The Formation of Structural Imperfections in Semiconductor Silicon

V. I. Talanin and I. E. Talanin

The Formation of Structural Imperfections in Semiconductor Silicon

The Formation of Structural Imperfections in Semiconductor Silicon

By

V. I. Talanin and I. E. Talanin

Cambridge Scholars Publishing

The Formation of Structural Imperfections in Semiconductor Silicon

By V. I. Talanin and I. E. Talanin

This book first published 2018

Cambridge Scholars Publishing

Lady Stephenson Library, Newcastle upon Tyne, NE6 2PA, UK

British Library Cataloguing in Publication Data
A catalogue record for this book is available from the British Library

ISBN (10): 1-5275-0635-5
ISBN (13): 978-1-5275-0635-0

CONTENTS

PREFACE

We are to admit no more causes of natural things than such as are both true and sufficient to explain their appearances
—Isaac Newton (25.XII.1642 – 20.III.1727)
Philosophiæ Naturalis Principia Mathematica, 1726

Over the past few decades, our knowledge of the solid state nature has increased significantly. At the same time the scope of application of crystalline solids in various fields of technology has greatly expanded. The increasing technological demands stimulate the rapid development of a relatively young area of modern natural science – solid state chemistry, the main tasks of which are as follows: synthesis of solids, research of their physical and chemical properties, reactions thereof, and ultimately creation of materials with predetermined properties.

All real solids (monocrystalline and polycrystalline) contain structural defects. Structural defects are violations of the periodicity of the spatial arrangement of atoms. The appearance of defects in crystals is inevitable, since they are formed in the process of a single crystal growth. The impact of defects on the physical properties of crystals is extremely diverse. It is determined by the nature of the binding forces in crystals, their energy structure (metals, semiconductors or dielectrics). If the fundamental physical properties of a substance are determined by its chemical composition and perfect structure, the introduction or change in the concentration of defects can change these properties, as well as impart new optical, electronic, mechanical and other characteristics to the substance. Creating a fairly complete picture of the nature and behavior of various defects is a prerequisite for a scientific approach to control structurally sensitive properties and processes in solids. Therefore, the most informative path to study any solid crystals is to consider their structure, formation, and properties as a joint and inseparable overall problem.

Semiconductor silicon occupies a completely unique position of all the variety of solids. Semiconductor (or electronic) silicon is considered to be basis of the electronic industry at present and in the foreseeable future. Discrete instruments and microelectronic integrated circuit are made of silicon. Requirements for the quality of silicon single crystals are

constantly increasing due to transition to production of large and very large scale integrated circuits and associated increase in the single crystal diameter and the degree of microelectronic circuit integration. Microelectronics requires to grow single crystals, which are completely dislocation-free, with a uniform distribution of doping and background impurities, with controlled and limited content of intrinsic structural point defects. Such stringent requirements stimulate intensive research into the nature of defect formation and improvement of techniques for obtaining modern dislocation-free silicon single crystals.

Requirements for the quality of modern microelectronic devices have made silicon the purest material in the world. Silicon single crystals are obtained by means of Czochralski method and floating zone melting method. Both methods ensure the production of the initial silicon with the total content of residual impurities $10^{11}…10^{12}$ cm^{-3}. The specific resistance of single crystals obtained by the floating zone melting method can reach up to 100 kΩ·cm, they show a large diffusion length of charge carriers and a low oxygen content. Such hyperpure crystals are an excellent research laboratory to study the general principles of defect formation. In addition, semiconductor silicon is the most suitable model for this kind of research as on of the most studied and used by humankind materials.

The growth of dislocation-free silicon single crystals by the Czochralski and floating zone melting methods is accompanied by the formation of structural imperfections known as grown-in microdefects. The formation of grown-in microdefects is mainly caused by intrinsic point defects (vacancies and interstitial silicon atoms) and impurity atoms of oxygen and carbon. The problem of controlling the nature, content, size, and nature of distribution of defects present in the dislocation-free silicon single crystal is primarily related to the development of effective methods for influencing the state of the ensemble of interacting point defects in the grown ingot. Advances in control of the point defects ensemble state ultimately determine the success of the quality management of electronic devices. Therefore, studying of formation and growth causes of various grown-in microdefects under different growing conditions of dislocation-free silicon single crystals is of high applied significance.

The problem of grown-in microdefects formation is both of technological (defect structure control in the process of crystal growing), and of fundamental scientific importance because its solution makes it possible to describe the physics of defect formation in hyperpure dislocation-free silicon single crystals. At the same time, it is impossible to solve the technological aspect of the problem of grown-in microdefects formation without understanding the physics of grown-in microdefects

formation process in dislocation-free silicon single crystals. This requires knowledge and correct physical model of grown-in microdefects formation and transformation to be adequately applied. This model is built using comprehensive experimental researches of dislocation-free silicon single crystals obtained by the Czochralski and floating zone melting methods at varying thermal conditions in the course of crystal growth.

The quantitative model of defect formation in dislocation-free silicon single crystal should be only developed based on such a qualitative mechanism, which adequately reflects a real crystal structure. The quantitative model of grown-in microdefects formation, in its turn, allows to simulate and to obtain dislocation-free silicon single crystals with a predetermined defect structure and to control it during further process effects. The quantitative model of grown-in microdefect formation should give an answer to the fundamental question of solid state physics, which consists in describing the kinetics of the grown crystal defect structure during its cooling. The development of such a model for the most perfect silicon crystals can serve as a basis for considering similar problems for other dislocation-free single crystals. The patterns of defect formation in dislocation-free single crystals are common, thus, silicon can be an example of structure analysis for all semiconductor and metallic dislocation-free single crystals.

Most publications about the defect structure of dislocation-free silicon single crystals are more or less associated with the investigation of point defects interaction in the course of dislocation-free silicon single crystals growth, elucidating the nature of the grown-in microdefects, and revealing the relationship between thermal conditions of crystal growth and formation of structural imperfections. A lot of international conferences carried out in recent years were devoted to these issues. However, up to the present time, there are no enough focused reviews in the scientific literature which would analyze the problems of grown-in microdefects growth and transformation from a common viewpoint. This monograph, to some extent, can compensate and eliminate these deficiencies.

The book considers experimental results of studying the nature of grown-in microdefects. The main attention is focused on the experimental and theoretical investigation of the point defects interaction in silicon, the elucidation of physical and chemical nature of grown-in microdefects, their transformation in the course of dislocation-free silicon single crystals growth, as well as the analysis of existing physical and mathematical models of the grown-in microdefects formation. The monograph is the result of a critical comprehension of a large number of original experimental and theoretical works presented in various scientific journals.

In a number of cases, there are significant differences in the experimental data and their interpretation. This difference is mainly due to the fact that there are two ways to solve the problem of defect formation in dislocation-free silicon single crystals. Followers of the first approach assume that there is rapid recombination of intrinsic point defects (IPDs) under the crystallization temperature and suggest that simulation of IPD dynamics in silicon may contribute to a quantitative understanding of the grown-in microdefects formation process and to their spatial distribution optimization inside the crystal. This approach assumes the dominant role of IPDs in the structural imperfection formation and leads to negation of the impurity involvement in this process. Followers of the second approach governed by the obtained experimental results deny the fact of IPD recombination in silicon at high temperatures and suggest that the problem of defect formation in dislocation-free silicon single crystals can be solved by creating a physical model based on the known experimental results to the fullest extent possible. In this case, it is assumed that defect formation in silicon is based on the interaction 'impurity – intrinsic point defect'. The main goal of this monograph is an attempt to understand these contradictions and to present a real picture of defect formation in dislocation-free silicon single crystals.

The monograph consists of six chapters. The first chapter considers features of (1) dislocation-free silicon single crystals growth by floating zone melting and Czochralski methods; (2) modern ideas about the defect structure arising in the process of their growth; (3) a review of experimental studies on the impurity kinetics of grown-in microdefects formation; (4) results of studies on various process-caused transformations of grown-in microdefects.

The second chapter is devoted to the analysis of physical simulation models of defect formation processes in semiconductor silicon. In particular, we considered early physical models of grown-in microdefects formation (equilibrium and nonequilibrium interstitial models, drop, vacancy and vacancy-interstitial models). Special attention was paid to the recombination-diffusion model proposed by V.V. Voronkov which can be considered as a symbiosis of all the pre-existing models. We considered a strong approximation of a mathematical model of intrinsic point defects dynamics developed on the basis of a recombination-diffusion model in detail. The main provisions of the heterogeneous (two-stage) model, as well as the origins of various approaches to solving the problem of defect formation in semiconductor silicon are briefly discussed.

The third chapter deals with critical issues for understanding the heterogeneous (two-stage) model. It is explained why the interaction

'impurity – intrinsic point defect' has an advantage over the IPD recombination processes in the course of crystal growth under high temperatures. It is shown how to reconcile the high-temperature precipitation process with the classical theory provisions related to the second phase particles nucleation.

The fourth chapter considers two new approaches to solve the problem of theoretical description of defect formation processes in the course of crystal growth: the high-temperature impurity precipitation model and the complex-formation model based on Vlasov equation solution for imperfect crystals. Firstly, we described the high-temperature impurity precipitation model in the course of crystal growth. We considered basic concepts of the microscopic theory of impurity kinetics in semiconductors and chose the model of dissociative diffusion-migration of impurities as a model for complex formation in the course of silicon single-crystal growth. We discussed the kinetics of high-temperature impurity precipitation process in dislocation-free silicon single crystals. As an alternative, we considered the problem of complex formation in semiconductor silicon in accordance with A. A. Vlasov model for solids. It was discovered that two nucleation theories of second phase particles, which are based on various approaches (classical nucleation theory and Vlasov model for solids), lead to identical results. A kinetic model of oxygen and carbon precipitates growth and coalescence during the grown silicon crystal cooling is presented.

The fifth chapter discusses the formation of microvoids and interstitial dislocation loops in the course of crystal growth. Formation processes of microvoids and interstitial dislocation loops within the framework of the point defect dynamics model were simulated. A vacancy-condensation model, as well as a kinetic model of interstitial dislocation loops formation and growth were proposed.

A general approach to the engineering of defects in silicon is given in the sixth chapter. The necessary conditions for defect engineering during crystal growth are briefly discussed. We considered the diffusion model structure of grown-in microdefects formation and transformation and its application to describe the defect formation in heat-treated silicon single crystals. The technique of defect structure virtual research is given. It is considered as an assistant tool to use modern information technologies in order to analyze and control defect structure of initial single-crystals and instruments made of such crystals. Presented is a computation algorithm for semiconductor silicon defect structure used in the development of software products.

The content of this book mostly reflects the authors' research area, thus, some issues related to point defect interaction were not included and

others were considered briefly and concisely due to limited volume of the book. Despite this, the authors do hope that this monograph can be useful both for professionals and students, as well as can be used as a reference material.

It should be noted that all chapters of this book are written by both authors and each of them has the same copyright to the material presented in the book. There is no conflict of interests between the authors.

CHAPTER ONE

GROWTH OF DISLOCATION-FREE SILICON SINGLE CRYSTALS FROM MELT AND DEFECT FORMATION

When we meet a fact which contradicts a prevailing theory, we must accept the fact and abandon the theory, even when the theory is supported by great names and generally accepted
—Claude Bernard (12.VII.1813 – 10.II.1878)
An Introduction to the Study of Experimental Medicine, 1865

The development of electronics is based on the development of microelectronics as the leading sub-sector of world electronic production; because microelectronic technologies are now the pinnacle of engineering in the field of high technologies and they determine the achievable technical level of the country's industrial potential. On the one hand modern rates of microelectronics development are associated with advances in the field of semiconductor technology, and on the other hand they lead to increasingly stringent requirements for the semiconductor industry. These requirements can be met by means of different technologies and materials, but due to the needs of mass production and relative cheapness of the material, the monocrystalline silicon grown by the Czochralski method is the main material in the microelectronic industry. Economic reasons led to a steady increase of grown single crystals in the diameter and length, as far as more crystals can be cut from a larger diameter wafer (the square dependence of area on diameter). Modern growth units in combination with developed growing modes and precision control systems allow growing high-quality single crystals with a diameter of up to 350 mm on an industrial scale and mastering the production of single crystals with a diameter of 450 mm. A greater output of suitable products is possible only in case of high axial and radial homogeneity in impurity composition and low content of grown-in microdefects in growing dislocation-free silicon single crystals.

1.1. Features of dislocation-free silicon single crystals growth by floating zone melting and the Czochralski methods

Two main methods of growing silicon single crystals are used in the industry: extraction from quartz crucibles (Czochralski method) and floating zone melting [1, 2]. To obtain silicon single crystals by the Czochralski method (hereinafter referred to as CZ-Si) polycrystalline silicon is placed in high purity quartz crucible heated to the melting point of silicon ($\sim 1683 \ldots 1685\,K$). A seed of a certain section and a given orientation cut from a single crystal is lowered into the melt and a part of the seed is melted slightly by raising the temperature. After this, the heater temperature is slowly lowered until crystallization on the seed begins. At this point, the seed is lifted, and the single crystal is drawn out of the melt. The diameter of the grown single crystal is regulated by the temperature of the heater, the rate of lifting the rod, the conditions for removing the heat of crystallization, and other parameters. To obtain silicon single crystals with a given type of conductivity and resistivity a doping impurity (boron, phosphorus, antimony, arsenic, aluminum, etc.) is introduced into the crucible with a charge or into the melt in pure form or in the form of ligature. The growing process demands suitable conditions for the dopant to be uniformly distributed throughout the volume of the single crystal. It is extremely difficult to create a strictly symmetrical thermal field; crystal or crucible (or both) rotate to equalize the temperature field, which makes it possible to grow symmetrical single crystals even at large asymmetric temperature gradients.

Due to the thermal field asymmetry so-called ‘screw thread’ is observed on the cylindrical surface of single crystals grown with rotation: Crystal growth rate increases when passing the cold area of the melt and more impurities are captured at this point. In hotter area the growth rate decreases. Such periodic microscopic fluctuations in the crystal growth rate cause the phenomenon of ‘remelting’, which is responsible for the banded distribution of impurities in the crystal longitudinal section and leads to the formation of grown-in microdefects in the swirl distribution along the crystal cross-section [3]. In addition to the ‘screw thread’, one can see annular irregularities on the surface of a single-crystal related to the fluctuations of the melt level, its temperature, rod movement velocity, etc.

The main shortcoming of CZ-Si crystal growth is the increased content of carbon (up to $5 \cdot 10^{16}$ cm^{-3} an over) and oxygen (up to $18 \cdot 10^{18}$ cm^{-3}), as

well as other impurities contained in the quartz crucible from which the ingot is drawn.

Unlike CZ-Si, silicon single crystals obtained by the floating zone method (hereinafter referred to as FZ-Si) are distinguished by a very low content of such background impurities as oxygen and carbon. The concentration of these impurities in some crystals may be below the sensitivity level of optical methods (less than $5 \cdot 10^{15}$ cm^{-3}).

To obtain FZ-Si a polycrystalline rod shall be vertically fixed in the unit clamps. The molten zone is created by induction heating, and this zone is retained by surface tension forces. The smaller the zone height, the larger ingot diameter it can occupy. A single-crystal seed is strengthened in the lower clamp and a molten drop is created at the end of the rod. Then the seed is moved upward and introduced into the melt. After seeding, the seed, along with the single crystal growing on it, is moved downward (or the inductor is lifted up). Repeated zone movement due to evaporation and difference in impurity distribution coefficients in liquid and solid states can lead to a very high degree of silicon purification. To produce silicon single crystals with a given level of resistivity, volatile compounds of the dopant (phosphine, diborane, arsine, etc.) are introduced into the unit chamber or polycrystalline rods are used preliminarily doped in the course of hydrogen reduction or monosilane decomposition. The pedestal growth is a variation of the floating zone melting method. In this case, the seed is installed in the upper clamp and the molten zone is created at the upper end of the rod.

Dislocation-free single-crystals make more than 95 % of the silicon single crystals obtained. Dislocation-free single crystals are grown by the Dash method [4]. This method consists in high-rate growing of a long thin monocrystalline neck with a diameter less or equal to the seed diameter after seeding. Once a section free from dislocations is found on a certain neck section, a conical and then a cylindrical part of a single crystal of a given diameter may be grown.

Theoretical analysis and practical growing of silicon single crystals in any crystallographic direction allow us to conclude that the growth of these crystals is accomplished by the appearance and development of planes {111}. In this case, growth begins with the formation of a two-dimensional nucleus. While the two-dimensional nucleus is developed in a tangential direction at a low rate because of the boundary large curvature a number of other nuclei are formed on its surface. This process continues until the curvature radius decrease in normal direction leads to the growth rate decrease. By this time, the curvature radius is increased in tangential direction and growth in this direction quickly outstrips growth in normal

direction. Once the face is overgrown with the layer formed, the process resumes.

Thermal stresses arising in a growing crystal as a result of curvature of isothermal surfaces, one of which is the crystallization surface, can lead to plastic deformation and structural defect formation. The number and distribution of structural defects and associated changes in electrical and physical properties of single crystals are largely determined by the magnitude and distribution of thermal stresses defined by thermal growth environment. The thermal growth environment can be defined by the crystallization front shape. For example, it is possible to obtain a simple relation, determined by the macroscopic growth front shape of a single crystal as a function of the drawing rate. It is necessary to preserve the condition $V_p = V_g$ (V_p – drawing rate; V_g – the rate of the heat flow across the interface or the growth rate of the crystal) to prevent liquid detachment from the crystal. This rate can be determined by Fick's equations. Thus, for a planar interface

$$\frac{\partial^2 T}{\partial z^2} = \frac{\partial T}{\partial t} = \frac{\partial T}{\partial z}\frac{\partial z}{\partial t} = \frac{\partial T}{\partial z}V_z. \qquad (1.1)$$

Hence, heat flow rate through a flat surface equals

$$V_z = \frac{\partial^2 / \partial z^2}{\partial T / \partial z}. \qquad (1.2)$$

For a spherical interface

$$\frac{\partial^2 T}{\partial r^2} + \frac{2}{r}\frac{\partial T}{\partial r} = \frac{\partial T}{\partial t} = \frac{\partial T}{\partial r}\frac{\partial r}{\partial t} = \frac{\partial T}{\partial r}V_r \qquad (1.3)$$

whence

$$V_r = \frac{\partial^2 T / \partial r^2}{\partial T / \partial r} + \frac{2}{r}. \qquad (1.4)$$

Thus, heat flow through a spherical surface $V_r = V_z + 2/r$, where T is a temperature; r is a distance from the interface. Hence, if $V_r = V_p$, then $V_p - V_z = 2/r$. If $V_p = V_z$ a flat interface is maintained; if $V_p > V_z$, a concave crystallization front arises, and if $V_p < V_z$ – a convex crystallization front arises. Type of the crystallization front has a significant influence on the temperature distribution at the interface. Curvature of the crystallization front is the main parameter used to estimate changes in thermal growth environment.

Radial temperature gradients arising in the crystal and determining thermal stress magnitude are proportional to the tangent of the isothermal surface curvature angle and the axial temperature gradients:

$$\frac{\partial T}{\partial r} = \frac{\partial T}{\partial a} tg\theta, \qquad (1.5)$$

where $\frac{\partial T}{\partial r}$ and $\frac{\partial T}{\partial a}$ are the radial and axial temperature gradients respectively; $tg\theta$ is the slope of the curve to the isothermal surface.

As the rate of the zone passage increases, the curvature of the crystallization front decreases. Decrease of the crystallization front curvature and increase of the passage rate can be explained by the following reasons:

- Firstly, as the passage rate increases, the amount of evolved crystallization heat increases;
- Secondly, the melting power should be increased to maintain a stable zone, which leads to more intensive melt mixing.

Both factors contribute to a more uniform temperature distribution in the zone area. An increase in the passage rate also leads to a decrease in the axial temperature gradient. Consequently, as the passage rate increases, the value of both parameters decreases on the right-hand side of Eq. (1.5), which corresponds to a decrease in the radial temperature gradient and the associated thermal stresses and structural defects.

As the crystal grows, the conditions of the heat transfer through the crystallization front and the melting front should be changed along the zone transfer path. So, as the zone moves, heat removal through the crystallization front should increase, and heat removal through the melting front should decrease. This should lead to increase of the axial temperature gradients in the growing crystal and increase of the crystallization front curvature. Since silicon thermal conductivity coefficient is a finite value, increase of the axial temperature gradient in the course of zone movement along the ingot should mainly appear when crystals are grown at lower rates of the zone passage.

The dependence of the axial temperature gradient on the rate of the zone shift was expressed in [5] by the empirical formula for the first time for small-scale crystals of FZ-Si (up to 30 mm):

$$\frac{dT}{dx} = 10 + (x - 16)^2 \exp(-61.2V_g - 0.28), \qquad (1.6)$$

where x is the distance from the crystallization front to a certain cross section, cm. An analytical determination of the two-dimensional

temperature field was proposed in [6, 7] for large-scale CZ-Si crystals (over 100 mm). According to this technique, the temperature field is set as follows:

$$1/T = 1/T_m + G_a x/T_m^2 \qquad (1.7)$$

where T_m is the crystallization temperature, x is the distance from the crystallization front, G_a is the axial temperature gradient. The temperature field is set both axial-wise and along the surface; a field along the crystal's surface to axial-wise field ratio changes incrementally. It was shown in [8] that the joint usage of formulas (1.6) and (1.7) to calculate the defect formation shows similar results. Similar results obtained by two methods prove the absence of fundamental differences between them, their interchangeability and the possibility of their application to crystals of any diameters [8].

The most typical shapes of the crystallization front for CZ-Si and FZ-Si are shown in Fig.1.1.

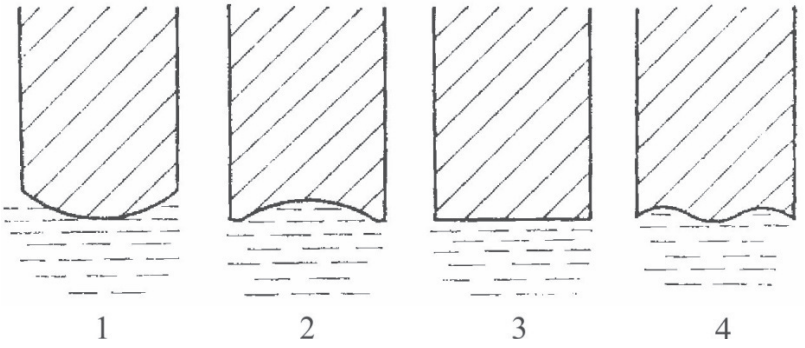

Fig. 1.1. The shape of the crystallization front during the growth of silicon single crystals: (1) convex; (2) concave; (3) flat; (4) undulating.

In fact, the crystallization front is not limited by a smooth surface, but by a stepped surface. Flat areas of different lengths can be often observed on the crystallization front, depending on the growth direction. In addition, macro- and microdepressions, protrusions, etc. may be formed in some cases. The shape of the crystallization front depends on the growth modes, and if silicon single crystals are grown in the [111] direction, a plane molecular smooth surface appears along the surface of the crystal-liquid contact with the rounded sections. In contrast to the flat growth front

(when $V_p = V_g$), as a rule being a stepped surface with a low step height, the formed face turns out to be mirror-smooth. If the crystallization front is convex, then the face is formed on a rise (deep in the liquid). If the front is concave towards the crystal, the face is formed on the peripheral part of the circle. It is established that this face coincides with the crystallographic face (111) of the silicon lattice. In addition to the horizontal face (111), lateral lower and upper faces (111) also appear on the crystallization front. When growing in directions different from [111], for example, [100], only the side faces come out to the crystallization front. It should be noted that the crystallization front surface of dislocation-free and dislocation silicon single crystals differs significantly. This difference is manifested primarily in the sharp increase of the face protrusion area (111) on the crystallization front in the course of the growth of dislocation-free silicon single crystals.

The channel inhomogeneity was discovered long ago and used to be the main reason causing an inhomogeneous distribution of impurities along the cross-section of silicon single crystals grown in the [111] direction. Channel inhomogeneity arises because of the face effect appearance under certain conditions causing the crystallization front face formation (111). For this crystal face is grown in a relatively more super-cooled melt than its surrounding, then impurity concentration in the crystal face area is higher. Although the channels are detected both when the crystallization front is concave (to the seed) and almost flat, they are formed mainly at the convex towards the melt crystallization front.

When single crystals are grown with a wave-type crystallization front, we observe a core-type and tubular-type channels. These channels appear in points of the face protrusion (111) on the crystallization front. Increase in size of a flat area of the crystallization front results in expanding a channel's width. A curvature decrease of the crystallization front leads to a wider central (core-type) channel and decreasing of a tubular-type channel diameter. A sharp change of the crystallization front can lead to the channel disappearance. The crystallization front is flat near the channel.

The main reason for the channel inhomogeneity formation is the growth of single crystal by the two-dimensional nucleation (coupled with the single crystal rotation and drawing in the direction [111]), which leads to increased super-cooling in the face protrusion (111) on the crystallization front area.

The number and distribution of structural imperfections largely depend on the magnitude and distribution of thermal stresses, determined by the thermal growth conditions. Since the crystallization front shape with sufficient accuracy reflects the isotherm corresponding to the silicon melting temperature, this shape identification and study allow us to

characterize a single crystal thermal growth conditions. The macroscopic shape of the crystallization front, in its turn, is determined by the crystal growth rate. Indeed, the growth rate increase causes the crystallization front curvature decrease and the axial temperature gradient decrease. The most technically simple way is to control the growth rate, while accurate measurements of the temperature gradient meet certain difficulties [9, 10].

1.2. Defect structure arising in the process of dislocation-free silicon single crystals growth

According to the generally accepted geometric (dimensional) classification [11], structural defects in crystals are subdivided into:

- point (zero-dimensional): vacancies, interstitial atoms (intrinsic and impurity atoms);
- linear (one-dimensional): dislocations of various types; flat (two-dimensional): stacking faults, interphase and intraphase interfaces;
- three-dimensional: voids, precipitates.

Structural imperfections called ‘grown-in microdefects’ are formed during high-temperature growth and subsequent cooling of high-purity dislocation-free silicon single crystals. Since the dislocation-free crystals are supersaturated by point defects (vacancies, self-interstitials, impurity atoms) in the cooling process, the formation of grown-in microdefects is due to the processes of IPD and impurity aggregation. The impossibility of complete material purification (presence of residual or background impurities) and occurrence of IPDs (vacancies and silicon self-interstitials) at the crystallization temperature even in special undoped high-purity silicon single crystals obtained by the floating zone method result in complex interaction processes and subsequent decomposition of the oversaturated solid solution of point defects during the crystal cooling [12]. Structural imperfections (micro-precipitates, dislocation loops, microvoids) formed in such processes are grown-in microdefects. Thus, pursuant to a contemporary view, the term microdefects is taken to involve any local disturbances of the lattice periodic behavior measuring from several tens of angstroms to several micrometers. They form an intermediate class between point and other types of structural defects and also are aggregates of IPDs and impurities [13]. In turn, microdefects formed during silicon processing were called the ‘post-growth’ microdefects.

Information about the presence of etch pits in dislocation-free silicon single crystals for the first time appeared in the second half of the 1960s

[14]. On the (111) plane, these pits have the shape of regular triangles with sides directed along [110]. Unlike ordinary dislocation etch pits, they have a flat bottom, and therefore were called as empty etch pits in those works. The [15] describes the arrangement of empty pits in a single crystal body and the influence of a number of factors on their appearance for the first time in detail, and assumes the vacancy origin of these defects.

De Kock began to classify the empty etch pits, having called them clusters. He introduced two types of clusters depending on the etch pit size: A-clusters (A-microdefects) and B-clusters (B-microdefects) [15, 16]. Taking into account that the macro-pattern of empty etch pit distribution along a single crystal cross-section in most cases resembles vortices, the authors of [17, 18] called these microdefects as swirl defects. It was shown that microdefects are located along impurity growth bands, which, in turn, reflect the shape of the crystallization front, determined by the thermal conditions of growth [19, 20]. The minimum spacing between the spiral bands corresponds to the ratio of the crystal growth rate to its rotation speed. As the crystal growth rate decreases, the deflection of the microdefect bands increases, which is explained by increase of the temperature gradient radial component [20]. Density of microdefects in the band was found to be higher than at the periphery of the center of the crystal. The authors [20] state that this may be caused by the fact that the temperature gradient radial component in the center of the crystal is always higher than at the periphery at the observed crystallization surface curvature. Both types of defects may be observed in the crystal body. Herewith, the distribution of B-microdefects (small etch pits) is often superimposed on the distribution of A-microdefects (large etch pits). The maximum size of B-microdefects is observed in areas where there are no A-microdefects. A- and B-microdefects can be found in the central part and are usually absent at the side crystal surface. Furthermore, B-microdefects are located closer to the single crystal surface than A-microdefects. The crystal surface can serve as a drain for intrinsic point defects, so, as a rule, the near-surface areas, contain few microdefects. The average concentration of A-microdefects in the crystal body is ~ 10^6…10^7 cm^{-3}, while average concentration of B-microdefects is ~ 10^9…10^{10} cm^{-3} [21, 22]. Experiments on crystal quenching have shown that B-microdefects are formed first [16, 19].

It should be noted that until the end of the 1970s grown-in microdefects were investigated mainly in small-sized FZ-Si crystals (26...30 mm in diameter). In silicon single crystals of 30 mm in diameter banded distribution of typical A-microdefects were found to be observed at the crystal growth rates V_g = 1.0…3.5 mm/min, uniform distribution

thereof at V_G < 1.0 mm/min, while banded distribution of B-microdefects was found to be observed at $V_G \leq 4.5$ mm/min [12]. Fig. 1.2 shows typical banded distribution of A-microdefects along the crystal cross-section, and Fig. 1.3 shows swirl distribution of B-microdefects in the (111) plane [23].

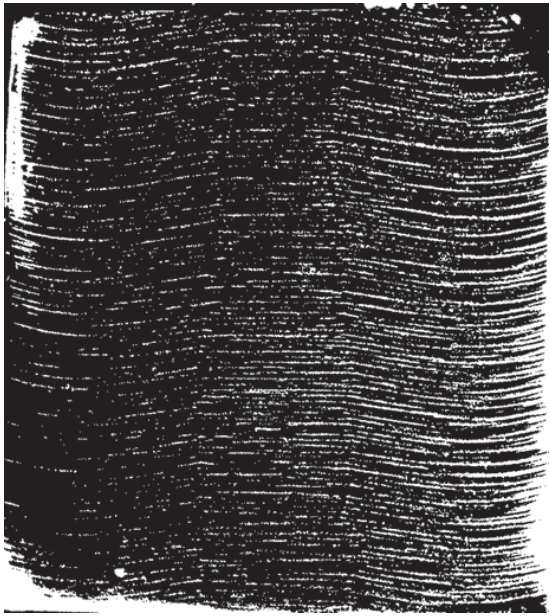

Fig. 1.2. Banded distribution of A-microdefects in the plane [112], selective etching, crystal diameter 30 mm

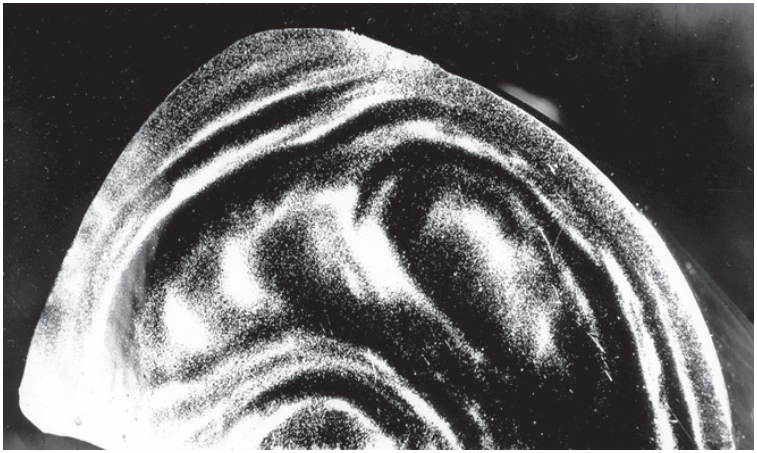

Fig. 1.3. Swirl distribution of B-microdefects in the plane [111], selective etching, crystal diameter 30 mm

As the size of the A-microdefects increases to a certain limit (ca. 40 μm at v_g = 1.0 mm/min) [19] dislocations arise in silicon single crystals [19, 24, 25]. With the help of transmission electron microscopy (TEM), it was shown that A-microdefects could act as sources of dislocation nucleation, which, pursuant to the authors [26], is due to the Frank-Read mechanism action, under the influence of compressive stresses in the center of the crystal resulting from the combined effect of radial and axial temperature gradients. Appearance of dislocations is seriously affected not only by the dimensions, but also by relative disposition of microdefects, and by distances between them, since their growth and interaction take place at temperatures corresponding to the plasticity zone [20].

Abe conducted an analysis of the impurity effect on microdefect formation and showed that the formation of A- and B-microdefects is enhanced by crystal doping with carbon and is impeded by oxygen [3]. The formation of microdefects is suppressed by doping with impurities of large covalent radii, for example, antimony. Banded distribution of A- and B-microdefects is associated with the sites of their nucleation. When the crystal is grown, temperature fluctuations occur due to crystal rotation and melt convection. As a result, microdefects grow following the crystal type of growth and stopping [3, 27, 28]. Periodic changes in the crystal growth rate cause respective periodic changes in the impurity concentration, in particular, carbon. It was shown [28] that the local maxima of the concentration of microdefects (bands of A- and B-microdefects) coincide

with areas of high phosphorus concentration. Based on the fact that banded distribution of A- and B-microdefects is also observed in phosphorus-free silicon and taking into account the similarity of phosphorus and carbon distribution [28, 29], the authors of [18, 30-32] concluded that the microdefects should be formed with the participation of carbon atoms. Foll et al. determined that concentration of microdefects increases as carbon content increases [18]. On this basis, it was concluded that the banded distribution of microdefects indicates a heterogeneous nature of their nucleation and its dependence upon periodic changes in crystal growth rate [18]. The critical crystal growth rate at which the remelting phenomenon is suppressed, which contributes to the nonuniform distribution of impurities in the crystal was calculated theoretically in [33] (for floating zone melting method ~ 5.3 mm/min). This value is in good agreement with the experimental results [34], under which disappearance of B-microdefects occurs. Based on these results, it can be concluded that temperature fluctuations and the presence of impurities (especially carbon [18, 32, 35, 36] and oxygen [37-40]) are the main factors responsible for the formation of A- and B-microdefects.

At a certain growth rate, it is possible to achieve the absence of large microdefects. For example, disappearance of A- and B-microdefects in FZ-Si crystals occurs at very low cooling rates, which is achieved by growing crystals at a growth rate of $V_g \leq 0.2$ mm/min [41]. At such low growth and cooling rates, the concentration of point defects as a result of their diffusion to the crystal surface decreases below a certain critical value necessary for the formation of microdefects [41]. In this case, the amplitude of impurity bands also decreases, which is related to the diffusion process in the solid state and respective composition homogenization. With an increase in crystal growth rate up to 4.0...4.2 mm/min A-microdefects are not detected, and at a growth rate of more than 4.5 mm/min B-microdefects are not detected as well [42-45]. Based on these experimental data, the authors of [15, 41] proposed methods for obtaining dislocation-free silicon single crystals without microdefects. However, obtaining homogeneous and defect-free silicon single crystals at very low growth rates is characterized by low process productivity, which is a very significant drawback [20]. In addition, in this case, it is difficult to maintain the dislocation-free mode, since dislocations may be generated during an unforeseen decrease in the crystal growth rate [19].

Until 1975, it was believed that A- and B-microdefects are vacancy clusters generated during the growing crystal cooling on various vacancy-oxygen complexes. However, TEM-studies of dislocation-free silicon single crystals revealed that A-microdefects are individual dislocation

loops of 1...5 μm size or clusters of such interstitial-type loops [26, 27, 42]. These investigations did not provide any direct study of B-microdefects in a 'pure' form in theory. Only pre-decoration of microdefects allowed to make an assumption about their interstitial origin [27]. Further detailed TEM-studies confirmed this hypothesis [45].

When crystals are grown at sufficiently high rates (above 4.5 mm/min for FZ-Si crystals), a new type of microdefects was observed as uniform distribution and could be identified as dim regions after preferential etching and decoration [46]. These defects were classified as C- or D-microdefects depending on their macrodistribution images [46]. Both types were visualized as the regions with uniform defect distribution of high density and, according to the authors of the paper [46], differed from each other by distribution geometry in these regions. The uniform D-microdefects distribution is focused in the form of a 'channel' in the central part of the crystal (Fig. 1.4a). At the same time, C-microdefects were observed as rings or circles of irregular shape, located at the most extensively cooled parts of the crystal. Later de Kock confirmed the existence of identical grown-in microdefects in small-scale CZ-Si crystals (50 mm in diameter), which were observed after selective etching [47, 48].

It should be noted that in [46] defects were named D-microdefects which were observed after selective etching in a uniform distribution in the form of a channel in the center of a 30 mm diameter FZ-Si crystal grown at $V_g \leq 6.0$ mm/min. With the help of TEM, the physical nature of D-microdefects (the sign of defect-induced lattice imperfection) discovered in [46], was studied in detail [21, 49]. It was shown that D-microdefects (and C-microdefects) formed in crystals grown at growth rates above 4.5 mm/min $\leq V_g \leq 6.0$ mm/min are interstitial by nature, i.e., they cause compression deformation in the crystal.

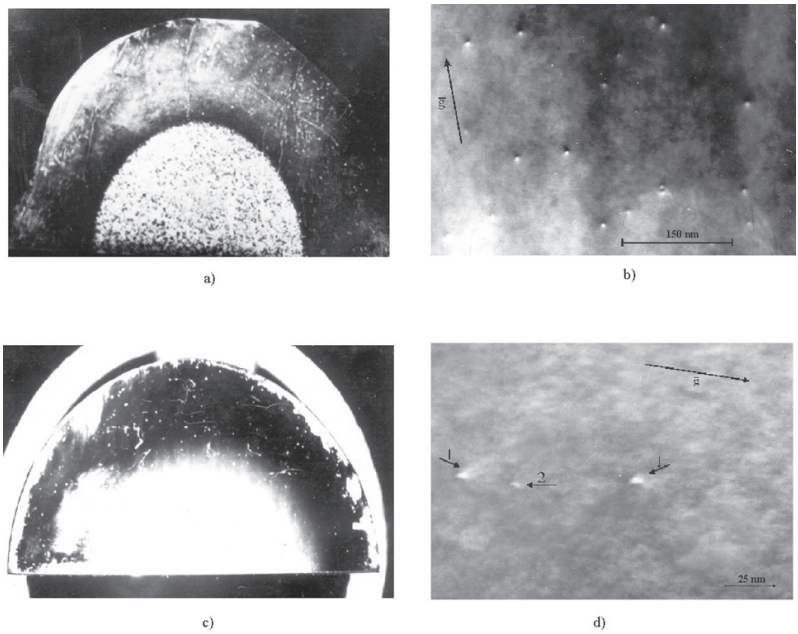

Fig. 1.4. D-microdefects and (I+V)-microdefects of FZ-Si crystals (crystal diameter 30 mm):
(a) D-microdefects, selective etching, plane (111); (b) D-microdefects, TEM, dark field, $\overline{g} = (\overline{2}20), s = 0$; (c) (I+V)-microdefects, selective etching, plane (111); (d) (I+V)-microdefects ((1) V-defects; (2) I-defects), TEM, dark field, $\overline{g} = (\overline{2}20), s = 0$.

Four years after the paper [46] Roksnoer and van den Boom also investigated uniform defects distribution in the center of a 30 mm diameter FZ-Si crystal grown at V_g > 6.0 mm/min [50]. On the basis of X-ray topography results coupled with subsequent copper decoration, it was assumed that D-microdefects are vacancy-type. This erroneous assumption had a great influence on subsequent theoretical studies of defect formation in silicon, since it formed the basis for the recombination-diffusion model of the grown-in microdefects formation (Voronkov model) [6]. Later it was shown that under these conditions (I+V)-microdefects are formed (Fig. 1.4c) [13]. (I+V)-microdefects are coexisting defects of the vacancy (V) and interstitial (I) type (Fig. 1.4d) [13, 51, 52].

It should be noted once again that all the above data refer to silicon single crystals with a diameter of 28...30 mm. However, the known data allow us to state that as the crystal diameter is increased; the growth rates are reduced resulting in the disappearance of A- and B-microdefects and the appearance of D-microdefects. For example, in [3] it is pointed out that in silicon single crystals with a diameter of 42 mm, D-microdefects are formed at a growth rate of 4.0 mm/min, while the formation of A- and B-microdefects in larger single crystals with a diameter of ~ 125 mm is suppressed at a growth rate V_g > 2.5 mm/min. These results can be explained by a decrease in the axial temperature gradient in the crystal, which occurs when the diameter of the grown crystal is increased. Therefore, defect formation in large-scale crystals is of great interest, since the modern electronic industry is characterized by an increasing tendency to use silicon single crystals of large diameters [53-55]. However, as shown in [53], defects ensemble in large-diameter crystals does not undergo serious changes, and, probably, mechanisms of defect formation are generally uniform for single crystals of any diameter. It should only be taken into account that as the diameters increase, the differences in the temperature growth conditions of such crystals become effective.

In the process of CZ-Si single crystal growth temperature growth conditions and content of impurities significantly differ from those applied to obtain silicon by the floating zone melting method. Carbon concentration in these crystals is one order of magnitude higher, and oxygen concentration is one or two orders of magnitude higher and makes ~ 10^{16}…10^{18} cm^{-3}. Furthermore, the Czochralski method is characterized by a lower cooling rate.

Etching patterns of A-, B-, and D-microdefects found in CZ-Si were identical to those found in FZ-Si crystals [47, 48, 50]. Banded distribution of A- and B-microdefects is observed in undoped or slightly doped monocrystals with a diameter of 50 mm grown at V_g ≤ 1.0 mm/min. Furthermore, at V_g ~ 1.0 mm/min A- and B-microdefects are formed in concentrations comparable to their concentration in silicon single crystals obtained by the floating zone melting method. At V_g ≥ 2.0 mm/min the formation of A- and B-microdefects is completely suppressed, and the presence of uniformly distributed D-microdefects is observed [56]. The distribution of A-microdefects depends on the amplitude of fluctuations in the crystal microscopic growth rate [57]. If the microscopic growth rate varies significantly, the banded distribution of microdefects takes place, otherwise the uniform distribution takes place. The critical growth rate at

which the A-microdefects disappear is ~ 2.0 mm/min [47]. This value decreases with the crystal diameter increase and with the axial temperature gradient decrease. As known, the axial temperature gradient near the crystallization front decreases as the growth rate increases and as the crystal diameter increases [54]. The value of 2.0 mm/min obtained by the authors of [47] is in good agreement with the calculated growth rate required to suppress the remelting phenomenon (~ 2.7 mm/min) [33] caused by temperature instability due to thermal convection.

Due to the high content of impurities in CZ-Si single crystals, the defect ensemble is also strongly dependent on residual and dopant impurities. For example, doping with acceptor impurities almost suppresses the formation of B- and D-microdefects, donor doping eliminates A-microdefects [58, 59]. Oxygen is present in CZ-Si single crystals in fairly high concentrations (up to ~ $2 \cdot 10^{18}$ cm^{-3}), it penetrates into silicon from a quartz crucible [15, 49, 60, 61]. Such a high content of oxygen determines its significant influence on such single crystals' parameters. Oxygen precipitation has a significant effect on the crystal electrical and mechanical properties [62-64], and it is in close interrelation with the defect structure of silicon single crystals [65-67]. In addition, the authors of [68-71] indicate that carbon should also be as important as oxygen in CZ-Si crystals, and that concentrations of B- and D-microdefects depend upon the carbon concentration [47, 57, 68, 72]. Based on these results, as well as on the identity of main types of microdefects in FZ-Si and CZ-Si crystals, and taking into account the strong dependence of microdefects in FZ-Si crystals on carbon impurity [18], it was concluded that carbon should play the key role in microdefects formation in CZ-Si crystals [73, 74].

In earlier papers devoted to CZ-Si crystals [47, 48], D-microdefects were identified based on the nature of their distribution, and for this reason, according to [46], they were for some time referred to as C- and D-microdefects. In addition, further research was conducted using various detection techniques, which led to a disparity in the names of the same defects. An attempt was made in [75] to classify microdefects in crystals grown by the Czochralski method on the basis of X-ray topography results coupled with selective decoration. D-microdefects of FZ-Si crystals were named as A'-microdefects in this paper. The authors of [75, 76] showed banded distribution of A'-microdefects. A type of defects called α-defects [75] was also identified. The dimensions of the etching patterns and the density of the A'- and α-microdefects were identical, but taking into account uniform distribution of α-defects in contrast to A'-defects, the authors of [75] identified them as a separate type of defects. Herewith,

theoretical results [6] showed that α-microdefects are formed at the boundary of interstitial- and vacancy-type growth, while A'-microdefects are formed in the course of vacancy-type growth [75]. The technique used by the authors could not specify the type of detected defects (interstitial or vacancy), and therefore α-microdefects were treated as defects of 'unknown nature' [65, 66, 75]. The situation with the nature of microdefects of the A'-type was also unclear. Repeatedly pointing out the identity of A'-microdefects with D-microdefects of FZ-Si and postulating the interstitial origin of A'-microdefects, the authors of [76-78] found the main differences between these two types of microdefects in the nature of their distribution: banded for A'-microdefects and uniform for D-microdefects. Subsequently, still pointing out the identity of both types of defects, but assuming the vacancy origin of D-microdefects [50], the A'-microdefects were regarded as defects of the vacancy origin and identified as

> '*oxygen microprecipitates formed as a result of joint oxygen-vacancy agglomeration'* [40, 65, 79-81].

New types of grown-in microdefects are observed in large-scale CZ-Si crystals (diameter over 100 mm). In particular, the formation of so-called oxidation-induced stacking faults (OSF-ring) after thermal oxidation of annular distribution along the cross-section perpendicular to the growth axis is the most typical at present[82, 83]. Stacking faults arise around plate-like oxygen precipitates, and bulk density of precipitates ($\sim 1.5 \cdot 10^7$ cm^{-3}) remains unchanged in spite of increasing oxidation duration. It means that precipitates formation process is completed in the course of the crystal growth [84]. The formation of oxidation-induced stacking faults was registered by means of TEM after heat treatment at 1373 K in steam within 5.0 min, although grown-in precipitates could not be observed. Since oxidation-induced stacking faults occur on oxygen precipitates formed in the process of growth, OSF-ring parameters should depend on the growing conditions. Investigation of the growth rate effect on distribution of grown-in microdefects in silicon single crystals with a diameter of 150 mm showed that the OSF-ring is observed in crystals grown at a moderate growth rate (0.7...0.8 mm/min) and is absent in crystals grown at 0.4 mm/min and 1.1 mm/min [84]. The critical growth rate at which the OSF-ring appearance or disappearance is observed in the center of the growing crystal is due to thermal conditions on the crystallization front. A change in thermal conditions is accompanied by a change in OSF-ring diameter contraction rate as the growth rate decreases:

the lower the axial temperature gradient, the faster the diameter of the ring is reduced.

The process of oxygen microprecipitates formation (nuclei of oxidation-induced stacking faults) is considered as a function of free vacancies concentration: formation of vacancy clusters dominates at a high concentration of nonequilibrium vacancies (in the central part of the vacancy zone), with its decrease (at the edge of the zone) interaction of vacancies and oxygen atoms with formation oxide particles take place [81]. Thus, the OSF-ring is formed at the edge of the vacancy area, the outer boundary of the ring adjoins the defect-free zone [85, 86]. The OSF-ring is formed due to nonuniform distribution of the axial temperature gradient at the crystallization front along the growing crystal radius, resulting in uneven radial distribution of the residual intrinsic defects. The formation of the OSF-ring is closely related to the dependence of oxygen precipitation kinetics on the concentration of free vacancies [81].

The microdefects detected by selective etching are differently distributed inside and outside the OSF-ring; the nature and distribution of microdefects vary substantially with the crystal growth rate change. The following types of defects are observed inside the ring at moderate and high growth rates, depending on the investigation methods:

- typical cone-shaped etching patterns detected in a result of selective etching (flow pattern defects, FPD) [87];
- double or triple octahedral voids with linear dimensions of 0.1...0.3 μm detected by the scattered IR radiation method (light scattering tomography defects, IR LSTD) [88];
- etch pits detected by selective etching, similar to FPD but not cone-shaped (Secco etch pits defects, SEPD) [87];
- single or double pyramid-shaped small pits with a diameter of 0.12...0.3 μm and a depth of about 0.14 μm, faceted with planes {111}, detected on the silicon wafer surface before and especially after washing in NH4OH:H2O2:H2O solution (crystal originated particles, COPs) [89];
- defects detected by optical interferometry (optical precipitate profiler defects, - OPPD) [90].

As it was illustrated in [90], the above listed defects are likely different forms of the same defect revealed by various methods: vacancy complexes formed inside the OSF-ring. The relationship between them can be expressed as follows: (IR LSTD = COPs = OPPD) = FPD + SEPD. Heat treatment at high temperatures in an oxidizing atmosphere result in

reduction of etch pit size until complete annihilation [84]. To explain this fact it was suggested that IR LSTD ability to form etching patterns detected as FPD is lost due to high-temperature heat treatment, which in its turn is caused by the oxygen oxide layer growth on the defect/matrix boundary during heat treatment [89, 90].

TEM-studies of crystals containing IR LSTD were for the first time carried out in [87, 91]. These studies allowed to determine the octahedral shape and sizes (100...300 nm) of LST-defects. Spectral analysis showed oxygen presence in these defects, the content of which in the defect center is significantly lower compared to its periphery and to ordinary oxide precipitate [87, 91]. Although TEM-studies failed to reveal the type of these defects (the sign of the crystal lattice imperfection) due the low oxygen content and the size of detectable defects compared to theoretically predicted void sizes in silicon [6], it was assumed that LST-defects are peculiar microvoids, which have a vacancy origin. This enabled to interpret all the defect types, identified by different techniques (A'-microdefects, IR LSTD, FPD, COPs), as a single type of defects identical to D-microdefects in FZ-Si crystals. Since according to [50] D-microdefects were erroneously defined as vacancy-type defects, assumptions [88, 91] qualified these defects as microvoids formed in a result of homogeneous nucleation [53, 81, 90, 92].

At the same time, detection of dislocation loops and interstitial-type clusters in CZ-Si crystals [84], taking into account the results of the IR LSTD study by sectional topography with synchrotron radiation, enabled the authors of [73, 93, 94] to conclude that these defects have interstitial origin. In [73] it was suggested that joint agglomeration of silicon and carbon self-interstitials, whose presence was detected in IR LSTD [72], should play a more important role than oxygen precipitation in the process of grown-in microdefects formation. Similar results were obtained in [74], where it was shown that OSF-rings are formed as per heterogeneous mechanism under simultaneous oxygen precipitation and agglomeration of silicon self-interstitials with atoms of ‘non-oxygen impurity’. The results obtained in [95] should also be noted, as microdefects in CZ-Si crystals were detected using the diffuse X-ray scattering method, and the authors concluded that A'-microdefects are interstitial by nature. In addition, vacancy-type defects were detected in crystal areas with interstitial-type defects [95].

The process of COPs and OPPD formation in a growing crystal with a diameter of 150 mm was investigated by direct thermocouple temperature measurement on the growing crystal axis as a function of change in distance to the crystallization front [96]. It is established that nucleation of

defects and growth of their sizes proceed in a narrow temperature range of 1343...1373K during the crystal cooling. The oxide film growth on the walls of COPs lying in the {111} planes was observed in the same range. The growing film thickness reached a maximum value of 0.015 μm at a temperature of 1343 K. It was also found that the activation energy of the oxide formation process resembles the activation energy of the oxygen atoms diffusion in silicon. This led to the conclusion that the oxide film growth rate is limited by the oxygen diffusion. On the basis of the obtained results, the authors of [96] propose the following qualitative model of the two-stage defect formation process. On the first stage, vacancy complexes grow rapidly in the cooling process in the temperature range of 1373...1343 K. It is assumed that this process, which takes place in a narrow temperature range, is due to the rapid agglomeration of vacancies during the crystal cooling. On the second stage, the oxide film grows on the inner side of the complex in the range of 1373...1173 K.

The presence of such vacancy-type defects in the initial silicon wafers adversely affects MOS devices since the defect linear size (0.1...1.0 μm) is commensurate with the size of VLSI elements, and also due to typical non-smooth octahedral shape of defects [87, 96]. Therefore, the problem of material defect structure control arises either at the crystal growth stage or at the stage of the device manufacturing. The second variant is economically correct, since the change in typical defect structure is associated with lower growth rates, which significantly increases the cost of crystals, or with an axial temperature gradient at the crystallization front uniformly distributed and controlled along the whole length of the growing single crystal, which is a very complicated technical task. It is possible to obtain single crystals with growth rates significantly exceeding the standard methods used in CZ-Si production technology, which allows to significantly reduce the size of the vacancy clusters due to the high speed passing of the crystal through the temperature range of vacancy complex formation and growth (1373...1343 K). Furthermore, high-temperature treatment of the wafer surface in an atmosphere of hydrogen allows to smooth undesirable surface pits or to eliminate them completely [89].

The perspective of growing crystals of diameters $\geq$ 400 mm with structural characteristics similar to crystals of a diameter up to 200 mm shows [53] that the necessity to reduce the growth rate (for example, up to 0.55 mm/min for a diameter of 300 mm, which makes half of value required for the diameter of 200 mm) below the critical rate to limit thermal stresses in the crystal makes the task to obtain ingots without OSF-ring rather complicated. Increase of cooling duration for large-diameter crystals in the growing process, and, therefore, increase of their

holding at temperatures of nucleation center formation of oxidation-induced stacking faults cause significant density increase. According to the data on the axial temperature distribution dependency upon time, cooling duration for crystals with diameters of 150 mm, 200 mm, and 300 mm at 1273 K – 1173 K makes 80 min, 105 min, and 165 min, respectively [53].

1.3. Experiments with impurity kinetics of grown-in microdefects formation

The complexity of solving the problem of defect formation in dislocation-free silicon single crystals is related to the following:

- Difficulty in fully accounting for the interaction of a large number of reacting system components (vacancies, silicon interstitials, oxygen, carbon, alloying impurities, iron, hydrogen, nitrogen, etc.).
- A critical influence of thermal conditions of crystal growth on the interaction of point defects, which in turn depend on the diameter of the growing crystal and the method of its growth.
- The exceptional complexity of observing such small dimensions and lattice distortions given by clusters of point defects that require the use of direct methods of investigation with the possibility of analyzing the sign of the deformation of the crystal lattice.

To solve this problem, it was necessary to do the following:

- Study the patterns of distribution and individual characteristics (size, shape, sign of crystal lattice deformation) of grown-in microdefects in FZ-Si and CZ-Si crystals obtained under different thermal conditions (for example, when the crystal growth rate changes from additional thermal treatments in the crystal growth process, with a change in crystal diameter during growth, etc.). This comprehensive research should be based on the use of small-scale FZ-Si (30 mm in diameter) and CZ-Si (50 mm in diameter) single crystals, since the entire spectrum of grown-in microdefects is observed in such crystals.
- Use of the most informative of research methods: selective etching (monitoring of distribution patterns of grown-in microdefects), transmission electron microscopy (monitoring of individual characteristics of grown-in microdefects), which has a resolving power from 2 nm, X-ray topography, etc.

- Study of the grown-in microdefects transformation, both in the process of crystal growth, and in a result of various types of processing (thermal treatments, epitaxy, ion implantation).

Most of such experiments with grown-in microdefects were carried out at the end of the twentieth century. Since the middle of the 1990s, theoretical investigation of grown-in microdefects began its rapid development on the basis of qualitative physical models of their formation. Since any model should be based on the experimental results, we briefly review the main results of experiments with each type of grown-in microdefects.

(I+V)-Microdefects. These are interstitial- (I) and vacancy-type (V) microdefects coexisting in the same areas of the crystal. They were first discovered during experiments with X-ray topography coupled with subsequent copper decoration [50]. However, the small size of defects did not allow to determine their physical nature, thus, the authors [50] erroneously assumed that only vacancy-type defects were detected At the same time, it was suggested in [34, 97] that simultaneous coexistence of vacancy- and interstitial-type defects is possible under certain temperature conditions. On this basis, the physical nature of defects detected in [50] was studied in detail in [21, 51] using TEM and it was shown that they really are (I+V)-microdefects.

(I+V)-microdefects are formed in FZ-Si crystals with a diameter of 30 mm at growth rates between 6.0...6.5 mm/min, and in CZ-Si crystals with a diameter of 50 mm at growth rates between 1.5...1.8 mm/min [12, 21, 23, 51]. In case of interstitial-type microdefects presence (of A-, B-, and D(C)-type) selective etching does not reveal microdefects distribution patterns in those areas of the crystal where (I+V)-microdefects are observed (for example, inside the D(C)-microdefects ring). If annular distribution of D(C)-microdefects vanishes, (I+V)-microdefects are observed as uniform distribution in the central part of the crystal (Fig. 1.4c). It was determined that at certain growth rates of a FZ-Si crystal 30 mm in diameter (V_g = 7.0 mm/min), the ratio of vacancy and interstitial-type defects is 1:4 [51]. If the growth rate rises, the number of vacancy-type microdefects in the total number of defects increases. When growing conditions are most close to the initial stages of defect formation (high growth rates or in experiments with crystal quenching in the process of growth), both vacancy- and interstitial-type defects coexist in approximately equal concentrations [21]. We have shown that the (I+V)-microdefects are the primary oxygen-vacancy and carbon-interstitial agglomerates formed on the impurity centers and they are the initial stage

of subsequent defect structure transformation of FZ-Si and CZ-Si crystals [12, 23, 45]. The coexistence of vacancy- and interstitial-type microdefects suggests that recombination of IPDs near the crystallization front is absent. Background oxygen and carbon impurities serve as the nucleation centers of (I+V)-microdefects, their influence determines the mechanism of microdefects subsequent growth and transformation. Compression areas near oxygen interstitials are the nucleation centers of oxygen-vacancy aggregates, excessive vacancies and other oxygen interstitials rush to these areas. Stretching areas around the substituting carbon atoms are the nucleation centers of carbon-interstitial aggregates, excessive silicon and oxygen self-interstitials rush to these areas [13, 52].

D(C)-Microdefects. For the first time, they were detected in FZ-Si (crystal diameter 30 mm) at growth rates exceeding 4.5 mm/min as uniform distribution and could be identified as dim regions after selective etching [46]. Initially, these defects were classified as D- and C-microdefects, based on differences in their distribution: uniformly distributed D-microdefects were concentrated in the central part of the crystal in the form of a channel, whereas C-microdefects in the form of circles and rings of irregular shape were located at the most extensively cooled parts of the crystal [46]. Standard channel distribution (Fig.1.4a) is typical for the impurity distribution in case of face effect occurrence. Comparing macro-patterns of the microdefects uniform distribution in Fig. 1.4a and Fig. 1.4c shows that the channel distribution of D-microdefects has sharp and clear boundaries, while a similar distribution of (I+V)-microdefects is vague and unclear. Carbon concentration determined by infrared absorption spectrums makes $N_c = 4.4 \cdot 10^{16}$ cm^{-3} in the channel area and $N_c = 2 \cdot 10^{16}$ cm^{-3} outside the channel. Such effect of the carbon impurity indicates a heterogeneous nature of microdefects nucleation. FZ-Si single crystal was obtained in vacuum at V_g = 6.0 mm/min. Channel distribution is typical for crystals with V_g = (5…6.0) mm/min. At higher growth rates (V_g > 6.0 mm/min), the channel may break in the crystal center and turn into annular distribution along a section perpendicular to the growth axis [12, 13, 45]. Fig. 1.5 presents a generalized distribution scheme of D-microdefects as a function of the growth rate. As the crystal growth rate raises, the inner area of the annular distribution increases (Fig. 1.5, Fig. 1.6), and at V_g ≥ 8.0 mm/min the annular distribution of D-microdefects vanishes.

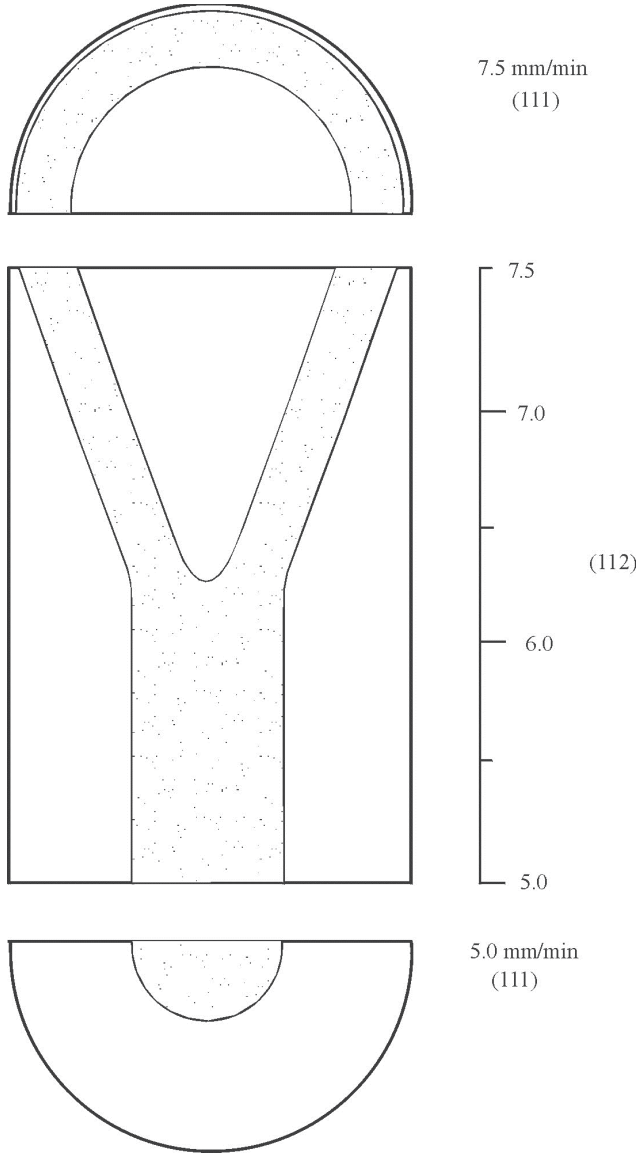

Fig. 1.5. Schematic representation of the divergence of the channel distribution of D-microdefects into the annular with increasing growth rate in FZ-Si single crystals (diameter 30 mm)

These defects were first detected in CZ-Si in [47, 48]. The first TEM-studies determined the size of the defects (~ 10 nm) and their concentration (~ 10^{13}…10^{14} cm^{-3}) [38]. Similar data were obtained after CZ-Si investigation by neutron scattering, which has a resolving power comparable to the TEM [98], and in the course of radiation experiments [99]. Defects of 6...8 nm in size, lying in the {100} planes with sides along the directions [110] were detected [98].

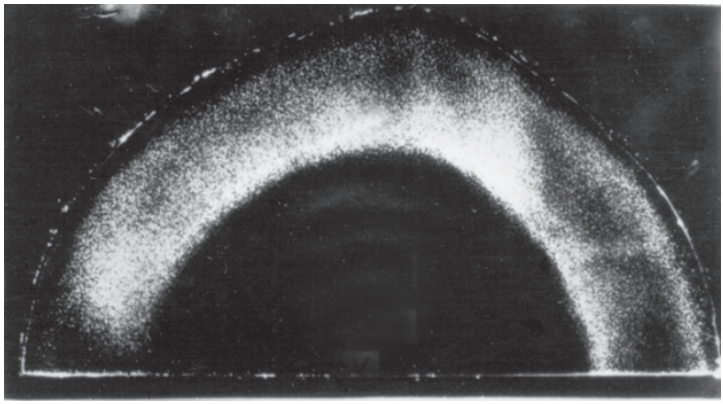

Fig. 1.6. The annular distribution of D-microdefects in the (111) plane of FZ-Si crystals (V_g = 7.5 mm/min)

However, as already mentioned above, it was difficult to detect physical nature of D(C)-microdefects, because in addition to the erroneous assertion on vacancy-type defect detection the author mistakenly named these defects as D-microdefects in [50]. The results of [50] gave rise to a discussion about the microdefect origin. Based on X-ray topography and decoration in combination with selective etching, and on different types of defect distribution, the D(C)-microdefects were divided into subclasses. It was assumed that some of them are interstitial- and others are vacancy-type defects [75-78]. Taking into account theoretical investigation [6] and experimental results [50], a number of investigators stood for the assertion of the vacancy origin of D(C)-microdefects [40, 65, 66, 100].

TEM showed that all observed D-microdefects and C-microdefects cause compression deformation in the crystal, i.e., they are interstitial-type defects (Fig. 1.7) [21, 23, 52]. The sizes of these defects are in the range of (3...10) nm, and their concentration is about ~$1 \cdot 10^{13}$ cm^{-3}. It was shown

that as the crystal growth rate decreases, the size of D-microdefects increases [21, 52].

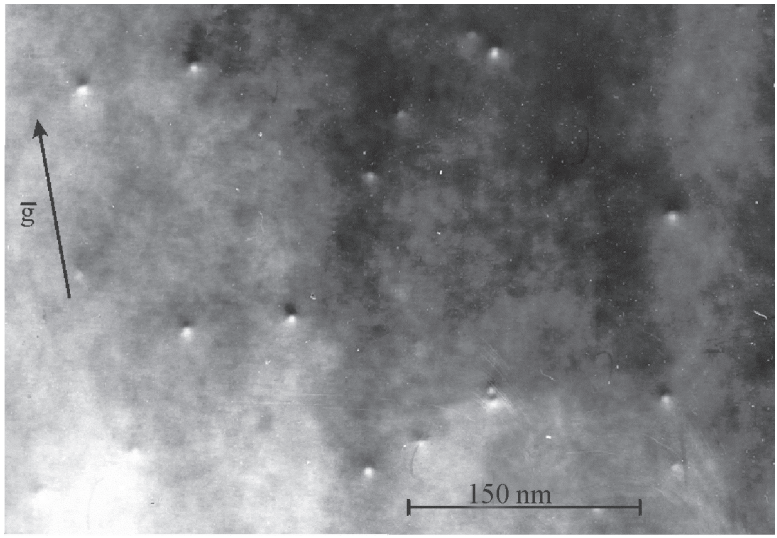

Fig. 1.7. TEM-image of D-microdefects, dark field, $s = 0$, $\bar{g} = (\bar{2}20)$

These experimental results were obtained by means of TEM for amplitude contrast by analyzing the diffraction image using black-and-white contrast and 2.5D methods. However, these methods have some drawbacks and limitations, related both to the inaccurate knowledge of the defect occurrence depth, and to the very small size of the defects investigated. Therefore, investigation of D-microdefects by means of independent TEM-method of direct crystal lattice resolution are of special value [49]. Detailed information about the delicate structure of D-microdefects was obtained by means of this method based on phase contrast and forming a crystal lattice image with a resolution of ~ 0.2 nm. Undoped FZ-Si single crystals of n-type with diameter 28…30 mm with ρ = 2000 Ωm·cm, grown in vacuum at V_g = 6 mm/min were investigated. The concentration of oxygen and carbon was determined from the IR absorption spectra and made: oxygen concentration < $1 \cdot 10^{16}$ cm^{-3} and carbon concentration – $1.6 \cdot 10^{16}$ cm^{-3}. The authors of [49] observed two types of TEM-images of D-microdefects: with a regular

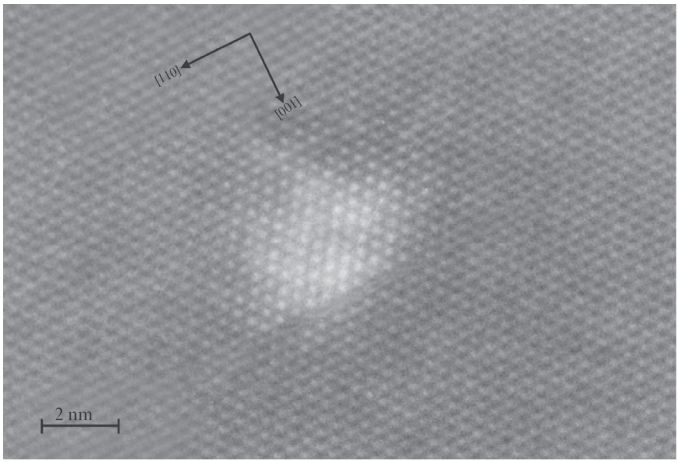

a)

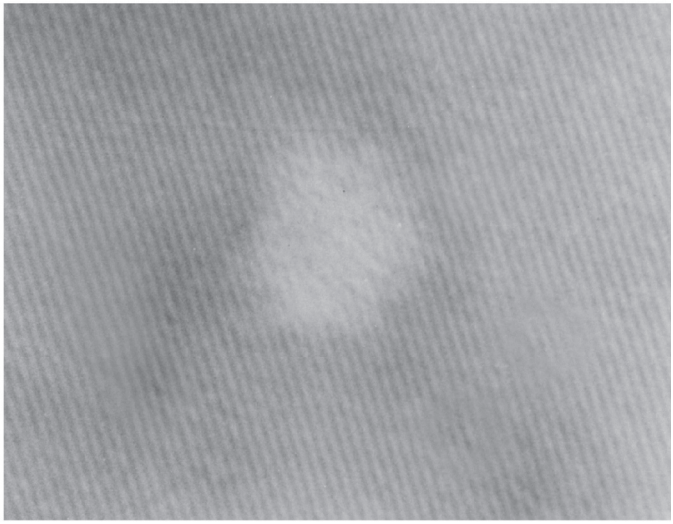

b)

Fig. 1.8. TEM-images (direct resolution) of D-microdefects in FZ-Si:
(a) periodic structure; (b) amorphous structure

(periodic) and irregular (amorphous) structure (Fig. 1.8). It was found that these defects cause compression deformation in the crystal lattice of silicon, i.e., they are interstitial-type defects. It is shown that they are small precipitates of SiO_2 and SiC [13, 23, 52]. Hence, two independent TEM methods (of amplitude contrast and direct lattice resolution) established the interstitial origin and two possible forms of D-microdefects detected in crystals.

Detailed TEM-studies showed that D-microdefects are entirely identical to C-microdefects n FZ-Si [12, 13, 21, 49] and CZ-Si [23, 101] as far as contrast of TEM images, the sign of lattice imperfection and sizes are concerned. Thus, these are interstitial-type defects. Also, the interstitial origin of these microdefects was confirmed when studying their behavior during radiation experiments [99].

Investigation statistics of C- and D-microdefects allows us to conclude that C-microdefects are a particular form of distribution of D-microdefects [101]. Furthermore, the location and distribution nature of C- and D-microdefects indicate that they are a specific stage preceding the formation of A- and B-microdefects [13, 52].

B-Microdefects. They are the next stage in the development of D(C)-microdefects. Essentially, it should be said that the D(C)-microdefects are small uniformly distributed B-microdefects, or that B-microdefects are banded distribution of large D(C)-microdefects [52].

B-microdefects were first observed in FZ-Si as etch pits with a flat bottom in the form of regular triangles with sides in the [110] direction on the (111) plane [14, 102, 103]. The two groups of etch pits were identified: 1) large, with a lower concentration, 2) small, with a higher concentration. The second group was classified as B-microdefects (B-clusters) [15, 16, 43]. Taking into account that the macro-pattern of etch pit distribution along a single crystal cross-section resembled vortices, these microdefects were called swirl defects [28]. It was found that banded distribution of B-microdefects is observed in the crystal longitudinal section at $V_g \leq 4.5$ mm/min (crystal diameter of 30 mm) [104].

These defects were first observed in CZ-Si in [47, 48]. Banded distribution of B-microdefects is observed in undoped (or slightly doped) crystals with a diameter of 50 mm grown at $V_g \leq 1.0$ mm/min. At $V_g \sim 1.0$ mm/min B-microdefects are formed in concentrations comparable to their concentration in silicon single crystals obtained by the floating zone melting method. At $V_g \geq 2.0$ mm/min the formation of B-microdefects is

completely suppressed, and the presence of uniformly distributed D(C)-microdefects is observed [56].

The average concentration of B-microdefects in the crystal body is ~10^9…10^{10} cm^{-3} [43]. Detailed TEM-studies showed the interstitial origin of B-microdefects (Fig. 1.9) [13, 27, 45, 52].

The sizes of these defects are in the range of 15...50 nm. As the crystal growth rate raises, the size of B-microdefects decreases [21, 52]. The geometric shape of some B-microdefects is revealed in case of deviation from the image dynamic conditions. In such a case they look like plates of a square and a rhomboid shape in the plane projection {111} (Fig. 1.10).

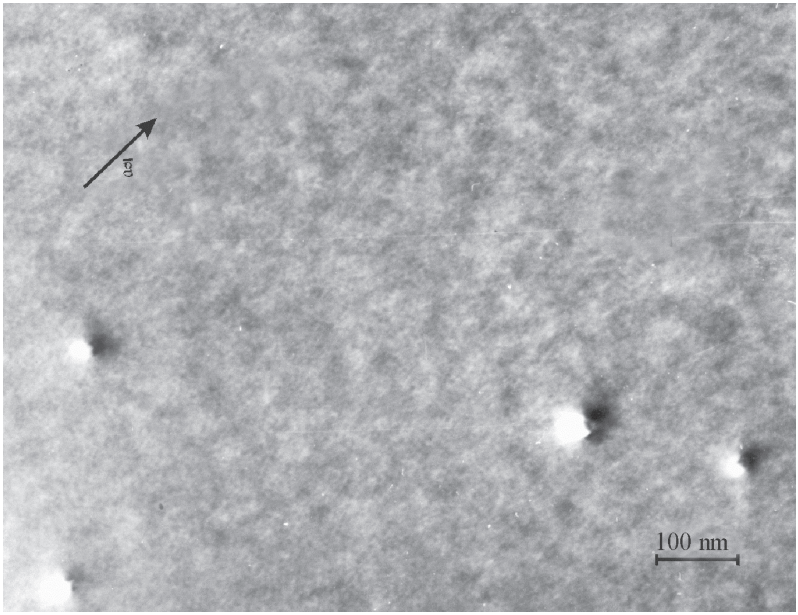

Fig. 1.9. TEM-image of B-microdefects, light field, $\bar{g} = (\bar{2}20)$, $s > 0$

Since the diagonals of the rhombus or the sides of the square are parallel to the diffraction vector $\bar{g} = (220)$, it can be said that such defects have a faceting in the [100] or [110] directions, lying in {100} planes, and form rhombuses and squares in the plane projection {111}. Similar planar agglomerations in {100} planes with faceting along the [110] directions were observed earlier by different authors in CZ-Si single crystals [38] and were identified by low-energy electron spectroscopy as oxygen precipitates [105]. With the help of high-resolution electron

microscopy, it was shown [38] that such agglomerations in the {100} planes are interstitial-type. It was determined that the structure of such clusters is amorphous and they are an amorphous phase of SiO2 [38]. The formation and growth of such flat agglomerates as a result of the oxygen precipitation causes a strong compression of the silicon lattice, and the removal of this compression leads to prismatic extrusion of interstitial dislocation loops [105-107]. It should be taken into account that in the experiments on establishing the sign of crystal lattice imperfection FZ-Si single crystals with oxygen and carbon content of less than $5 \cdot 10^{15}$ cm^{-3} were investigated, i.e., so-called oxygen-free crystals [21]. Nevertheless, some of the B-microdefects have the correct geometric shape (Fig. 1.11), which indicates the heterogeneous nature of grown-in microdefects nucleation.

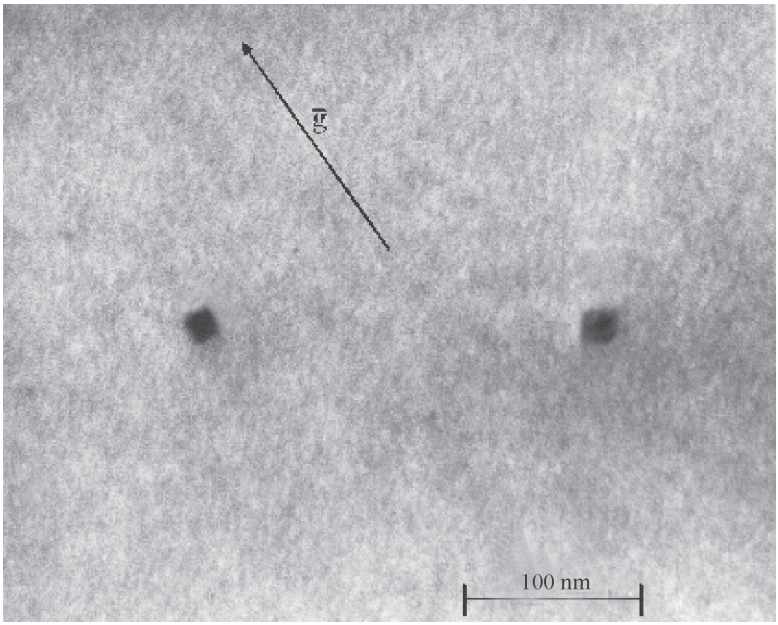

Fig. 1.10. TEM-image of B-microdefects with square and rhomboid shapes, dark field, $\bar{g} = (\bar{2}02)$

A-Microdefects. A-microdefects were first observed simultaneously with B-microdefects in FZ-Si in the form of the same etch pits with a flat bottom [14, 102, 103]. Large etch pits with a lower concentration were

classified as A-microdefects (A-clusters) [15, 16, 43]. They were also called swirl defects, since the macro-pattern of their distribution along the crystal cross-section transpired in the form of a discontinuous spiral [28]. Banded distribution of typical A-microdefects (Fig. 1.2) is observed at crystal growth rates V_g = 1…3.5 mm/min min and uniform distribution thereof is observed at V_g < 1.0 mm/min [104]. As the growth rate decreases, the A-microdefects increase in size, their concentration decreases and they are evenly distributed in the crystal body. The distance between the microdefect bands is usually associated with the distribution of impurities and can be determined by the formula: $h - V_g/w$ (where w is a single crystal rotation rate).

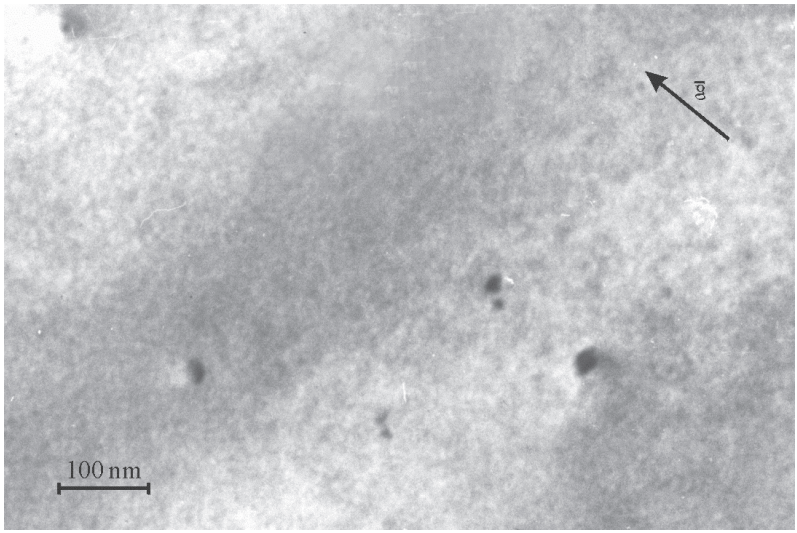

Fig. 1.11. TEM-image of B-microdefects with various forms, dark field, $\bar{g} = (\bar{2}20)$

These defects were first observed in CZ-Si in [47, 48] as well. Uniform distribution of A-microdefects is observed in undoped or slightly doped monocrystals with a diameter of 50 mm grown at $V_g \leq 1.0$ mm/min. At V_g ~ 1.0 mm/min A-microdefects are formed in concentrations comparable to their concentration in silicon single crystals obtained by the floating zone

melting method. At $V_g \geq 2.0$ mm/min the formation of A- and B-microdefects is completely suppressed, and the presence of uniformly distributed D(C)-microdefects is observed [56]. The critical rate (the rate of A-microdefects disappearance) ~ 2.0 mm/min) decreases as the crystal diameter increases and as the axial temperature gradient decreases [47]. The axial temperature gradient near the crystallization front decreases as the growth rate increases and as the crystal diameter increases [3].

The average concentration of A-microdefects in the crystal is ~ 10^6 cm^{-3} [43, 104]. Experiments on crystal quenching have shown that B-microdefects are formed earlier than A-microdefects [16, 19].

The distribution of A-microdefects depends on the amplitude of fluctuations in the crystal microscopic growth rate: if the microscopic growth rate varies significantly, the banded distribution of microdefects takes place, otherwise the uniform distribution takes place [57]. In [19, 20] the swirl distribution of A- and B-microdefects was investigated. It was shown that microdefects are located along impurity growth bands, which, in turn, reflect the shape of the crystallization front. The minimum spacing between the spiral bands corresponds to the ratio of the crystal growth rate to its rotation speed. As the crystal growth rate decreases, the deflection of the microdefect bands increases due to increase of the temperature gradient radial component [20]. Density of microdefects in the band is higher than at the periphery, which is caused by the fact that the temperature gradient radial component in the center of the crystal is always higher than at the periphery at the observed crystallization surface curvature.[20]. The distribution of B-microdefects (small etch pits) is often superimposed on the distribution of A-microdefects in the crystal body. The maximum size of B-microdefects is observed in areas where there are no A-microdefects. Both types of microdefects can be found in the central part and are usually absent at the side crystal surface. B-microdefects are located closer to the crystal surface than A-microdefects. The crystal surface can serve as a drain for intrinsic point defects, so, as a rule, the near-surface areas, contain few microdefects.

Detailed TEM-studies of A-microdefects showed that they are individual dislocation loops with a size of 1...5 μm or clusters of such interstitial-type loops (Fig. 1.12) [21, 26, 27, 42]. Analysis of loop configurations showed that A-microdefects constitute interstitial-type dislocation loops with Burgers vector $\bar{b} = 1/2[110]$ lying in planes {110} and {111} [21, 27, 42]. Such complex interstitial-type dislocation loops decorated with background impurities and corresponding to A-microdefects, were also observed in CZ-Si single crystals [47]. A-microdefects can arise

under the action of two different mechanisms: condensation of silicon self-interstitials and generation of dislocation loops caused by the elastic stress field around precipitates.

As the size of the A-microdefects increases to a certain limit (~ 40 μm at V_g = 1.0 mm/min) dislocations arise in silicon single crystals [19, 24, 25]. A-microdefects could act as sources of dislocation nucleation, which is due to the Frank-Read mechanism action, under the influence of compressive stresses in the center of the crystal resulting from the combined effect of radial and axial temperature gradients [67]. Appearance of dislocations is affected by the dimensions, relative disposition of microdefects and distances between them [26].

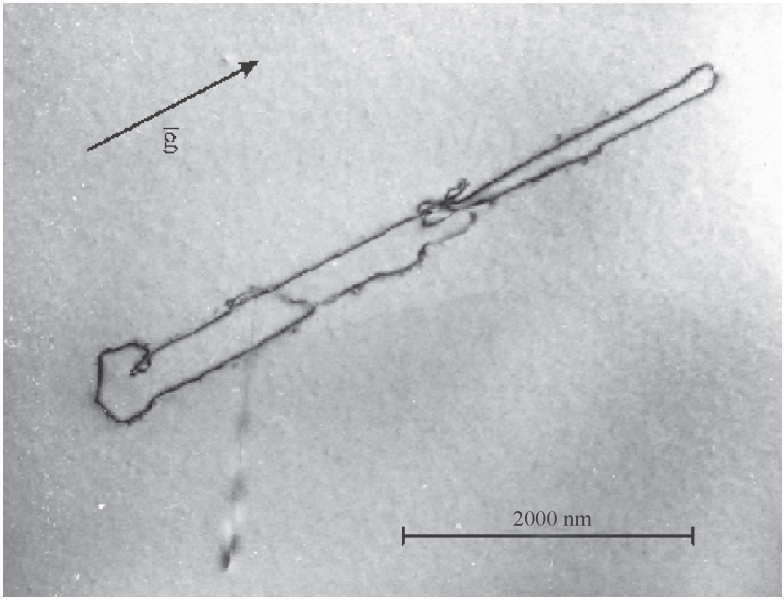

Fig. 1.12. TEM-image of A-microdefect in the form of overgrown dislocation loops, light field, $\bar{g} = (0\bar{2}2)$

Initial defect ensemble transformation. The foregoing data are based on a number of experiments we conducted [12, 13, 23, 45, 101, 104]. Statistical processing of experimental results enabled us to make a schematic representation of the microdefect distribution in FZ-Si and CZ-Si with a change under the changing crystal growth rate (Fig. 1.13) [52].

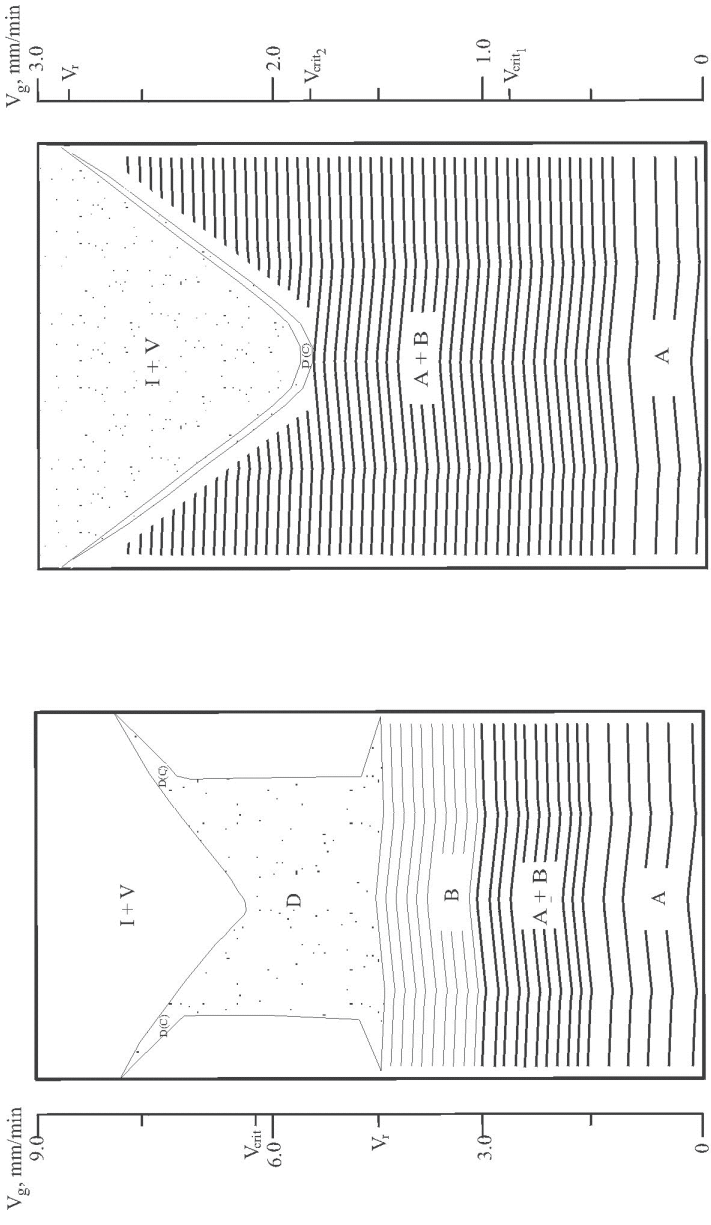

Fig. 1.13. Scheme of formation and transformation of microdefects in silicon single crystals (plane (111)): a) crystal FZ-Si, diameter of 30 mm; b) crystal CZ-Si, diameter of 50 mm

With gradual increase of growth rate, one type of microdefects in FZ-Si crystals is replaced progressively with the other type. Banded distribution of large A-microdefects is replaced by banded distribution of small B-microdefects. After the rate V_r reaches a certain value (at which the remelting phenomenon is suppressed) B-microdefects are replaced with uniform D-microdefect distribution.

The value V_r for FZ-Si is ~ 4.5 mm/min [12]. Above a certain critical growth rate V_{crit}, the vacancy-type microdefects begin to occur in crystals, while before V_{crit} only interstitial-type microdefects could be detected. If $V_g > V_r$ interstitial-type D-microdefects usually converge in a channel, which afterwards at $V_g \geq V_{crit}$ begins to diverge towards the periphery of the crystal. If the crystal growth rate continues to rise, the ring size diminishes (in plane (111)), and at V_g ~ 8…9.0 mm/min the ring of interstitial-type microdefects disappears, while vacancy-type and interstitial-type microdefects ((I + V)-microdefects) coexist within the whole crystal body in approximately equal concentrations.

Thus, as the crystal growth rate decreases, the interstitial-type microdefects are continuously transformed. Above V_{crit} = 6…6.5 mm/min vacancy-type microdefects occur and their concentration continues to increase up to V_g ~ 9.0 mm/min, when both concentrations of vacancy-type and interstitial-type microdefects become approximately equal [52].

When CZ-Si 50-mm crystals are grown, uniform microdefect distribution is typical for 1.5 mm/min < V_g < 2.0 mm/min. However, according to the theoretical model of grown-in microdefects formation [6], interstitial-type A- and B-swirls should occur only at $V_g < V_{crit1}$, where V_{crit1} is defined as a theoretical rate characterized by the vacancy-type microdefects occurrence and the interstitial-type microdefects vanish [100]. According to our estimation for CZ-Si crystals with a diameter of 50 mm, this rate will be in the range 0.8...1.2 mm/min [23]. Fig. 1.14a shows the distribution of microdefects in the plane (112) of a CZ-Si crystal grown at rates from 1.8 mm/min to 2.8 mm/min. The V-shaped defect distribution is a uniformly distributed D(C)-microdefects which have concentrations from 10^{13} cm^{-3} to 10^{14} cm^{-3} and sizes from 4 nm to 12 nm

(Fig. 1.14b). (I+V)-microdefects are observed inside the V-shaped defect distribution (Fig. 1.14c).

Experimental results enable us to state that there is no area where only vacancy-type growth occurs in FZ-Si and CZ-Si crystals. Hence, the type of growth characterized by vacancy-type microdefects should be called as vacancy-interstitial-type of crystal growth. The boundary of the vacancy-type microdefects occurrence (vanish) shall be determined based on the evaluation of real thermal growth conditions, i.e., for CZ-Si $V_{critmin} = V_{crit2}$.

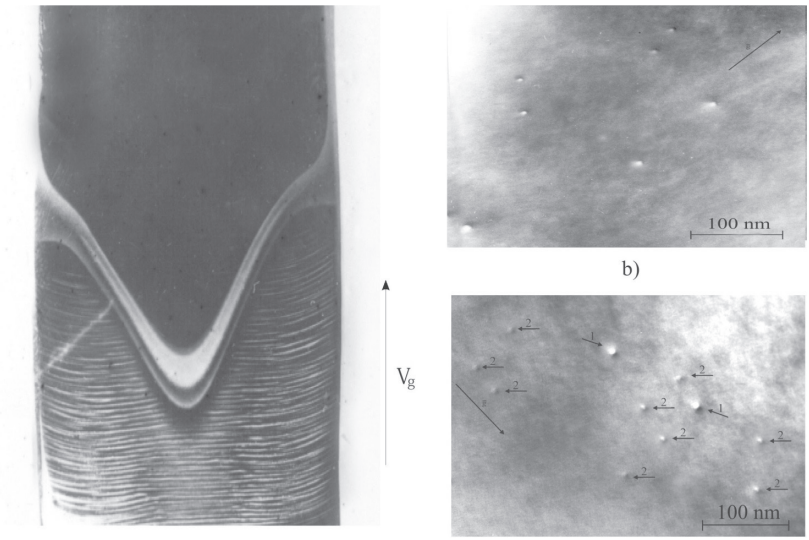

Fig. 1.14. D(C)-microdefects and (I+V)-microdefects of CZ-Si crystals (diameter of 50 mm; V_g=1.8…3.0 mm/min): (a) selective etching, plane (112);
(b) TEM-image of D(C)-microdefects in V-shaped distribution, dark field, $\overline{g} = (\overline{2}20), s = 0$
(c) TEM-image of (I+V)-microdefects inside the V-shaped distribution, ((1) V-defects; (2) I-defects), dark field, $\overline{g} = (\overline{2}20), s = 0$

The difference in distribution geometry of D(C)-microdefects (channel and ring in FZ-Si; only ring in CZ-Si) is defined by remelting phenomenon. In the process of growing crystals are subject to local melting caused by temperature instability due to thermal convection [9]. If this phenomenon is not suppressed, a banded distribution of microdefects and impurities appears in the crystal.

If the growth rate in the Czochralski method is increased to 2.7 mm/min, the remelting phenomenon can be minimized, and the banded distribution of microdefects turns into uniform, however, the banded distribution of impurities remains [33]. The change in thermal growth conditions causes the suppression of remelting phenomenon occurs in FZ-Si interstitial-type growth and in CZ-Si vacancy-interstitial-type growth [101].

Thus, the transformation of the initial defect structure during growth of the dislocation-free single FZ-Si and CZ-Si crystals follows the pattern:(I+V)-microdefects → D-microdefects → B-microdefects → A-microdefects [13, 52].

When the crystal is grown at $V_g < V_{crit}$ (FZ-Si) or $V_g < V_{crit2}$ (CZ-Si) and outside the D(C)-microdefect ring, the interstitial-type I-microdefects continue to grow and transform into interstitial-type D(C)-microdefects. Due to absorption of oxygen atoms vacancy-type V-microdefects change their sign of imperfection to the interstitial-type and transform into interstitial-type D(C)-microdefects [12, 45, 108].

At the same time, the transition between the vacancy-interstitial type of crystal growth and the interstitial type of growth does not occur sharply, but takes some time. For example, the authors of [109] studied the areas of FZ-Si and CZ-Si crystals obtained in the interstitial-type growth (low crystal growth rates), which is characterized by the formation of interstitial-type D(C)- and B-microdefects. For TEM-studies of D(C)- and B-microdefects ca. five hundred CZ-Si samples and one thousand FZ-Si samples were used (Table 1.1)

Table 1.1. The determination of the ratio between interstitial and vacancy microdefects in the interstitial growth regime [109]

Crystal type	Ingot number	Growth rate, mm/min	Number of samples	Interstitial defects, %	Vacancy defects, %	Defect type
FZ-Si	1	4.0	198	97.8	2.2	B
FZ-Si	2	6.0	206	95.8	4.2	D
FZ-Si	3	6.0	186	96.1	3.9	D
FZ-Si	4	5.0	221	97.5	2.5	D
FZ-Si	5	3.0	201	98.0	2.0	D
CZ-Si	1	1.0	242	99.2	0.8	B
CZ-Si	2	1.5	237	98.5	1.5	B

One or two vacancy-type defects occur on one hundred of interstitial-type defects in samples with B-microdefects. At the same time three-four vacancy-type defects occur on one hundred of interstitial-type defects in samples with D(C)-microdefects. Vacancy-type D(C)- and B-microdefects were similar to respective interstitial-type microdefects in sizes and image contrast [109].

In [95] studied diffuse X-ray scattering by grown-in microdefects in CZ-Si crystals (V_g = 0.5…1.0 mm/min, diameter 100 mm, oxygen concentration ~ 10^{18} cm^{-3}, boron concentration ~ 10^{15} cm^{-3}) with different thermal prehistory determined by growth conditions using a three-crystal diffractometer. The change in the crystal lattice associated with the grown-in microdefects formation and their sign of power (positive for interstitial-type grown-in microdefects and negative for vacancy-type grown-in microdefects) depends on the origin of observed defects. The X-ray diffuse scattering method by defects enables to evaluate not only the sign of power of grown-in microdefects but also to detect the simultaneous presence of grown-in microdefects with different signs of power, which is very effective for studying grown-in microdefects even if they are contained in crystals at low concentrations.

The authors of [95] observed defects both with positive and negative power in crystals grown in interstitial-type growth. It is established that dominant-type defects are accompanied by defects with a power of the opposite sign in the investigated crystal area [95]. Unfortunately, the authors of [95] did not report quantitative measurements of the observed defects.

The grown-in microdefects in CZ-Si single crystals were studied by X-ray topography on the basis of the Bormann effect [110]. Based on the theory of the Bormann contrast of intensity of crystal lattice defects with slowly varying deformation fields, intensity signals of B-microdefects were investigated. The principal possibility of recording B-microdefects by topography based on the Borrmann effect was shown [110]. The possibility of unambiguous determination of the matrix imperfection sign, i.e., the origin of B-microdefects, by the X-ray topography method based on the Borrmann effect is theoretically shown.

Experiments showed that the detected B-microdefects are coherent inclusions of the second phase (SiO_2 and SiC). Dislocation loops (A-microdefects) were not observed by the authors of [110]. Along with defects of predominantly interstitial origin, defects with an opposite black-and-white image contrast (vacancy-type B-microdefects) were observed on topograms. It has been experimentally established that 99% of B-microdefects are interstitial-type defects and 1% of them are vacancy-type defects [110].

Three independent investigation methods (TEM, amplitude contrast method [109], diffuse X-ray scattering [95], X-ray topography based on the Bormann effect [110]) established that vacancy-type D(C)- and B-microdefects are formed in the course of interstitial-type growth of FZ-Si and CZ-Si crystals. The concentration of such defects is at least two orders of magnitude lower than the concentration of interstitial-type D(C)- and B-microdefects. The formation of other vacancy-type defects remains a discussion. The existence of vacancy-type dislocation loops (vacancy-type A-microdefects) and vacancy-type tetrahedra of stacking faults was not observed experimentally. Furthermore, it was suggested that the formation of vacancy-type A-microdefects is unfavorable from the viewpoint of thermodynamics [111]. To obtain a vacancy-type tetrahedron of the packing defect it is necessary to cut out the tetrahedron of the lattice, to remove the atomic layer from one of its faces, and then to put back the reduced tetrahedron symmetrically. Such a tetrahedron is energetically more favorable than a dislocation loop [112]. However, it was shown the formation of voids is energetically much more favorable than the vacancy-type tetrahedra of stacking faults for a diamond-type lattice [112].

Microdefects of large-scale crystals. As already mentioned, an increase in the silicon single crystal diameter leads to a significant change in the temperature growth conditions. Therefore, the role of vacancy condensation increases in the process of silicon ingot cooling. In the past decade different researchers observed so-called microvoids in the vacancy-interstitial-type growth in large-diameter silicon crystals that further cause

the degradation of semiconductor devices [113, 114]. Furthermore, dislocation-free growth is possible in a limited range of crystal growth rates. As a result, the spectrum of grown-in microdefects and the pattern of their distribution in the crystal are considerably narrowed. Under these conditions, a ring of D(C)-microdefects (often mistakenly defined as an OSF-ring), A-microdefects (L-pits) outside the D(C)-microdefect ring and (I+V)-microdefects inside the D(C)-microdefect ring may exist in the crystal (Fig. 1.15).

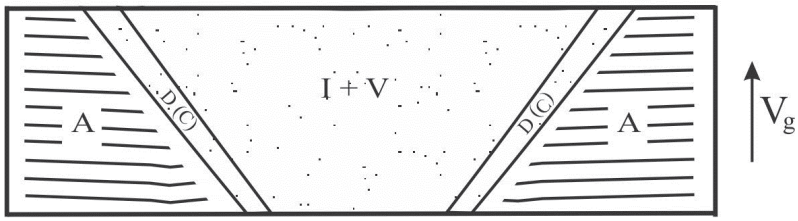

Fig. 1.15. Schematic image of the defect structure of large-scale silicon single crystals with a change in the growth rate

In our opinion, the OSF-ring in FZ-Si crystals is generated on the microprecipitates of the annular distribution of D(C)-microdefects after thermal treatments (Fig. 1.13). Uniform distribution of the (I+V)-microdefects over the entire body is observed only in CZ-Si crystals with a diameter of 50 mm. In crystals with diameters more than 70 mm, such a distribution is not observed due to the appearance of a grown-in ring of D(C)-microdefects [101]. This statement is supported by the TEM results for defects observed in the area of grown-in microdefect ring [52]. It was found that only interstitial-type defects are observed near the ring, while vacancy-type defects are not detected [52]. Similar investigations inside the ring distribution reveal the presence of interstitial- and vacancy-type defects coexisting like in FZ-Si crystals.

The range of growth rates at which the annular distribution is observed, as shown in [53], is within the range 1...2 mm/min for CZ-Si crystals 80 mm in diameter and ~ 0.5...0.8 mm/min for CZ-Si crystals 300 mm in diameter. As a result of changes in the temperature growth conditions, D-microdefects in CZ-Si single crystals determined similarly to D-microdefects in FZ-Si crystals are observed only in the ring distribution. Most probably, the absence of a channel distribution of D-microdefects in CZ-Si crystals is due to the fact that $V_{crit} < V_r$. Such a ring of uniformly distributed D(C)-microdefects divides the area of banded distribution of

interstitial-type microdefects and the area of coexistence of (I+V)-microdefects, which is similar to FZ-Si crystals. The formation of the annular distribution of D-microdefects is due to the thermal growth conditions of silicon crystals and the plane protrusion (111) to the crystallization front (the facet effect). In particular, a change in thermal growth conditions is accompanied by a change in diameter contraction rate of the D-microdefect ring and a decrease of their growth rate: the lower the axial temperature gradient, the faster the diameter of the ring is reduced.

The classic theory of stacking fault formation states that they are nucleated on swirl-defects [115]. According to [115] the mechanism of stacking fault formation is as follows: (a) the heterogeneous nucleation of microdefects leads to the formation of silicon-impurity complexes; (b) complexes grow and collapse with the formation of a stacking fault surrounded by a locked dislocation with $\bar{b} = 1/3[111]$; (c) loops with a stacking fault are converted into prismatic loops by reaction $1/3[111]+1/6[11\bar{2}] \rightarrow 1/2[110]$, forming A-microdefects.

Ravi also suggested [115] that SiC microprecipitates may be responsible for stacking fault formation more than SiO_2 microprecipitates. This enables to explain the results of [74], where it is shown that defects in the are of the OSF-ring are microprecipitates of SiO_2 and Si + some 'non-oxygen impurity'. Experimental results indicate that SiC microprecipitates are the second type of microprecipitates [52]. The radial distribution of microdefects along the (111) plane confirms the identity of the mechanisms of microdefect transformation in both types of crystals from vacancy- and interstitial-type microdefects through large precipitates to dislocation loops.

Changes in thermal conditions of the crystal growth (in particular, the growth rate, axial and radial temperature gradients, diameter) enable to obtain a V-shaped or W-shaped distribution of the OSF-ring along the plane (112) [116]. For example, if the axial temperature gradient in the center of the crystal is greater than at the crystal surface near the crystallization front, it is possible to obtain the W-shaped distribution of the OSF-ring by decreasing the crystal growth rate [116].

As it was mentioned, we call defects in the OSF-ring area as '*D-microdefects in the ring distribution*', since they are identical to D-microdefects in the channel distribution of FZ-Si crystals [13]. At the same time, it is well known that the channel inhomogeneity in dislocation-free silicon single crystals is the main reason causing an inhomogeneous distribution of impurities along the cross-section of single crystals grown

in the [111] direction [9]. The channel inhomogeneity in single crystals is explained by the influence of the facet effect according to which a face (111) is developed on the crystallization front under certain conditions. Since this face grows in a more supercooled melt than its environment, the impurity concentration in the vicinity of the face is higher [9]. The channel inhomogeneity is observed at any form of the crystallization front but only there where (111) crystal face may protrude the surface. With the convex crystallization front we observe a core-type, growth axially developing, channel. When single crystals are grown with a wave-type crystallization front, we observe a core-type and tubular-type channels. Increase in size of a flat area of the crystallization front results in expanding a channel's width. A curvature decrease of the crystallization front leads to a wider central (core-type) channel and decreasing of a tubular-type channel diameter [117]. When the crystallization front is concaved in the crystal, the face effect looks like a ring on (111) plane periphery.

Interstitial-type dislocation loops are defects outside the D(C)-microdefect ring [116, 118]. Defects observed in CZ-Si crystals at $V_g < V_{crit2}$ (Fig. 1.13) are clusters of interstitial-type defects (based on the results of TEM-studies) [73, 83, 93, 94]. It should be noted that according to the classification of grown-in microdefects these are A- and B-microdefects. 'Interstitial-type dislocation loops' and 'clusters of interstitial-type defects' are the old terms used before 1973, i.e. before the Dutch school of microdefect lettering was introduced. Temperature range of A-microdefects formation for FZ-Si makes ~ 1353…1393 K and for CZ-Si makes ~ 1223…1323 K [119].

The common term 'voids' or 'microvoids' currently refers to defects inside the D(C)-microdefect ring in CZ-Si crystals. Microvoids are vacancy complexes inside the D(C)-microdefect ring [90]. As indicated above, historically they were detected by different techniques: (1) cone-shaped patterns caused by selective etching (flow pattern defects, FPD) [87]; (2) double or triple octahedral voids detected by the scattered IR radiation method (light scattering tomography defects, IR LSTD) [88]; (3) non-cone-shaped patterns caused by selective etching (Secco etch pits defects, SEPD) [87]; (4) single or double pyramid-shaped pits with a diameter of 0.12...0.3 μm and a depth of 0.14 μm faceted with planes {111}, detected on the silicon wafer surface before and especially after washing in $NH_4OH:H_2O_2:H_2O$ solution (crystal originated particles, COPs) [89]; (5) defects detected by optical interferometry (optical precipitate profiler defects, OPPD) [90]. As already noted, the relationship between these types of the same defect can be described by formula (IR

LSTD = COPs = OPPD) = FPD + SEPD [90]. Temperature range of microvoids formation makes ~ 1403...1343 K for CZ-Si crystals [120-122].

Since microvoids are formed in large-scale crystals, the growth of which are characterized by relatively high growth rates, small curvature of the crystallization front and small axial temperature gradient, then under these conditions a purely vacancy agglomeration can take precedence over the oxygen-vacancy agglomeration at a certain stage of crystal cooling due to high cooling rate [121]. Single or double microvoids with octahedral thermodynamic equilibrium shape will be formed as a result of vacancies condensation. It is shown that single microvoids are formed at a relatively high cooling rate and a low oxygen concentration, and double microvoids are formed at a high oxygen concentration and a relatively low cooling rate, while the oxide layer on the walls of microvoids increases, and this oxide layer prevents their further growth [121].

Dependence of microvoids shape and structure on oxygen concentration, as well as formation and growth of microvoids in a narrow temperature range of crystal cooling, enable us to ask: are microvoids the secondary defects we observe, and do they conceal the defect producing them? The answer to this question was given by heat treatment experiments on crystals with microvoids. Fig. 1.16 shows TEM-images of a microvoid before and after heat treatment in vacuum for 30 min at T = 1373 K [122].

It is noteworthy that such a short-term heat treatment causes a sharp reduction in size and a change in structure of microvoids and, most importantly, the formation of precipitates of quite a considerable size. It was established that first small voids and then large voids of double microvoids are reduced and vanished [122]. Detailed observations show that the process of microvoid shrinking starts from the adjacent area between the two voids [121]. Hence, the process of microvoid formation is heterogeneous. The octahedral microvoids are formed owing to vacancies' agglomeration in course of consequent as-grown on nuclei crystal's cooling. They occur both oxygen-vacancy and carbon-interstitial agglomerates that are formed at higher temperatures. Under certain thermal growth conditions for large-scale silicon crystals the vacancy supersaturation becomes the prevailing factor and vacancies are deposited on oxygen-vacancy and carbon-interstitial aggregates (temperature range of microvoids formation and growth is ~ 1373...1343 K, growth interval of oxide film on their walls is ~ 1323 ... 1173 K [114, 121, 122]). This statement is confirmed by the experimental fact of oxygen presence in some microvoids and carbon presence in other microvoids [72].

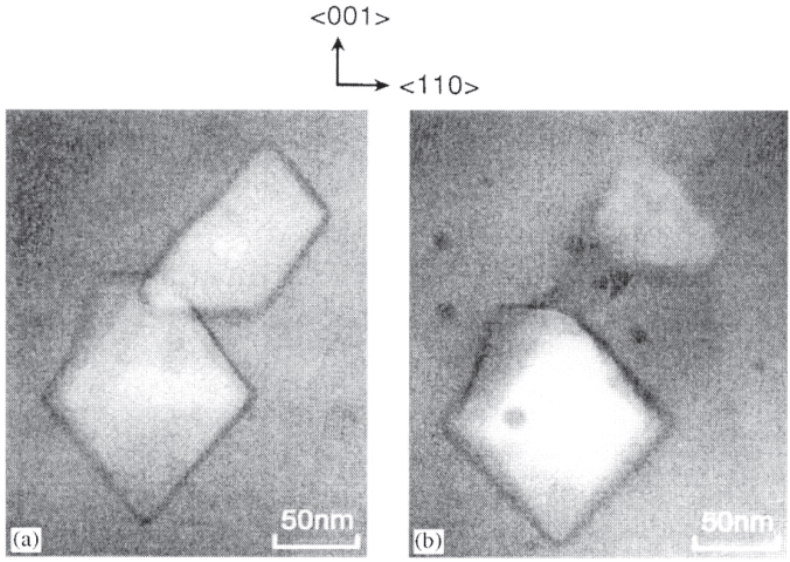

Fig. 1.16. The process of microvoid reduction as a result of heat treatment in a vacuum for 30 min at T = 1373K [122]: (a) before heat treatment; (b) after heat treatment.

Classification of the grown-in microdefects. Two approaches were used to classify grown-in microdefects in FZ-Si and CZ-Si single crystals until recently. The first approach is based on the results of experimental studies of the distribution patterns of microdefects in (111) and (112) planes as a function of the crystal growth rate. The Dutch and German scientists (Dr. A.J.R. de Kock (born.1939) et al.) in 1970-1980 [27, 42-44, 47, 48, 102, 111] and Soviet (Dr. E.G. Sheikhet and Dr. I.E. Talanin et al.) scientists in 1973-1987 [21, 32, 46, 49, 51, 123], the so-called experimental classification of grown-in microdefects was constructed, which was based on the use of selective etching, X-ray topography with decorating and TEM. The Dutch research group introduced the names of A- and B-microdefects, the Soviet (Russian) group introduced the names of C-, D- and (I+V)-microdefects. Further studies in terms of experimental classification established the origin of B-, C-, D- and (I+V)-microdefects [12, 13, 23, 45, 52, 124], which in turn allowed the final experimental classification (Table 1.2, 1.3).

Table 1.2. Classification of grown-in microdefects in dislocation-free silicon single crystals FZ-Si (diameter 30 mm).

Type	Physical nature	Size, nm	V_g, mm/min	Distribution in (112) plane	N, cm^{-3}
A	Interstitial dislocation loops	Up to 50000	1…3.5	Band	~ 10^6
B	Interstitial, precipitates	20…50	≤ 4.5	Band	~ 10^{10}
D (C)	Interstitial, precipitates	4…10	> 4.5	Uniform, as ring in (111) plane	~ 10^{13}
I + V	Interstitial + vacancy, precipitates	4…12	> 6.0	Uniform	~ 10^{13}

The classification was constructed taking into account the thermal growth conditions and the sign of of defect-induced lattice imperfection (origin of mircrodefects). The obtained experimental results indicated the identity of defect formation processes in FZ-Si and CZ-Si crystals, and hence the identity of the classification of grown-in microdefects in both types of crystals [101].

Table 1.3. Classification of grown-in microdefects in dislocation-free silicon single crystals CZ-Si (diameter 50 mm).

Type	Physical nature	Size, nm	V_g, mm/min	Distribution in (112) plane	N, cm^{-3}
A	Interstitial dislocation loops	Up to 50000	≤ 2.5	Band	~ 10^6
B	Interstitial, precipitates	30…80	≤ 2.5 and > 0.5	Band	~ 10^{10}
D (C)	Interstitial, precipitates	4…12	1.8…2.7	Uniform, as ring in (111) plane	~ 10^{13}
I + V	Interstitial + vacancy, precipitates	4…12	> 2.0	Uniform	~ 10^{13}

The second approach to the classification of grown-in microdefects in dislocation-free silicon single crystals should be considered as a process one. Since the middle of the 1990s, most publications have focused on large-scale crystals (100 mm in diameter and larger) [53-55]. The larger the diameter of the grown crystal, the lower the growth rate at which these microdefects are observed, due to the decrease in the axial temperature gradient in the crystal. Interstitial-type dislocation loops and microvoids, which make the main contribution to the further degradation of semiconductor devices, become most relevant in large-scale crystals. These defects within the framework of process classification are considered to be the main ones for dislocation-free silicon single crystals [81, 92, 119].

Silicon single crystals contain a significant amount of growth impurities (doping and background) that leads to the creation of complex semiconductor-impurity systems in crystals, which under certain conditions (temperature, impurity concentration) are a disintegrating solid solution. The absence of sinks for IPDs determines their active participation in the process of decomposition of a solid solution of point defects. As shown by our experimental results, the main and decisive factor for the decomposition of a solid solution of point defects in semiconductor silicon is the formation of primary defects both in the form of oxygen-vacancy aggregates (identified by us as SiO_2 microprecipitates) and in the form of carbon-interstitial aggregates (identified by us as SiC microprecipitates). The heterogeneous nature of the defects nucleation determines, in fact, the entire further process of defect formation in semiconductor silicon.

The main feature of the decomposition of a solid solution of point defects is the generation of secondary defects that accompany the growth of a new phase particle and is determined by the difference in matrix and precipitate atomic volumes. The resulting secondary defects are localized, mainly, in the form of agglomerates near the precipitates. In investigated high-purity CZ-Si and FZ-Si crystals such secondary defects are interstitial-type A-microdefects (interstitial-type dislocation loops) and octahedral vacancy microvoids. It should be noted that in general case Frank loops, helicoids, dipoles, etc. can also be assigned to secondary defects in semiconductor silicon. As a result, distortions of the crystal lattice are determined more rather by secondary defects than by the new phase particles (their total volume is insignificant because of low solubility of the impurity in silicon), but rather by secondary defects. They are spread for a distance of a few micrometers from the new phase particles

they are generated by, and fill almost the entire crystal body, and create problems for further crystal use.

Based on an analysis of experimental results of grown-in microdefects formation, a new physical classification can be proposed [52]. This classification is based on the assumption that the oxygen-induced vacancy agglomerates and the carbon-induced interstitial agglomerates are the driving factors of the formation mechanism of microdefects on the impurity centers. Under certain thermal conditions of crystal growth this defect formation process is accompanied by the generation of interstitial-type dislocation loops and microvoids. In this case, the primary grown-in microdefects are oxygen-vacancy and carbon-interstitial agglomerates (B-, D- and (I+V)-microdefects). Formation of any type of grown-in microdefects is caused by changes in the crystal thermal growth conditions. This classification is simpler and reflects the physics of defect formation processes in dislocation-free single crystals of silicon.

The physical classification of grown-in microdefects involves the participation in the defect formation process of other impurities (doping impurities, nitrogen, iron, etc.) and other impurity centers, since the formation of defects in dislocation-free silicon single crystals involves the decomposition of solid solutions of IPDs on the impurity centers.

1.4. Research of grown-in microdefects transformation under various process effects

High-temperature treatments. In the production of semiconductor devices and integrated circuits, single crystals or silicon structures undergo a series of sequential process operations associated with their heat treatment, which leads to defects that are added to the initial grown-in microdefects (post-growth microdefects), as well as to their interaction and transformation. Recently, silicon with high resistivity is used in the form of bulk single crystals and epitaxial layers for manufacture of power semiconductor devices, high-speed integrated circuits, radiation detectors and photodetectors.

In CZ-Si the background oxygen impurity leads to the formation of different types of precipitates. The morphology, size, and density of precipitates depend on doping temperature and density, initial oxygen concentration, presence of various impurities and thermal history of the crystal. The formation of oxygen precipitates is accompanied by the generation of silicon self-interstitials, which, in turn lead to the appearance of dislocation dipoles, loops, or stacking faults, depending on the doping temperature and some other conditions [37, 125].

The authors of [21, 123] showed that some of grown-in B-microdefects in initial FZ-Si single crystals, as well as part of D(C)-microdefects in heat-treated FZ-Si single crystals, are oxygen-containing precipitates. Similar microdefects in heat-treated CZ-Si crystals lying in the planes {100} with sides along the directions [100] or [110] were observed by various authors [38, 126-128]. It was found that the remaining parts of B- and D(C)-microdefects in FZ-Si and CZ-Si crystals are carbonaceous precipitates [21, 23, 52].

High-temperature treatments of FZ-Si dislocation-free silicon single crystals inevitably lead to a change in the bulk distribution of microdefects and also affect their growth and transformation from one type to another [52]. It is established that during the epitaxy, the A-microdefects in the dislocation-free substrate are transformed into dislocations; the initial B-microdefects are enlarged and transformed following this pattern: B-microdefects $\rightarrow$ dislocation loops (A-microdefects) $\rightarrow$ dislocations. The transformation of D(C)-microdefects into a dislocation is hampered by the diffusion of IPDs and background impurities [52]. For example, TEM-studies of heat-treated substrates from FZ-Si single crystals obtained at growth rates of 2...8.0 mm/min (heat treatment for 180 min at T $\cong$ 1453 K in a hydrogen atmosphere) reveal black-and-white contrast defects under dynamic conditions. This indicates a continuous process of defect formation under the thermal influence on a crystal. TEM-studies of heat-treated substrates with initial D(C)-microdefects (V_g = 6.0 mm/min) showed an increase in the size of microdefects to 10...14 nm (minor defects). In turn, defects with strong deformation contrast of a complex type were founded in substrates with initial B-microdefects (Fig. 1.17). Defects of this type (large defects) are also observed in heat-treated substrates of crystals obtained at other growth rates, which definitely indicates the transformation of the initial defect structure in the process of high-temperature treatment during epitaxial growth [52].

Data on transformation of smaller microdefects into larger microdefects obtained during epitaxy experiments were confirmed in a complex of experiments on heat treatment of crystals [52]. For example, two single crystals of FZ-Si were investigated: one of them was grown at a V_g = 6.0 mm/min and at a certain time, its growth stopped for 60 min, the other was grown at a constant growth rate V_g = 6.0 mm/min and then cut into four parts (cylinders), with each of the four parts being bisected along the plane{112}. One of the halves of each cylinder was etched to reveal patterns of microdefects distribution, and four others were heat treated for

60 min in vacuum at temperatures of 1073 K, 1173 K, 1273 K, 1373 K, respectively. As a result of crystal growth stopping a set of all known types of interstitial-type microdefects was formed, each of them being typical for crystals obtained at determined growth rates (Fig. 1.18). Here they are present in one crystal, which makes it possible to explain their appearance solely by thermal treatment. Since the stopping of growth can be regarded as a change in the real temperature conditions, that is, the crystal receives additional treatment at different temperatures at points located below the stopping place for a certain time. This leads to formation of various types of microdefects in the crystal [52]. TEM-studies of crystal areas with A-microdefects show the presence of dislocation loops of interstitial type with a size of 2...20 μm, the dislocation lines of which are strongly decorated by background impurities due to additional heat treatment (Fig. 1.19). 20...60 nm interstitial-type defects are revealed in the crystal areas with B-microdefects.

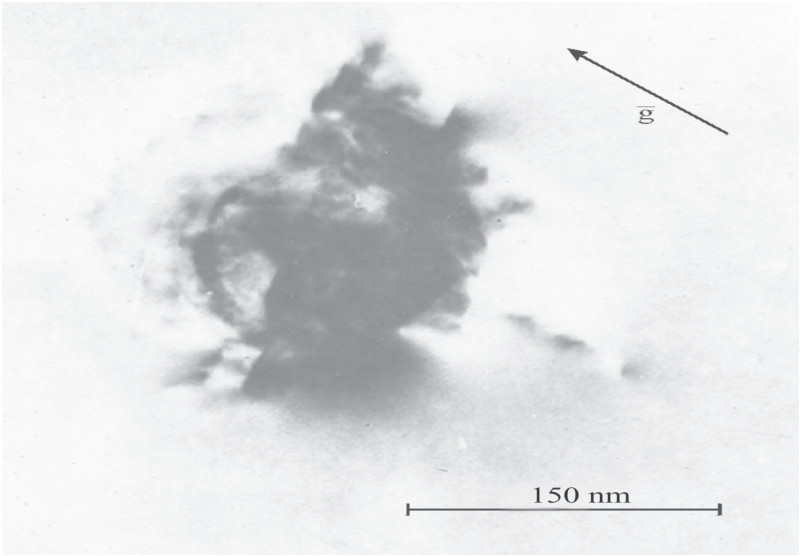

Fig. 1.17. TEM-image of a defect of a complex type with a strong deformation contrast, light field, $\overline{g} = (\overline{2}20)$

The interstitial-type defects of black-and-white contrast up to 15 nm in size were detected in the crystal areas with D(C)-microdefects. Heat treatment of the second crystal is accompanied by a redistribution of defects and an increase in their sizes. Thus, heat treatment at 1373 K promotes an increase in the size of D(C)-microdefects up to 10...12 nm. The defects with a strong size deformation contrast of 100...500 nm were observed in crystals, which were heat-treated to 1373 K (Fig. 1.20) [52].

To investigate the effect of heat treatment on the defect structure of CZ-Si crystals, two crystals of 80 mm in diameter were grown in direction [111] and doped with phosphorus at V_g = 0.6 mm/min and V_g = 2.0 mm/min [23]. The resistivity of the crystals measured under ambient temperature immediately after growth at V_g= 2.0 mm/min made 7…10 Ωm·cm, and at V_g = 0.6 mm/min it made 18…30 Ωm·cm. Each crystal was subjected to heat treatment in the growing vessel at 923 K within 60 min in the ambient air medium. It was established that after heat treatment the etch pit sizes become smaller and the swirl distribution in the bottom part of the crystal disappears. In crystals grown at V_g = 0.6 mm/min, we identified big etch pits (~10^3 cm^{-2}), after heat treatment, which were absent in crystals grown at V_g = 2.0 mm/min. The view of microdefects distribution changes due to heat treatment: the concentration of microdefects increases, their size decreases and the swirl distribution disappears in the bottom part of the crystal where carbon concentration is higher [23].

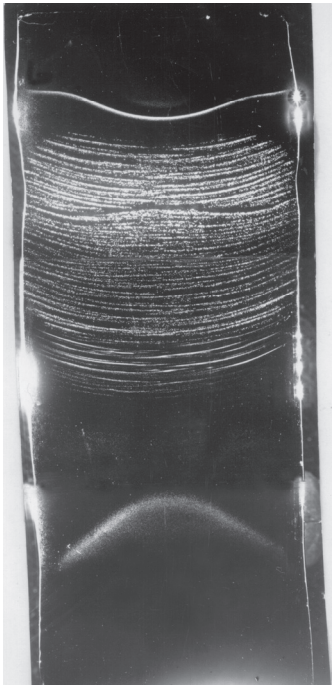

Fig. 1.18. The distribution of microdefects of various types in the FZ-Si crystal grown at V_g = 6.0 mm/min, after stopping crystal growth

CZ-Si crystal grown at V_g = 2.5 mm/min (50 mm in diameter) was heat treated at 1373 K for 600 min [23]. TEM-studies enabled to reveal both image black-and-white contrast defects of 10...20 nm in size and more complex-shaped defects with a strong deformation contrast of 300...600 nm, being sources of dislocation loops, in the area of the D(C)-microdefect ring (Fig. 1.21a). The largest complex-shaped defects (up to 700...900 nm), which can also be the sources of dislocation loops, were found inside the D(C)-microdefect ring (Fig. 1.21b). These data correlate well with the results of [129, 130]. The obtained experimental results allowed the authors of [12, 52] to determine the basic model concepts of transformation mechanism of interstitial-type microdefects.

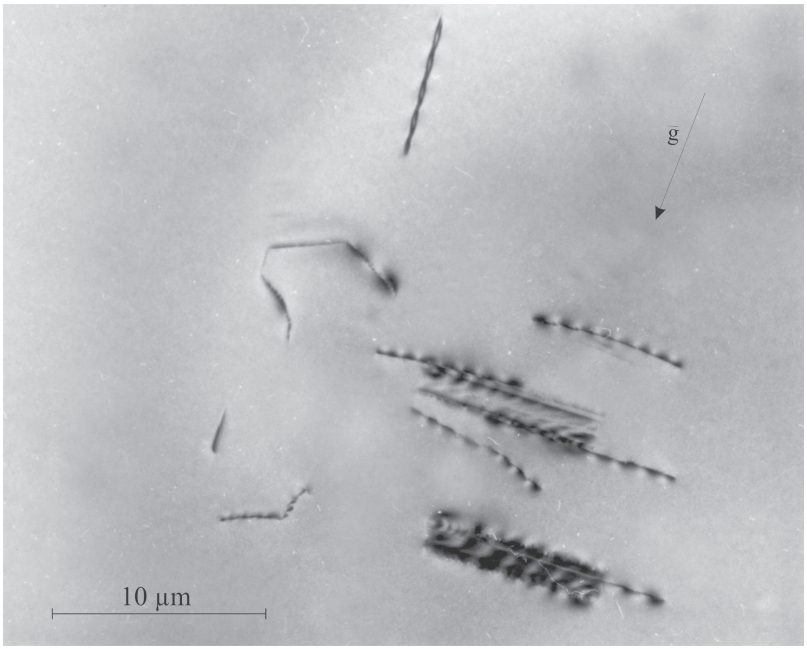

Fig. 1.19. TEM-image of A-microdefects in heat treated crystal, light field, $\overline{g} = (20\overline{2})$

Dislocation activity. Grown-in microdefects are stress concentrators of the crystal lattice and can become sources of dislocations under certain conditions. Conditions for the dislocation activity of microdefects are realized during silicon processing in the course of manufacturing devices made of it. X-ray topography methods were used to study dislocation loops generated by microdefects. The loops were created by deformation (uniaxial compression) at a temperature of 973 K in helium or air medium [25].

Dislocation activity of various types of grown-in microdefects is different. B-microdefects were the most active ones, since loops of the same size were observed at lower loads than in samples with A-microdefects. The dislocation activity of A-microdefects depended on the size of defects: larger defects showed higher activity. D(C)-microdefects showed activity at loads 2.5 times higher than conditions for B-microdefects [25]. The sources of dislocation loops in the form of grown-in microdefects refer primarily to the symmetric type of Frank-Read

sources (A-microdefects) and spiral Bardeen-Hering sources (B-microdefects) with fixation points undetectable by topography. However, if the mechanisms of loop generation by A- and B-microdefects are different in detail, the final result of both type sources application is the same: sliding loops. The small dislocation activity of D(C)-microdefects is explained by the small size of these defects and the difficulty of the first loop formation [25].

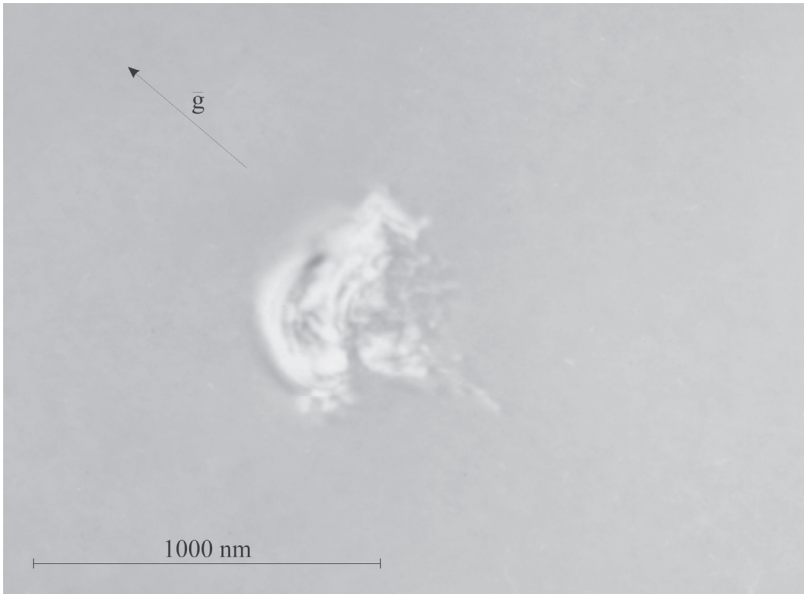

Fig. 1.20. TEM-image of defect of a complex type with strong deformation contrast in heat treated crystal, light field, $\bar{g} = (\bar{2}20)$

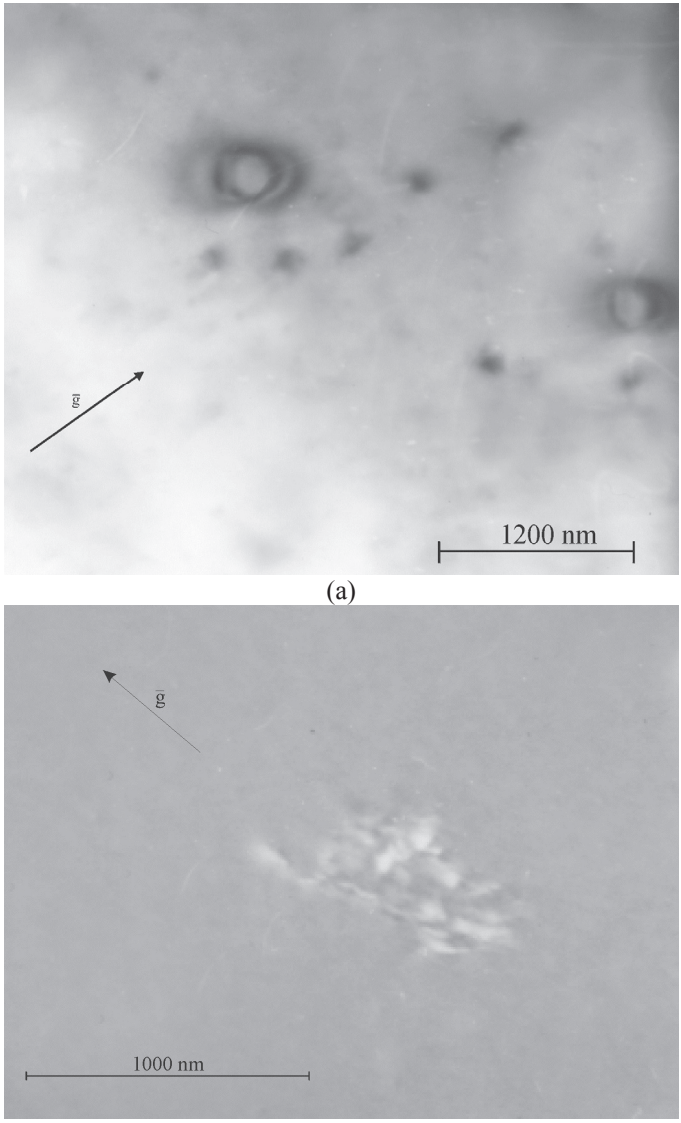

Fig. 1.21. TEM-images of defects of a complex type after heat treatment CZ-Si crystals, $\overline{g} = (2\bar{2}0)$ (a) in the region of the D-microdefects ring; (b) inside the ring of D-microdefects

Radiation impact. Investigations of the effectiveness of radiation defect interaction (vacancies and silicon interstitials) with grown-in microdefects of a certain type make it possible to estimate the origin of microdefects indirectly. For example, it was established in [99] that the decrease in the rate of E-centers introduction in FZ-Si crystals (V_g < 6.0 mm/min) with the interstitial-type grown-in microdefects is explained by the presence of defects that create compressive stresses around them. Due to this, they effectively capture free vacancies, which lead to a decrease in the introduction rate of secondary vacancy-type radiation defects (E-centers). Intensive capture of vacancies leads to an increase in the lifetime of silicon self-interstitials, and, consequently, an increase in the introduction rate of interstitial-type defects. The experiment showed a simultaneous increase in the introduction rate of C_i-C_s complexes. In contrast, in FZ-Si crystals (V_g > 6.0 mm/min) there was a slight decrease of the introduction rate of E-centers and C_i-C_s complexes. This decrease can mean that there are sinks for both vacancies and silicon self-interstitials [99].

Studies of various types of grown-in microdefects rearrangement due to the different nature of their interaction with nonequilibrium point radiation defects in the processes of neutron-transmutation doping and post-radiation doping showed that the formation of a high concentration of nonequilibrium point defects upon irradiation and subsequent thermal treatment would cause transformation of microdefects with the participation of impurity atoms even at relatively low temperatures: (I+V)-microdefects → D(C)-microdefects → B-microdefects → A-microdefects [131]. The absence of swirl defects (A- and B-microdefects) in the initial single crystals does not ensure their absence after neutron-transmutation doping and subsequent heat treatment. A decrease in concentration of residual impurities of oxygen and carbon allows us to change the doping type towards lower temperatures, and therefore it is possible to obtain, more perfect single crystals by suppressing reactions of interaction of point defects, generated by irradiation, with residual impurity atoms after neutron-transmutation doping and heat treatment [131].

Ion implantation of surfaces is widely used in microelectronics for the dosed introduction of impurities into the surface layers of crystals with the purpose of locally changing the electrical properties of the original wafers. At the same time, the ion implantation process is accompanied by the introduction of a large number of radiation defects into the crystal surface layer [132, 133], which adversely affects the quality and manufacturability of semiconductor devices and microcircuits. Generation of defects in ion

implantation process is determined by the primary and secondary collision of implanted ions with the original crystal atoms [134]. In these collisions, a high concentration of point defects (vacancies, silicon self-interstitials) occurs. The implanted ions are usually in electrically inactive positions in the lattice. Therefore, process doping is carried out to reduce the concentration of radiation defects and to convert doping impurities into an electrically active state, as well as to restore the crystal structure [135]. A number of papers indicate that typical defects observed in implanted layers after doping are dislocation loops, dislocation interlacing, and microdefects [132]. With the implantation of boron, phosphorus, and arsenic followed by doping, a large number of elongated dislocation loops, dipoles, and rod-like defects, which are interstitial-type defects, are found in the resulting structure [136-138]. Some authors note that doping in an oxidizing atmosphere leads to the formation of stacking faults that arise as a result of the interaction of point defects with the flow of self-interstitials that appear during oxidation [134, 139]. A generalization of the published results of earlier experiments allows to state that silicon self-interstitials play the main role in the inter-defect interaction processes after ion implantation [140, 141].

To study this provision precisely, as well as to clarify the interaction process of grown-in microdefects with point defects arising during implantation, a special cycle of experiments was carried [52]. CZ-Si single crystals with a precisely defined type of grown-in microdefects were used. A crystal of 50 mm in diameter had banded distribution of A- and B-microdefects with a growth rate V_g = 0.5 mm/min; and banded distribution of B-microdefects was observed with a growth rate V_g = 1.0 mm/min. Uniform distribution of small (I+V)-microdefects with a growth rate V_g = 2.5 mm/min was observed. Arsenic and antimony ions were implanted into the substrates made of these crystals. The substrates were studied as specially doped or undoped. Depending on the type of initial grown-in microdefects, various combinations of secondary structural imperfections were observed: the entire spectrum of which consisted of microdefects with the size of 4...20 nm; precipitates with the size of 30…130 nm; dislocation loops with the size of 40…100 nm; direct segments of dislocations; hexagonal formations [52]. It was found that these defects cause compression deformation in the crystal lattice in all cases, i.e. they are interstitial-type defects. Most likely this is due to the fact that vacancies in a crystal are captured by various sinks (dislocation loops, precipitates, complexes), while the silicon self-interstitials interact with carbon atoms which are effective sinks for them. Implanted samples

contain arsenic atoms, vacancies, silicon self-interstitials, atoms of oxygen and carbon background impurities. Researchers in [139] point to that in such a case the SiAs complex generation is more energy favorable, while the VAs_2 complex generation is not proved experimentally [142]. Based on the coexistence of vacancy- and interstitial-type defects ((I+V)-microdefects), the probable interaction mechanism in such system can be depicted as follows. SiAs complex generation is accompanied by the process when free vacancies are absorbed by the interstitial-type defects. Thus, both interstitial-type defects grow emitting silicon self-interstitials that results in their excess number and further interaction with carbon atoms. Vacancy-type microdefects, in their turn, interact with oxygen atoms and change their sign of imperfection from the vacancy-type to the interstitial-type in the course of transformation.

Obtained experimental results analysis shows that in course of ion-implantation and further process doping, CZ-Si grown-in microdefects growth and transformation occur, following by decomposition of oversaturated silicon-arsenic solid solution. The structural imperfections transformation is as follows: grown-in microdefects + point defects $\rightarrow$ dislocation loops + precipitates $\rightarrow$ plate-time formations + dislocations [52].

Electrical activity. The values of the resistivity and lifetime of nonequilibrium carriers are the important characteristics of silicon single crystal quality since their values are determined by the content of certain impurities and recombination centers in a single crystal. Recombination of nonequilibrium carriers takes place on the crystal lattice defects, complexes of defects, and in zones of local stresses in a crystal, etc. The electrical activity of impurities and defects essentially determines the applicability and functioning of semiconductor devices and microcircuits.

The author of [143] investigated electrical and physical parameters of n-type FZ-Si single crystals obtained at a variable growth rate from 2.0 to 7.5 mm/min, therefore, containing a set of microdefects of all types: A-, B-, D(C)- and (I+V)-microdefects. After the measurements, the samples were doped in vacuum at a temperature of 1373 K for 60 min. Then, the same parameters were remeasured. Experimental results are shown in Table 1.4.

The average value of the resistivity at the peripheral ring of each face is greater than the average value at the center of each face (for V_g = 2.0; 4.0; 6.0 mm/min). With increasing concentration of D(C)-microdefects, the ρ and τ decrease. At the same time, for the crystal samples with V_g = 7.5 mm/min, the situation is inverse [143]. Properties of the original

samples are changed due to the heat treatment effect. High-temperature doping leads to a significant decrease in the lifetime of nonequilibrium carriers regardless of the values of the resistivity and the initial lifetime. The decrease in the lifetime is apparently due to the outside impurity diffusion and the formation of additional recombination centers.

Table 1.4. Electrophysical parameters of single-crystal silicon obtained under different technological conditions

Crystals growth rate, mm/min (type of microdefects)	Without annealing		After annealing, T = 1373K, t = 60 min	
	ρ, Ωm·cm	τ, μs		ρ, Ωm·cm
2.0 (A)	$2.1 \cdot 10^3$	220	2.0 (A)	$2.1 \cdot 10^3$
4.0 (B)	$2.45 \cdot 10^3$	260	4.0 (B)	$2.45 \cdot 10^3$
6.0 (D)	$3.1 \cdot 10^3$	360	6.0 (D)	$3.1 \cdot 10^3$
7.5 (I + V)	$2.9 \cdot 10^3$	380	7.5 (I + V)	$2.9 \cdot 10^3$

The recombination activity of A-microdefects, which are dislocation loops of interstitial type, is determined by the presence of their broken bonds and their subsequent capture of carriers.

B-microdefects constitute clusters of silicon self-interstitials and a new phase impurities or microparticles. The presence of such violations in the crystal body leads to the appearance of deformation stress fields, under the influence of which an atmosphere of impurities or their complexes being the main recombination centers in such material is formed near the microdefects. In crystals with A- and B-microdefects, the recombination of charge carriers takes place in centers that contribute to the lower half of the bandgap the acceptor energy levels E_V+0.41eV и E_V+0.30 eV with the asymmetry of the capture cross sections σ_p/σ_n=4.5 and σ_p/σ_n=4.0 respectively[144]. For the third (D(C)-microdefects) and the fourth ((I+V)-microdefects) groups of samples, it can be assumed that the lifetime of charge carriers is limited by their diffusion to sinks with a high local recombination rate. D(C)-microdefects can act as such sinks in the third group crystals, and small inclusions of impurities (in particular oxygen) can act as such sinks in the fourth group samples.

The scanning electron microscopy (EBIC method) was used to investigate the defect structure of FZ-Si crystals obtained at V_g = 1.0; 6.0

mm/min ($\rho \approx 100$ Ωm·cm; $N_P \approx 10^{14}$ cm^{-3}; $N_{O_i} < 1 \cdot 10^{16}$ cm^{-3}; $N_{C_S} = 1.6 \cdot 10^{16}$cm^{-3}) in vacuum after irradiation with electrons. Radiation defects in crystals with A-microdefects (V_g = 1.0 mm/min) and with D(C)-microdefects (V_g = 6.0 mm/min) were generated as a result of irradiation by electrons with E = 3.5 MeV of integral flow and F_e = $5 \cdot 10^{14} \ldots 5 \cdot 10^{15}$cm^{-2} at irradiation temperature not exceeding 333 K [99]. Different recombination activity of A- and D(C)-microdefects and their different behavior from the viewpoint of radiation defect accumulation as a result of electron irradiation were detected. After irradiation, the recombination activity of A-microdefects almost vanished, while in D(C)-microdefects remained almost unchanged. The authors explain this by the fact that most of vacancies in crystals with A-microdefects are used to neutralize the recombination field in the vicinity of A-microdefects. The remaining number of vacancies is recombined with silicon self-interstitials and used to form E-centers, the concentration of which, however, will be small. The excess of silicon self-interstitials apparently does not interact with the dislocation loop, first because of the same sign of elastic imperfection and, secondly, because silicon self-interstitials have a donor state in the bandgap and a positive charge [99]. Most likely, silicon self-interstitials interact with carbon atoms which are effective sinks for them. This interaction can lead to the formation of interstitial carbon Cs with the subsequent formation of a pair $C_i + C_s$.

A much lower energy of the elastic interaction of D-microdefects and a greater energy of the Coulomb interaction of negatively charged vacancies and positive capture centers lead to the formation of E-centers ($P^+ + V^-$) and divacancies. At the same time silicon self-interstitials will effectively interact with carbon, as in the case of crystals with A-microdefects. Hence, the recombination activity of D(C)-microdefects will not decrease [99]. The authors of [99] state that the electrical activity of microdefects (in the sense of their effect on the values ρ and τ) decreases pursuant to the following pattern: A → B → D(C).

The authors of Ref. [145] analyzed the dependence of the lifetime of the minority carriers (τ) and the concentration of the main carriers (n_0) upon the temperature (T = 100...400 K), as well as the dependence of τ upon the excitation level of the minority charge carriers ($\gamma = \Delta n/n_0 = 10^{-4} \ldots 10^{0}$) obtained before and after irradiation with various gamma-ray fluxes Co^{60}. Upon irradiation all the studied crystals effectively form the E-centers, through the levels of which recombination of the minority

carriers occurs. However, the degree of lifetime radiation change was not the same in crystals irradiated with the same gamma-ray flux. The analysis of the dose temperature dependences τ_F determined the coefficients K_τ of lifetime radiation change ($K_\tau F = 1/\tau_F - 1/\tau_0$ where F is the gamma-ray fluence, and τ_0 is the lifetime before irradiation) shown in Table 1.5. The Table 1.5 also shows calculated introduction rates ($\eta = dN/dF$, where N is a radiation defects concentrations) of E-centers (η_E) and C_i-C_s centers (η_C).

Table 1.5. The values of K_τ and rates of introduction η_E and η_C [145].

Group	Defect types	K_τ, $cm^2 \cdot s^{-1}$	η_E, cm^{-1}	η_C, cm^{-1}
I	D	$1.2 \cdot 10^{-10}$	$4.0 \cdot 10^{-4}$	$5.2 \cdot 10^{-4}$
II	A + B	$(4…6.0) \cdot 10^{-11}$	$(1…4.0) \cdot 10^{-4}$	$(8…5.0) \cdot 10^{-4}$
III	A	$(5…13.0) \cdot 10^{-11}$	$(1…4.0) \cdot 10^{-4}$	$(8…5.0) \cdot 10^{-4}$

The change of K_τ can be caused only by a decrease in η, since the origin and parameters of the defects (for example, the capture coefficients of electrons and holes on the levels of radiation defects) were the same in crystals of all three groups. Analysis of the temperature dependences of Hall coefficient showed that the introduction rate of the E-centers (η_E) correlates with the K_τ value [145]. Decrease in the introduction rate of E-centers in crystals of II and III groups can be caused by the presence of sinks for the vacancies generated by irradiation. Such defects can be clusters or precipitates of silicon self-interstitials and atoms of oxygen and carbon background impurities, creating compressive stresses around themselves. Due to this, they effectively capture free vacancies, which lead to a decrease in the introduction rate of secondary vacancy-type radiation defects including E-centers and thus coefficients K_τ. The sweep of K_τ coefficients from sample to sample (their sizes were 1.5×2.0×13.0 mm^3) is explained by the banded distribution of grown-in microdefects in the crystal.

Intensive capture of vacancies leads to increase in the lifetime of silicon self-interstitials, and, consequently, an increase in the introduction rate of interstitial-type defects. Alongside with decrease in η_E, the experiment showed an increase in the introduction rate of Ci-Cs (η_C), complexes occupying the level $E_2 = E_c - 0.17$ eV. In contrast, crystals of I group showed a slight decrease of η_E and η_C. Apparently, there are sinks for both vacancies and silicon self-interstitials [145].

As a rule, the main goal of any technology model development intended for a certain device manufacture is to ensure the maximum output of suitable products and to maintain the device characteristics within the specified parameters. Defects located in the space-charge area have a significant (mainly negative) effect on the quality and manufacturability of semiconductor devices and microcircuits. Investigations of the current-voltage characteristics of Schottky barriers showed that the breakdown voltage depends on the type and concentration of grown-in microdefects [146]. The reverse breakdown voltage for Schottky barriers made on silicon wafers containing A- and B-microdefects is less than for silicon wafers containing B-microdefects and even less than for Schottky barriers made of silicon containing D(C)-microdefects. The values of the reverse currents for Schottky barriers containing only D(C)-microdefects are the lowest in comparison with the barriers made of silicon with (A+B)-microdefects and B-microdefects [146]. The electrical activity of microdefects depends on the content of impurities, temperature growth conditions of single crystals, and on process operations of device manufacturing [146]. In [143], power diode structures were created and investigated on crystals containing similar types of grown-in microdefects. Statistical processing of reverse breakdown voltage measurement results showed that this parameter is 18% lower for diode structures made of silicon wafers with (A+B)-microdefects and 25% lower for structures made of silicon wafers with A-microdefects compared to structures made of silicon with D(C)-microdefects. If the temperature of the finished device functioning is increased to 200 ^{0}C, the breakdown voltage of diodes of all three groups decreases but the nature of dependence upon the type of microdefects remains. One of the reasons for this apparently is an increase of the efficiency of recombination processes on microdefects, which are very efficient recombination centers. The presence of electrically active microdefects of A-, B-, and D(C)-types in the space-charge area leads to a smooth increase in the reverse current and to the appearance of the so-called ‘soft’ current-voltage characteristic [143].

Conclusions to chapter 1. A brief analysis of the experimental results on formation and transformation of grown-in microdefects in dislocation-free silicon single crystals makes it possible to draw the following conclusions:

1. The change of thermal growth conditions, in particular, the controlled change in the crystal growth rate, leads to a consistent change in the type of microdefects observed. The increase of crystal growth rate leads to disappearance of swirl-microdefects and appearance of D-microdefects uniformly distributed in the form of channels and rings. The

disappearance of swirl-microdefects can be explained by the suppression of the remelting phenomenon in FZ-Si and CZ-Si crystals.

2. An increase in crystal growth rate leads to a decrease in the curvature of the crystallization front, which facilitates the face protrusion (111) on the crystallization front and the formation of channel and annular distributions of D-microdefects. This process confirms the heterogeneous origin of microdefects. A decrease in the curvature of the crystallization front leads to a decrease in temperature gradients, but in turn, the axial temperature gradient is not constant along the entire crystal diameter. Therefore, the axial temperature gradient usually increases from the center of the crystal to its edge, which leads to the formation of a V-shaped distribution of D-microdefects along the plane (112) with an increase in the crystal growth rate.

3. The coexistence of vacancy and interstitial-type microdefects in FZ-Si and CZ-Si crystals obtained at high growth rates suggests that the process of recombination of IPDs close to the crystallization temperature is almost absent. The decomposition of the supersaturated solid solution of IPDs (vacancies and silicon self-interstitials) due to the crystallization temperature occurs simultaneously according to two mechanisms: vacancy and interstitial.

4. The nucleation centers of grown-in microdefects are oxygen and carbon background impurities and their influence determines the mechanism of subsequent growth and transformation of microdefects. Compression areas near oxygen interstitials are the nucleation centers of oxygen-vacancy aggregates, excessive vacancies and other oxygen self-interstitials rush to these areas. Stretching areas around the substituting carbon atoms are the nucleation centers of carbon-interstitial aggregates, excessive silicon and oxygen interstitials rush to these areas.

5. Let us summarize the main experimental results obtained by means of TEM-studies of grown-in microdefects of various types. For FZ-Si crystals:

- A-microdefects are interstitial-type dislocation loops with the size of 1...20 μm with the Burgers vector $\overline{b}$ = 1/2[110], lying in the planes{111} and {110}.
- B-microdefects are interstitial-type precipitates of carbon and oxygen background impurities with the size of 20...50 nm, some of which have the correct geometric shape and lie in the planes{100}.
- D-microdefects are interstitial-type precipitates of carbon and oxygen background impurities of 4...10 nm in size having a regular and amorphous internal structure. The two forms of existing B-microdefects, the proximity of their sizes, the same contrast of the

TEM-images suggest that the D-microdefects are uniformly distributed small B-microdefects.

- C-microdefects are entirely identical to D-microdefects as far as contrast of TEM images, the sign of lattice imperfection and the size are concerned. Therefore, there is no need to separate them into a distinct type;
- (I+V) -microdefects are formed near the crystallization front and are precipitates of background carbon and oxygen impurities of interstitial (I) and vacancy (V) types.

For CZ-Si crystals:

- Microdefects in the area of annular distribution are clusters of interstitial-type point defects with dimensions of 4...12 nm.
- Interstitial- and vacancy-type microdefects ((I+V)-microdefects) coexist inside the annular distribution;
- There is no difference between the microdefects in the ring area and D-microdefects in FZ-Si crystals with regard to their sizes, sign of lattice imperfection and macrodistribution geometry;

6. Microvoids are formed in large-scale silicon single crystals as a function of thermal growth conditions.

7. The nature and regularities of the grown-in microdefect formation in FZ-Si and CZ-Si crystals are identical.

8. The initial defect structure of dislocation-free silicon single crystals determines the processes of defect formation and the emerging defect structure when producing silicon structures and devices.

Based on the currently available experimental results on grown-in microdefects formation investigation during crystal growth, it can be concluded that the nomenclature of grown-in microdefects in accordance with the generally accepted classification of defects includes three types: loops, and microvoids. Their formation is due to the temperature conditions of crystal growth. This conclusion allows to abandon the cumbersome and inconvenient alphabetic classification of grown-in microdefects (A-microdefects, B-microdefects, etc.) and to consider defect formation during the silicon crystal growth in a unified complex.

CHAPTER TWO

PHYSICAL MODELING OF DEFECT FORMATION PROCESSES IN DISLOCATION-FREE SINGLE CRYSTALS OF SILICON

I formulate no hypotheses
—Isaac Newton (25.XII.1642 – 20.III.1727)
Philosophiæ Naturalis Principia Mathematica, 1713

Modeling is one of the main methods of cognition, it is a form of reflection of reality and consists in clarifying or reproducing certain properties of real objects, objects and phenomena with the help of other objects, processes, phenomena, or using an abstract description in the form of image, a plan, a map , a set of equations, algorithms and programs.

The possibilities of modeling, i.e., the transfer of the results obtained during the construction and study of the model to the original are based on the fact that the model displays (reproduces, simulates, describes) certain features of the object of interest to the researcher. Modeling as a form of reflection of reality is widespread, and a fairly complete classification of possible types of modeling is extremely difficult, if only because the concept of "model" is ambiguous. For natural and technical sciences, the following types of modeling well known:

- Conceptual modeling, in which a set of already known facts or representations of an object or system is interpreted with the help of some special signs, symbols, operations on them, or with the help of natural or artificial languages.
- Physical modeling, in which the model and the modeled object represent real objects or processes of a unified or different physical nature, and between the processes in the original object and in the model there are some similarity relations which resulting from the similarity of physical phenomena.

- Structural-functional modeling, in which models are schemes (flowcharts), graphs, drawings, diagrams, tables, figures, supplemented by special rules for their integration and transformation.
- Mathematical (logical-mathematical) modeling, in which modeling, including the construction of a model, is carried out by means of mathematics and logic.
- Simulation (software) modeling, in which the logical-mathematical model of the investigated object is an algorithm for the functioning of the object implemented as a software package for a computer.

Types of modeling are not exclusive and can be used in the study of complex objects either simultaneously or in some combination. Furthermore, in some sense, the conceptual and structural-functional modeling are indistinguishable among themselves, since the same block diagrams are special signs with the established operations on them.

Traditionally, modeling on electronic computers was understood only as simulation modeling. However, with other types of modeling a computer can be also very useful, except perhaps for physical modeling, where the computer can also be used but rather for the purposes of controlling the modeling process. In mathematical modeling the implementation of one of the main stages (construction of mathematical models based on experimental data) is currently unthinkable without a computer. In recent years, thanks to the development of the graphical interface and graphics packages, computer modeling has been widely developed.

2.1. Early physical models of the formation of grown-in microdefects

The experimental results described in the previous chapter showed that the processes of nucleation and growth of grown-in microdefects directly depend on the presence of background impurities of carbon and oxygen in crystals. The presence in dislocation-free silicon single crystals at comparable concentrations of both background impurities of oxygen and carbon, and IPDs (silicon interstitial atoms and vacancies) leads to complex processes of interaction between them. Microdefects are the products of the decomposition of supersaturated solid solutions. Such supersaturated solid solutions are formed by impurities (doping and background) and IPDs. The decomposition can occur either directly during the cooling of as-grown silicon single crystals, or during subsequent thermal treatments or any other external effects on the crystal. It should be

taken into account that in the processes of decomposition of supersaturated solid solutions of IPDs and impurities in the course of subsequent technological treatments or external influences, the initial microdefect structure of silicon takes part. Therefore, the grown-in microdefects of silicon single crystals and microdefects of heat-treated silicon cannot be directly correlated. In this connection, there is a need for a clear division of the concept of microdefects into grown-in microdefects and post-growth microdefects.

Historically, there are a number of models for the formation of grown-in microdefects, differing of original physical concept and the degree of validity. Most of them are qualitative models and cannot explain the variety of available experimental results. At the heart of each model there are representations about the types and natures of the dominant point defects in the growing crystal, which are then transformed into microdefects in the cooling process. Almost all physical models of the formation of grown-in microdefects were proposed in 1975-1982 when the physical nature of A-microdefects was reliably established, while other grown-in microdefects could be represented only by indirect data.

The equilibrium interstitial model [18]. This is based on the assumptions [147, 148] that the dominant point defects that are in equilibrium at the melting temperature are silicon interstitial atoms with a concentration of ~ 10^{16} cm^{-3}, and the concentration of vacancies is small. During crystal cooling, a supersaturation occurs with point defects, which leads to rapid coalescence of interstitial atoms as a result of which metastable three-dimensional agglomerates (B-microdefects) are formed. The nucleus of agglomerate being heterogeneous in nature contains silicon interstitial atoms and carbon atoms and consists of approximately 100 atoms [149]. B-microdefects absorb interstitial silicon atoms and growed to 10^6...10^8 atoms [149]. Upon reaching this critical size, they become unstable and collapse with the formation of interstitial dislocation loops (A-microdefects). The thermodynamic calculation of the model was carried out in [18, 149, 150]. However, near the melting point the equilibrium concentrations of vacancies and silicon interstitial atoms are comparable, since the energies of formation of vacancies and interstitial silicon atoms are close in magnitude [6]. Also within the framework of this model it is impossible to explain the occurrence of vacancy-type microdefects.

The nonequilibrium interstitial model [27]. The authors of the model did not draw a conclusion about the type of prevailing point defects, referring only to the direct relationship between the formation of swirl defects and the process of crystal growth, in particular, with the

phenomenon of remelting. Within the framework of this model, the formation of A- and B-microdefects was considered as a two-stage process of condensation of silicon interstitial atoms (similar to the equilibrium model). In contrast to the equilibrium model, it was assumed that the excess concentration of silicon interstitial atoms is formed due to the capture of additional nonequilibrium interstitials of silicon from the melt at the time of crystallization, due to remelting upon rotation of the crystal in an asymmetric temperature field. If remelting occurs, the microscopic growth rate becomes negative and the average positive microscopic growth rate should be greater than the macroscopic growth rate. Since reverse remelting is unlikely at high macroscopic growth rates, the average microscopic rate and capture of nonequilibrium point defects can decrease with increasing macroscopic rate. Critical nuclei for the condensation of silicon interstitial atoms are formed by the heterogeneous association of interstitial atoms with background impurities of carbon and oxygen. The further process of growth of B-microdefects is analogous to the equilibrium interstitial model.

The drip model [151]. The authors of this model thought that due to temperature fluctuations in the process of crystal growth in a superheated solid region behind the "crystal-melt" interface, liquid microdroplets are formed. After cooling microdefects appear in the areas where the droplets were located. When these local sections melt, the surface tension and volume decrease, causing a tensile stress in the matrix which should stimulate the flow of interstitial silicon atoms and impurities towards the microdroplet and the reverse flow of vacancies. As a result, during crystallization of microdrops inside them an excess concentration of interstitial atoms is formed, which corresponds to interstitial B-microdefects. When the field reaches critical stresses, conditions are created for the generation of A-microdefects. The thermodynamic calculation of the model was carried out in [152, 153]. In [123] about droplet and nonequilibrium interstitial models it was pointed that microdefects are formed even under conditions that virtually eliminate additional remelting.

The vacancy model [154]. This was based on the assumption that the main equilibrium defects in crystals are vacancies. Within the model framework the formation of microdefects was considered as a result of the condensation of excess vacancies during the crystal cooling. The appearance of dislocation loops of interstitial type was explained by means of a hypothetical process of rearrangement of the inner surface of a flat "vacancy pore" which is accompanied by the appearance of a stream of atoms displaced from the surface to the edges of the cavity. It was

believed that these atoms exist in the liquid state and subsequent crystallization leads to the appearance of a dislocation loop containing a stacking fault of the interstitial type. Further displacement of the surfaces of the cavity should lead to the appearance of a complete dislocation loop of interstitial type. It should be noted the following: it is completely unobvious that the alleged surface rearrangement is energetically justified.

The vacancy-interstitial model [17]. This model is proposed by S.M.Hu from the premise of the incorrectness of isolating one type of defects and neglecting the other; independently of him, the same approach was proposed by E.Sirtl [155]. Within the model framework it is assumed that the silicon interstitial atoms and vacancies coexist in equilibrium at high temperatures. Hence, upon cooling the crystal is supersaturated by both types of point defects. This supersaturation is removed due to two processes of condensation of silicon interstitial atoms and vacancies, which lead to the formation of dislocation loops of interstitial type (A-microdefects) and vacancy clusters (B-microdefects).

In [111] A.J.R. De Kock made a critical review of all the above models. The analysis showed that none of the models fully explains the available experimental data. Equilibrium, nonequilibrium, and drip models do not explain the occurrence of vacancy-type microdefects in crystals. Surface rearrangement considered within the framework of the vacancy model is energetically unfavorable. The vacancy-interstitial model does not explain the influence of the growth rate and the axial temperature gradient, as well as the fact of changing the types of microdefects with increasing crystal growth rate. But, at the same time, the author of the review chose the vacancy-interstitial model, believing it to be the most worthy among others.

2.2. Recombination-diffusion model for the formation of grown-in microdefects

An attempt to solve this situation was the development of V.V.Voronkov in 1982 recombination-diffusion model, which can be considered as a symbiosis of all pre-existing models [6]. The basis of the recombination-diffusion model was the following: an experimentally established with the help of TEM of the interstitial nature of A-microdefects [27, 42]; theoretical calculation of the possibility of formation of "vacancy voids" during cooling of silicon and germanium crystals [112]; the assumption of the vacancy nature of D(C)-microdefects [50]. Within the framework of this model, the type of dominant IPDs is determined by their recombination at the initial point of crystal cooling,

i.e., at temperatures close to the melting point. The result of recombination selection depends on the ratio of the fluxes of transfer of IPDs of the growing crystal (which is resposible for the crystal growth rate, V_g) and the diffusion of IPDs near the crystallization front (which is responsible for the axial temperature gradient, G_a). For large values of the ratio V_g/G_a the diffusion contribution is assumed to be small, and such defects dominate ("survive") whose initial concentration in the crystal were higher [6, 156, 157]. At small V_g/G_a the diffusion contribution is assumed to be the main, and such defects dominate, whose diffusion coefficient above. Thus, it is assumed that at a certain constant value of $V_g/G_a = C_{crit}$ almost complete mutual annihilation of IPDs should occur, which corresponds to the growth conditions of a "defect-free" crystal or "defect-free" region in a crystal. Hence, within the framework of the recombination-diffusion model, it is assumed that IPDs play a decisive role in the aggregation processes. In this model the mathematical apparatus was used for the first time, which made it possible to relate the defective crystal structure to the distribution of thermal fields in crystals during their growth, which was achieved by introducing the growth parameter V_g/G_a into consideration. The physical essence of the recombination-diffusion model is based on the assumption that rapid recombination (earlier ~ 10^{-6} s, later ~ 0.3 s [6]) between the IPDs at the initial time near the crystallization front determines the type of dominant IPDs in the crystal.

It was assumed in [6] that for $V_g/G_a < C_{crit}$ only interstitial A-microdefects are formed as the result of aggregation of silicon interstitial atoms. For $V_g/G_a > C_{crit}$ only vacancy D(C)-microdefects are formed (in the terminology of Ref. [50]) as a result of aggregation of vacancies. In [81, 119, 158], starting from [112], within the framework of technological classification V.V. Voronkov pointed that for $V_g/G_a < C_{crit}$ only interstitial dislocation loops are formed, and only microvoids are formed for $V_g/G_a > C_{crit}$. Hence, the IPDs with a lower concentration and greater diffusion mobility (at the melting point) are silicon interstitial atoms and vacancies become the dominant type of defects [6, 159, 160].

According to [6] C_{crit}=3.3·10^{-5} cm^2/(s·K) and later estimates [86] give the C_{crit}=2.3·10^{-5} cm^2/(s·K).

It is concluded that when $V_g/G_a < C_{crit}$ the crystal is grows in the interstitial growth regime, and for $V_g/G_a > C_{crit}$ the crystal grows in the vacancy growth regime [6]. Large-scale crystals are grown in the vacancy growth mode [53]. It is assumed that the primary defects in the vacancy growth mode are vacancy clusters (octahedral voids) as defects with the lowest energy, which can not turn into dislocation loops [6, 81, 92]. Hence, in crystals obtained at $V_g/G_a > C_{crit}$ the observed vacancy microdefects should clustering into voids [81]. In accordance with the recombination-diffusion model, the formation of a "defect-free" region at $V_g/G_a = C_{crit}$ is postulated, which separates the regions of formation of microvoids and interstitial dislocation loops. It is assumed that this region directly borders on the region of OSF-defects, which in real crystals is the boundary between microvoids and interstitial dislocation loops. It is assumed that in the vacancy growth mode in a crystal, under certain conditions, a joint vacancy-oxygen aggregation due to vacancy supersaturation takes place [81]. The OSF-ring within the framework of this model is the region of distribution of small oxygen precipitates of the vacancy type [81, 85, 161, 162].

According to the recombination-diffusion model, the length of the region near the crystallization front on which recombination can occur is determined by the formula [6]:

$$\ell = \frac{2kT_m^2}{(\Delta H_i + \Delta H_v)G_a}, \qquad (2.1)$$

where k is a Boltzmann constant; T_m is a melting temperature; G_a is a axial temperature gradient; ΔH_i and ΔH_v is a energies of formation of interstitial atom and vacancy, respectively. According to the estimates of Ref. [6], the scale of this region for FZ-Si crystals is ca. 2 mm, for crystals CZ-Si ~ 10 mm.

It should be understood that within the recombination-diffusion model the interaction between impurities and IPDs is not taken into account [119]. Later it was theoretically shown that the introduction of impurity (boron, carbon, arsenic) leads to a shift in the interface between the growth regions [163-165]. It is assumed that during crystal cooling in the

temperature range 1683...1423K the invisible clusters of vacancies (D(C)-microdefects) or silicon interstitial atoms (B-microdefects) are formed depending on the growth regime. It is asserted that these clusters at 1223K $<T \leq$ 1423K are transformed into microvoids or interstitial dislocation loops (A-microdefects), respectively [119]. This transformation process leads to a sharp decrease in the concentrations of IPDs in the corresponding parts of the crystal. In this connection, it is assumed that the residual IPDs participate in the formation of oxygen clusters (complexes) in these regions as the crystal is further cooled [166]. It is assumed that relatively large oxygen clusters with a concentration of $10^9...10^{10}$ cm^{-3} are formed in the temperature range 1223...1023K, and they are the main centers of nucleation of precipitates during subsequent heat treatments [166].

The recombination-diffusion model assumes that the process of defect formation in dislocation-free silicon single crystals occurs in four stages: (1) Rapid recombination of IPDs near the crystallization front. (2) Formation in a narrow temperature range of 1423...1223K depending on the thermal growth conditions of the microvoids or interstitial dislocation loops. (3) The formation of oxygen complexes in the temperature range 1223...1023K. (4) Formation and growth of precipitates as a result of subsequent heat treatments.

Hence, the essence of the recombination-diffusion model is the presence of recombination selection at temperatures close to the melting point; in the assumption of the vacancy nature of the primary grown-in microdefects; in the presence of separate independent regions with interstitial and vacancy microdefects. The recombination-diffusion model, developed first for crystals grown by the floating zone method [6, 40, 78], was subsequently proposed for crystals grown by the Czochralski method [81, 166].

When in the mid of 1990s the existence of microvoids in large-scale crystals was experimentally confirmed [88, 91], the Voronkov's model began to be considered the base both for explaining experimental data and for subsequent theoretical models. In particular, the theoretical model of the point defects dynamics is based on the Voronkov's model. In the model of the point defects dynamics, an attempt is made to relate the defective structure of the crystal to the thermal processes occurring in the melt as a result of consideration of four processes of interaction of IPDs (recombination, diffusion, convection, thermal diffusion) [162, 167-170]. In this case, the crystal is considered as a dynamic system or a solid-state chemical reactor for the transfer and interaction of point defects, their complexes and aggregates. The model of the point defects dynamics

includes the convection, diffusion, thermal diffusion and recombination of IPDs [169], however, recombination playing the most critical role near the melting point [167, 171-175]. It is believed that the formation of grown-in microdefects, their dimensions, concentration and spatial distribution are determined by the dynamics of the crystal and the temperature gradients in the crystal. The analogy with chemical reactions suggests that modeling the point defects dynamics in silicon can lead to a quantitative understanding of the process of formation of grown-in microdefects and to optimize their spatial distribution within the crystal [167]. The model of the point defects dynamics completely ignores the process of interaction of IPDs with impurities during crystal growth [119].

If we analyze all stages of defect formation in silicon on the basis of a recombination-diffusion model, we see that this model based on the postulate of the recombination of IPDs near the crystallization front during the crystal growth. This postulate proceeds from the assumption that recombination of intrinsic defects in the high-temperature region occurs in the same way as in the low-temperature region. As a result of this assumption, the recombination-diffusion model by isolating individual regions of the crystal with different types of IPDs makes it very easy to explain the homogeneous formation of dislocation loops and microvoids. Control of these areas of the crystal with the help of thermal growth conditions (growth method, growth rate and temperature gradients) makes it possible to develop mathematical models for the formation of such defects.

We note that the second stage of the defect formation process in accordance with the recombination-diffusion model corresponds to the available experimental results. In fact, depending on the growing method and the thermal growth conditions of the crystals, the formation of microvoids and interstitial dislocation loops occurs in a narrow temperature range at temperatures $T \leq T_m - 300$ [114, 119, 121, 122].

However, the third and fourth stages of the defect formation process which are associated with impurity precipitation in silicon are very inconclusive. And also the postulate about recombination of IPDs near the crystallization front leads to the primacy of IPDs over impurity atoms which contradicts most of the experimental data on impurity precipitation during crystal growth [39, 52, 176, 177]. For example, in the classical paper [122] it is shown that microvoids are formed on already formed impurities precipitates. Trying to eliminate this contradiction within the framework of the recombination-diffusion model, it was suggested that during the crystal cooling the vacancies are bound by oxygen and nitrogen

atoms and to form complexes [178, 179]. With subsequent thermal treatments the complexes develop into precipitates.

Contradictions between the experimental and theoretical results are due to the fact that until recently the theoretical description of impurity precipitation during the crystal cooling after grown was impossible. The classical theory of nucleation of particles of the second phase is based on the fact that the decomposition of a solid solution begins with the nucleation process, i.e., physically clear centers are formed and their then grow. This growth leads to the isolation of a new phase inside the initial solid solution. In general, the precipitation of the second phase occurs in three stages: (1) a local fluctuation of the chemical potential (formation of the nucleus), (2) the formation of a stable nucleus, (3) growth and coalescence of precipitates [180]. According to the thermodynamic theory of fluctuations, the distribution function of nuclei of various sizes is $f_0(R) \sim \exp\left\{-\frac{\Delta G(R)}{kT}\right\}$, where ΔG is a minimum energy is for creating the nucleus of the desired size, k is a Boltzmann constant [180, 181]. In this case the formation of a critical nucleus at high temperatures is very problematic. The classical theory of nucleation of particles of the second phase indicates that critical nuclei of small dimensions are more likely to arise in the low-temperature region [49]. The critical size of the nucleus increases with increasing temperature [50, 182]. That is why in the theoretical papers of the apologists of the recombination-diffusion model are pointed that when the crystal is cooled from the melting point to temperatures of 1173±50K, the impurity atoms do not participate in defect formation processes. In this case, as has been repeatedly pointed out above, the model of the point defects dynamics which is based on the basic positions of the recombination-diffusion model ignores the process of interaction of IPDs with impurities [119].

It should be noted that recently a partial "revision" of the recombination-diffusion model takes place, which leads to a certain convergence of its individual supporters with the provisions of alternative qualitative model of defect formation which will be considered below. Thus, in [183-185] the question of the influence of the growth parameter V_g/G_a on the formation of micropores and dislocation loops was critically examined. It is assumed that for a given melt zone, diameter, and crystal length, the temperature gradient at the crystallization front is a function of the growth rate of the crystal. Furthermore, a bold assumption is made about the coexistence of vacancy and interstitial clusters in growing crystals [184]. Such a drift of followers of the postulate of

recombination of IPDs near the crystallization front to the basic positions of the alternative model testifies about desire to explain the existing experimental results on the investigation of defect formation during the growth of silicon single crystals that do not fit into the framework of the recombination-diffusion model. Such a main experimental result is the presence of impurity precipitation during crystal growth [13]. Note that such "revisionist" views were immediately criticized [186, 187].

2.3. Model of the point defects dynamics

Based on the recombination-diffusion model the mathematical model of the point defects dynamics in silicon has been developed, which quantitatively explains the homogeneous character of the formation of microvoids and dislocation loops and is the basis for understanding the relationship between the defect structure of the crystal and the processes occurring in the melt [119]. The calculation of defect concentrations is made from the assumption of rapid recombination of vacancies and silicon interstitial atoms in a narrow region near the crystallization front, which leads to the fact that the primary defects are in equilibrium concentrations [6]. Based on the flux of defects in the interior of the crystal, it is possible to obtain the concentration of the remaining primary defects after passing through a narrow recombination region. With further crystal cooling during their growth, the primary defects are collected in clusters: microvoids in the region of prevalence of vacancies and dislocation loops in the region of dominance of silicon interstitial atoms [119].

The model of the point defects dynamics in the general case consists of three model approaches: rigorous, lumped, and discrete-continuous [188]. The rigorous model requires the solution of integral-differential equations for the concentration of point defects and in this model the distribution of grown-in microdefects is a function of the coordinates, time and time of evolution of the microdefect size distribution [81, 119, 158, 172, 189]. A lumped model uses the approximation of the mean defect radius by the square root of the mean defect area [188]. This approximation is taken into account in the additional variable, which is proportional to the total surface area of the defect. A lumped model is effective in calculating the two-dimensional distribution of grown-in microdefects [178, 188]. Both models use the classical theory of nucleation, suggesting the calculation of the formation of stable nuclei and the kinetics of diffusion-limited defect growth. The discrete-continuous model assumes a complex approach: solving discrete equations for the smallest defects and solving Fokker-Planck equations for larger defects [162, 190, 191]. Let us repeat that all

these models quantitatively explain the homogeneous character of the formation of microvoids and dislocation loops [119]. The formation of microvoids or dislocation loops begins at temperatures $T \le T_m - 300$ [6, 192]. It is assumed that impurity precipitation occurs only at the stage of thermal treatment of the crystal [119, 178, 179, 188].

A rigorous model describing the dynamics of defects in a crystal includes the kinetics of Frenkel reactions, the nucleation of point defects, the growth of clusters, and the balance of point defects [119]. In the kinetics of Frenkel reactions mutual annihilation and the formation of pairs of point defects in the entire volume of the crystal are considered. In the section on nucleation of point defects a series of bimolecular reactions is considered. In the cluster growth section the motion of point defect complexes in the direction from the melt-crystal interface is considered.

The balance of IPDs includes their diffusion and convection, Frenkel reactions and their expenditure on the formation of clusters. The basic equations of balance of point defects are written as follows:

$$\frac{\partial C_i}{\partial t} = \frac{\partial\left(D_i \frac{\partial C_i}{\partial z}\right)}{\partial z} - V_g \frac{\partial C_i}{\partial z} - k_{IV}(C_i C_v - C_{i,e} C_{v,e}) - $$
$$- 4\pi D_i (C_i - C_{i,e}) \int_0^t R_{cl,i}(z,\tau,t) J_{cl,i}(\xi,\tau) d\tau - J_{cl,i}(z,t) m_i^* \qquad (2.2)$$

$$\frac{\partial C_v}{\partial t} = \frac{\partial\left(D_{vi} \frac{\partial C_{vi}}{\partial z}\right)}{\partial z} - V_g \frac{\partial C_{vi}}{\partial z} - k_{IV}(C_i C_v - C_{i,e} C_{v,e}) - $$
$$- 4\pi D_v (C_{vi} - C_{v,e}) \int_0^t R_{cl,v}(z,\tau,t) J_{cl,v}(\xi,\tau) d\tau - J_{cl,v}(z,t) m_v^* \qquad (2.3)$$

Here $J_{cl,j}$ is a concentration of critical clusters, m^* is a amount of monomers, R_{cl} is a radius of critical cluster, z is a distance from the crystallization front, $J(\xi,\tau)$ is a cluster formation rate, k_{IV} is a recombination factor, τ is a cluster formation time, $\xi = z - \int_\tau^t V_g d\tau'$, где τ' is the time between t and τ.

In equations (2.2) and (2.3), the first term is responsible for the change in the concentration of point defects due to their diffusion, the second term is the same due to their convection, the third term is the same due to the Frenkel reactions, the fourth term is the same due to their spending on existing clusters, the fifth term is the same due to the formation of new

clusters. The rate of expenditure of point defects to the formation of new clusters is negligible and can be ignored [119].

The diffusion-limited growths rates of clusters for any z and t formed for the corresponding ξ and τ are described by the following equations:

$$\frac{\partial R_{cl,i}^2(z,\tau,t)}{\partial t} = \frac{2D_i}{\psi_{i,cl}}(C_i - C_{i,e}) - V_g \frac{\partial R_{cl,i}^2(z,\tau,t)}{\partial z} \tag{2.4}$$

$$\frac{\partial R_{cl,v}^2(z,\tau,t)}{\partial t} = \frac{2D_v}{\psi_{v,cl}}(C_v - C_{v,e}) - V_g \frac{\partial R_{cl,v}^2(z,\tau,t)}{\partial z} \tag{2.5}$$

where ψ is a density of monomers in the cluster.

The nucleation rate equations are described as follows:

$$J_{cl,i}(z,t) = [4\pi R_{cl,i}(m_i^*) D_i C_i]\left(k_b T \ln\frac{C_i}{C_{i,e}}(12\pi F_i^* k_b T)^{1/2}\right)[\rho_{site} e^{(-F_{iv}^*/k_b T)}] \tag{2.6}$$

$$J_{cl,v}(z,t) = [4\pi R_{cl,v}(m_v^*) D_{vi} C_v]\left(k_b T \ln\frac{C_{vi}}{C_{v,e}}(12\pi F_v^* k_b T)^{1/2}\right)[\rho_{site} e^{(-F_v^*/k_b T)}] \tag{2.7}$$

where F^* is the maximum change in free energy.

The initial length (or height) of the crystal is taken as zero. For a crystal of finite length *h* the equilibrium conditions are assumed to prevail over the entire surface including the crystal-melt interface:

$$h(t=0) = 0 \tag{2.8}$$

$$C_i(z=0,t) = C_{i,e} \tag{2.9}$$

$$C_v(z=0,t) = C_{v,e} \tag{2.10}$$

$$C_i(z=h,t) = C_{i,e} \tag{2.11}$$

$$C_v(z=h,t) = C_{v,e} \tag{2.12}$$

The initial size of the critical cluster is negligible compared to the size of the microdefect. Hence, the initial size of a stable cluster has a negligible effect on its final size. The initial size of a stable cluster (nucleus) is calculated based on the number of monomers in the critical cluster:

$$R_{cl,i}(\xi,\tau) = \left(\frac{3}{4\pi}\frac{m_i^*}{\psi_{i,cl}}\right)^{1/3} \tag{2.13}$$

$$R_{cl,v}(\xi,\tau)=\left(\frac{3}{4\pi}\frac{m_v^*}{\psi_{vi,cl}}\right)^{1/3} \tag{2.14}$$

Equations (2.2)-(2.12), together with the energy balance of the hot zone are control and quantitatively determined the dynamics of point defects. In the semiconductor industry the quality of the crystal is often determined based on the total concentration or total density and is represented by the average size of existing clusters. The total density of clusters is calculated by summing clusters of different sizes in the current state:

$$N_{cl,i}=\int_0^t J_{cl,i}(\xi,\tau)d\tau \tag{2.15}$$

$$N_{cl,v}=\int_0^t J_{cl,v}(\xi,\tau)d\tau \tag{2.16}$$

The average radius of a cluster is defined as follows:

$$R_{cl,i,avg}=\left(\frac{\int_0^t R_{cl,i}^3(z,\tau,t)J_{cl,i}(\xi,\tau)d\tau}{\int_0^t J_{cl,i}(\xi,\tau)d\tau}\right)^{1/3} \tag{2.17}$$

$$R_{cl,v,avg}=\left(\frac{\int_0^t R_{cl,v}^3(z,\tau,t)J_{cl,v}(\xi,\tau)d\tau}{\int_0^t J_{cl,v}(\xi,\tau)d\tau}\right)^{1/3} \tag{2.18}$$

where the sign "avg" denotes the mean.

The model of the point defects dynamics is one-dimensional in nature, and, consequently, the influence of radial diffusion prevailing near the surface of the crystal is not taken into account here. Therefore, the model can be applied to the axial distribution of defects in a crystal at fixed radial positions far from the surface.

The energy balance can be calculated using quasi-stationary approximations [119]. Time-dependent changes in the temperature profile in the growing crystal are obtained by calculating the temperature profiles at different crystal lengths at different growth stages. The basic assumptions for the calculations are follows: (1) The system is axisymmetric. (2) The melt can be approximated as a solid. (3) Two solids are in perfect contact. (4) The energy transition from the open end occurs through radiation and convection. (5) The energy balance at the crystal-

melt interface is key to determining the shape of the interface. (6) The convection between the two phases seems to be in good agreement with the heat and mass transfer coefficients. (7) The conditions of constant temperature accurately determine the boundary of the computational domain.

The temperature field in the growing crystal in reference to the fixed crystal-melt interface varies only in the early stages of growth, when the crystal is still very small. When the length of the crystal increases, the temperature fields in the crystal a strong change. Hence, it is assumed [119] that the temperature field in a long crystal must be regarded as a temperature field in the cross section of the crystal. Therefore, the calculation of the nonequilibrium dynamics of point defects can be performed under the assumption that the growing crystal passes through the quasistationary temperature field of a long crystal [119]. Hence, according to the authors of [119], the distribution of defects in the crystal can be predicted on the basis of the assumption of a fixed temperature field in reference to the interface.

The mathematical model of the point defects dynamics is the process of defect formation in the form of a homogeneous formation of clusters and their development without the participation of impurity. The calculation of the concentrations of primary defects is made from the assumption of a rapid recombination of vacancies and silicon interstitial atoms in a narrow region near the crystallization front, which leads to the fact that the primary defects are in equilibrium concentrations. Based on the flux of defects in the interior of the crystal it is possible to obtain the concentration of the remaining primary defects after passing through a narrow recombination region. In this case the main type of primary defects is determined by the growth parameter V_g/G_a: when the growth parameter exceeds the threshold value, vacancies are the primary type of defects, and for the parameter V_g/G_a less than the threshold one, the silicon interstitial atoms [6]. With further crystal cooling during the growth process, the primary defects are collected in clusters: microvoids in the region of prevalence of vacancies and interstitial dislocation loops in the region of predominance of silicon interstitial atoms. It is shown that the growth of such clusters becomes advantageous only at a size greater than some critical point and it is necessary to overcome the energy barrier to form the nucleus of the cluster. The value of this barrier decreases with decreasing temperature, as a result of which the rate of formation of new defects is extremely low at a temperature below the threshold and sharply increases as the nucleation temperature approaches. With further cooling, the

nucleation rate decreases, since the concentration of the predominant type of IPDs decreases due to diffusion deposition on the clusters. The value of the nucleation temperature, for example, for microvoids depends on the primary concentration of vacancies and decreases when it decreases [81, 92]. The interaction between the IPDs and impurities in the model of the point defects dynamics and outside its framework is completely ignored [119].

Proceeding from the basic assumptions of the model of the point defects dynamics [6, 81, 92, 119], the authors of [7] investigated the influence of axial temperature gradients on the crystallization front and radial inhomogeneity in their distribution on the processes of vacancy-interstitial recombination and the formation of microvoids. Based on the analysis of numerous calculated data obtained during global thermal modeling of thermal zones, a method for specifying a two-dimensional temperature field that reflects the main changes in temperature distributions in a crystal is proposed [7]. The analytical simplicity of specifying a two-dimensional temperature field made it possible to recommend it for parametric and test calculations.

For a two-dimensional thermal field the used of the known axial temperature dependence [6]: $\frac{1}{T} = \frac{1}{T_m} + \frac{G_a Z}{T_m^2}$; here Z is a distance from the crystallization front. Consider a crystal with a length L = 60 cm. The length of the crystal is divided into two sections (Z_0, Z_1) and (Z_1, Z_2). It is assumed that at a distance L = 60 cm ($Z = Z_2$) from the crystallization front ($Z = Z_0$), the radial inhomogeneity of the temperature field disappears and the temperature is T = 1173 K.

On the first section the temperature field is given by:

- Along the axis

$$\frac{1}{T} = \frac{1}{T_m} + \frac{G_a Z}{T_m^2} \qquad (2.19)$$

- Along the crystal surface

$$\frac{1}{T} = \frac{1}{T_m} + \frac{G_e Z}{T_m^2} \qquad (2.20)$$

where the indices "a" and "e" mean directions along the axis or along the crystal surface, respectively.

On the crystallization front, G_a varies for 19 variants through 5.0 K/cm from 91.0 to 1.0 K/cm, here G_e is selected from the given ratio

$p = G_e/G_a$. Also considered 19 variants of variation p = 1.96...1.06 with a step of 0.05.

On the second section the temperature field is given by:

- Along the axis

$$\frac{1}{T} = \frac{1}{T_1} + \frac{G_{a1}(Z - Z_1)}{T_1^2} \quad (2.21)$$

- Along the crystal surface

$$\frac{1}{T} = \frac{1}{T_1} + \frac{G_{e1}(Z - Z_1)}{T_1^2} \quad (2.22)$$

Here T_1 is calculated from equations (2.19) and (2.20) and a given coordinate Z_1, which depends on the gradient from the following given formula: $Z_1 = a - b(G_a - g)$. Parameters are selected as: a=11, b=0,1, g=1. The gradient values at the beginning of the second section G_{a1} and G_{e1} are calculated from the equalities (2.21) and (2.22) for given $Z = Z_2$ and $T_{a2} = T_{e2}$ = 1173 K [7].

The proposed method of analytical determination of a two-dimensional thermal field in a crystal allows one to simulate situations with different values of G_a and G_e at short distances from the crystallization front in the region where the (V+I)-recombination process occurs. At large distances corresponding to the temperature range 1373...1273 K, the values of the axial gradients are rather low (~ 10 K/cm). To manage gradients at lower temperatures, one can also use this analytical approach making it more complicated by specifying of the input data for the third accounting section.

The two-dimensional temperature distribution in a crystal 60 cm long changed in time in accordance with the proposed procedure from large values G_a = 81.0 K/cm to small G_a = 16.0 K/cm. The calculations allow us to represent the influence of the axial gradient G_a and the ratio G_e/G_a on the behavior of the (V+I)-border and the radial position of the OSF-ring in a convenient graphical form [7].

The greatest practical interest is the effect of the crystal cooling rate during its growth on the concentration and size of microvoids. Using the distribution of residual (V+I)-concentrations after recombination, the process of formation of microvoids was calculated [161]. As the gradient

G_a is increased in the range 16…71 K/cm, the voids concentration N_v increases from $4.0 \cdot 10^4$ to $2.4 \cdot 10^5$ cm^{-3}, and the void size R_v decreases from 290.0 to 95.0 nm. Thus, as the axial temperature gradient is increased at the crystallization front, the decrease of voids size and the increase in their concentration are observed [7].

The authors of [7] note that the growth of defect-free regions (without microvoids) corresponding to the minimum concentration of vacancies is possible by substantially increasing the cooling rate of the ingot. However, in the open thermal zones these regions are very small and concentrated near the lateral surface of the crystal where the greatest axial temperature gradients occur at the crystallization front. In the ingot center these gradients are much smaller.

It is established that when the diameter of the ingot increases from 100 to 200 mm, a radial inhomogeneity of the axial gradient (p increases from 1.3 to 1.9) occurs with a simultaneous decrease of G_a in 1.5…2.0 times [7]. For a more significant expansion of the defect-free area it is necessary to reduce the parameter p and increase G_a. To obtain a defect-free area, a decrease in the residual concentration of vacancies needed C_v up to 10^{12} cm^{-3} [6]. In Ref. [116] this is achieved by radial inversion of the gradient region (when the central gradients are higher than the marginal gradients). This transforms the V-shaped form of the OSF-ring into a W-shaped. The proposed approach makes it possible to perform a parametric study of such possibilities without reference to a specific thermal zone [7].

A further modernization of this approach was made in [170], where the effect of cooling conditions on the process of defect formation in a growing single crystal based of an analytical specification of the temperature field in a crystal and a modernized model of defect formation was investigated. In the modernized model for the formation of grown-in vacancy microdefects, unlike the previous [7], multidimensionality of the process of vacancy transfer is taken into account. To realize this model, taking into account the axial symmetry and nonstationarity of the growing process, a numerical algorithm and a computational program are developed within the framework of the global thermal modeling complex CRYSTMO [193].

The algorithm for calculating the distribution of the IPDs (vacancies V and silicon interstitial atoms I) as a result of the (V+I)-recombination process in the nonstationary formulation is retained by the previous [194]. However, the algorithm for calculating of vacancy microdefects

(microvoids) formation has been substantially reworked in comparison with the previous one-dimensional approach [161].

In accordance with this algorithm, the decrease in the residual concentration of vacancies C_v occurs due to their diffusion to the resulting microvoids. Their common flow Q_v is obtained as a result of the integration of flows for voids of different sizes (radius R_v):

$$Q_v = 4\pi D_v (C_v - C_{ve}) N_v \langle R_v \rangle = 4\pi D_v (C_v - C_{ve}) \int I_v(t') R_v(t', t) dt' \quad (2.23)$$

The flux refers to the element of the crystal at time t; C_{ve} is a equilibrium concentration of vacancies. The diffusion coefficient of vacancies D_v depends on the temperature T and the position of the element of the crystal under consideration:

$$D_v = D_{vm} exp[-E_{vD}/(kT) + E_{vD}/(kT_m)] \quad (2.24)$$

where T_m is a silicon crystallization temperature; k is a Boltzmann constant; D_{vm} is a diffusion coefficient at the crystallization front; E_{vD} = 0.35 eV is a energy barrier for diffusion of vacancies.

The equilibrium distribution of vacancy concentration is given in the form

$$C_{ve} = C_{vm} exp[-E_v/(kT) + E_v/(kT_m)] \quad (2.25)$$

where C_{vm}= $8.84 \cdot 10^{14}$ cm^{-3} is a concentration of vacancies at the crystallization front; E_v = 4.5 eV is a energy barrier of formation of vacancies [7]. The following notation is used in Eq. (2.23): N_v is a current voids density (these voids are formed at the moment of time preceding the current moment, when $t' < t$); $\langle R_v \rangle$ is the average radius of voids present at the current moment in the element under consideration; $I_v(t')$ is the rate of void formation in the element under consideration at time t'; $R_v(t', t)$ is the radius of the voids formed at time t' and grown for a period from t' to t.

The defect growth rate I_v is a function of temperature T and concentration C_v, which are depending on time and position in the crystal. The stationary formula for I_v describes well the formation of voids in

silicon due to the high diffusion of vacancies and, hence, of the rapid entry of vacancies in the void [161]:

$$I_v = \sigma_{Si} D_v C_v \sqrt{16\pi/3F_v kT}\, exp(-F_v/kT) \quad (2.26)$$

where σ_{Si} is a surface energy of the void; F_v is an energy barrier of void formation. The vacancy diffusion equation, taking into account the vacancy losses, is written as follows:

$$\partial C_v / \partial t = div(D_v grad C_v) - Q_v \quad (2.27)$$

To solve this equation, according to Eq. (2.23), it is necessary to know every position of the crystal, i.e., the entire prehistory of defect growth, which seems to be a very complicated calculation problem.

The authors of [170] solve this problem in the following approximate way. The average radius $\langle R_v \rangle$ in Eq. (2.23) is replaced by the value $\langle R_v^2 \rangle^{1/2}$. This value is not accurate, but close enough to $\langle R_v \rangle$.

Equation for $\langle R_v^2 \rangle$ is described as

$$\langle R_v^2 \rangle = \frac{\int I_v(t') R_v^2(t', t) dt'}{N_v} \quad (2.28)$$

where current void density N_v is calculated as the integral of the nucleation rate:

$$N_v = N_{v0} + \int I_v(t') dt' \quad (2.29)$$

and its initial value is taken as $N_{v0} = 0$. On the next step an auxiliary quantity U_v is introduced as an integral in the equation (2.28)

$$U_v = \int I_v(t') R_v^2(t', t) dt' \quad (2.30)$$

and then the vacancy flux to the voids can be written

$$Q_v = 4\pi D_v (C_v - C_{ve})(U_v N_v)^{1/2} \quad (2.31)$$

Thus, the problem is reduced to the calculation of three fields: $C_v(\bar{r}, t)$, $N_v(\bar{r}, t)$ and $U_v(\bar{r}, t)$, where $\bar{r}$ is a radius-vector of the element of the crystal, characterizing its position. With this approach there is no need to store the history of defect formation, and instead of the pore size distribution, two quantities are used: U_v and N_v. And the derivative $\partial U_v / \partial t$ is not expressed through the void density function, but through

N_v, and C_v due to the simple kinetic equation for R_v^2. From (2.30) we can obtain the kinetic equation for U_v (where ρ_{Si} is the resistivity of silicon):

$$\partial U_v/\partial t = (2/\rho_{Si})D_v(C_v - C_{ve})N_v \quad (2.32)$$

Finally, taking into account the crystal growth rate V_g the system of equations for the three fields C_v, U_v and N_v, taking into account the vacancy diffusion equation (2.28), is written as follows:

$$\frac{\partial C_v}{\partial t} = -V_g \frac{\partial C_v}{\partial z} + D_v div(grad C_v) - 4\pi D_v (C_v - C_{ve})(U_v N_v)^{1/2} \quad (2.33)$$

$$\frac{\partial U_v}{\partial t} = -V_g \frac{\partial U_v}{\partial z} + \frac{2}{\rho_{Si}} D_v (C_v - C_{ve}) N_v \quad (2.34)$$

$$\frac{\partial N_v}{\partial t} = -V_g \frac{\partial N_v}{\partial z} + I_v(r, t) \quad (2.35)$$

The system of equations (2.33)-(2.35) is a mathematical formulation of the model. The most important result of the simulation consists in calculating the density $N_v(\bar{r}, t)$ and the average voids radius $\langle R_v \rangle$ for the region of the crystal remote from the crystallization front, in which the microdefect formation process is completed.

In the calculation of the formation of grown-in microdefects the analytical formulation of temperature fields in a crystal uses the approach proposed earlier [7] which realized for the (V+I)-recombination process with some features for temperature fields far from the crystallization front. In contrast to [7], to take into account the variation of temperature gradients far from the crystallization front, the region of the crystal adjacent to the crystallization front (z = 0…60 cm) is divided into three accounting sections. In this case the temperature of the crystal decreases from 1683 to 1473 K in the first region, from 1473 to 1173 K in the second region, and T = 1173 K on the third region. Variations in the temperature gradient in the second region occur in the temperature range of the formation of grown-in microdefects [119] and are decisive. In the third region the temperature of the crystal is sufficiently low and no effect on the defect formation process [170].

It is assumed that the axial temperature gradient at the center of the crystallization front is fixed: G_a = 51.0 K/cm. Radial inhomogeneity of the gradient at the crystallization front G_a/G_e = 0.67, i.e., on the edge of a

crystal G_a = 76.5 K/cm. The parameter $V_g/G_a = 0.134$ $mm^2/(K \cdot min)$, then the critical growth rate $(V_g)_{crit} = 0.683$ mm/min. The range of variation in the crystal growth rate was analyzed: $V_g = (1.0 \ldots 0.67)(V_g)_{crit}$ or V_g = 0.683…0.45 mm/min. The effect on the ingot's cooling rate also turns out to be a change in the axial temperature gradient G_a far from the crystallization front for the range of microvoids formation temperatures (1200 K < T < 1400 K) [170]. Such changes can be achieved by changes in the construction, for example, increase in the axial temperature gradient is provided by increase in the flow of heat from the crystal to the thermal shield [195].

Before calculating the process of microdefect formation it is necessary to calculate the distribution of IPDs after the (V+I)-recombination process when the temperature field in the crystal is specified in the manner described above.

Comparison of the calculation results with the data of Ref. [7] shows that large values of the density and, hence, smaller values of the size of microdefects are obtained. This is explained by the fact that the influence of two-dimensional diffusion of vacancies in calculating their losses on the formation of grown-in microdefects has been taken into account, otherwise, according to [161], substantially higher values of the size of microdefects are obtained.

The model of the point defects dynamics in this approach and in its various modifications [7, 100, 119, 120, 157, 162, 167, 169-172, 174] is in good agreement with the experimental results on the homogeneous formation of microvoids. At the same time, a theoretical description of the homogeneous formation of A-microdefects (interstitial dislocation loops) is not entirely correct, since the deformation mechanism for the formation of dislocation loops is not taken into account. This directly follows from the fact that the model of the point defects dynamics cannot explain defect formation processes that pass during the cooling of the crystal in the temperature range $\sim(T_m - 300K)$, since this model does not take into account the process of interaction of IPDs and impurity atoms. This significant drawback is due to the fact that the physical model (recombination-diffusion model [6]), which is the basis for the model of point defect dynamics, is partial, since it does not describe all experimental results on the formation and transformation of grown-in microdefects. The assumption that complex formation with the participation of an impurity occurs at temperatures below 1173 K allows

authors of various mathematical models of the process of oxygen precipitation to transfer the experimental results of the study of heat-treated single crystals on the formation of grown-in microdefects [38, 125, 176, 196-198]. Mixing the systems of grown-in and post-growth microdefects leads to a distortion of the real process of defect formation, despite the further development and improvement of modern methods of computer modeling [120, 170, 194, 199]. Therefore, the model of the point defects dynamics cannot be considered a quantitative model.

2.4. Heterogeneous (two-stage) model of grown-in microdefect formation

A heterogeneous (two-stage) model for the formation of grown-in microdefects, as a physical model, has been actively developed in recent times on the basis of the synthesis of numerous experimental and theoretical studies [12, 13, 45, 200]. The fundamental difference of this model from all varieties of the model of the point defects dynamics is in relation to the question about recombination of IPDs at high temperatures.

This model is based on experimental studies of the conditions and causes of the formation of grown-in microdefects. Thus, recently, with the help of TEM the entire nomenclature of grown-in microdefects in FZ-Si and CZ-Si crystals of various diameters were studied; standard patterns of macro-distribution of grown-in microdefects are revealed depending on thermal conditions of crystal growth; the transformation of grown-in microdefects during various technological treatments was observed; the physical nature (sign of the crystal lattice deformation) of all types of grown-in microdefects were determined [13, 27, 42, 84, 122]. The experimental results of the study of the processes of transformation of grown-in microdefects under various thermal treatments, as well as during technological effects, for example, ion implantation and epitaxy, confirm the conclusion that the mechanisms and processes of formation, growth and transformation of microdefects in single crystals of FZ-Si and CZ- Si are identical [101]. During crystal growth, a continuous process of transformation of the original defect structure takes place. Technological impacts (high-temperature treatments, radiation treatments) on dislocation-free silicon single crystals lead to inevitable change in the bulk distribution and transformation of interstitial microdefects. This transformation is accompanied by the enlargement of microdefects and a decrease in their concentration.

The main points of the heterogeneous (two-stage) model of grown-in microdefect formation are the following:

- Recombination of IPDs at high temperatures can be neglected.
- Background impurities of carbon and oxygen are involved in the process of defect formation as nucleation centers.
- The decomposition of a supersaturated solid solution of point defects during crystal cooling from the crystallization temperature occurs according to two independent mechanisms (or branches): vacancy and interstitial.
- The basis of the defect formation process is the primary agglomerates that are formed during the crystal cooling from the crystallization temperature due to the interaction of point defects "impurity + IPD".
- During crystal cooling at $T \le T_m - 300$ temperature secondary grown-in microdefects are formed.
- The formation of secondary grown-in microdefects is due to the action of coagulation (microvoids and interstitial dislocation loops) and deformation (interstitial dislocation loops) mechanisms.
- The vacancy and interstitial branches of the heterogeneous (two-stage) model have a symmetry that consists in the parallelism of defect formation processes during the decomposition of a supersaturated solid solution of point defects, the consequence of which is the formation of vacancy and interstitial grown-in microdefects of the same type and the growth of dislocation-free silicon single crystals in the vacancy-interstitial growth regime.

The main points of the heterogeneous (two-stage) model for the formation of grown-in microdefects in dislocation-free silicon single crystals were considered in [12, 13, 45, 52, 101, 104, 108, 201-203] and on their basis we can speak about following.

Dislocation-free silicon single crystals are devoid of effective internal sinks (macroscopic defects) for IPDs, and the lateral surface of the ingot, due to purely diffusion limitations, cannot also be an effective external sink [117]. In real silicon single crystals the concentration of background impurities (oxygen and carbon) is often higher than the concentration of IPDs. These impurities contribute to increase in the temperature of formation of the initial aggregates, i.e., they facilitate the process of their formation. In this connection, the presence in the dislocation-free silicon single crystals both impurities and IPDs leads to complex processes of interaction between them [52]. The key (fundamental) role in defect formation is played by the processes of interaction between IPDs and impurities. These processes determine the defect structure of dislocation-free silicon single crystals [200]. The decomposition of supersaturated

solid solutions of point defects begins near the crystallization front and proceeds during the crystal cooling.

The heterogeneity of the model is determined by the fact that the decisive factor in the start of the process of defect formation in dislocation-free silicon single crystals is the formation of primary "impurity + IPDs" complexes, whereas in the recombination-diffusion model underlies the interaction "IPDs + IPDs". Therefore, in the recombination-diffusion model, it is concluded that the formation of grown-in microdefects is based on the decomposition of a supersaturated solid solution of IPDs that occurs during the crystal cooling from the crystallization temperature. Hence, in all modifications of this model, it is *a priori* considered that all types of grown-in microdefects are different stages of the formation of only two grown-in microdefects: the microvoids and interstitial dislocation loops. Consequently, a heterogeneous (two-stage) model for the formation of grown-in microdefects and a recombination-diffusion model are in contradiction with each other. And this contradiction is due to different understanding of the process of recombination of IPDs near the crystallization front.

The heterogeneous model is based on two stages of defect formation in the process of crystal cooling (the formation of primary and secondary grown-in microdefects) and is therefore also defined as a two-stage mechanism for the formation and transformation of grown-in microdefects.

For a vacancy branch, it is theoretically possible to expect both a purely vacancy and a vacancy-impurity aggregation. Vacancy-impurity aggregation begins before the purely vacancy aggregation. This is because the process of formation of impurity particles upon absorption of vacancies from their supersaturated solid solution is thermodynamically profitable [202].

The formation of microprecipitates results in excess of the matrix volume, and one vacancy for each two oxygen atoms will be absorbed. Then the process bifurcates. First, further absorption of vacancies and impurities by a growing microdefect leads to a decrease in the concentration of vacancies. As a result, precipitates begin to additionally absorb oxygen without the participation of vacancies, their size will grow, and the deformation around them will changing from vacancy to interstitial with the formation of interstitial D-microdefects [12, 45, 101]. Further aggregation is accompanied by the emission of silicon interstitial atoms.

These assumptions, made on the basis of a careful analysis of TEM-studies of grown-in microdefects are found experimental confirmation in the works of Novosibirsk scientists [204-207]. Detailed studies of the

kinetics of point defects clusters nucleation upon irradiation of thick silicon crystals in a high-voltage electron microscope have shown that in the center of the irradiation zone where the irradiation intensity reaches $6 \cdot 10^{19}$ e·cm^2/s are observed the signs of accumulation of vacancies in the temperature range 293...643K [207]. The resulting secondary defects were defects of interstitial type, which, in conditions of accumulation of vacancies, suggested the possibility of nucleation of interstitial defects on vacancy clusters. This assumption was confirmed by investigations in a high-resolution electron microscope, which made it possible to fix successive stages of the transformation of the vacancy cluster into interstitial [206]. Most vividly this effect is show in the high-purity FZ-Si. Furthermore, based on TEM-studies it was suggested that interstitial grown-in microdefects with small displacement vectors can be formed in large-scale silicon in the mode of vacancy growth (in the terminology of the model of point defect dynamics) [204]. In fact, these works are independent experimental confirmation of the adequacy of the heterogeneous (two-stage) mechanism of formation and transformation of grown-in microdefects that describes the real defect structure of dislocation-free silicon single crystals.

Secondly, in the interstitial mode of crystal growth, a small number of primary grown-in microdefects are "surviving" causing a tensile deformation in the crystal matrix. These precipitates begin to absorb additional vacancies with formation of vacancy D-microdefects. With interstitial mechanism, there are also nucleation centers based on interstitial oxygen atoms. However, carbon atoms play a catalytic role in this case. Supersaturation with interstitial silicon atoms leads to the appearance of "carbon + silicon interstitial atoms" complexes.

The supersaturation by silicon interstitial atoms leads to the formation of micro-precipitates of SiC, and can also lead to joint precipitation of oxygen and carbon. An increase in the size of interstitial microdefects causes a substantial decrease in the concentration of interstitial silicon atoms, which creates conditions for impurity precipitation. In this case the formation of particles of the impurity phase is accompanied by the emission of silicon atoms into the interstices. As a result, interstitial D-microdefects are formed [21, 49, 51].

Hence, during the crystal growth the "vacancy-oxygen" aggregation occurs during the decay of a supersaturated solid solution of vacancies, as well as "interstitial-carbon" aggregation in the decay of a supersaturated solid solution of silicon interstitial atoms [52, 108, 201]. D-microdefects are uniformly distributed small B-microdefects which are then transformed into A-microdefects [13]. In general, A-microdefects can be formed by the

transformation of B-microdefects both due to the mechanism of prismatic extrusion, and due to condensation of silicon interstitial atoms [13].

2.5. About various approaches to solving the problem of defect formation in silicon

Examination of the recombination-diffusion and heterogeneous models shows that their difference, basically, lies in the question of the role of an impurity in the formation of grown-in microdefects. Two tendencies can be clearly seen in resolving this issue. The first trend is to develop a qualitative model of a phenomenon, followed by a search for facts that support this model. By this way went V.V. Voronkov (born. 1936), when he proposed the main points of the recombination-diffusion model [6]. From these positions, the priority of IPDs in the formation of grown-in microdefects was postulated and the participation of the impurity was denied. All subsequent variations of mathematical models of the theory of point defect dynamics were based on these positions.

From a theoretical viewpoint, such a solution was possible but it is almost impossible to imagine that an impurity, whose concentration is two or four orders of magnitude higher than the concentration of IPDs, does not participate in defect formation. The absence of a theoretical description of impurity precipitation upon cooling of the crystal during growth was the main reason for this approach. This approach led to the disregard of any experimental studies that disproved the theoretical constructions of the recombination-diffusion model of the formation of grown-in microdefects.

The second trend was based on complex experimental studies on the basis of which a heterogeneous model for the formation of grown-in microdefects was proposed [52]. The development of this model required considerable time and theoretical study of the possibility of impurity participation in defect formation processes. By this way went Zaporozhye scientific group, which was established in the late 1960s and headed by Dr. E.G. Sheikhet (09.VII.1938 – 12.VII.1988). The E.G. Sheikhet was one of the pioneers in the study of the fine structure of elementary semiconductors in the USSR, his original scientific works have always outperformed foreign scientific publications on 5-6 years. He received new results with great scrupulousness and repeatedly checked them using various methods and techniques. Over the course of two decades, his work determined the progress in the formation of the most important ideas about defect formation processes in high-pure silicon single crystals. He proposed and developed a set of experimental studies, which ultimately

allowed his followers to begin to actively solve the problem of the formation of grown-in microdefects, to which he devoted his entire life.

The E.G. Sheikhet was the first in the world to create a complete classification of grown-in microdefects in small-scale FZ-Si crystals (the so-called "experimental" classification) [46]. It was first reported in 1975 at the IV International Symposium on Growth and Synthesis of Semiconductor Crystals and Films in Novosibirsk. He first showed that at high crystal growth rates (> 4.5 mm/min for FZ-Si) new types of grown-in microdefects (C-microdefects and D-microdefects) are observed in the form of patterns of uniform defect distribution after selective etching and X-ray topography with decoration [46].

The E.G. Sheikhet showed that the main process that determines the development of grown-in microdefects is the diffusion of IPDs in the temperature gradient field. The formation of grown-in microdefects occurs at nucleation centers which are the atoms of background impurities of carbon and oxygen. Depending on the growing conditions (growth rate, temperature gradient, cooling rate), a continuous sequence of nucleation, development and transformation of one type of defects to another is realized [32].

Scientific work of E.G. Sheikhet and his followers went with a creative competition with a Moscow scientific group (V.V. Voronkov et al.). Such creative competition led to the emergence of new ideas, the development of methods of experimental research, which ultimately contributed to the solution of the problem of the formation of grown-in microdefects in silicon. Unfortunately in the early 1980s, the ideas of E.G. Sheikhet did not find broad support which was mainly due to the following three factors. First, in 1982 by Voronkov's the recombination-diffusion model for the formation of grown-in microdefects was proposed [6]. When constructing his model V.V. Voronkov proceeded from the results of the work of Roksnoer [50]. In turn, this work was the second factor that interfered with the perception of ideas E.G. Sheikhet. This is because E.G. Sheikhet called as "D-microdefects" the defects that were observed after selective etching in a uniform distribution in the form of a channel in the center of a 30 mm diameter FZ-Si crystal grown at 6.0 mm/min. Probably Roksnoer was not aware about paper of E.G. Sheikhet 1977 [46], and in 1981 Roksnoer defined as "D-microdefects" the defects that also have a uniform distribution in the center of the FZ-Si crystal with a diameter of 30 mm, but grown at 7…8.0 mm/min [50]. Based on the results of X-ray topography after copper decoration, Roksnoer suggested that D-microdefects are vacancy-type defects [50]. This assumption fit well into the theoretical concept of V.V. Voronkov, and was used in the

development of the model for the formation of grown-in microdefects. As shown by further experimental studies, the D-microdefects of the classical classification of E.G. Sheikhet [46] and D-microdefects by Roksnoer [50] are different types of grown-in microdefects. The E.G. Sheikhet et al. are showed that D-microdefects in FZ-Si crystals are only interstitial defects [21, 123]. They also determined that the "D-microdefects by Roksnoer" are coexisting defects of the vacancy and interstitial type (the so-called (I+V)-microdefects in accordance with [21, 45, 51]). However, due to the difference in the thermal growth conditions of the crystals, the distribution of D-microdefects at the center of CZ-Si is similar to the same distribution in CZ-Si the E.G. Sheikhet was not found, which was the third problematic factor.

The E.G. Sheikhet understand that his point of view can only be protected by means of statistically reliable experimental results. Therefore, E.G. Sheikhet developed a plan for complex experimental work to solve the problem of grown-in microdefects in dislocation-free silicon single crystals, which provided for the unification of production efforts and the largest laboratories for structural analysis of USSR and other countries. In the mid of 1980s under the leadership of E.G. Sheikhet was the first in the world to establish the physical nature (the sign of the crystal lattice deformation) of all types of growth microdefects (A-, B-, C-, D- and (I+V)-microdefects) in small-scale dislocation-free FZ-Si single crystals [21, 51, 123]. The E.G. Sheikhet et al. for the first time experimentally prove the fact of oxygen precipitation in the "oxygen-free" FZ-Si [21, 49, 51].

The experimental results obtained by E.G. Sheikhet already testified that from the viewpoint of the physics of defect formation the diffusion-recombination model of V.V. Voronkov is incorrect. However, two factors prevented further research: the early death of E.G. Sheikhet and also the death of the USSR and the collapse of the economy in the "new post-Soviet states".

After the death of E.G. Sheikhet the Zaporozhye (Russian) scientific group (headed by the follower of E.G. Sheikhet the Prof. Dr. I.E. Talanin (born. 1952)) continued the work and completed all the necessary experiments only by the year 2000. However, due to the fact that until the mid of 1990s the Zaporozhye (Russian) group did not function, the Voronkov model was widely recognized. The heterogeneous (two-stage) mechanism developed by the Zaporozhye (Russian) group was the best confirmation of the significance of the works and ideas of E.G. Sheikhet [52]. Recently developed mathematical models for the formation of grown-in microdefects confirm the experimental results on which the

heterogeneous (two-stage) mechanism of grown-in microdefect formation is based. The process of interaction of IPDs with impurities which starts near the crystallization front is a fundamental process, and this is determining process in the formation of the defect structure of highly perfect dislocation-free silicon single crystals during their growth. The approach, which combines the obtaining and analysis of numerous experimental data (in particular, on the study of the characteristics of individual grown-in microdefects of all types under different thermal conditions of crystal growth), with the construction of mathematical models for the formation of grown-in microdefects on the basis of experimental data, is most productive for solving problems of defect formation in dislocation-free silicon single crystals.

Conclusions to chapter 2. Grown-in microdefects determine not only the initial defect structure of dislocation-free silicon single crystals, but also the subsequent processes of transformation of this structure as a result of technological influences. Therefore, the study of the mechanism of formation of grown-in microdefects and the construction of a theoretical model of defect formation on its basis is the key both to solving the problem of controlling the defect structure of the crystal and to understanding the fundamental interactions of point defects. The solution of the problem of constructing a theoretical model of defect formation in dislocation-free silicon single crystals should be sought in the way of constructing mathematical models adequate to real experimental data.

Any modifications of the model of the point defects dynamics are not such theoretical model of defect formation, since neither the quantitative nor the qualitative the formation of all types of grown-in microdefects (except microvoids) this model cannot be described. The physical model (recombination-diffusion model), on which is based on the model of point defect dynamics, is particular, since it does not describe all the experimental results on the formation and transformation of grown-in microdefects. At the same time, the heterogeneous (two-stage) model gives a good qualitative description of the experimental results on the investigation of the defective structure of silicon.

CHAPTER THREE

PHYSICAL BASIS OF A HETEROGENEOUS (TWO-STAGE) MODEL OF GROWN-IN MICRODEFECT FORMATION

A mathematician may say anything he pleases, but a physicist must be at least partially sane
—Josiah Willard Gibbs (11.II.1839 – 28.IV.1903)
Quoted in: R. B. Lindsay, "On the Relation of Mathematics and Physics" Scientific Monthly ***59*** *(1944)*

When using a heterogeneous (two-stage) model of grown-in microdefect formation, two questions arose:

(1) Why the "impurity + IPD" interaction in the high-temperature region has an advantage over the recombination processes of IPDs?

(2) On which basis can be conform the high-temperature precipitation process to the classical theory of nucleation of particles of the second phase?

The answers to these two simple questions are key in constructing a theoretical model of defect formation that would be adequate to the experimental results of studies of the defective structure of silicon. In this case it becomes possible to consider the participation in the formation of structural defects during the crystals cooling after growing not only their IPDs but also impurities.

3.1. Recombination of intrinsic point defects in silicon and the classical theory of nucleation

The problem of recombination of IPDs in dislocation-free silicon single crystals is crucial both in the quantitative model of the point defects dynamics [167-173] and in the qualitative recombination-diffusion model of the formation of grown-in microdefects [6, 40, 81, 92]. According to these approaches, recombination near the melting point plays a decisive role in selecting the dominant type of IPDs in a single crystal (vacancies or

silicon interstitial atoms). The type of defects that dominates determines the further process of defect formation.

At the same time, experimental studies [49, 51, 52] disprove the assumption [6, 192] on the recombination of IPDs near the crystallization front. The facts of the coexistence of vacancy and interstitial grown-in microdefects confirm that the decomposition of a supersaturated solid solution of point defects in dislocation-free silicon single crystals occurs by two mechanisms: vacancy and interstitial. The presence of two simultaneous decay paths of a supersaturated solid solution of point defects indicates a significant difficulty in the process of recombination between IPDs, since in this case there is no the only one type of dominant point defects and the only one type of grown-in microdefects.

The results of experimental studies allow us to say that the thoughts set forth by A.J.R. De Kock in [111] about the correctness of the assumptions of the vacancy-interstitial model of S.M. Hu have not lost their relevance. To explain the experimental results and theoretical assumptions of S.M.Hu, we must take into account the basic concepts of the model of stretched configurations of IPDs at high temperatures and a recombination barrier [147, 208-212]. The thermodynamic estimates and calculations based on them [12, 213] confirm both the validity of the experimental results and the incorrectness of the model of the point defects dynamics and the recombination-diffusion model for the formation of grown-in microdefects.

A microscopic model of the recombination barrier was elaborated in detail in [209, 210]. The essence of this model is that the dependence of the barrier on temperature is determined by the configuration of IPDs at high temperatures. Within the framework of this model, it is assumed that at high temperatures the IPDs are stretched into several atomic volumes (11 atoms occupy 10 cells), i.e., around the point defect there is a disordered region extending isotropically up to the atoms of the second coordination sphere. According to [209, 210], recombination can occur only in the case of simultaneous compression of both defects in the surroundings of one atomic volume. Since extended defect configurations have a greater number of microstates than a point defect, this compression reduces the entropy, and, hence, the entropy barrier $\Delta S < 0$ exists. As the temperature is lowered, the barrier decreases significantly and disappearing at low temperatures, and defects easily recombine. This is due to a change in the configuration of IPDs, which are stretched at high temperatures, and at low temperatures have a pointlike dumbbell configuration [210]. It should be noted that the theory of extended defect

configurations, as well as the recombination barrier, has been confirmed in a number of papers [204-207, 214-216].

In the high-temperature region the temperature dependence of the configuration entropy for extended defect can be represented in the following form [217]:

$$S_c(T) = S_\infty(1 - T_k/T) \quad (3.1)$$

where S_∞ is a limit value of S_c (at $T \to T_m$); T_k is a characteristic temperature.

Suppose that T_k is the minimum temperature for the formation of structural imperfections in dislocation-free silicon single crystals. Then we estimate T_k = 450 ^{0}C = 723 K as the average temperature of formation of thermodonors in silicon. From this $S_c(T) = S_\infty(1 - 723/T)$. In accordance to [210], $S_c(1373K) = -11.5k$ (where k is a Boltzmann constant). Then we can get $S_\infty = -24.3k$. Hence,

$$S_c(T) = -24.3k(1 - 723/T) \quad (3.2)$$

According to the model [218], the free energy of the recombination barrier is $\Delta G = -T \cdot \Delta S$, since the contribution of the enthalpy ΔH is negligible. The temperature dependence of the height of the recombination barrier is controlled by the entropy of the formation of point defects. Then

$$\Delta G(T) = -T[-S_c(T)] = TS_c(T) \quad (3.3)$$

Approximate estimate at $T = T_m$ gives $\Delta G(1683K)$ = 2.014 eV.

The experimental results on self-diffusion in silicon show that the diffusion coefficient obeys the Arrhenius dependence over a wide temperature range $D(T) = D_0 exp(-E_a/kT)$, with the activation energy E_a~ 4…5 eV and the pre-exponential factor D_0 much larger than for metals [218]. However, the question about contribution of various mechanisms (vacancy or interstitial) remains vacant. We use the classical data of J.H. Mayer [219], in accordance with which in the temperature range T = 1320…1658 K

$$D(T) = 1460exp(-5.02/kT) \quad (3.4)$$

Approximate estimate at $T = T_m$ gives D(1683 K) = 1.42·10^{-12} cm^2·s^{-1}. The silicon interstitial atoms dominate at high temperature. Therefore, we estimate the recombination time at a high temperature τ_1 using formula

$$\tau_1 = \Omega / 4\pi D(T) r_0 \exp(-\Delta G(T)/kT) \quad (3.5)$$

where Ω is a lattice volume with allowance for the model [210]; $r_0 = 3 \cdot 10^{-8}$ cm is a recombination radius.

The estimate at $T = T_m$ gives $\tau_1 = 316$ s. The estimate using the new data [220] and [218] gives the values $\tau_1 = 132$ s and $\tau_1 = 110$ s, accordingly.

The recombination factor $k_{IV}(T)$ is described by the theory of diffusion-limited reactions together with the kinetic activation barrier [168]. In the case of high temperatures

$$k_{IV}(T) = 4\pi r_0 D(T) \exp(-\Delta G(T)/kT)/\Omega c_s \quad (3.6)$$

where $c_s = 5 \cdot 10^{22}$ cm^{-3} is a density of atoms.

The estimate at $T = T_m$ gives $k_{IV}(1683K) = 6.3 \cdot 10^{-26}$ cm^3/s. The criterion of "rapid recombination" was introduced in [100, 172] $k_{IV}(1683K) \cdot C_{Vm} \geq 20 s^{-1}$ (where $C_{Vm} = 11.7 \cdot 10^{14}$ cm^{-3} is a vacancy concentration at $T = T_m$). For the considered conditions of the model of the point defects dynamics, the "fast recombination" criterion is not satisfied.

Let us consider the low-temperature region. A number of experimenters suggest the breakdown of Arrhenius in the region of 1323 K, suggesting of the action of various mechanisms before and after this temperature [218]. It was shown in [218] that at 1353 K a transition occur between the silicon interstitial atoms that dominate in self-diffusion at high temperatures and vacancies dominating in self-diffusion at low temperatures.

We estimate the recombination time at a low temperature τ_2 using formula [221]:

$$\tau_2(T) = \tau_\infty \cdot \exp(C/TS_c) \quad (3.7)$$

In this case a separate evaluation of the energy barrier at T = 1373 K ($\Delta G = \Delta H = C$ = 1.4 eV) was made in [222] by comparing the experimentally measured lifetime of the vacancies to the rate of growth of the diffusion-limited reaction. The value $\tau_\infty = 634.13$ s we obtain from (3.7) at $T = T_m$. Then

$$\tau_2(T) = 634.13 \exp\left(-\Delta G/TS_c(T)\right) \quad (3.8)$$

The estimate at $T = T_m$ gives τ_2 = 316.4 s, and at T = 723 K we obtain $\tau_2 \rightarrow 0$ (when estimating without taking into account the vibrational entropy). In the case of low temperatures the recombination factor $k_{IV}(T)$ is determined by the formula

$$k_{IV}(T) = 4\pi r_0 [D_I(T) + D_V(T)] exp(-\Delta G/kT)/\Omega c_s \quad (3.9)$$

where $D_I(T) = 1.76 \cdot 10^{-2} exp(-0.937/kT)$ $cm^2 \cdot s^{-1}$ and $D_V(T) = 1.70 \cdot 10^{-2} exp(-0.457/kT)$ $cm^2 \cdot s^{-1}$ [219]. The estimate at T = 723 K gives $k_{IV}(T) \approx 10^{-9}$ $cm^3 \cdot s^{-1}$ and the "fast recombination" criterion is well satisfied.

The results of thermodynamic calculations show that in the region of high temperatures, i.e., at temperatures close to the melting point, the equilibrium concentrations of vacancies and silicon interstitial atoms in dislocation-free silicon single crystals coexist simultaneously, and the supersaturated solid solution of IPDs decays simultaneously by two mechanisms: vacancy and Interstitial. Thermodynamic calculations confirm the experimental data obtained by TEM that the process of recombination of IPDs is difficult in dislocation-free silicon single crystals near the crystallization front due to the presence of a recombination barrier [13, 213]. As a result, it can be said that vacancies and silicon interstitials atoms find their sinks on the background impurities of oxygen and carbon, respectively.

At the same time, thermodynamic calculations show that, under conditions of low-temperature studies (for example, in ion implantation), recombination of IPDs occurs at a good rate. Theoretical calculations confirm the model of the entropy barrier, the essence of which is that the decrease in the barrier is due to a decrease in the configuration entropy with decreasing temperature.

Experimental and theoretical confirmation of the fact that the rate of recombination of IPDs near the crystallization front is close to zero means that two diffusion mechanisms (interstitial and vacancy) that correspond to two mechanisms (branches) of the heterogeneous mechanism of formation and transformation of growth microdefects should observed.

3.2. About the accordance of process of the high-temperature precipitation and the classical theory of nucleation

Decay of the solid solution begins with the process of nucleation, i.e., the formation of physically distinct centers, which then grow. This growth leads to the isolation of a new phase inside the initial solid solution. In general, precipitation of the second phase occurs in three stages: (1) a local fluctuation of the chemical potential (formation of the nucleus), (2) formation of a stable nucleus, (3) growth and coalescence of precipitates [181].

The change in the free energy of a crystal ΔG when the nucleus is formed has the form

$$\Delta G = \Delta G_V + \Delta G_S + \Delta G_L \tag{3.10}$$

where ΔG_V is a change in free energy as a result of a change in the chemical composition in the volume (has a negative sign); ΔG_S is a change in free energy due to the formation of interphase boundary; ΔG_L is a change in free energy due to changes in the volume of the nucleus [181]. If we find equations for ΔG_V, ΔG_S and ΔG_L, and substitute them in (3.10), we obtain

$$\Delta G = \alpha R^3 \left(\Delta g_V + \Delta g_L\right) + \beta R^2 \Delta g_S \tag{3.11}$$

where α is a geometric factor, taking into account the shape of the nucleus; β is a nucleus shape coefficient; R is a linear characteristic size of the nucleus; Δg_V is the difference in the volume energies of the phases per unit volume; Δg_S is the surface energy of the nucleus per 1 cm^2; Δg_L is a the change in the bulk elastic energies of the nucleus and crystal, per unit volume. When the inequality is fulfilled $|\Delta g_L| > |\Delta g_V|$, the formation of the nucleus begins. In this case the curve $\Delta G(R)$ will have the shape of a curve with a maximum that corresponds to the critical size of the nucleus R_C. If the size of the nucleus $R < R_C$, then such nucleus will dissolve. If the size of the nucleus $R > R_C$, then such nucleus will grow [181].

The critical size of the nucleus R_C can be found from the condition of the maximum of the curve $d\Delta G(R)/dR = 0$

$$R_C = \left| \frac{2\beta\Delta g_S}{3\alpha(\Delta g_V + \Delta g_L)} \right| \tag{3.12}$$

Then the corresponding value of the energy $\Delta G_C = 3\beta R_C^2 \Delta g_S$. It can be shown that $\Delta G_V = kT \ln\left(C_X / C_X^{eq}\right)$, where C_X is a impurity concentration; C_X^{eq} is the equilibrium impurity concentration, which depends on the temperature [181, 182]. Then

$$R_C = \frac{2\beta\Delta g_S}{kT \ln\left(C_X / C_X^{eq}\right)} \tag{3.13}$$

A more complete theoretical described of the critical size of the nucleus is given in [223]:

$$R_C = \frac{2\sigma u V_p}{kT \ln(S_X S_i^{-\gamma_i} S_v^{\gamma_v}) - 6\mu\delta\varepsilon u V_p} \tag{3.14}$$

where $S_X = C_X / C_X^{eg}, S_i = C_i / C_i^{eg}, S_v = C_v / C_v^{eg}$ is a supersaturation, respectively, of impurity atoms, silicon interstitial atoms and vacancies; σ is a surface interface energy density between the precipitate and the matrix; μ is a silicon shear modulus; δ and ε is a relative linear and volume deformations of the discrepancy between the precipitate and the matrix; γ_i and γ_v is a the fraction of silicon interstitial atoms and vacancies attributable to one impurities atom attached to the precipitate; V_p is a volume of a molecule of precipitate; $u = (1 + \gamma_i x + \gamma_v x)^{-1} \cdot (\frac{1+\varepsilon}{1+\delta})^3$. It follows from (3.13) and (3.14) that the critical size of the nucleus increases with increasing temperature [182].

The formation and development of the growth microdefective structure of silicon is due to the thermal growth and cooling conditions of the crystal. This fact has been proved experimentally and is not in doubt either in the model of point defect dynamics [119, 192] nor in the heterogeneous (two-stage) model [52]. The temperature distribution along the length of the ingot during its cooling, depending on the thermal parameters of the

growing, varies according to the law $1/T = 1/T_m + G_a Z/T_m^2$, where Z is a distance from the crystallization front [6]. We note that in the general case it is necessary to take into account the radial inhomogeneity of the temperature field. We introduce into this formula the growth rate of the crystal and obtain

$$T(t) = \frac{T_m^2}{T_m + V_g G_a t} \tag{3.15}$$

In this interpretation the growth parameter V_g/G_a is a parameter that controls the process of defect formation in silicon. At the same time, in the recombination-diffusion model this parameter is treated only as a criterion that separates the regions of existence of microvoids and dislocation loops.

We introduce the dependence $T(t)$ in equation (3.14) with allowance for the fact that C_v^{eq}, C_i^{eq} depend on T

$$R_C = \frac{2\sigma u V_p}{kT(t)\ln(S_X S_i^{-\gamma_i} S_v^{\gamma_v}) - 6\mu\delta\varepsilon u V_p} \tag{3.16}$$

On Fig. 3.1 are shown the results of calculations of the critical radii of precipitates of oxygen and carbon from the temperature for a CZ-Si crystal with such parameters: crystal growth rate $V_g =$ 0.6 mm/min, axial temperature gradient $G_a =$ 2.5 K/mm, $C_{O,C} =$ 10^{18} cm^{-3} for the concentration of oxygen and carbon, accordingly [224].

Minimum values $R_C =$ 0.81 nm (oxygen precipitate) and $R_C =$ 1.1 nm (carbon precipitate) are reached in the initial state at $T = 1682K$ and increase with decreasing temperature. At a $T \approx 1455K$ the critical radii of precipitates of oxygen and carbon have the same values (~ 3.6 nm), and then the critical oxygen radius grows faster. The increasing of the critical radius of precipitates during the crystal cooling leads to a sharp decrease in their growth rate and, accordingly, a sharp decrease in the precipitation rate.

For a FZ-Si crystal (with such parameters: crystal growth rate $V_g =$ 6.0 mm/min, axial temperature gradient $G_a =$ 130.0 K/cm, $C_O =$ $8 \cdot 10^{16}$ cm^{-3} for oxygen concentration and $C_C =$ 10^{16} cm^{-3} for carbon concentration) slightly higher minimum values $R_C =$ 0.813 nm (oxygen precipitate) and

$R_C =$ 1,107 nm (carbon precipitate) are reached in the initial state at $T = 1682K$ and also increase with decreasing temperature. For both groups of crystals, the minimum values R_C (at $T = 1682K$) increase with increasing the growth rate of the crystal or the axial temperature gradient at the crystallization front. For example, the Fig. 3.2 shows the dependence $R_C(V)$ for oxygen precipitates at constant G_a and $T = 1682K$. Note that the larger the value V_g (or G_a), the more steep the growth of the values of the function $R_C(V_g)$ or $R_C(G_a)$ is observed in crystals of both groups [224].

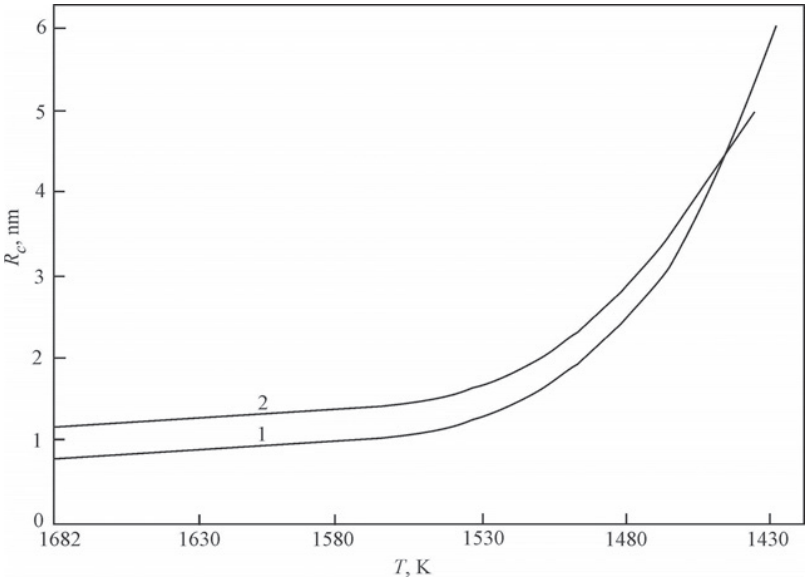

Fig. 3.1. Temperature dependences of critical radii of precipitates of oxygen (1) and carbon (2): V_g = 0.6 mm/min, G_a = 2.5 K/mm, $C_{O,C}$ = 10^{18} cm^{-3}

A first-order phase transition proceeds through the formation of a so-called activated complex [225]. This state corresponds to the highest point of the pass of the lowest energy barrier separating the original (reagents) and the new (reaction products) phase in the reaction coordinate space. For the ordinary first-order phase transition, the activated complex is the

critical nuclei of the new phase in the volume of the initial phase, i.e., the activated complex is dissimilar or heterogeneous [226].

If a first-order phase transition occurs in a solid, then to form the nucleus of a new phase it is necessary to take into account the elastic stresses arising both in the nucleus and in the matrix of the initial material. Moreover, if the elastic energy or some other factors sharply increase the energy of formation of critical nuclei directly in the initial phase, this inhomogeneous state ceases to play the role of an activated complex for a chemical reaction or a phase transition, since these nuclei cease to correspond to the lowest energy barrier separating the initial and a new phase [226].

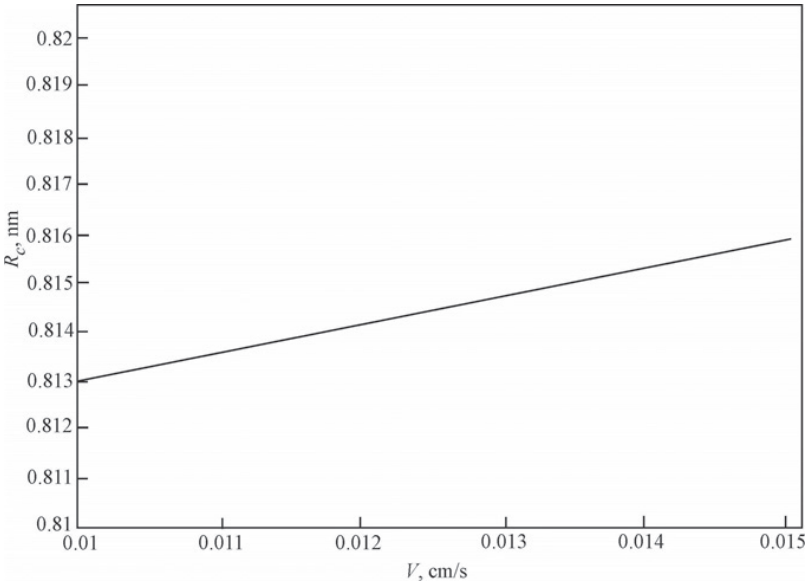

Fig. 3.2. Change of R_C for oxygen precipitates ($G = const$ and $T = 1682K$)

This is possible if the crystal structure of the new phase differs from the crystalline structure of the initial phase, and the density of the new phase is smaller than the density of the initial phase, and also in the case of incoherent coupling of the crystal lattices of the new and old phases. This remark concerns the use of formula (3.14), since it is valid only for the case of coherent conjugation of phases.

Under these conditions, at first, another homogeneous state is formed from the initial state, which will play the role of an intermediate state, and the nuclei of the final phase, i.e., the new activated complex, will already be formed from it [227].

Thus, it was shown in [227] that the transition from Si to SiC occurs via an intermediate state which including Si saturated by dilatation dipoles (stable objects consisting of an atom C located in the interstice of Si and a silicon vacancy). Elastic dilatation energy, as well as elastic energy due to coherent coupling, makes the energy of formation of the critical SiC nucleus directly in Si too large. Saturation of Si with dilatation dipoles smoothly reduces the barrier for the formation of SiC up to values close to kT, after which the formation of SiC from a homogeneous intermediate state occurs very rapidly throughout the entire volume of the intermediate state [227]. It should be taken into account that in the high-temperature region this barrier is much lower than the barrier for the recombination of IPDs [213].

Taking into account the influence of the thermal growth conditions of silicon single crystals in the form of a dependence $T(t)$ it is possible to theoretically describe the conditions for nucleation, growth and coalescence of precipitates from the crystallization temperature to room temperature. In this case the Vanhellemont-Clayes model [223] is applicable not only to the description of the formation of precipitate nuclei in silicon during the thermal action, but also extends to the cooling of the crystal during growth. With such a consideration, even in the initial stage of crystal cooling, point defects interact with one another. The interaction of the "impurity + IPDs" is of a fundamental nature and determines the defect structure of the crystal.

The process of high-temperature precipitation is not only adequate to the experimental results of the study of grown-in microdefects, but also does not contradict the classical theory of nucleation of particles of the second phase. Furthermore, it makes it possible to extend the action of the mathematical apparatus of the classical theory of nucleation to the formation of nuclei in a solid during its cooling after growing.

Conclusions to chapter 3. The process of recombination of IPDs in dislocation-free single crystals of FZ-Si and CZ-Si near the crystallization front is impossible due to the presence of a recombination barrier. At temperatures close to the melting point the vacancies and silicon interstitial atoms in the dislocation-free silicon single crystals coexist simultaneously. When the crystal is cooled, the decomposition of the supersaturated solid solution of point defects occurs in two branches

(vacancy and interstitial) in accordance with the heterogeneous (two-stage) model for the formation of grown-in microdefects.

High-temperature precipitation and the classical theory of nucleation complement each other and expand the possibilities of a theoretical description of the processes of nucleation in solids. The introduction and allowance in the initial equations of the classical theory of the nucleation of thermal conditions of crystals growth makes it possible to show that critical nuclei of small dimensions are more likely to arise near the crystallization front. When the crystal is cooled with decreasing temperature, processes of growth and coalescence of precipitates occur. Depending on the thermal growth conditions, the initial defect structure of the crystal is formed, which in general includes such grown-in defects as impurity precipitates, dislocation loops and microvoids.

CHAPTER FOUR

HIGH-TEMPERATURE PRECIPITATION OF IMPURITY IN DISLOCATION-FREE SILICON SINGLE CRYSTALS

There is no certainty in sciences where one of the mathematical sciences cannot be applied, or which are not in relation with these mathematics
—Leonardo di ser Piero da Vinci (15.IV.1452 – 02.V.1519)
Quoted in: J.-P. Richter, "The Literary Works of Leonardo da Vinci". London: S. Low, Marston, Searle & Rivington, 1883

The solution of the technological aspect of the problem of the formation of grown-in microdefects is impossible without an understanding of the physics of defect formation of grown-in microdefects in dislocation-free silicon single crystals. This requires knowledge and adequate application of a qualitative physical model for the formation and transformation of grown-in microdefects, which is constructed with the help of complex experimental studies. The development of a quantitative defect formation model in dislocation-free silicon single crystals should be based only on such a qualitative mechanism that adequately reflects the real structure of the crystal. The quantitative model of the formation of grown-in microdefects, in turn, makes it possible to simulate and obtain dislocation-free single crystals of silicon with a predetermined defect structure and to control it with subsequent technological influences. The quantitative model for the formation of grown-in microdefects should give an answer to the fundamental question of solid state physics, which consists in describing the kinetics of the defective crystal structure during its cooling after growing.

Investigation of properties and modeling of the defect structure of dislocation-free silicon single crystals makes it possible to construct a defect formation model that will predict the physical properties of silicon crystals. The basis for verification of mathematical models is experimental studies of defect formation processes in as-grown silicon single crystals.

The construction of a theoretical model for the formation of grown-in microdefects in dislocation-free silicon single crystals is important scientific and practical problem that is relevant from the viewpoint of developing the physical foundations for the purposeful creation of materials with the necessary complex of physical properties.

The solution of the problem of the formation of grown-in microdefects allows an answer to the questions about interaction of point defects during crystal growth, to explain the initial defect structure of the crystal, to understand the formation of post-growth defects and to explain the effect of defects on the physic-chemical properties of silicon. These questions are special relevant for the physics of semiconductors, since structural defects with impurities have a very strong effect on the most important electrical, optical, and photoelectric properties of semiconductor crystals. Therefore, this problem and its solution for the most perfect silicon crystals can serve as a basis for considering similar problems in other semiconductor crystals.

The presence in dislocation-free silicon single crystals the background impurities (carbon, oxygen) and IPDs leads to complex processes of interaction between them. The result of these processes is the nucleation and subsequent transformation of microdefects of various types. At the earliest stages near the crystallization front there are simultaneously silicon interstitial and vacancy atoms, and the recombination processes between them are negligible because of the entropy barrier.

During the crystal cooling, after passing through the diffusion zone, an excessive (nonequilibrium) concentration of IPDs arises. The disappearance of excess IPDs takes place in sinks, whose role in this process is played by uncontrolled (background) impurities of oxygen and carbon [13]. The formation of complexes between IPDs and impurities occurs because they are both a source of internal stresses in the lattice (elastic interaction), and also because of the Coulomb interaction between them (if defects and impurities are present in the charged state). In the mathematical models described below the elastic interaction and the absence of a recombination process of IPDs in the high-temperature region are taken into account.

The decomposition of a supersaturated solid solution of point defects occurs simultaneously along two mechanisms, as a result of which the formation of oxygen-vacancy and carbon-interstitial complexes occurs simultaneously near the melting point, on the basis of which interstitial and vacancy grown-in microdefects are formed.

Such idealized system is characteristic of undoped dislocation-free single crystals of FZ-Si grown in a vacuum with oxygen and carbon

impurity concentration of less than $5 \cdot 10^{15}$ cm^{-3}. It should be taken into account that such a system allows the possibility of joint interaction O_i and C_s. Furthermore, in real industrial crystals FZ-Si and CZ-Si the presence and interaction of other point defects (for example, iron, nitrogen, doped impurities, etc.) should be taken into account. A heterogeneous (two-stage) model for the formation of grown-in microdefects makes it possible to describe the defective structure of a crystal as a structure consisting of two subsystems: a subsystem of primary grown-in microdefects (impurities precipitates) and a subsystem of secondary grown-in microdefects (microvoids and dislocation loops).

4.1. Basic concepts of the microscopic theory of impurity kinetics in semiconductors

Impurities in semiconductors at high temperatures show different migration effects in the crystal. The most common effect is the decay of a supersaturated solid solution, which includes diffusion as an integral part of a multistage process [228]. Migration phenomena include the process of dissociative diffusion, which is the simultaneous migration of impurity atoms through the interstices of the crystal lattice and vacancies with a changing position, i.e., by trapping the vacancy of an impurity atom and the formation of a free interstice [229-232]. Here, the difference from the decay phenomenon is that in diffusion, as a technological process, the diffusant enters the sample from an external source and in the decay's from the internal (from the nodes of the crystal lattice). Regardless of the model of the migration process, their common feature is firmly established: the interaction of impurity atoms with other point defects. A consistent account of such interactions requires introducing a variable diffusion coefficient, for which it is necessary to know its functional dependence on the concentration of all components of the kinetic process. A direct introduction to the theory of the variable diffusion coefficient is practically impossible, which is connected with [233]:

- The dependence of the concentrations of the components on each other and their continuous variation in time.
- A change in the charge of impurity atoms, especially amphoteric ones, with a change their crystalline position.
- The ability of impurity atoms to form of associated defects.

A more productive approach is to use the equivalence of diffusion and quasi-chemical descriptions of changes in the concentration of point

defects. In this case the migration of impurities with a variable crystal-chemical position is interpreted as some chemical reactions of the impurity transition from the node (s) to the interstice (i) with the formation of a vacancy and vice versa for a semiconductor, for example, n-type, taking into account the electron charge [229, 232]:

$$A_S^{(Z_S)} + Ze^- \underset{K_2}{\overset{K_1}{\leftrightarrow}} A_i^{(Z_i)}{}_{\downarrow K_3} + V_{\downarrow K_4}^{(Z_V)}, \tag{4.1}$$

where the superscript denotes the magnitude of the charge of each component. The output of interstitial atoms and vacancies into the sinks in formula (4.1) is also treated as quasi-chemical reactions with rate constants K_3 and K_4. The authors of [229, 232] derived formula (4.1) taking into account the conditions [234]: (1) Identity of sinks for all defects. (2) The sinks are uniformly distributed in the crystal. (3) Number of sinks constantly. (4) The capacity of drains is unlimited and sinks do not create elastic stress fields.

The next important quasi-chemical reaction is the interaction of the impurity in the node and the vacancy with the formation of associated defect $X^{(Z_X)}$ [233]:

$$A_S^{(Z_S)} + V^{(Z_V)} \underset{K_6}{\overset{K_5}{\leftrightarrow}} X_i^{(Z_X)}{}_{\downarrow K_7} + Z'e^-. \tag{4.2}$$

The numbers of electrons participating in the reactions (4.1) and (4.2) are determined by the condition of charge conservation:

$$Z = Z_S - Z_V - Z_i, \quad Z' = Z_X - Z_V - Z_S. \tag{4.3}$$

Then changes in time of medium bulk concentrations can be written in the form of the following kinetic equations [231]:

$$\begin{aligned}
\frac{dC_S}{dt} &= -K_1 C_S n^Z + K_2 C_i C_V - K_6 C_S C_V + K_5 C_X n^{Z'}, \\
\frac{dC_i}{dt} &= K_1 C_S n^Z - K_2 C_i C_V - K_3 (C_i - C_i^0), \\
\frac{dC_V}{dt} &= K_1 C_S n^Z - K_2 C_i C_V - K_6 C_S C_V + K_5 C_X n^{Z'} - K_4 (C_V - C_V^0), \\
\frac{dC_X}{dt} &= -K_5 C_X n^{Z'} + K_6 C_S C_V - K_7 (C_X - C_X^0),
\end{aligned} \tag{4.4}$$

where, according to [228, 233],

$$K_1 = K_2 \frac{C_i^0 C_V}{C_S^0} n_0^{-Z}, \quad K_2 = 4\pi r_0 (D_i + D_v),$$
$$K_3 = \gamma\rho D_i, \quad K_4 = \gamma\rho D_v, \quad K_5 = K_6 \frac{C_V^0 C_S^0}{C_X^0} n_0^{-Z'}, \qquad (4.5)$$
$$K_6 = 4\pi\rho_0 D_v, \quad K_7 = \gamma\rho D_X,$$

D_i, D_v, D_X is a diffusion coefficients of defects; ρ is a density of sinks per unit area; γ is a multiplier determined by the geometric shape of the sink (≈ 1); r and ρ_0 is a effective radii of capture of pairs "interstitial atom + vacancy" and "substitute atom + vacancy", respectively. The rate constants of direct and backward reactions are interdependent and their relationship is determined from the equilibrium condition, when $dC_S / dt = 0$ and $dC_X / dt = 0$.

The system (4.5) is supplemented by the neutrality condition of the crystal, which makes it possible to determine the concentration of free electrons [233]:

$$n = Z_S C_S + Z_i C_i + Z_V C_V + Z_X C_X + n_i^2 / p, \qquad (4.6)$$

where the last term is the electron concentration.

The systems of equations (4.4)-(4.6) are nonlinear, therefore, for their solution it is necessary to adopt certain assumptions leading to their linearization. The first type of assumption is the approximation of the equilibrium defect concentration [208], when it is assumed that the concentration of the most mobile defects is equal at each instant of time to the thermodynamically equilibrium concentration at a given temperature. However, point defects at each instant of time are in quasi-equilibrium with each other, and the presence of a nonequilibrium fraction of one type of defects leads to an excess content of others. Therefore, the second assumption (approximation of nonequilibrium concentration of defects) is based on the assumption that the excess concentrations of all defects are much lower than their equilibrium concentrations [233].

Dissociative diffusion-migration of impurities with a variable crystal-chemical position is described by the reactions (4.1). In determining of dissociative diffusion, one should take into account the surface concentration, which decreases in the sample bulk in time and in coordinate. The time constant (the measure of the time decrease) is determined by the migration mechanism in the sample volume, and the dependence on the coordinate is determined by the shape of the sample and the boundary conditions of the diffusion task [233].

Since the value of the diffusion coefficient is a combination of the partial diffusion coefficients of the components and their concentrations, the analysis of the diffusion process shows its microscopic nature. In general, the analysis of the diffusion problem is cumbersome, but at the same time, a more simplified theory is often sufficient for a qualitative or semiquantitative interpretation of the experimental data. Such simplifications are: (1) Application of the approximation of the equilibrium concentration of defects. (2) Not taking into account the charge of defects. (3) Not taking into account the reaction diffusion (only two defects are considered: impurity atom and vacancy). Then the system of kinetic equations (4.4) is substantially simplified [233]:

$$\frac{dC_S}{dt} = -K_1 C_S + K_2 C_i C_v, \tag{4.7}$$

$$\frac{dC_i}{dt} = K_1 C_S - K_2 C_i C_v - K_3 (C_i - C_i^0), \tag{4.8}$$

$$\frac{dC_v}{dt} = K_1 C_S - K_2 C_i C_v - K_4 (C_v - C_v^0). \tag{4.9}$$

The constants are determined in accordance with (4.5), but when Z = 0.

In general, sinks can be dislocations, surfaces, impurity atoms. In our case (dislocation-free silicon single crystals; the considered of initial moment of interaction of point defects at temperatures close to the melting point), the most important role is played by the impurity atoms. Mathematical description of diffusion is carried out for the cases of constant, variable and mixed sources and sinks of vacancies and interstitial impurity atoms.

Interpretation of diffusion in multicomponent systems is difficult in connection with the need to take into account the interaction of impurity atoms. In the general case, numerical methods for solving equations are used, and only in some approximations it is possible to obtain simple analytic expressions convenient for comparison with experiment [231]. Always the most important is the preliminary qualitative analysis of the experimental data, which allows substantiating the correctness of the inclusion or exclusion of certain factors from the mathematical model.

In a widely used model of successive diffusion, a simplifying interpretation is possible when the diffusion coefficient of the previously introduced impurity is much larger than the impurity diffusion coefficient introduced in the subsequent stage. This allows us to identify our task with the task of the diffusion of impurity into a uniformly doped sample [229, 230]. Differences between sequential and simultaneous diffusion are associated with different types of initial conditions: (1) If the constant concentration of the components is specified at the boundary, this is the

process of simultaneous diffusion. (2) If a condition is set at the boundary for the absence of a flux of one of the components that is at the initial instant of time in the bulk of the sample, this is a process of successive diffusion. The analysis of complex impurity profiles obtained both in experiments with sequential and simultaneous diffusion of impurities in semiconductors is most logically considered within the framework of the approach of thermodynamics of irreversible processes [231, 235-238]. The equations of flows of diffusing components in the framework of linear thermodynamics of irreversible processes in the case of two components are written as follows [233]:

$$\frac{\partial C_1}{\partial t} = D_{11}\frac{\partial^2 C_1}{\partial x^2} + D_{12}\frac{\partial^2 C_2}{\partial x^2},$$
$$\frac{\partial C_2}{\partial t} = D_{21}\frac{\partial^2 C_1}{\partial x^2} + D_{22}\frac{\partial^2 C_2}{\partial x^2}. \qquad (4.10)$$

In the general case, the initial and boundary conditions have this form for successive diffusion: $C_1(x,0) = C_1^0, \quad C(\infty,t) = C_1^0, \quad C_2(0,t) = C_2^0, \quad C_2(\infty,t) = 0,$

$C_2(x,0) = 0, \quad D_{11}\frac{\partial C_1}{\partial x} + D_{12}\frac{\partial C_2}{\partial x}\Big|_{x=0} = 0,$ and for simultaneous diffusion:

$C_1(x,0) = C_2(x,0) = 0$ at x > 0, $C_1(\infty,t) = C_2(\infty,t) = 0, \quad C_1(0,t) = C_1^1, \quad C_2(0,t) = C_2^1,$

where C_1^0, C_2^0, C_1^1, C_2^1 is a constants.

When the two components are simultaneously diffused at a sufficiently large distance from the surface, the concentrations of the components decrease monotonically into the interior of the sample. Near the surface the maximum in the distribution of components may appear. Hence, one of the signs of the interaction of components is the nonmonotonic character of the impurity distributions [233].

The basis of the thermodynamics approach for irreversible processes, in addition to the interaction model of diffusing components through internal fields (electrical and elastic), was the basic interaction model: the complexation model [229, 230]. The mechanism of formation of complexes may be different, but regardless of the nature of the forces leading to the formation of complexes, any model assumes that the range of action of these forces should be small. In this case, in analyzing the migration of point defects, the complex can be considered as a point defect.

Diffusion impurity kinetics in the formation of mobile complexes is described by a system of equations that accompany the diffusion reaction of the components $A + B \leftrightarrow Q$, and in general they have the form [233]:

$$\begin{aligned}
\frac{\partial H_A}{\partial t} &= D_A \frac{\partial^2 H_A}{\partial x^2} - K_1 H_A H_B + K_2 Q, \\
\frac{\partial H_B}{\partial t} &= D_B \frac{\partial^2 H_B}{\partial x^2} - K_1 H_A H_B + K_2 Q, \\
\frac{\partial Q}{\partial t} &= D_Q \frac{\partial^2 Q}{\partial x^2} + K_1 H_A H_B - K_2 Q,
\end{aligned} \tag{4.11}$$

where H_A, H_B is a concentration of free components A and B; Q is a concentration of complexes; K_1, K_2 are the rate constants of the formation and decay of complexes.

The system of equations (4.11) does not have analytic solution. Therefore, to obtain dependencies $H_A(x,t)$, $H_B(x,t)$, $Q(x,t)$ this system is usually solved by numerical methods on a computer.

If we introduce the time for establishing the chemical equilibrium τ of the reaction $A + B \leftrightarrow Q$ in a homogeneous closed system, then the system (4.11) can be considered for small times $t << \tau$ (when the interaction of the diffusing components can be neglected and all three components independently diffuse into the sample) and for long times $t >> \tau$ [239]. For long times, two cases are possible.

Near the surface of the sample, when $x << \sqrt{Dt}$ (D is a arbitrary diffusion coefficient: D_A, D_B or D_Q) the terms of order $1/\tau$ describing the change in concentration with time can be neglected, and then the system of equations (4.11) goes into:

$$\begin{aligned}
D_A \frac{\partial^2 H_A}{\partial x^2} - K_1 H_A H_B + K_2 Q = 0, \\
D_B \frac{\partial^2 H_B}{\partial x^2} - K_1 H_A H_B + K_2 Q = 0, \\
D_Q \frac{\partial^2 Q}{\partial x^2} + K_1 H_A H_B - K_2 Q = 0.
\end{aligned} \tag{4.12}$$

This system of equations describes the stationary profiles of the components near the surface of the sample.

Far from the surface ($x >> \sqrt{Dt}$) the terms describing the interaction between the components become much larger than the rest of the terms, and it follows from (4.11) [232]:

$$K_1 H_A H_B = K_2 Q. \tag{4.13}$$

The missing two equations are obtained after taking into account the remaining terms in equations (4.11). In order that in the equations only commensurable terms are contained, we add the first two equations (4.11) with the third:

$$\frac{\partial H_A}{\partial t} + \frac{\partial Q}{\partial t} = D_A \frac{\partial^2 H_A}{\partial x^2} + D_Q \frac{\partial^2 Q}{\partial x^2},$$
$$\frac{\partial H_B}{\partial t} + \frac{\partial Q}{\partial t} = D_B \frac{\partial^2 H_B}{\partial x^2} + D_Q \frac{\partial^2 Q}{\partial x^2}, \qquad (4.14)$$

which together with (4.13) form a complete system of equations. This system of equations coincides with the system of equations (4.11), and describes the consistent dissemination of components from the surface into the interior of the sample [229]. Taking into account the finite length of the sample L, we obtain the following transition conditions for the system of equations (4.11) in (4.12), (4.14):

$$\sqrt{Dt} << x << L, \ \tau << t << L^2 / D. \qquad (4.15)$$

The systems of equations (4.12)-(4.14) describe the nonstationary process of dissemination of components from the surface in the sample bulk.

Consideration of the task with a homogeneous initial distribution of the impurity allows us to introduce the Boltzmann substitution $\lambda \equiv x/2\sqrt{Dt}$, which essentially simplifies the system of equations (4.12), (4.14) [233]:

$$d_A^2 H_A'' + d_Q^2 Q'' + 2\lambda(H_A + Q)' = 0,$$
$$d_B^2 H_B'' + d_Q^2 Q'' + 2\lambda(H_B + Q)' = 0, \qquad (4.16)$$
$$H_A H_B = KQ,$$

where $d_A^2 \equiv D_A$, $d_B^2 \equiv D_B$, $d_Q^2 \equiv D_Q$; strokes denote differentiation under λ.

The system of equations (4.16) can also be written in terms of the complete components $N_A \equiv H_A + Q$ and $N_B \equiv H_B + Q$:

$$d_A^2 (N_A - Q)'' + d_Q^2 Q'' + 2\lambda N_A' = 0,$$
$$d_B^2 (N_B - Q)'' + d_Q^2 Q'' + 2\lambda N_B' = 0, \qquad (4.17)$$
$$(N_A - Q)(N_B - Q) = KQ.$$

The solution of the system of equations (4.16) is considered for cases of sequential, simultaneous and mutual diffusion. The boundary conditions have the following form [233]:

For a sequential diffusion

$$H_A\big|_{\lambda=0} = H_A(0); \qquad H_A\big|_{\lambda=\infty} = H_A(\infty), \qquad (4.18)$$
$$d_B^2 H_B' + d_Q^2 Q'\big|_{\lambda=0} = 0; \qquad H_B\big|_{\lambda=\infty} = H_B(\infty);$$

For a simultaneous diffusion

$$H_A\big|_{\lambda=0} = H_A(0); \qquad H_A\big|_{\lambda=\infty} = H_A(\infty), \qquad (4.19)$$
$$H_B\big|_{\lambda=0} = H_B(0); \qquad H_B\big|_{\lambda=\infty} = H_B(\infty);$$

For a mutual diffusion

$$H_A\big|_{\lambda=-\infty} = H_A(-\infty); \qquad H_A\big|_{\lambda=+\infty} = 0, \tag{4.20}$$

$$H_B\big|_{\lambda=-\infty} = 0; \qquad H_B\big|_{\lambda=+\infty} = H_B(+\infty).$$

Sequential diffusion corresponds to the absence of two flows at the sample boundary $\left.\frac{\partial H_B}{\partial x}\right|_{x=0} = 0, \left.\frac{\partial Q}{\partial x}\right|_{x=0} = 0$ when solving the system of equations (4.11). Simultaneous diffusion corresponds to the definition of at least two concentrations at the sample boundary. Mutual diffusion corresponds to the diffusion homogenization of the sample, half of which is doped by component A, and other by component B.

In the general case, the system of equations (4.16) with the boundary conditions (4.18)-(4.20) does not have analytic solutions; therefore, for analyzing the form of impurity profiles, consider some limiting cases [230].

1. *Strong complexation* ($K \to 0$). The approach of strong complexation physically means that the reaction $A + B \leftrightarrow Q$ is sharply shifted toward the formation of the complex. Formally, from (4.13) with ($K = 0$) follows that the concentration of at least one of the free components is zero, i.e., $H_A = 0$ or $H_B = 0$. In the general case this leads to the fact that on the axis λ two regions are formed, separated by a singular point λ_0. Within each of the regions there is an independent diffusion of the complex Q and one of the free components H_A or H_B. From the conditions of continuity of concentration H_A and H_B at the point λ_0 are zero, i.e., the components H_A and H_B migrate to a point λ_0, whose physical meaning is the front of the chemical reaction of complex formation Q.

2. *Weak complexation* (K >> H_A, H_B). The approximation of weak complexation corresponds to a shift in the reaction $A + B \leftrightarrow Q$ toward the formation of free components. From (4.16) in the zero approximation ($K = \infty$) follows $Q^{(0)} = 0$ and the components A and B diffuse independently. In the next approximation $Q^{(1)} = \frac{H_A^{(0)} H_B^{(0)}}{K} << H_A, H_B,$ which allows us to construct the usual perturbation theory.

3. *The linear approximation* ($\Delta N_A << N_A$, $\Delta N_B << N_B$). Change in the concentration of the complete components during diffusion is much less

than the concentration values. This condition allows linearizing the system of equations (4.17).

4. *Approximation of close coefficients of diffusion.* In the case $D_A = D_B + D_Q$ the system of equations (4.17) has a simple analytic solution.

The solutions obtained in [229-231, 233] show that the most transparent and informative, and allowing a simple physical interpretation is the case of strong complexation. Complex profiles of complete components N_A and N_B in this approximation, arise from the superimposition of profiles of free components H_A and H_B and complexes Q. The formation of the front of the chemical reaction is associated with the possibility of dividing the sample into two regions in which only one of the two free components can migrate (H_A or H_B). Therefore, the appearance of a reaction front is possible only under boundary conditions that allow the existence of free components H_A and H_B in two different regions. If the boundary conditions do not satisfy this requirement, then the reaction front is not formed [233].

Consideration of the kinetic processes of impurity interactions shows that as a transparent and informative mathematical model for the formation of mobile complexes, one should choose the strong complexation approximation of the model of successive diffusion, which allows the simple physical interpretation and may be the most adequate for the physical model.

Under the conditions of model the successive diffusion, the IPDs can be considered as a component that is at the initial instant of time in the bulk of the sample, and the background impurities as a component at the sample boundary and introduced into the sample. In this case, it is possible not to distinguish the diffusion of the impurity inward from the surface of the sample and the decomposition of the supersaturated solid solution. Since only the surface of the crystal is used as a source or sink, the analytical solution is possible for the one-dimensional case [233].

4.2. Model of dissociative diffusion-migration of impurities

In the diffusion of two components (A, B), taking into account the instantaneous reaction of complex formation, we obtain:

$$A + B \leftrightarrow Q, \qquad (4.21)$$

then the thermodynamic equilibrium condition between the free impurity A, B and an impurity bound to the complexes Q, can be written in the form:

$$\mu_A + \mu_B = \mu_Q , \tag{4.22}$$

where μ_A, μ_B is a chemical potentials of a free impurity, μ_Q is a chemical potential of complexes [229].

If the complete concentration of impurities A and B (N_A, N_B) is small in comparison with the concentration of the main substance, then in this approximation $\mu_Q \approx \ln N_Q$ and the equilibrium condition (4.22) can be written in the form [229, 230]:

$$\frac{(N_A - Q)(N_B - Q)}{Q} = k(T), \tag{4.23}$$

where Q is a concentration of complexes, k(T) is the constant of complexation reaction, which depending on temperature (at constant pressure). At k = 0 the whole impurity is bound to the complexes (approximation of strong complexation).

It should be taken into account that in the diffusion equations for complexation the total impurity flux is composed of a free impurity flux and an impurity flux bound to complexes [229, 230]:

$$\frac{\partial N_A}{\partial t} = D_A \frac{\partial^2 (N_A - Q)}{\partial x^2} + D_Q \frac{\partial^2 Q}{\partial x^2} \tag{4.24}$$

$$\frac{\partial N_B}{\partial t} = D_B \frac{\partial^2 (N_B - Q)}{\partial x^2} + D_Q \frac{\partial^2 Q}{\partial x^x} , \tag{4.25}$$

where N_A, N_B is a impurities cocentration; D_A, D_B, D_Q is a diffusion coefficients of free components A, B and complexes, respectively.

The coefficient of diffusion of complexes depends on the mechanism of formation of complexes and on the type of components that form complexes. In particular, if a complex is formed by two interacting atoms, then the diffusion coefficient D_Q is much smaller than the diffusion coefficients of the atoms (D_A, D_B). Therefore, considering the complexes to be inactive, it is possible to neglect the last terms in Eqs. (4.24), (4.25):

$$\frac{\partial N_A}{\partial t} = D_A \frac{\partial^2 (N_A - Q)}{\partial x^2} \tag{4.26}$$

$$\frac{\partial N_B}{\partial t} = D_B \frac{\partial^2 (N_B - Q)}{\partial x^2} \tag{4.27}$$

Since the complexes do not move, the boundary conditions are written for the free impurity. Since the time to establish the equilibrium between the complexes and the free impurity is much smaller than the characteristic diffusion times, it is possible to set as initial conditions the complete impurity concentration [229].

In [230], the task of the successive diffusion of component A into a sample one-doped with component B was considered, taking into account the complexation at the initial and boundary conditions:

$$\begin{aligned} &N_A(x,0) = 0 \\ &N_B(x,0) = N_B(\infty) \\ &N_A(0,t) - Q(0,t) = H_A(0) \\ &\frac{\partial}{\partial x}\left[N_B(x,t) - Q(x,t)\right]_{x=0} = 0 \end{aligned} \tag{4.28}$$

Then the diffusion equation will be written as follows:

$$\left.\begin{aligned} &\frac{1}{2}\left[N_A - N_B - k + \sqrt{k^2 + 2k(N_A + N_B) + (N_A - N_B)^2}\right]' + 2\lambda N_A' = 0 \\ &\frac{1}{2}\left[N_B - N_A - k + \sqrt{k^2 + 2k(N_A + N_B) + (N_A - N_B)^2}\right]' + 2\lambda d^2 N_B' = 0 \end{aligned}\right\}, \tag{4.29}$$

where $\lambda = \frac{x}{2\sqrt{D_A \cdot t}}$ is a Boltzmann substitution; strokes denote differentiation under λ, $d^2 = \frac{D_A}{D_B}$, D_A, D_B is a coefficients of diffusion of components.

The solution of the system of equations (4.29) with the corresponding boundary conditions (the diffusion of impurity A from a constant source into a semiconductor homogeneously doped with impurity B, and impurity B does not evaporate) in the case of strong complexation (k = 0) is as follows [230]:

$$N_A = \begin{cases} N_{B1} + H_A(0)\left[1 - \frac{erf(\lambda / d_A)}{erf(\lambda_0 / d_A)}\right], \lambda < \lambda_0 \\ 0, \lambda > \lambda_0 \end{cases} \tag{4.30}$$

$$N_B = \begin{cases} N_{B1}, \lambda < \lambda_0 \\ N_{B0}\left(1 - \frac{erfc(\lambda d)}{erfc(\lambda_0 d)}\right), \lambda > \lambda_0 \end{cases} \tag{4.31}$$

where $N_{B1} = \frac{N_{B0} e^{-\lambda_0 d^2}}{\sqrt{\pi}\lambda_0 derfc(\lambda_0 d)}$, (4.32)

and the λ_0 is determined from equation:

$$\frac{e^{\lambda_0^2(1-d^2)} erf(\lambda_0)}{erfc(\lambda_0 d)} = \frac{N_{A0}}{N_{B0}} \tag{4.33}$$

We rewrite the system of equations (4.23)-(4.25) for the diffusion impurity kinetics of mobile complexes in the term of complete components, i.e. with $N_A = H_A + Q$ and $N_B = H_B + Q$:

$$d_A^2 (N_A - Q)'' + d_Q^2 Q'' + 2\lambda N_A' = 0 \tag{4.34}$$

$$d_B^2(N_B - Q)'' + d_Q^2 Q'' + 2\lambda N_B^{'} = 0 \tag{4.35}$$

$$(N_A - Q)(N_B - Q) = k(T)Q \tag{4.36}$$

where $d_A^2 = D_A; d_B^2 = D_B; d_Q^2 = D_Q; D_Q$ is a diffusion coefficient of the complex; strokes denote differentiation under λ.

We note that, as was shown above, the solution of the system of equations is considered for the three most frequently encountered cases, which are defined as sequential, simultaneous and mutual diffusion. Under the conditions of our physical model (a two-stage mechanism for the formation of grown-in microdefects), we can speak of successive diffusion, when the condition for the absence of a flux of one of the components located at the initial instant of time in the sample bulk is specified at the interface. The boundary conditions in this case have the following form:

$$H_A\big|_{\lambda=0} = H_A(0); \quad H_A\big|_{\lambda=\infty} = H_A(\infty) \tag{4.37}$$

$$d_B^2 H_B^{'} + d_Q^2 Q^{'}\big|_{\lambda=0} = 0; \quad H_B\big|_{\lambda=\infty} = H_B(\infty)$$

As was mentioned above, in the general case the system of equations (4.34)-(4.36) with the boundary conditions (4.37) does not have analytic solutions; therefore, for the analysis of the type of impurity profiles, it is necessary to consider limiting cases. Consider the strong complexation (k = 0) approximation, which physically means that the reaction $A + B \leftrightarrow Q$ is sharply shifted toward the formation of the complex. In addition, formally, from the system of equations (4.34)-(4.36) for k = 0 it follows that the concentration of at least one of the free components is zero, i.e., $H_A = 0$ or $H_B = 0$ (the impurity completely binds to complexes).

The solution of the task of diffusion of component A into a semi-infinite sample uniformly doped with component B, under the condition that there is no evaporation of component B from the sample and the presence of free component A at the sample boundary, has the form [233]:

$$H_A = N_A - Q = \begin{cases} (N_A(0) - N_{B1})\left[1 - \dfrac{erfc(\lambda / d_A)}{erfc(\lambda_0 / d_A)}\right], & \lambda \le \lambda_0 \\ 0, & \lambda > \lambda_0 \end{cases} \tag{4.38}$$

$$H_B = N_B - Q = \begin{cases} 0, & \lambda \le \lambda_0 \\ N_B(\infty)\left[1 - \dfrac{erfc(\lambda / d_B)}{erfc(\lambda_0 / d_B)}\right], & \lambda > \lambda_0 \end{cases} \tag{4.39}$$

$$Q = \begin{cases} N_{B1}, & \lambda \geq \lambda_0 \\ N_{B1}\dfrac{erfc(\lambda / d_Q)}{erfc(\lambda_0 / d_Q)}, & \lambda < \lambda_0 \end{cases} \quad (4.40)$$

$$N_{B1}S_1(\lambda_0 / d_Q) = N_B(\infty)S_1(\lambda_0 / d_B)$$
$$N_{B1}S_1(\lambda_0 / d_Q) = \{N_A(0) - N_{B1}\}S_2(\lambda_0 / d_A) \quad (4.41)$$

where $S_1(x) = \dfrac{\exp(-x^2)}{\sqrt{\pi}xerfc(x)}; S_2(x) = \dfrac{\exp(-x^2)}{\sqrt{\pi}xerf(x)}; N_A(0) - N_{B1} = H_A(0).$

Under the conditions of a two-stage mechanism for the formation of grown-in microdefects, we assume that component A is a background impurities (oxygen or carbon), and component B is an IPD (vacancy or silicon interstitial atom) [8]. For the vacancy branch of the mechanism, we consider the interaction of "oxygen + vacancy" (O+V), for the interstitial branch of the mechanism the "carbon + silicon interstitial atom" (C+I). In the calculations the following quantities were used [8]: $H_A(0) = H_o(0) = 4 \cdot 10^{15} cm^{-3}(FZ - Si)$; $H_A(0) = H_o(0) = 8 \cdot 10^{16} cm^{-3}(CZ - Si)$; $C_V = 8.84 \cdot 10^{14} cm^{-3}$; $D_V = 4 \cdot 10^{-5} cm^2/s$; $D_o = 0.17 \exp(-2.54/kT)$, $k = 8.6153 \cdot 10^{-5} eV/K$, $H_A(0) = H_c(T_m) = 4 \cdot 10^{15} cm^{-3}(FZ - Si)$, $H_A(0) = H_c(0) = 1 \cdot 10^{16} cm^{-3}(CZ - Si)$, $C_I(0) = 6.31 \cdot 10^{14} cm^{-3}$, $D_I = 4.75 \cdot 10^{-4} cm^2/s$, $D_c = 1.9 \cdot \exp(-3.1/kT)$.

The solution of equations (4.32) and (4.33) has a physical meaning ($N_{B1} \sim 10^{12}...10^{14}\ cm^{-3}$) only for $\lambda \approx 0.01$, which corresponds to $\sim 3 \cdot 10^{-4}$ mm. We note that in the strong complexation approximation the λ_0 is interpreted as the boundary of the front of the complex formation reaction. Since x is a length of the crystal, and the value $x = 0$ is the position of the crystallization front, then we can say that the process of complexation occurs near the crystallization front [240].

These calculated data are confirmed by early experimental studies of the initial stages of the defect formation process [12]. In these experiments, quenching of undoped FZ-Si single crystals with a diameter of 30 mm, grown in vacuum at different growth rates (2.0; 3.0; 6.0; 9.0 mm/min) was studied. At the right time, the molten zone was blown sharply by a directed flow of argon. These experiments allowed us to determine the formation temperatures of microdefects (Table 4.1) [12].

Table 4.1. The temperatures of formation of microdefects of various types

Growth rate, mm/min	Conditions of growth	Type of microdefects	Distance from the crystallization front, mm	Temperatures of formation, ± 20 K
2.0	Quenching	A	23	$T_A = 1373$
3.0	Quenching	B	-	$T_B = 1653$
6.0; 9.0	Quenching	D; I+V	-	$T_{D;\ I+V} = 1653$

Quenching of FZ-Si crystals grown at V_g = 6.0 mm/min leads to the formation of a so-called "defect-free region" between the crystallization front and the region with D-microdefects. TEM-studies showed that in the "defect-free region" there are both interstitial and vacancy defects of 2...7 nm in size and their concentration ~ $4.5 \cdot 10^{13}$ cm^{-3} ((I+V)-microdefects). In FZ-Si crystals grown at V_g = 9.0 mm/min, after their quenching, interstitial and vacancy microdefects were found at approximately comparable concentrations. When studying the separation surface, it was found [12] that dislocations are introduced at distances not exceeding 1...3 mm from the crystallization front due to thermal shock. Therefore, it is difficult to determine exactly the beginning of the process of formation of primary grown-in microdefects. Taking this fact into account and proceeding from the results of Table. 4.1, we can say that the primary grown-in microdefects are formed near the crystallization front.

On Fig. 4.1a,b is shown the T(x) dependences for FZ-Si crystals (diameter 30 mm) and CZ-Si (diameter 50 mm). For FZ-Si crystals the T(x) dependence was determined in accordance with the empirical relationship [5]:

$$\frac{dT}{dx} = 10 + (x-16)^2 \exp(-61.2V_g - 0.28), \qquad (4.42)$$

where x is the distance from the crystallization front to the considering cross section.

For CZ-Si crystals it was assumed that $G_{FZ-Si} \approx 3G_{CZ-Si}$, where G is a axial temperature gradient. For FZ-Si crystals on Fig. 4.1 are shown the dependencies at V_g = 1…9.0 mm/min and for CZ-Si at V_g = 0.5…3.0 mm/min. The radial temperature gradient was not taken into account in the calculations; the distribution of defects in the crystal along the diameter is uniform. Theoretical calculations was made for the vacancy (O+V) and

interstitial (C+I) branches of the two-stage mechanism for the formation of grown-in microdefects. On Fig. 4.2a,b are shown calculated dependencies $C_V / C_V(0), C_{Q1} / C_{Q1}(0)$ in dependence from length of CZ-Si crystals in the range of growth rates 0.5…3.0 mm/min (where $C_V(0)$ and $C_{Q1}(0)$ is the concentrations of vacancies and complexes (O+V) near crystallization front, accordingly). On Fig. 4.3a,b are shown calculated dependencies $C_I / C_I(0), C_{Q2} / C_{Q2}(0)$ in dependence from length of CZ-Si crystals in the range of growth rates 0.5…3.0 mm/min (where $C_I(0)$ and $C_{Q2}(0)$ is the concentrations of silicon interstitial atoms and complexes (C+I) near crystallization front, accordingly). Similar calculated dependencies were obtained depending on the length of the FZ-Si crystal in the range of growth rates 1...9.0 mm/min (Fig. 4.4; 4.5) [240].

At the next stage of the calculations, the analytical appointment of the two-dimensional temperature field was made by the method [7]. The technique assumes tasking of the temperature field in the following form: $1/T = 1/T_m + G_a x / T_m^2$. According to [7], the temperature field is given along the crystal axis and along its surface; the ratio of the field along the surface to the field along the axis varies by a certain step. On the crystallization front G_a is varied for six crystal growth rates of CZ-Si (0.5...3.0 mm/min) and nine growth rates for FZ-Si crystals (1.0...9.0 mm/min) (Fig. 4.6…4.10) [240]. Also were calculated a radial distribution of concentrations for CZ-Si and FZ-Si crystals (Fig. 4.11…4.14).

The numbers of 1...9 and 0.5...3 on Fig. 4.11, and 4.12, and 4.13, and 4.14 denote the growth rates of the crystal from V_{g1} = 1.0 mm/min to V_{g9} = 9.0 mm/min and from V_{g1} = 0.5 mm/min to V_{g3} = 3.0 mm/min, accordingly.

The tasking of the two-dimensional temperature field by the method [7], developed for large-scale CZ-Si crystals, leads to results similar to those obtained for the tasking of the temperature field by the method [5] developed for small-scale FZ-Si crystals. The obtaining of similar results by two methods indicates the absence of fundamental differences between them, their interchangeability and the possibility of their application to crystals of any diameters [8].

Let us estimate the applicability of the mathematical model for the formation of primary grown-in microdefects based on the experimental results of small-scale crystals for large-scale crystals with diameters greater than 100 mm grown in the vacancy regime (in the terminology of

Ref. [119]). In our model for a range of growth rates of 0.5...3.0 mm/min in the interval of distances 6...10 cm from the crystallization front, the concentration of vacancies decreases by an order of magnitude. These intervals correspond to the temperature of vacancy microvoids formation (~ 1423...1373 K). It was shown [7] that for large-scale single crystals of CZ-Si the value of G_a decreases rapidly with distance from the crystallization front to values below 10 K/cm. For standard values G_a = 81…31 K/cm this decrease occurs at distances of 6...12 cm from the crystallization front, which corresponds to the temperature range T = 1423...1373 K [194]. At T = 1423 K, the vacancy concentration becomes lower by an order of magnitude [119]. In accordance with the data of [7, 119], these conditions lead to the formation of microvoids in the temperature range 1423...1373 K.

Analysis of the calculated data shows their good agreement with the experimental data and the provisions of the two-stage model for the formation of grown-in microdefects. This concerns the temperatures of formation of primary grown-in microdefects from experiments on quenching of crystals (Table 4.1) and also values of concentrations (I+V)-microdefects and D(C)-microdefects, determined by TEM-studies $(\sim 10^{13}...10^{14}\ cm^{-3})$ [13]. Therefore, it can be said that the dissociative model of impurity diffusion is in good agreement with the experimental results and can serve as a theoretical basis for the complexation process within the framework of two-stage mechanism of grown-in microdefect formation.

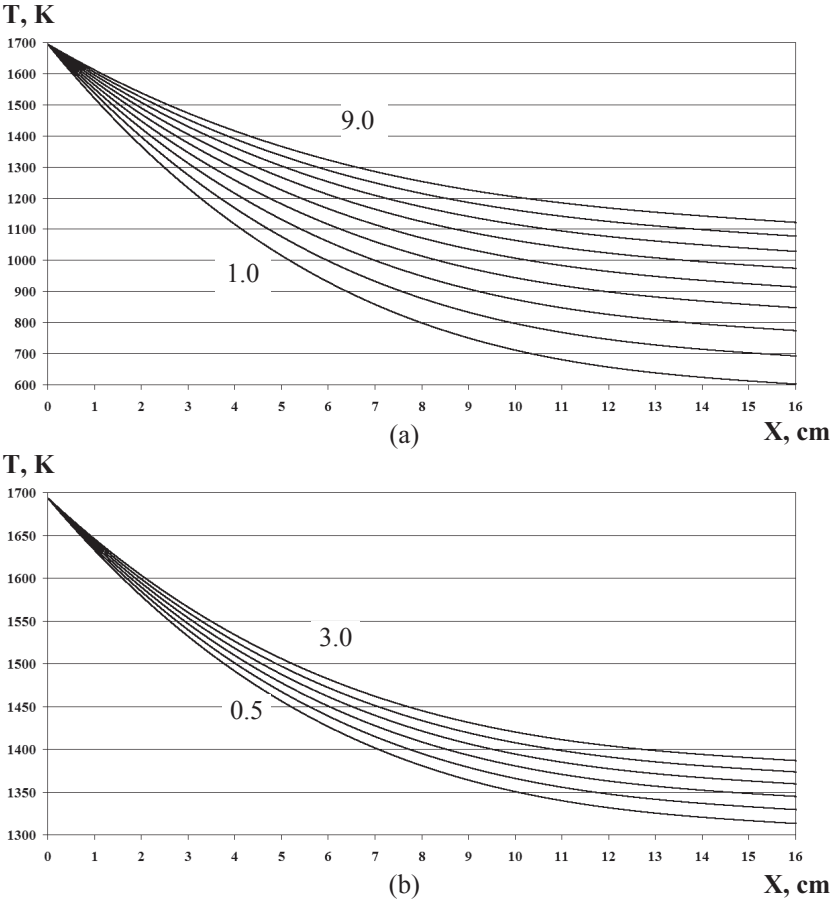

Fig. 4.1. The curves T(x):
(a) for FZ-Si grown at V_g = 1…9.0 mm/min,
(б) for CZ-Si grown at V_g = 0.5…3.0 mm/min.

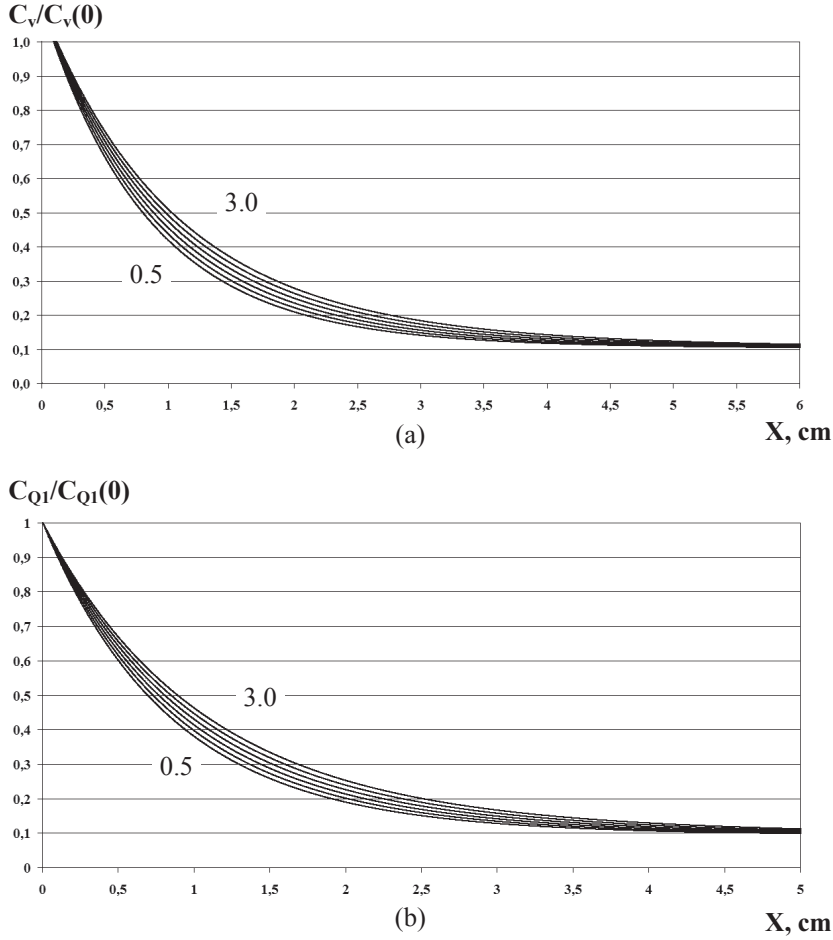

Fig. 4.2. The curves
(*a*) $C_V / C_V(0)$, (*b*) $C_{Q1} / C_{Q1}(0)$ in dependence from length of CZ-Si crystal

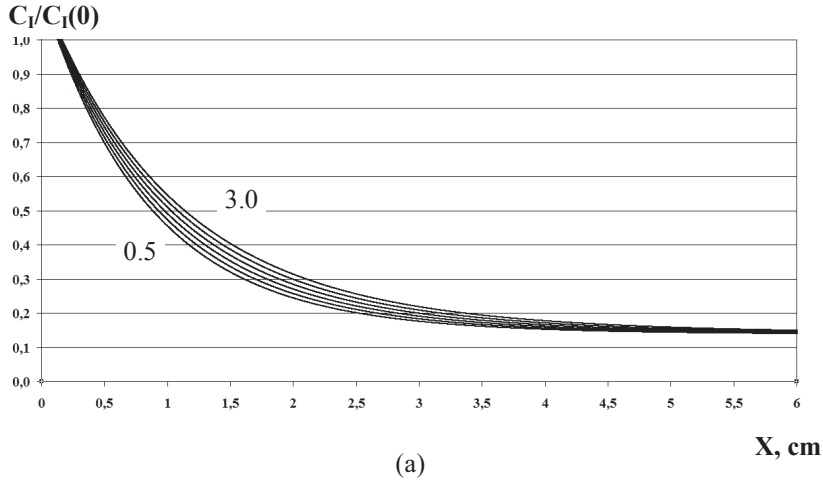

(a)

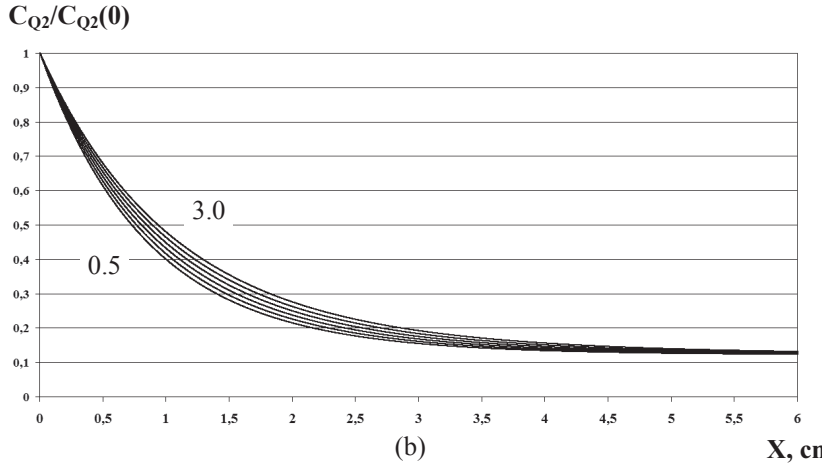

(b)

Fig. 4.3. The curves
(*a*) $C_I / C_I(0)$, (*b*) $C_{Q2} / C_{Q2}(0)$ in dependence from length of CZ-Si crystal

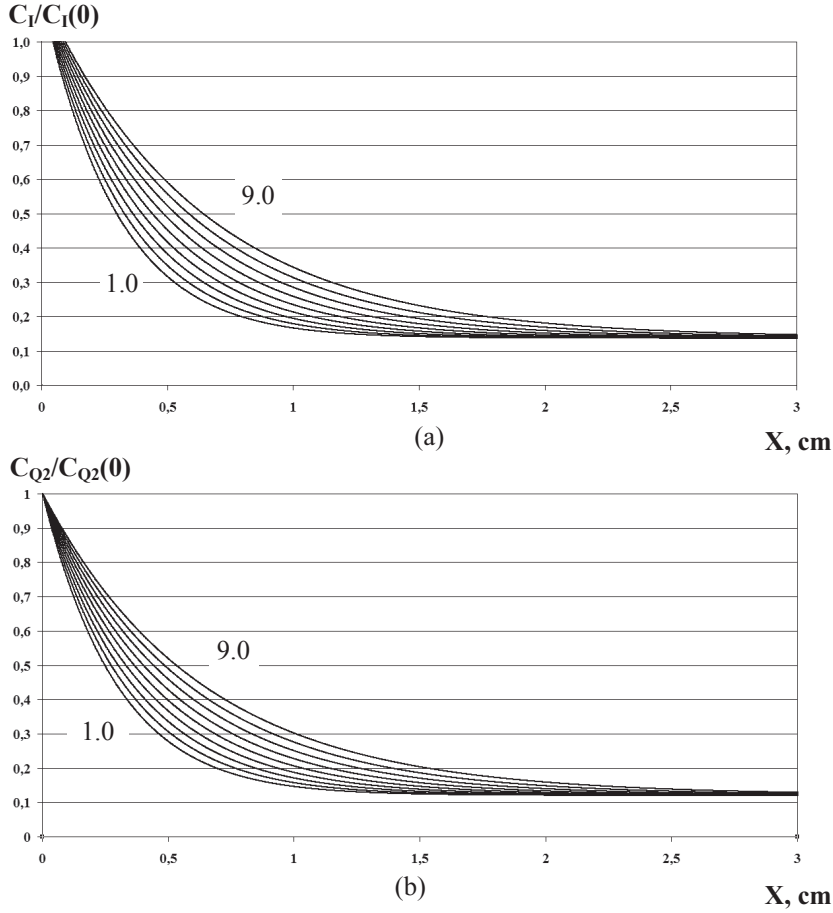

Fig. 4.4. The curves
(*a*) $C_I / C_I(0)$, (*b*) $C_{Q2} / C_{Q2}(0)$ in dependence from length of FZ-Si crystal

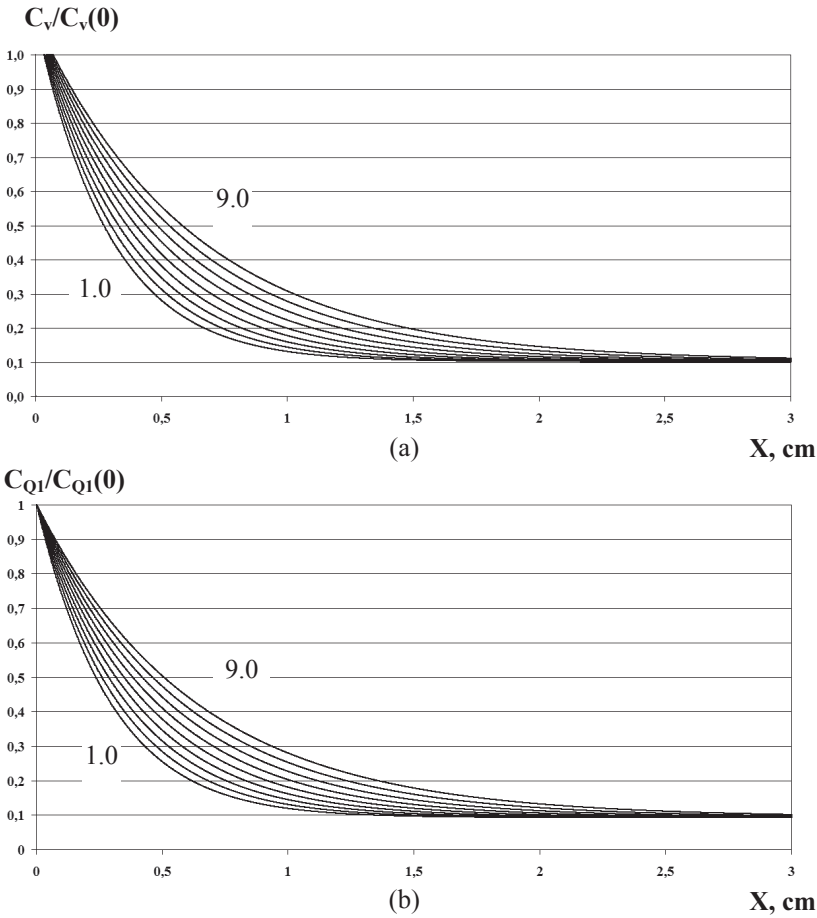

Fig. 4.5. The curves
(*a*) $C_V / C_V(0)$, (*b*) $C_{Q1} / C_{Q1}(0)$ in dependence from length of FZ-Si crystal

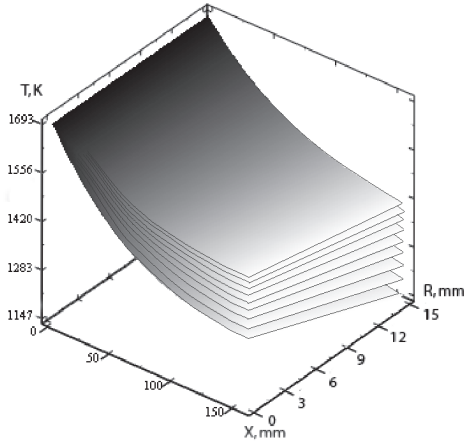

(a)

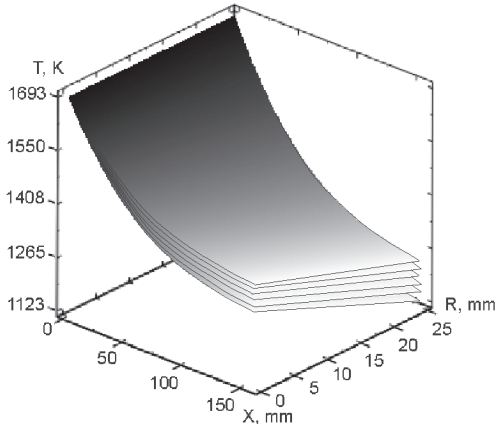

(b)

Fig. 4.6. The set of flatness T(x):
(a) for FZ-Si grown at V_g = 1…9.0 mm/min,
(b) for CZ-Si grown at V_g = 0.5…3.0 mm/min

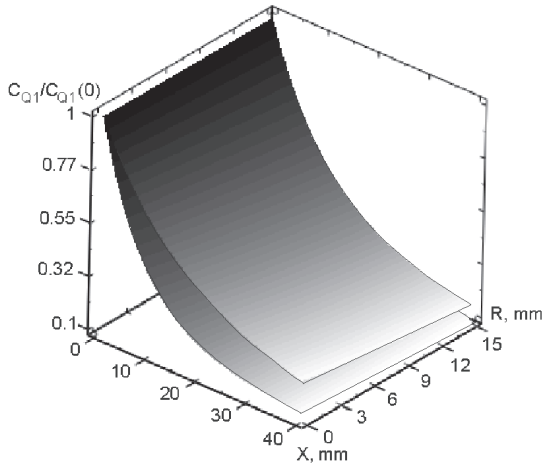

(a)

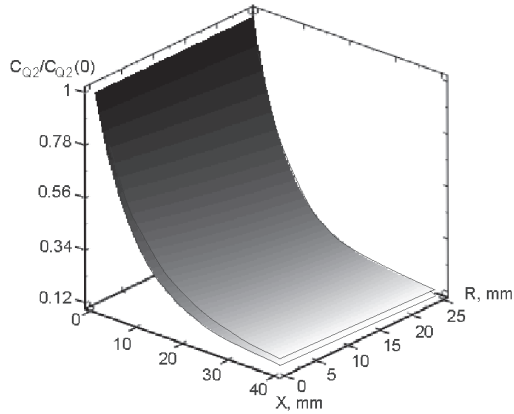

(b)

Fig. 4.7. The set of flatness:
(a) $C_{Q1} / C_{Q1}(0)$ for FZ-Si,
(b) $C_{Q2} / C_{Q2}(0)$ for CZ-Si

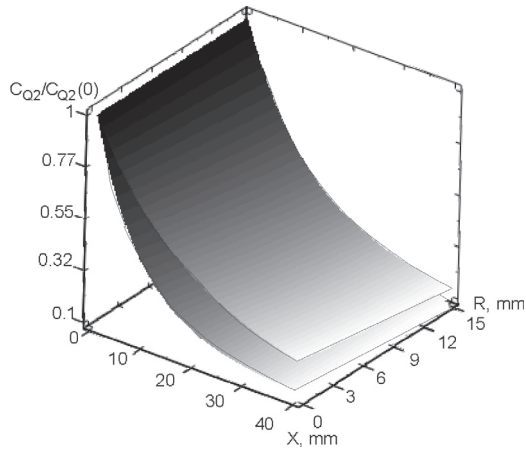

(a)

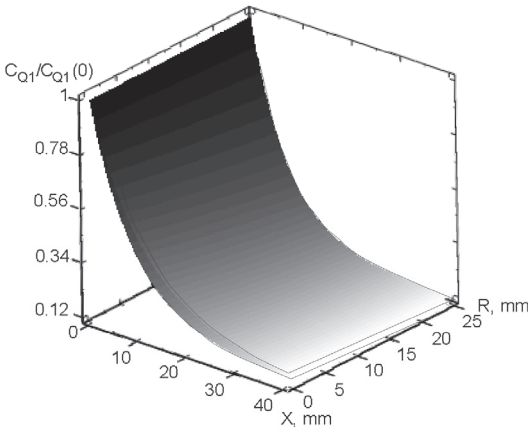

(b)

Fig. 4.8. The set of flatness:
(a) $C_{Q2} / C_{Q2}(0)$ for FZ-Si,
(b) $C_{Q1} / C_{Q1}(0)$ for CZ-Si

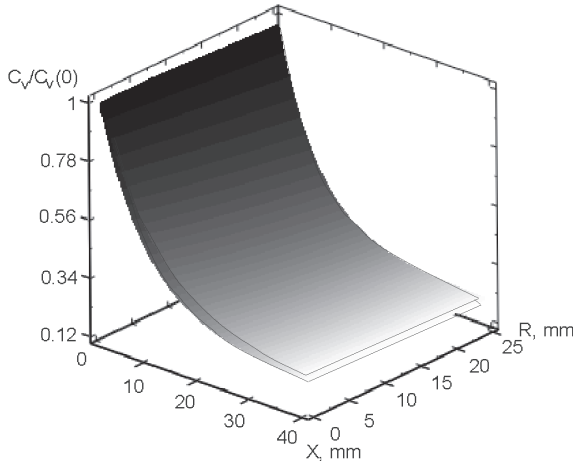

(a)

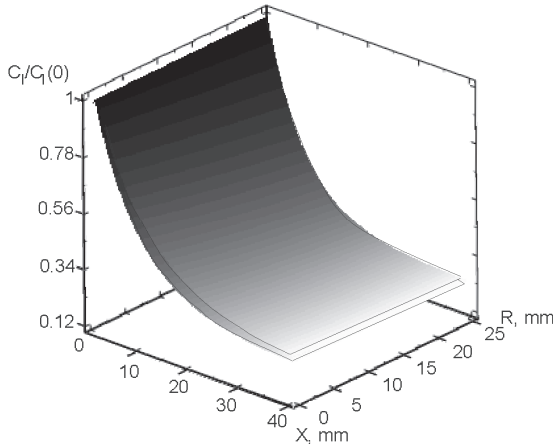

(b)

Fig. 4.9. The set of flatness:
$(a)\ \ C_v / C_v(0)$, $(b)\ \ C_I / C_I(0)$ for CZ-Si

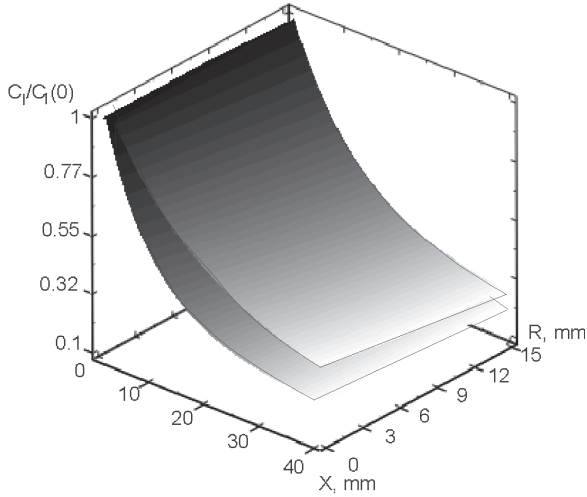

(a)

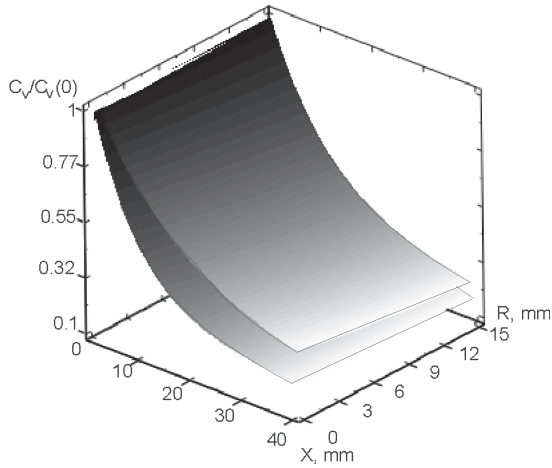

(b)

Fig. 4.10. The set of flatness:
$(a)\ \ C_I / C_I(0)$, $(b)\ \ C_v / C_v(0)$ for FZ-Si

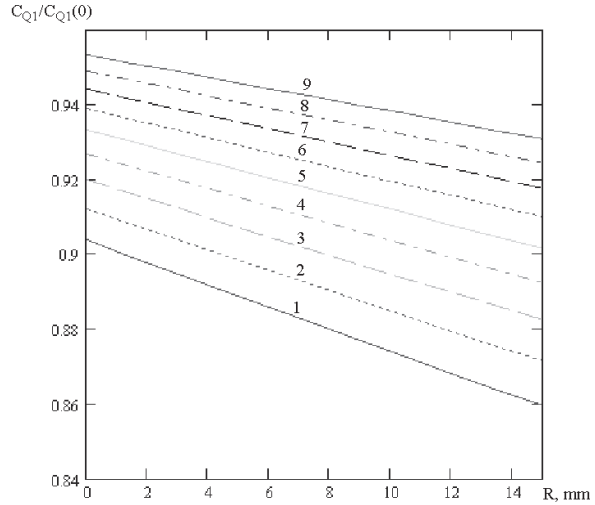

(a)

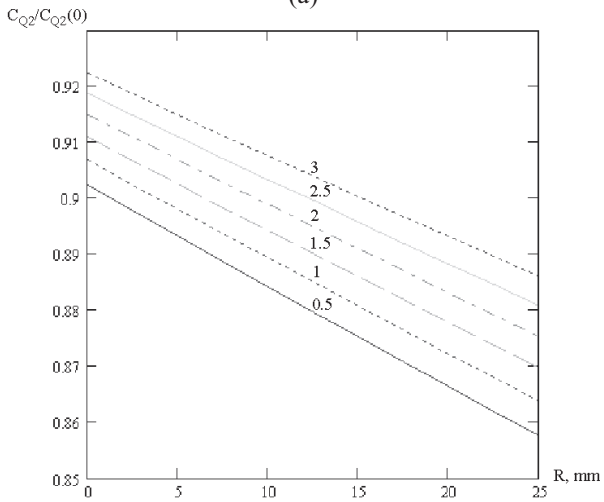

(b)

Fig. 4.11. Radial dependences
(*a*) $C_{Q1} / C_{Q1}(0)$ for FZ-Si,
(*b*) $C_{Q2} / C_{Q2}(0)$ for CZ-Si

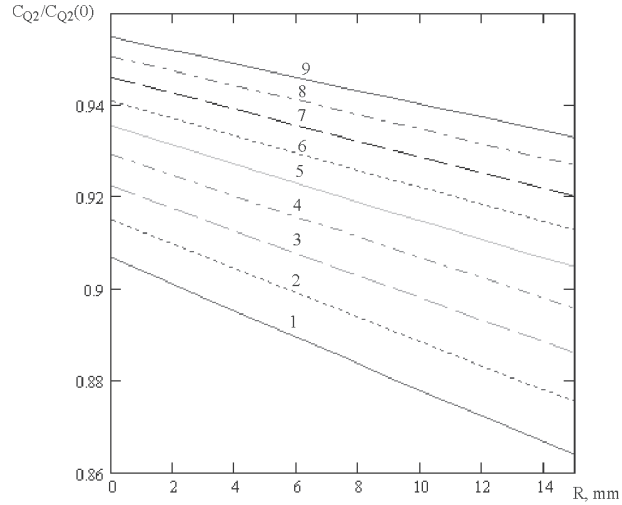

(a)

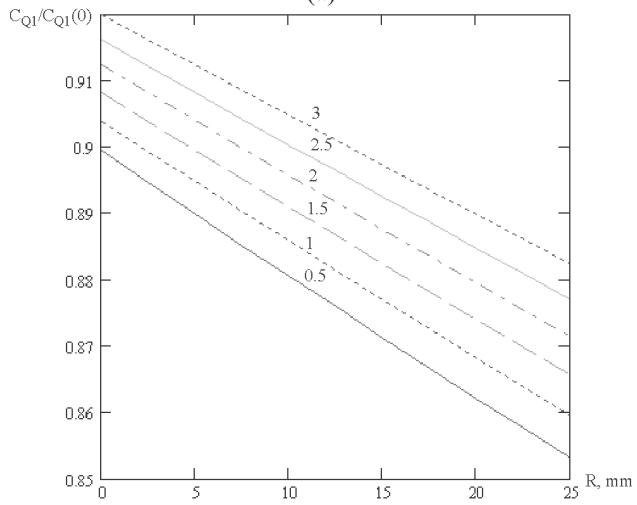

(b)

Fig. 4.12. Radial dependences
(a) $C_{Q2} / C_{Q2}(0)$ for FZ-Si,
(b) $C_{Q1} / C_{Q1}(0)$ for CZ-Si

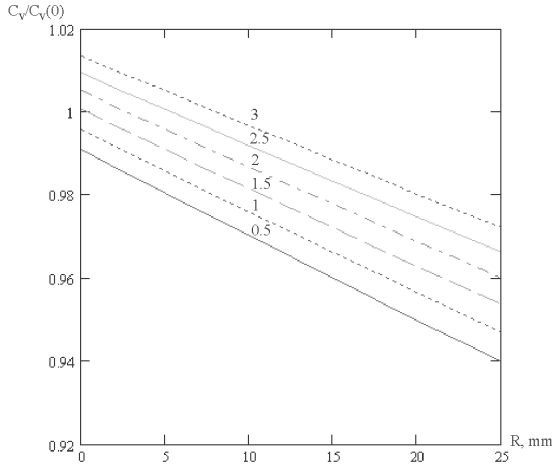

(a)

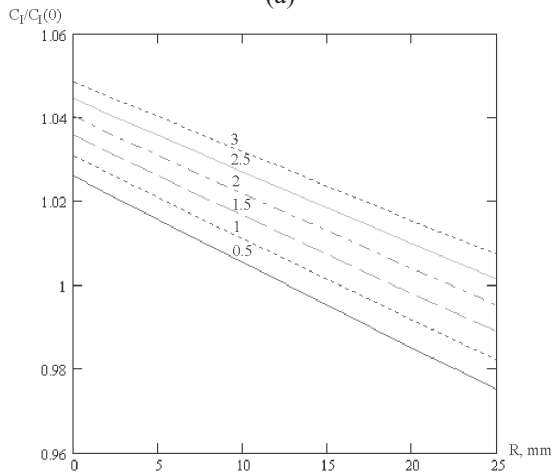

(b)

Fig. 4.13. Radial dependences
$(a)\ \ C_v / C_v(0)$, $(b)\ \ C_I / C_I(0)$ for CZ-Si

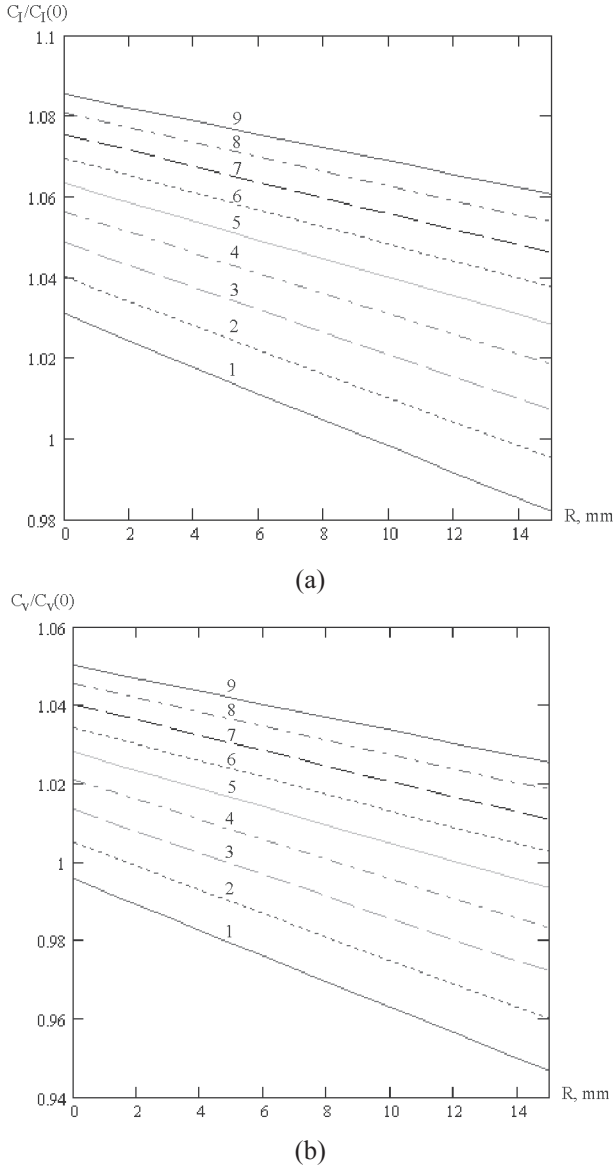

Fig. 4.14. Radial dependences
$(a)\ \ C_I / C_I(0)$, $(b)\ \ C_v / C_v(0)$ for FZ-Si

4.3. Kinetics of the high-temperature precipitation process in dislocation-free silicon single crystals

Calculations in the framework of the dissociative diffusion-migration model of impurities showed that the boundary of the front of the complexation reaction ("oxygen + vacancy" and "carbon + silicon interstitial atom") is at a distance of ~ $3 \cdot 10^{-4}$ mm from the crystallization front [12, 240]. This approximation is relevant at the initial stages of nuclei formation, when their dimensions are small and the application of the Fokker-Planck continual differential equations is impossible. In [241], a modern approach was considered in the form of systems of interrelated discrete differential equations of quasi-chemical reactions for describing the initial stages of nucleation of new phases and a similar system of continual differential equations of the Fokker-Planck.

Grown-in microdefects have been considered as clusters of particles of various kinds, the formation and decomposition of which can be represented in form as a reaction consisting of random processes of attachment and detachment of particles X:

$$\begin{aligned} A_n + X &\xrightarrow{g(n,r,t)} A_{n+1} \\ A_n &\xrightarrow{d(n,r,t)} A_{n-1} + X \end{aligned} \qquad (4.43)$$

where A_n is a cluster A consisting of n particles of X; $g(n,$ r, $t)$ is a cluster A_n growth rate; $d(n,$ r, $t)$ is a cluster A_n decay rate. The concentration of clusters A_n at the point **r** is determined by function $f(n,$ r, $t)$. The variation on time of this function is described by a system of discrete kinetic differential equations:

$$\frac{\partial f(n,r,t)}{\partial t} = J(n,r,t) - J(n+1,r,t), (n = 2,3,...,n_{\max}) \qquad (4.44)$$

$$J(n,r,t) = g(n-1,r,t) f(n-1,r,t) - d(n,r,t) f(n,r,t)$$

The conservation of the number of particles X is described by equation:

$$\frac{\partial f(1,r,t)}{\partial t} = -J(2,r,t) - \sum_{n=2}^{n_{\max}} J(n,r,t) \qquad (4.45)$$

where $n_{\max}$ is the maximum number of particles X contained in the cluster A. Using the expansion of the functions g, d and f which smoothly depend on n in the Taylor series up to the second order, from the system of discrete equations we obtain a continual partial differential equation (the Fokker-Planck equation) [197]:

$$\frac{\partial f(n,r,t)}{\partial t} = -\frac{\partial I(n,r,t)}{\partial n} \tag{4.46}$$

In this case, the flow of monomers in a space of sizes n is equal to

$$I(n,r,t) = Af - B\frac{\partial f}{\partial n} \tag{4.47}$$

and the kinetic coefficients A and B are described by equations

$$A = g - d - \frac{\partial B}{\partial n}, B = \frac{g+d}{2} \tag{4.48}$$

The flows J and I when solving the system of equations (4.44) and (4.46), are joined at the point $n=n_{min}$. Then the particle conservation law (4.45) is transformed to the form

$$\frac{\partial f(1,r,t)}{\partial t} = -J(2,r,t) - \sum_{n=2}^{n_{min}-1} J(n,r,t) - \int_{n_{min}}^{n_{max}} I(n,r,t)dn \tag{4.49}$$

Equation (4.46) is a diffusion-drift equation describing the evolution of the distribution function f in a space of sizes n. The system of equations (4.44)-(4.49) makes it possible, within the framework of a unified model, to consider the processes of nucleation and the subsequent growth of clusters. A conditional boundary separating small and large clusters is considered to be the value $n = n_{min}$ which in the calculations is assumed to be from 10 to 20. This value is the boundary between the size region in which the thermodynamic approach to the description of physical processes is right ($n>n_{min}$) and the area where it is necessary to take into account the clusters atomic nature ($n<n_{min}$).

To describe the kinetics of simultaneous nucleation and growth (dissolution) in a supersaturated solid impurity solution in silicon of new-phase particles of several types, a system consisting of oxygen, carbon, vacancies and interstitial silicon atoms was considered. Interactions in such system during the crystal cooling from 1683K lead to the formation of precipitates of oxygen and carbon [52]. For the formulation and interpretation of computational experiments, a dimensional analysis of the kinetic equations and conservation laws was performed using the characteristic time constants and the critical sizes of the defects. With the help of this analysis, a comparative analysis of the joint evolution of oxygen and carbon precipitates was made and the computational scheme for numerical solution of the equations was optimized.

The nucleation and evolution in the process of crystal cooling of a system of grown-in microdefects, which consists of oxygen precipitates and carbon precipitates, are described by systems of coupled differential equations (4.44)-(4.49) for each type of defects. The connection between these systems is realized through the laws of conservation of point defects,

which determine the current values of their concentrations in the crystal and effect on the rates of growth and dissolution of clusters of both types. For a thin plane-parallel wafer of large diameter, when the conditions in a plane parallel to the surface of the crystal can be considered homogeneous and consider only diffusion along the normal to the surface (the z axis), the mass balance of point defects in the crystal is described by a system of diffusion equations for the silicon interstitial atoms, oxygen atoms, carbon and vacancies:

$$\begin{aligned}
\frac{\partial C_o}{\partial t} &= D_o \frac{\partial^2 C_o}{\partial z^2} - \frac{\partial C_o^{SiO_2}}{\partial t} \\
\frac{\partial C_c}{\partial t} &= D_c \frac{\partial^2 C_c}{\partial z^2} - \frac{\partial C_c^{SiC}}{\partial t} \\
\frac{\partial C_i}{\partial t} &= D_i \frac{\partial^2 C_i}{\partial z^2} + \frac{\partial C_i^{SiO_2}}{\partial t} - \frac{\partial C_i^{SiC}}{\partial t} \\
\frac{\partial C_v}{\partial t} &= D_v \frac{\partial^2 C_v}{\partial z^2} - \frac{\partial C_v^{SiO_2}}{\partial t} + \frac{\partial C_v^{SiC}}{\partial t}
\end{aligned} \tag{4.50}$$

Equations (4.50) take into account that oxygen precipitates are both sinks for oxygen atoms and vacancies, and sources of interstitial silicon atoms. Then

$$\begin{aligned}
C_o^{SiO_2} &= \sum_{n_o=2}^{n_o^{\min}-1} n_o \cdot f_{SiO_2}(n_o,z,t) + \int_{n_o^{\min}}^{n_o^{\max}} n_o \cdot f_{SiO_2}(n_o,z,t)dn_o \\
C_v^{SiO_2} &= \gamma_v C_o^{SiO_2}, C_i^{SiO_2} = \gamma_i C_o^{SiO_2}
\end{aligned} \tag{4.51}$$

At the same time, carbon precipitates are sinks for carbon atoms and interstitial silicon atoms, as well as sources of vacancies. Then

$$\begin{aligned}
C_c^{SiC} &= \sum_{n_c=2}^{n_c^{\min}-1} n_c \cdot f_{SiC}(n_c,z,t) + \int_{n_c^{\min}}^{n_c^{\max}} n_c \cdot f_{SiC}(n_c,z,t)dn_c \\
C_v^{SiC} &= \gamma_v^* C_c^{SiC}, C_i^{SiC} = \gamma_i^* C_c^{SiC}
\end{aligned} \tag{4.52}$$

In the general case the proportionality multipliers $\gamma_v, \gamma_i, \gamma_v^*, \gamma_i^*$ may depend on the values n_o, n_c and are determined by the conditions of thermodynamic equilibrium [242]. In addition, the recombination of pairs of interstitial silicon atoms and vacancies is not taken into account in Eqs. (4.50) [213].

The system of interrelated Fokker-Planck equations can be transformed to a dimensionless form:

$$\frac{\partial \widetilde{f}_{SiO_2}}{\partial \tau} = -\frac{\partial I_{SiO_2}}{\partial \widetilde{\upsilon}_O} \qquad (4.53)$$
$$\frac{\partial \widetilde{f}_{SiC}}{\partial \tau} = -\frac{t_0}{t_c}\frac{\partial I_{SiC}}{\partial \widetilde{\upsilon}_c}$$

where $\tau = \frac{t}{t_o}$ is s dimensionless time. The time constants in equations (4.53) are given as $t_O = (n_O^{cr,0})^2 / g_{SiO_2}^0; t_c = (n_c^{cr,0})^2 / g_{SiC}^0$, where critical growth rates of precipitates $g_{SiO_2}^0 = N_O^0 \upsilon_O \exp(-G_{act}^{SiO_2} / kT); g_{SiC}^0 = N_O^0 \upsilon_c \exp(-G_{act}^{SiC} / kT)$. The normalized sizes of the precipitates are defined in Eqs. (4.53) as $\widetilde{\upsilon}_O = n_O / n_O^{cr,0}; \widetilde{\upsilon}_c = n_c / n_c^{cr,0}$, where n_O^{cr}, n_c^{cr} is the normalizing critical sizes of precipitates. The values $N_O^0 = 4\pi (r_O^{cr,0})^2 \delta_{SiO_2} C_O^{eq}; N_c^0 = 4\pi (r_c^{cr,0})^2 \delta_{SiC} C_c^{eq}$ is the quantities of particles in the vicinity of the corresponding precipitates with critical sizes. The function of size distribution of precipitates in equations (4.53) is normalized to the initial concentrations of the corresponding nucleation centers:

$$\widetilde{f}_{SiO_2} = \frac{f_{SiO_2}}{f_{SiO_2}^0}; \widetilde{f}_{SiC} = \frac{f_{SiC}}{f_{SiC}^0} \qquad (4.54)$$

Particle flows in the right-hand sides of equations (4.53) are described by equations

$$A_{SiO_2} = (\widetilde{g}_{SiO_2} - \widetilde{d}_{SiO_2}) n_O^{cr,0} - \frac{\partial B_{SiO_2}}{\partial \widetilde{\upsilon}_O}; A_{SiC} = (\widetilde{g}_{SiC} - \widetilde{d}_{SiC}) n_O^{cr,0} - \frac{\partial B_{SiC}}{\partial \widetilde{\upsilon}_O}; \qquad (4.55)$$

in which the notation for normalized kinetic coefficients is

$$A_{SiO_2} = (\widetilde{g}_{SiO_2} - \widetilde{d}_{SiO_2}) n_O^{cr,0} - \frac{\partial B_{SiO_2}}{\partial \widetilde{\upsilon}_O}; A_{SiC} = (\widetilde{g}_{SiC} - \widetilde{d}_{SiC}) n_O^{cr,0} - \frac{\partial B_{SiC}}{\partial \widetilde{\upsilon}_O}; \qquad (4.56)$$

$$B_{SiO_2} = \frac{\widetilde{g}_{SiO_2} + \widetilde{d}_{SiO_2}}{2}; B_{SiC} = \frac{\widetilde{g}_{SiC} + \widetilde{d}_{SiC}}{2} \qquad (4.57)$$

The normalized rates of growth and dissolution of precipitates in Eqs. (4.56)-(4.57) have the form

$$\widetilde{g}_{SiO_2} = \frac{g_{SiO_2}}{g_{SiO_2}^0}; \widetilde{g}_{SiC} = \frac{g_{SiC}}{g_{SiC}^0}; \widetilde{d}_{SiO_2} = \frac{d_{SiO_2}}{g_{SiO_2}^0}; \widetilde{d}_{SiC} = \frac{d_{SiC}}{g_{SiC}^0} \qquad (4.58)$$

The critical size of the precipitates can be determined in accordance with [242]:

$$r_O^{cr} = \frac{2\sigma u V_p}{kT\ln(S_0 S_i^{-\gamma_i} S_v^{\gamma_v}) - 6\mu\delta\varepsilon u V_p} \quad (4.59)$$

$$r_C^{cr} = \frac{2\sigma u V_p}{kT\ln(S_c S_i^{\gamma_i} S_v^{-\gamma_v}) - 6\mu\delta\varepsilon u V_p} \quad (4.60)$$

The number of impurity atoms in compressed precipitates with radii r_O and r_C is defined as [223, 243]:

$$n_{O,C} = \frac{4\pi r_{O,C}^3 \cdot (1+\gamma_i x+\gamma_v x)}{3V_p}\left(\frac{1+\delta}{1+\varepsilon}\right)^3 \quad (4.61)$$

where V_p is the precipitate volume, x is the fraction of impurity atoms per one IPD, $x \le 2$, $\gamma_i \le ½$, $\gamma_v \le ½$.

The following data were used in the calculations: $V_p = 4.302\cdot10^{-2}$ nm^3 (SiO_2); $V_p = 2.04\cdot10^{-2}$ nm^3 (SiC); σ = 310 erg/cm^2 (SiO_2); σ = 1000 erg/cm^2 (SiC); μ = $6.41\cdot10^{10}$ Pa; δ = 0.3; ε = 0.15; $\gamma_i = 0.4; \gamma_v = 0.1$; x = 1.5; δ_{SiO_2} = 0.5431 nm; $\delta_{SiC} = 0.4359nm$; $C_O^{eq} = 8\cdot10^{16}cm^{-3}$; $C_c^{eq} = 1\cdot10^{16}cm^{-3}$; $G_{act}^{SiO_2} = 2.54eV$; $G_{act}^{SiC} = 3.17eV$ $D_O = 0.17\exp(-2.54eV/kT); D_c = 1.9\exp(-3.1eV/kT);$, , $k = 8.6153\cdot10^{-5} eV/K$ [241].

When analyzing the evolution of grown-in microdefects during the crystal cooling, the important parameters are the characteristic constants in the space of sizes: the critical dimensions of the corresponding grown-in microdefects and the characteristic time constants associated with them, which determine the scale of the time variation of the distribution function of microdefects in size. The time constants in Eqs. (4.53) allow us to calculate the normalizing dimensions $n_O^{cr,0}$ and $n_C^{cr,0}$ by substituting in (4.59)-(4.60) the values of supersaturations corresponding to the complete escape of oxygen and carbon atoms to the precipitates. In addition, in each Eqs. the supersaturations of the remaining point defects are assumed to be equal to unity.

The increase in the supersaturations of point defects (oxygen and carbon atoms, interstitial silicon atoms and vacancies) leads to a decrease in the corresponding critical size of the precipitates and promotes the acceleration of their growth. The decrease in the characteristic times also leads to acceleration of precipitation processes with increasing

supersaturations of point defects. The reverse trend is observed when the crystal is cooled from the crystallization temperature [241].

The important feature of the characteristic times is the inverse proportionality to the multiplications of the characteristics of point defects (diffusion coefficients and equilibrium concentrations):

$$t_o \sim (D_o C_o^{eq})^{-1}, \quad t_c \sim (D_c C_c^{eq})^{-1} \tag{4.62}$$

Since the multiplication for the oxygen atoms significantly exceeds the analogous multiplication for the carbon atoms, the rate of evolution of the distribution function over the size of carbon precipitates will exceed the same rate for oxygen precipitates. This fact means that the development of the microdefect structure of dislocation-free silicon single crystals in the process of crystal cooling after growth is determined mainly by the rate of growth of oxygen precipitates. Detailed quantitative information on the characteristics of the primary grown-in microdefects can be obtained by numerical calculations of equations (4.53).

The algorithm for solving the problem of simulating the simultaneous growth and dissolution of oxygen and carbon precipitates due to the interaction of point defects during crystal cooling from the crystallization temperature is based on the application of a monotonic explicit first-order difference scheme for the Fokker-Planck equations (4.53) [241].

On Fig. 4.15 and Fig. 4.16 are shown the dependencies of the critical radius of precipitates of oxygen and carbon, respectively. Near the crystallization front (at T = 1682 K), the size of the critical nucleus of oxygen precipitate is 0.81 nm, and the size of the critical nucleus of carbon precipitate is ca. 1.1 nm. The minimum values $n_o^{cr} = n_o^{cr,0}$ and $n_c^{cr} = n_c^{cr,0}$ are reached in the initial state at T = 1682 K and increase with decreasing temperature. The increase in the critical radius of precipitates during crystal cooling leads to a sharp decrease in their growth rate and, correspondingly, to a sharp decrease in the kinetics of their precipitation [241].

Modeling of the kinetics of defect formation upon cooling of a growing crystal exponentially in the temperature range from 1682 K to 1403 K is shown in Fig. 4.17 and Fig. 4.18. In this computational experiment it was assumed that the concentrations of nucleation centers for oxygen and carbon precipitates are $\sim 10^{12}$ cm^{-3}. These values correspond to the experimental data obtained by TEM [52]. On Fig. 4.17 shows the distribution function in size of spherical oxygen precipitates, and on Fig. 4.18 the same function for carbon precipitates.

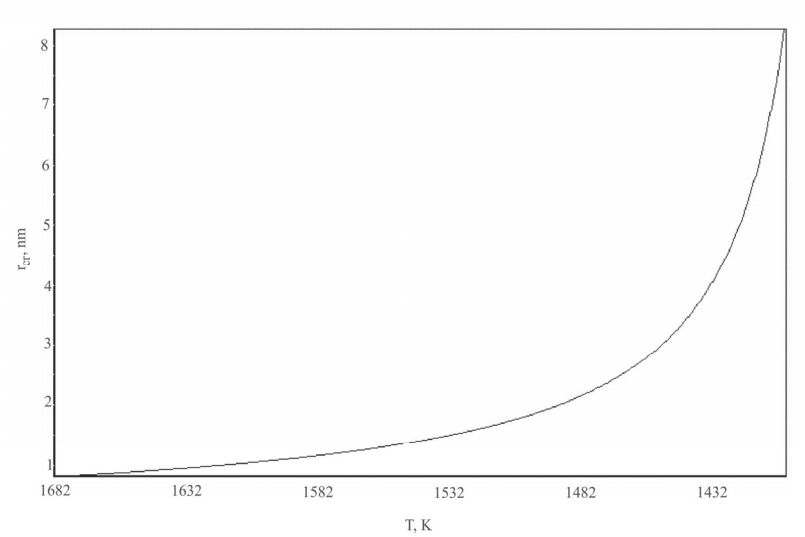

Fig. 4.15. Dependence of the critical radius of oxygen precipitate on temperature upon cooling of the crystal after growing

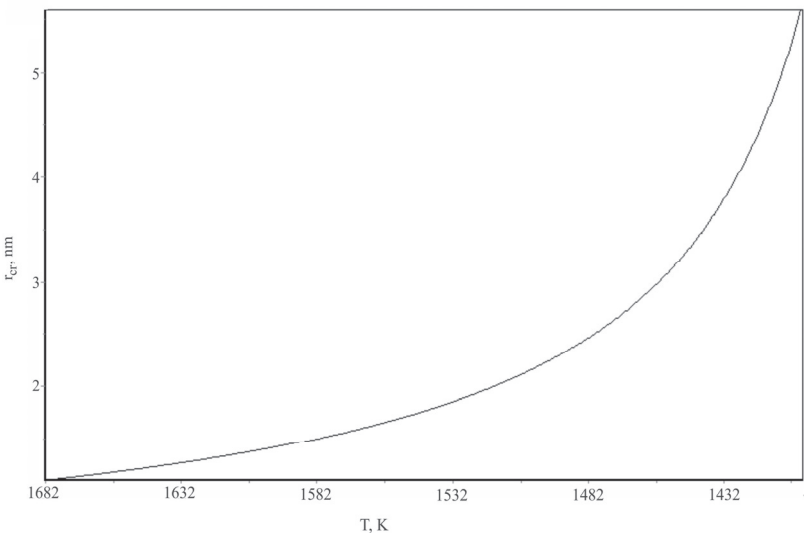

Fig. 4.16. Dependence of the critical radius of carbon precipitate on temperature upon cooling of the crystal after growing

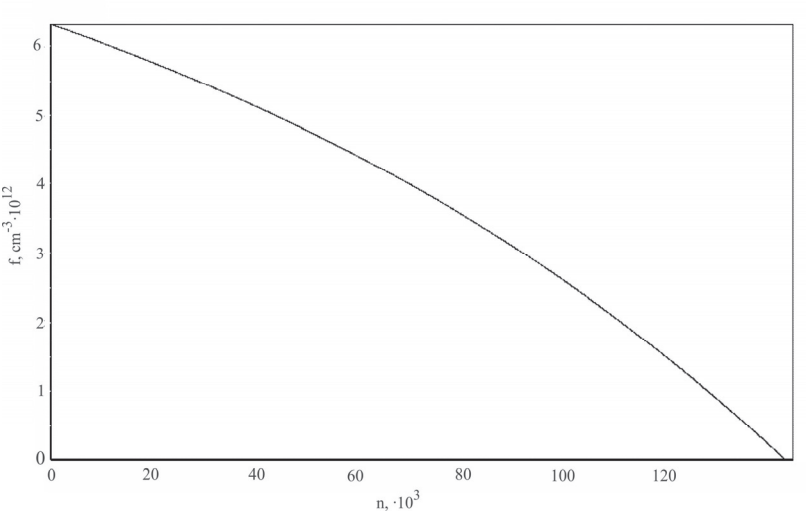

Fig. 4.17. The size distribution function of oxygen precipitates upon cooling of the crystal after growing

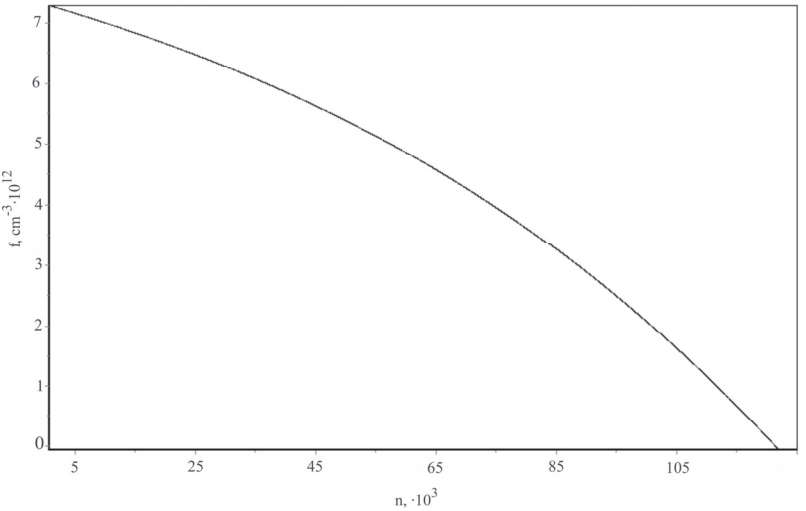

Fig. 4.18. The size distribution function of carbon precipitates upon cooling of the crystal after growing

These dependences demonstrate a significant influence of IPDs (vacancies and interstitial silicon atoms) on the dynamics of mass transfer of point defects between oxygen and carbon precipitates. The absorption of vacancies by the growing precipitates of oxygen leads to the emission of silicon atoms into the interstices. The silicon interstitial atoms, in turn, interact with growing carbon precipitates, which in the process of their growth supply vacancies for growing oxygen precipitates. Such interaction leads to the fact that, firstly, the growth of precipitates is not so strongly suppressed due to a slower increase in the supersaturation of IPDs in the bulk of the growing crystal and, secondly, the critical radius of formation of carbon precipitates increases more slowly, which contributes to a faster growth of carbon precipitates.

The higher rate of evolution of the size distribution function of carbon precipitates may be due to the higher mobility of interstitial silicon atoms in comparison with vacancies in the high-temperature region. It can be assumed that the mutual formation and growth of precipitates of oxygen and carbon leads to a slowing down of the rate of evolution of the size distribution function of oxygen precipitates despite their smaller critical size at the initial time, due to the influence of carbon impurity.

In [72], using low-energy electron spectroscopy and Auger electron spectroscopy, it was shown that the emerging carbon precipitates are prevent the growth of oxygen precipitates, simultaneously causing the formation of new oxygen precipitates. Similar results were obtained in Refs [71, 127], where it was determined by TEM that precipitates of oxygen and carbon are formed upon cooling of a 150 mm diameter crystal growing at a $V_g / G_a > C_{crit}$ in a temperature range of 1682...1403 K. These precipitates are precursors and centers for the formation of microvoids during the crystal cooling below 1403 K [114, 121, 122]. In [244] the formation of plate-like and amorphous carbon precipitates, which lie in the {111} and {100} planes, was proved by TEM.

The results of approximate calculations of partial differential equations of the Fokker-Planck type [241] correlate well with the results of the analytical solution of the equations of the consecutive dissociative diffusion model in the strong complexation approximation [240]. The main advantage of these two models is that they supplement each other. So the distribution functions of the critical sizes of oxygen and carbon precipitates can be found only from the Fokker-Planck continual differential equations, whereas the dissociative diffusion model in the strong complexation approximation cannot be determine this functions. In turn, the dissociative diffusion model makes it possible to analyze the

processes taking place in the diffusion region near the crystallization front. It should be especially noted that these mathematical models, together with the experimental results on the study of quenched crystals, show that nucleation processes pass very rapidly near the crystallization front.

4.4. Complexation in semiconductor silicon within the framework of Vlasov's model for solids

Plasma is the fourth state of matter and is found everywhere: gas-discharge plasma, cosmic plasma, solid-state plasma, etc. A.A.Vlasov (07.VIII.1908 – 22.XII.1975) on the basis of the kinetic equation (Vlasov's equation) for the first time theoretically described the properties of plasma [245]. At a number of Soviet scientists, his ideas provoked sharp rejection. In his famous paper "On the oscillations of electron plasma", L.D.Landau (09.I.1908 – 01.IV.1968) wrote a very sharp remark [246]:

«*These equations were used by A.A. Vlasov for investigation of the vibrations of plasma. However most of his results are incorrect*».

However, in the field of plasma physics, the history of science is judge of the A.A.Vlasov and his opponent's. Today, many papers and monographs are devoted to the studied of Vlasov's equation and its various applications in the field of plasma physics [247].

In his following papers A.A.Vlasov went further and suggested using Vlasov's equation to theoretically describe the properties of gases, liquids and solids [248, 249]. Therefore, in paper [250], which was not published in the English version, L.D.Landau, and V.L.Ginzburg (21.IX.1916 – 08.XI.2009), and their supporters were even tougher [251]:

«*Recently (in 1944-1945) in print appeared a number of works by AA Vlasov, dedicated to generalization of the concept of the electron plasma and solid state theory. In these works, the author concludes that in the self-consistent field method accounting of the interaction forces at large distances reveals new dynamic properties of polyatomic systems and leads to a change in our perceptions of gas, liquid, solid in the direction of combining them with the concept of plasma, etc. Consideration of these works of Vlasov's led us, however, to the conclusion about their complete failure and about the absence of the results of scientific value*». Relatively recently (in 2000) V.L. Ginzburg wrote the following: «*I do not know about any Vlasov's achievements in solid state theory and the general theory of many particles (outside of plasma physics)*».

We were interested in such animosity towards the ideas of A.A.Vlasov for solids and we decided to study this question.

In the last century, two approaches were proposed for describing the physical properties of solids from the viewpoint of their atomic structure: the classical and probabilistic. The process of defect formation is always considered on the basis of classical ideas about the periodic structure of a crystal. The classical approach postulates the concept of a crystal lattice. These representations are based on such physical limitations: (1) Localization of each atom in the vicinity of a fixed lattice site. (2) The concepts of probability and the mechanical description of the behavior of particles do not contradict each other. (3) The premise that the set of atoms in a crystal is an integer. The Born theory of the crystal, in which statistical and quantum-mechanical methods were used, led to important results. In particular, one of such results is the creation of the classical theory of the nucleation and growth of particles of the second phase in solids [181]. At the same time, another model of the crystal was developed in [245, 248]. In this model, the periodic structure of crystals is not a consequence of restrictions on the freedom of movement of atoms across the crystal, but is due to the specificity of the statistical laws of particle motion that correspond the periodic structure and the freedom of moving atoms, as a result of which the probability of encountering an atom in interstitial states is always different from zero [248]. The model is based on the solution of the kinetic Vlasov's equation, which is a system of equations describing the evolution of a particle continuum with a pair interaction potential [252]. The solution of this equation under certain conditions leads to a description of the ideal periodic structure of the crystal [248]. However, to describe the real structure of the crystal, Vlasov's model for solids model was not used [251].

The basis of Vlasov's model is the following basic physical provisions [248]: (1) The rejection of the principle of spatial and velocity localization of particles (in terms of classical mechanics), which takes place independently of force interactions. (2) The introduction of force interactions by analogy with classical mechanics, but taking into account the new principle of non-localization of particles. (3) The behavior of each particle of the system is described by means of an extended *f*-function in the phase space. With this approach, the ideas of continuity and corpuscularity are combined, since the initial method of describing the motion of a particle is associated with an extended function, and the particle's pointlike is manifested only in the particular case [245].

In the general case, Vlasov's equation describes the evolution of the distribution function $f(x, v, t)$ of the continuum of interacting particles

in Euclidean space in terms of the rate v and the coordinate x at time t. This equation has the form

$$\frac{\partial f}{\partial t} + \left(\frac{\partial f}{\partial x}, v\right) + \left(\frac{\partial f}{\partial v}, F\right) = 0$$
$$F = -\frac{\partial}{\partial x}\int K(x,y)f(y,v,t)dvdy \qquad (4.63)$$

where K is a paired interaction potential, which in real tasks depends on the distance $|x-y|$, and F is the total force with which all particles act on one of them, which is at time t at the point x [253]. To distinguish the types of interactions, one usually speaks of the systems of Vlasov's equations (the Vlasov-Poisson equations, Vlasov-Maxwell, Vlasov-Einstein, and Vlasov-Yang-Mills equations) [253].

The problem of constructing a theory of the crystalline state on the basis of the first principles is reduced to the choice of the initial system of equations for the distribution function and to the development of methods for their solution. The solution found allows us to calculate the equilibrium properties of the crystal from a given interaction potential, at a given temperature and particle density [254].

To describe the stationary properties of a crystal, the notion of the particle distribution density is use $\rho(r) = \int f(r,v)dv$. The molecular field is determined not by the exact but only probable locations of the atoms, which is shown by the potential function containing the particle probability density with allowance for the temperature distribution of the particles [248]. The choice of the pair interaction potential depends on the task under consideration. Then the non-local model of the crystal is based on the following nonlinear equations that make it possible to calculate the molecular potential and the density of the particle location under thermal equilibrium conditions [248]:

$$V(r) = \lambda kT \int_{-\infty}^{\infty} K_{1,2}(r)exp\left(-\frac{K_{1,2}(r)}{kT}\right)dr$$
$$\rho(r) = \lambda kTexp\left(-\frac{K_{1,2}(r)}{kT}\right) \qquad (4.64)$$

where k is a Boltzmann constant; $K_{1,2}$ is a pair interaction potential; λ is a some characteristic number. The initial equations are equations for two particles under steady state conditions $\left(\frac{\partial}{\partial t} = 0\right)$ [245]. The characteristic number is those values of some parameter λ, for which equations (4.64)

have solutions different from trivial [245]. If the position of one of the particles is taken as point of origin, then we can determine $\rho(0) = \lambda kT$ [248]. Finding the characteristic numbers in Vlasov's model for solids is the most important task.

The characteristic number λ can be determined from the main criterion for the existence of a crystalline state, and the crystallization condition can be written as follows:

$$\frac{4\pi N}{kT_m}\int_0^\infty K_{1,2}^*(\rho)\rho^2 d\rho = 1 \qquad (4.65)$$

Where N is a number of particles; T_m is a melting (crystallization) temperature of the crystal; $K_{1,2}^* = -K_{1,2}$ [248].

To achieve this goal, it is necessary to evaluate the possibility of creating stable complexes and the evolution of their distribution density, depending on the nucleation temperature in the temperature range from T_m=1682K to T=1382K. The choice of the lower limit of temperature is due to the fact that in this temperature range from the crystallization front, the formation of "impurity + IPD" complexes occurs with the further development of impurity precipitates [255]. The choice of the upper temperature limit, in turn, is also due to the fact that, depending on the thermal growth conditions of the crystal, at temperatures $T < T_m - 300$ begins the formation of interstitial dislocation loops or microvoids [256]. It has been shown theoretically and experimentally that in this temperature range (from ctystallization temperature to $T \sim T_m - 300$) in non-doped dislocation-free silicon single crystals near the crystallization front, "silicon+carbon" and "silicon+oxygen" complexes are formed [52, 240, 241]. The process of precipitation (nucleation, growth and coalescence of second-phase particles) passes through the whole range of cooling temperatures ($T \sim 1683 \ldots 300K$) after growing [224].

Interactions between the atoms of substances, and accordingly their properties, are determined on the basis of information on the potential of interatomic interaction. The exact form of the interaction potential of two atoms is determined from quantum mechanical calculations, and the resulting potentials are usually represented by functions with a large number of parameters, which makes it difficult to analyze them analytically. Therefore, it is usual need to operate with model potentials that contain a small number of parameters.

Now there are many approaches to constructing interatomic potentials for materials with covalent bonds. Models potentials such as Lennard-Jones potential, Mee-Lennard-Jones potential, Stillinger-Weber potential,

Morse potential, Tersoff multi-particle potentials, Brenner multiparticle potential are extensively used [257]. To describe the real substances on the basis of the model potentials of interatomic interaction, it is necessary to identify their parameters. The selection of the parameters of the potential can be carried out according to either individual thermodynamic properties or from a certain set of them for different thermodynamic conditions. A single-valued determination of the interatomic potential for silicon crystals is difficult [258]. Therefore, theoretical predictions use in their formalism various adjustable parameters whose behavior under different temperature conditions is difficult to predict or justify.

To estimate the parameters of formation the "silicon + carbon" and "silicon + oxygen" complexes, we represent the interatomic interaction in the form of a Mee-Lennard-Jones potential:

$$U(r) = K_{1,2}(r) = \frac{D}{(b-a)}\left[a\left(\frac{r_0}{r}\right)^b - b\left(\frac{r_0}{r}\right)^a\right] \quad (4.66)$$

where D and r_0 is a depth and a coordinate of the minimum of potential; b and a is a parameters, $b > a$. In the formation of a stable bond between atoms $r = \sqrt[6]{2}r_0$ and $U(r) = U_{min}$. For silicon, the potential parameters are a=2.48, b=4.0, D=2.32 eV; for carbon the potential parameters are a=2.21, b=3.79, D=3.68 eV; for oxygen the potential parameters are a=2.6, b=4.2, D=3.38 eV [259-265].

Since the system under investigation consists of dissimilar atoms, the values of the cross parameters of the potential were determined according to the Lorentz-Berthelot combination rule [266]. Calculations of the parameters of potential gave the following results: for a "silicon + carbon" complex a=2.345, b=3.895, D=2.922 eV; for a "silicon + oxygen" complex a=2.541, b=4.101, D=2.812 eV. Then we obtain for a "silicon + carbon" complex U_{1min}=2.840 eV, and for the "silicon + oxygen" complex U_{2min}=2.710 eV.

To determine the characteristic numbers of the "silicon + oxygen" (λ_1) and "silicon + carbon" (λ_2) complexes, we use equation (4.65) at the number of particles in the complex N=2 and $K(\rho) = kT\left(1 - e^{-\frac{K_{1,2}}{kT}}\right)$ [247]. The calculations gave the following results: $\lambda_1 - 4.482 \cdot 10^8 eV^{-1}$ and $\lambda_2 = 1.099 \cdot 10^9 eV^{-1}$[267].

Equation (4.64) is written for the conditions of temperature equilibrium of the system. Since the minima of interatomic potentials correspond to the stable equilibrium arrangement of atoms in "silicon + oxygen" and "silicon + carbon" complexes, then one can determine the density of the complex distribution as a function from cooling temperature of the crystal

$$\rho(T) = \lambda kT exp\left(-\frac{V_{1min,2min}}{kT}\right) \quad (4.67)$$

The evolution of the distribution density upon cooling of a growing crystal in the temperature range from 1682 K to 1382 K is shown in Fig. 4.19 and Fig. 4.20.

In this computational experiment, it was assumed that the concentration of nucleation centers for carbon and oxygen complexes is $\sim 10^{12}$ cm^{-3}. These values correspond to the experimental data obtained by TEM [52]. On Fig. 4.19 is shown the results of calculating the density distribution of "silicon + carbon" complexes, and on Fig. 4.20 shows the results of calculations the density distribution of "silicon + oxygen" complexes [267].

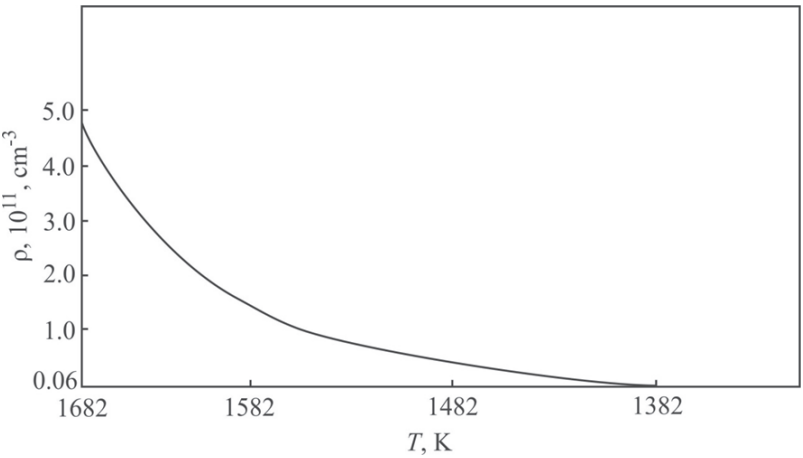

Fig. 4.19. Temperature dependence of the distribution density of "silicon + carbon" complexes

The calculations of complexation with the help of Vlasov's model for solids allow us to make the following three observations. First, the actual equality of the values of the distribution density of "oxygen + silicon" complexes ($\rho_1 = 0.493$) and "carbon + silicon" ($\rho_2 = 0.492$) near the

crystallization front ($T = 1682K$) is experimentally confirmed. With the help of TEM, it was shown that at high crystal growth rates interstitial and vacancy defects are formed at approximately equal concentrations [52].

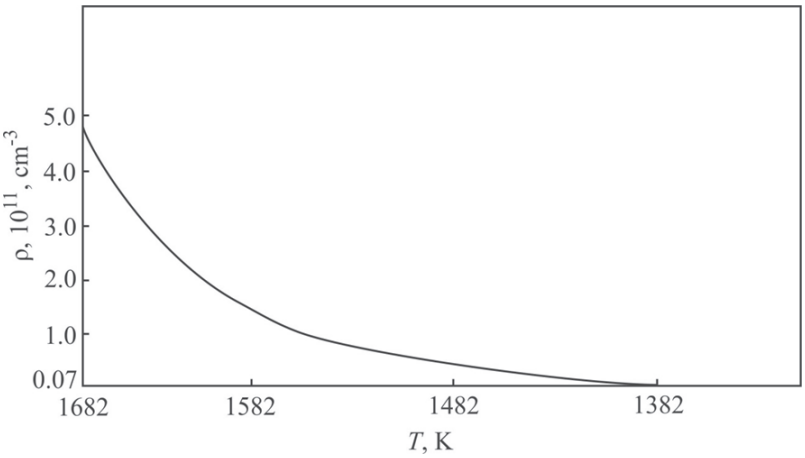

Fig. 4.20. Temperature dependence of the distribution density of "silicon + oxygen" complexes

Secondly, when calculating the homogeneous formation of microvoids and interstitial dislocation loops in accordance with the model of point defect dynamics, their formation temperatures were determined: for microvoids ~ 1333K and for interstitial dislocation loops ~ 1153K [256]. Vlasov's model does not operate with the concepts of the crystal growth rate and the axial temperature gradient, which are used in the classical theory of nucleation and growth of particles of the second phase in solids [268]. However, the condition of transition to the coalescence stage ($T \sim 1683 - 300K$), when the entire impurity is bound and take place the supersaturation on IPDs [268], corresponds to the end of the complexation process. This correspondence is typical for large-scale silicon single crystals (with a diameter of more than 100 mm). At the same time, for small-scale silicon single crystals, as the classical theory of nucleation shows, the coalescence stage begins already at $T \sim 1683 - 20K$ [268]. Hence, the classical theory of nucleation and growth of particles of the second phase in crystals and Vlasov's model for solids describe the processes of high-temperature precipitation, which is the basis of the process of defect formation in crystals.

Third, until recently, the evolution of the distribution density upon cooling a growing crystal in the temperature range from 1682K to 1382K (Figs. 4.19 and 4.20) could indicate the impossibility of applying Vlasov's model to real crystals, since it contradicted the classical theory of nucleation and growth of second-phase particles in solids. However, the model of high-temperature impurity precipitation created by us made it possible to extend the action of the mathematical apparatus of the classical theory of nucleation to the formation of nuclei in a solid during its cooling after growing [224]. As a result, two theories of nucleation of particles of the second phase, which are based on various epistemological approaches (the classical theory of nucleation and Vlasov's model for solids) lead to identical results. And Vlasov's model for solids does not require the introduction of additional parameters such as the growth rate and the axial temperature gradient of the crystal.

4.5. Kinetic model of growth and coalescence of precipitates of oxygen and carbon during the cooling of silicon crystal after growing

The growing undoped silicon crystal should be considered as a multicomponent and multiphase system, in which oxygen, carbon, silicon interstitial atoms and vacancies play the role of components, and the precipitates of oxygen, carbon and agglomerates of IPDs (microvoids and interstitial dislocation loops) are the new phase.

Various theoretical models for the analytical description of the decomposition of a supersaturated solid solution of oxygen in semiconductor silicon, as a rule, take into account the presence of only one type of particles of a new phase, namely, oxygen precipitates [176, 269-273]. Recently, papers have appeared about precipitation of carbon in silicon [274, 275]. Some papers consider the interaction of two subsystems of particles of a new phase during the thermal treatment of silicon single crystals [276]. All such theoretical models correspond to the formation of post-growth microdefects as a result of technological effects (heat treatment, irradiation, etc.), while ignoring the influence of the original defective structure (grown-in microdefects) on this process.

In the model of point defect dynamics, it is assumed that the impurity precipitation occurs at the last stage of the formation of the initial defective structure during the cooling of the crystal after growing at temperatures below 1123 K [119, 162, 243, 277]. As indicated above, in the latest variations of this model it is envisaged that part of the vacancies (v) in the temperature range 1683K...1373K due to interaction with

impurities of oxygen (*O*) and nitrogen (*N*) binds into complexes *vO*, vO_2, *vN* [179, 278]. After the formation of microvoids, these complexes grow, absorbing vacancies. In this model, the growth of complexes occurs due to the injection of silicon interstitial atoms, and the interaction of the impurity with interstitial silicon atoms is ignored [179, 278].

In our model for the formation of grown-in microdefects, a combined modeling method based on the solution of differential equations for small-size clusters and the Fokker-Planck equation for large-size clusters in the cooling temperature range 1683...1373K was used [8, 241]. In these studies, it was shown theoretically for the first time that the precipitation process begins near the crystallization front and is due to the disappearance of excess IPDs in sinks, whose role is played by oxygen and carbon impurities.

As noted above, in the classical theory of nucleation and growth of new-phase particles, the precipitation process in a crystal can be considered as a first-order phase transition, and the kinetics of this process can be divided into three stages: the formation of new-phase nuclei, growth of clusters and coalescence stage [180].

At the second stage, the aggregates grow without changing their number. In this case, a significant decrease in the degree of supersaturation of the solid solution occurs. Let the kinetics of growth of precipitates pass through a reversible scheme $A_iC + A \leftrightarrow A_{i+1}C$, which corresponds to growth of precipitates at nucleation centers C with concentration N_c that does not change over time. The nucleation centers capture and emit monomers, which are described using the system of equations [279]:

$$\begin{aligned} \frac{dN_0}{dt} &= -k_0 N N_0 + g_1 N_1, \\ \frac{dN_i}{dt} &= -N_i\left(k_i N + g_i\right) + g_{i+1} N_{i+1} + k_{i-1} N N_{i-1}, \\ \frac{dN}{dt} &= -N\sum_{i=0} k_i N_i + \sum_{i=1} g_i N_i, \end{aligned} \tag{4.68}$$

where N_i is the average concentration of nucleation centers that joined i particles; N is the monomers concentration; $k_i N$ is the capture rate of the monomer for the nucleation center; g_i is the monomer emission rate for the nucleation center. At the initial time, only monomers and nucleation centers are in the system. The growth of precipitates is limited by the diffusion of monomers. Kinetic coefficients $k_i = 4\pi R_i D$, where R_i is the

radius of capture of a free particle by a cluster of i particles; D is a diffusion coefficient of a free particle.

For the system (4.68), the law of conservation of nucleation centers $N_c = \sum_{i=1} N_i(t)$ and the law of conservation of the total number of particles, both monomers and precipitates, are carried out $N(0) = N(t) + \sum_{i=1} iN_i$, where $N(0)$ is the concentration of monomers at the initial time. Then the average number of particles at nucleation centers:

$$i = \frac{\sum_{i=0} iN_i}{\sum_{i=0} N_i} = \frac{N(0) - N(t)}{N_c} \tag{4.69}$$

At a $i >> 1$ for the description of the process, the Fokker-Planck equation is used [278], which, when the principle of detailed equilibrium is fulfilled $g(i) = k(i-1)N_E C_E(i-1) \;/\; C_E(i) \approx k(i)N_E$, has the form [279]:

$$\frac{\partial C(i,t))}{\partial t} = -(N(t) - N_E)\frac{\partial}{\partial i}(k(i)C(i,t)) + (N(t) + N_E)\frac{\partial^2}{2\partial i^2}(k(i)C(i,t)) \tag{4.70}$$

where N_E is the equilibrium concentration of monomers.

In the case of precipitation limited by diffusion, for the expected value $i(t)$ one can use the macroscopic equation [279] corresponding to equation (4.70):

$$\frac{di}{dt} = k_0(N - N_E)(i(t) + m)^{\alpha}, \tag{4.71}$$

where $k_0 = 4\pi R_i D$, m is an initial size of cluster; α is a parameter that depends on the geometry of the clusters.

Formulas (4.69) and (4.71) allow us to write down a differential equation describing the change in the concentration of monomers during the decomposition of a solid solution [279]:

$$\frac{dN(t)}{dt} = -k_0 N_c^{1-\alpha}(N(t) - N_E) \times (N(0) + mN_c N(t))^{\alpha} \tag{4.72}$$

The kinetics of the decrease in monomer concentration obtained from numerical solutions of the system of initial equations (4.68) coincides with the one obtained from equation (4.72) within the error of numerical methods [279]. The solution of the original system (4.68) for real systems is practically impossible because of the large dimensionality of the system of equations, while with the equation (4.72) no complexities arise [279].

The kinetics of the decrease in the monomer concentration as a result of the decomposition of the solid solution at $m = 0$ has a form:

$$\frac{N(t)-N_E}{N(0)-N_E} = \exp\left\{-N_c\left[(1-\alpha)(N(0)-N_E)^{\alpha}k_0 t\right]^{\frac{1}{1-\alpha}}\right\} \qquad (4.73)$$

Solving equation (4.72) together with (4.69) one can calculate the average radius of precipitate:

$$R(t) = \sqrt[3]{\frac{3bi(t)}{4\pi}} \qquad (4.74)$$

Soon there comes the third stage of the process, when the particles of the new phase are large enough, the supersaturation is small, new particles are no longer formed, and the determining role is played by coalescence, which is accompanied by the dissolution of small particles and the growth of large particles. The condition for the transition to the coalescence stage is the ratio $u(t) = \frac{R(t)}{R_{cr}(t)} \approx 1$, where $R_{cr}(t)$ is the critical radius of precipitate. Under this condition, the precipitate is in equilibrium with the solution ($\frac{dR}{dt} = 0$). At a $R(t) > R_{cr}(t)$ precipitate grown, and when $R(t) < R_{cr}(t)$ precipitate dissolves. With time the $R_{cr}(t)$ increases and the number of particles per unit volume (n) decreases [180, 280]. The solution of the system of equations describing this process, as shown in [281], is possible only in the case when the supersaturation of the solute tends to zero.

In the crystallization of one-component melts, temperature fields are formed and the new phase separations interact with each other by means of generalized temperature fields [282]. The asymptotic solution of the system of equations describing this process, similar to solving diffusion isothermal coalescence equations [283], is possible when supercooling of the melt $\Delta T=T_c-T_0$ tends to zero (where T_c is a average crystal temperature, T_0 is a equilibrium crystal temperature) [284].

Let us consider a solid solution containing single-component spherical precipitates of a new phase with initial size distribution function of $f_0(R)$. The system in which the solid solution is located is thermally insulated and there are no sources of matter. The initial temperature and the concentration of the solid solution are equal to $T_c(0)$ and $c_c(0)$, and the solid solution is in the coalescence stage.

Since the system in which the solid solution dissolves is thermally insulated, the heat of the phase transition that is emitted during coalescence will increase the temperature of the entire system, and this in

turn will lead to a change in the equilibrium concentration c_0 [284]. In this case, supersaturation will tend to zero more rapidly than in the case of isothermal coalescence, since with increasing temperature c_0 increases [285]. This will lead to a drop in the concentration gradient between the solution and the emitted a new phase and the rate of growth of the precipitates will decrease. Hence, the diffusion and thermal fields become self-consistent and the system of non-isothermal coalescence equations must contain both the mass balance equation and the heat balance equation. A system of equations describing non-isothermal coalescence [284]:

$$\frac{\partial f(R,t)}{\partial t}+\frac{\partial}{\partial R}\left[f(R,t)dR/dt\right]=0, f_0(R)=f(R,0) \qquad (4.75)$$

$$Q(T_c)=c_c(t)+\chi\int_0^\infty f(R,t)R^3dR \qquad (4.76)$$

$$T_c(t)=T_c(0)+\frac{L\chi}{c_p\rho_t}\int_0^\infty\left[f(R,t)-f_0(R)\right]R^3dR \qquad (4.77)$$

where (4.75) is the equation of continuity in the space of sizes for the distribution function of precipitates on size; (4.76) is the mass balance equation; (4.77) is the equation for the amount of heat emitted; $f_0(R)$ is the initial function of size distribution of precipitates; $T_c(0)$ is the initial temperature of solid solution; $\chi=4\pi/3\upsilon$; υ is the volume per atom in new phase precipitates; $Q(T_c)$ is the total amount of the substance in precipitates and in solution; $c_c(t)$ is the concentration of solute in solid solution; L is the heat of phase transition per atom of the formed phase; c_p is the heat capacity at constant pressure per unit mass of solid solution; ρ_e is the solid solution density. The average temperature of the solid solution is a function of the amount of material in the new phase precipitates, i.e., equations (4.76) and (4.77) are related to each other.

In order that the system of equations (4.75)-(4.77) be complete, it is necessary to find the dependence of the growth rate of precipitates dR/dt on the radius R:

$$\frac{dR}{dt}=-D\upsilon\frac{\partial c}{\partial r} \qquad (4.78)$$

where D is the diffusion coefficient of the phase-forming component; $\frac{\partial c}{\partial r}$ is the gradient of the concentration of atoms at the boundary of the

precipitate, which can be obtained from the quasi-stationary solution (since supersaturation is small) of the solution of diffusion equation (4.79) written in spherical coordinates with the boundary conditions (4.80):

$$\frac{\partial^2 c}{\partial r^2} + \frac{2}{r}\frac{\partial c}{\partial r} = 0, \tag{4.79}$$

$$c_{r\to\infty} = c_c(T_c), c_{r=R} = c(R), D\frac{\partial c}{\partial r} = \beta\upsilon\left(c(R) - c_R\right) \tag{4.80}$$

where β is the specific boundary flow, which takes into account the rate of incorporation of the emission of atoms into the precipitate; c_R is the concentration of atoms which are in equilibrium with a precipitate of radius R; $c(R)$ is the concentration at the surface of new phase precipitate. Concentrations c_c, $c(R)$, c_R are in the case of non-isothermal coalescence the temperature T_c functions. The equation for the precipitate growth rate (4.81) is obtained from the solution of equation (4.79) with the condition (4.80):

$$\frac{dR}{dt} = \frac{2\sigma D\upsilon^3\beta c_0(T_c)}{kT_c(D+\beta\upsilon R)R^2}\left(R/R_k - 1\right) \tag{4.81}$$

where $c_0(T_c)$ is the equilibrium concentration of solute at temperature T_c; σ is the surface tension at the boundary of new phase precipitate. It follows from equation (4.81) that two processes are possible that limit the growth rate of precipitate [284]:

(1) diffusion processes at $D << \beta\upsilon R$

$$\frac{dR}{dt} = \frac{2\sigma D\upsilon^2 c_0(T_c)}{kT_c R^2}\left(R/R_k - 1\right) \tag{4.82}$$

(2) processes on the boundary of precipitate at $D >> \beta\upsilon R$

$$\frac{dR}{dt} = \frac{2\sigma D\upsilon^3 c_0(T_c)\beta}{kT_c R}\left(R/R_k - 1\right) \tag{4.83}$$

Equations (4.75)-(4.77) with one of the equations (4.82) or (4.83) constitute a complete system of equations describing the process of non-isothermal decomposition of the solid solution in the coalescence stage. The authors of [284] showed that in closed systems in the absence of sources (sinks) of heat and matter in the case of nonisothermal coalescence, the dependence of the change in the distribution functions of precipitates of a new phase on the sizes, their density, critical and average sizes, is the same as for isothermal coalescence [283]. Only constants that

depend on temperature are changed. The solution of equations (4.75)-(4.77) together with (4.82) or (4.83) is carried out by the method developed in [283]. In the general case, the size distribution of precipitates has the following form [286]:

$$f(R,t) = \frac{n(t)}{R_{cr}(t)} P(u)$$

$$u = \frac{R(t)}{R_{cr}(t)} \tag{4.84}$$

$$P(u) = \begin{cases} -\dfrac{16u \cdot \exp\left[\dfrac{3u}{u-2}\right]}{(u-2)^5}, & u < 2 \\ 0, & u > 2 \end{cases} \tag{4.85}$$

The average size of the precipitates is proportional to the cube root of time [284]:

$$R_{sr}(t) = \sqrt[3]{R_{cr}^3(t_0) + \frac{4D\beta t}{9}} \tag{4.86}$$

where D is the diffusion coefficient of impurity atoms; $\beta = \left(\frac{\sigma\Omega}{kT}\right) N(0)$; $R_{cr}(t_0)$ is the initial critical radius; σ is the surface tension of the "precipitate / solid solution" interface; Ω is the atomic volume.

Concentration of precipitates:

$$n(t) = \frac{M(t_0)}{t/t_0} \tag{4.87}$$

where t_0 is an initial critical time; $M(t_0)$ is a initial concentration of precipitates.

The following data were used in the calculations [268]: $V_p = 4.302 \cdot 10^{-2}$ nm^3 (SiO_2); $V_p = 2.04 \cdot 10^{-2}$ nm^3 (SiC); σ = 310 erg/cm^2 (SiO_2); σ = 1000 erg/cm^2 (SiC); $\mu = 6.41 \cdot 10^{10}$ Pa; $\delta = 0.3$; $\varepsilon = 0.15$; $b = 0.25nm$; $D_O = 0.17\exp(-2.54eV/kT)$; $D_c = 1.9\exp(-3.1eV/kT)$; $k = 8.6153 \cdot 10^{-5} eV/K$.

The modeling of precipitation of oxygen and carbon was carried out using the kinetic model of the growth of spherical precipitates under the diffusion mechanism of growth. The analysis was carried out in the approximation that the growth of precipitates occurs at a fixed number of

nucleation centers. The model takes into account a uniform precipitation in bulk.

Four separate groups of calculations were carried out, which simulated the precipitation processes during the growth of large-scale and small-scale FZ-S- and CZ-Si crystals [268]. The first group of calculations (I) was carried out with the following parameters: crystal growth rate V_g = 0.6 mm/min, the axial temperature gradient G_a=2.5 K/mm, $N(0)$= 10^{18} cm^{-3} for oxygen and carbon concentrations. These conditions correspond to the growth of large-size single CZ-Si crystals. The second group of calculations (II) was carried out with the following parameters: crystal growth rate V_g = 6.0 mm/min, the axial temperature gradient G_a= 130 K/cm, $N(0)$= 10^{18} cm^{-3} for oxygen and carbon concentrations. The third group of calculations (III) was carried out with the following parameters: crystal growth rate V_g = 6.0 mm/min, the axial temperature gradient G_a= 130 K/cm, $N(0)$= $8\cdot10^{16}$ cm^{-3} for oxygen concentration and $N(0)$= 10^{16} cm^{-3} for carbon concentration. The fourth group of calculations (IV) was carried out with the following parameters: crystal growth rate V_g = 6.0 mm/min, the axial temperature gradient G_a= 130 K/cm, $N(0)$= $4\cdot10^{15}$ cm^{-3} for oxygen concentration and $N(0)$= $4\cdot10^{15}$ cm^{-3} for carbon concentration. Groups II, III and IV correspond to growth conditions for small-scale single FZ-Si crystals. For all four groups $T = \frac{T_m^2}{T_m + VGt}$, where T_m is a melting temperature; $N(0) = 0{,}1N_{\text{E}}$, $N_c = M(t_0) = 10^{13}\,см^{-3}$; $\alpha = 1/3$ (precipitates of spherical shape).

The result of calculations in groups I and II allow us to compare the precipitation processes in CZ-Si and FZ-Si crystals and analyze them at an almost maximum content of oxygen and carbon impurities. The kinetics of the decrease in the concentration of oxygen and carbon monomers in CZ-Si crystals is shown on Fig. 4.21. The change in the average size of the precipitates of oxygen (1) and carbon (2) is shown on Fig. 4.22, and their initial concentration is determined from experiments on quenching of crystals $(\sim 10^{12}...10^{13}\ cm^{-3})$ [52].

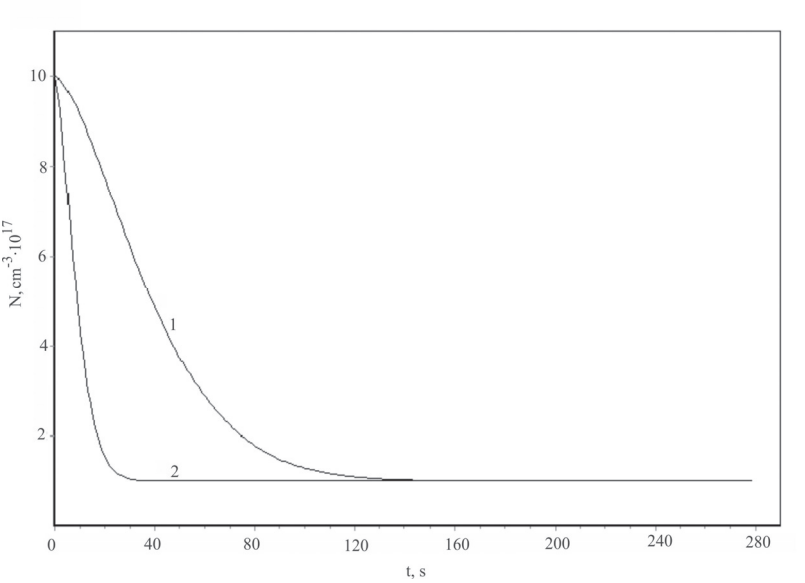

Fig. 4.21. The change in the concentration of the monomers of oxygen (1) and carbon (2) during the cooling of the CZ-Si crystal from the crystallization temperature

An analysis of the obtained results and the data of [8, 241] shows that the phase transition occurs by the mechanism of nucleation and growth of a new phase, both of which are not separated in time and are parallel.

The condition of transition to the coalescence stage is $R(t) \approx R_{cr}(t)$, which is performed when $T \approx 1423K$. Taking into account the computational errors, this temperature in large-scale crystals corresponds to the beginning of the microvoids formation region (at V_g = 0.6 mm/min). In this region the entire impurity is bound and a supersaturation arises in the vacancies, which is removed by the formation of vacancy microvoids. When the thermal growth conditions change (for example, at V_g = 0.3 mm/min [119]) supersaturation occurs on the interstitial silicon atoms, which leads to the formation of interstitial dislocation loops. In this case the condition $R(t) \approx R_{cr}(t)$ is performed at $T \approx 1418K$. Hence, the coalescence stage in large-scale silicon single crystals begins at

temperatures close to the formation temperatures of clusters of IPDs (these are vacancy microvoids or interstitial dislocation loops).

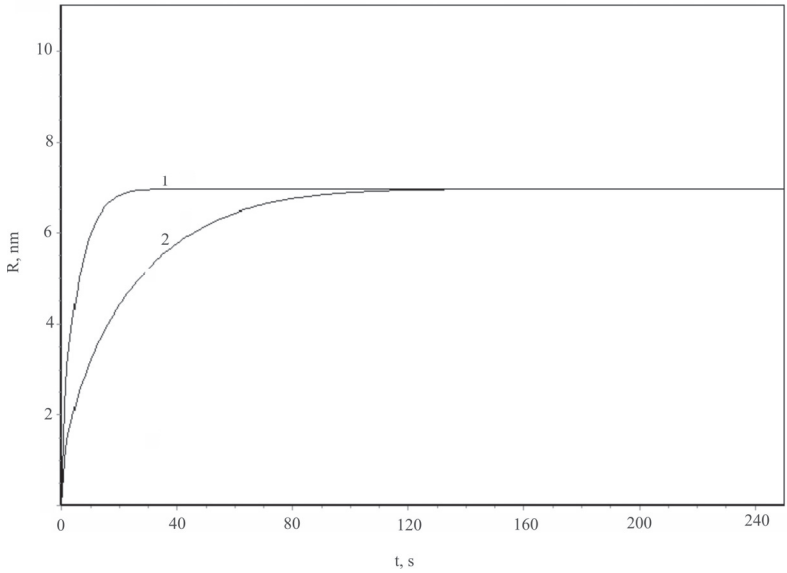

Fig. 4.22. The change in the average size of the precipitates of oxygen (1) and carbon (2) during the cooling of the CZ-Si crystal from the crystallization temperature

A Fig. 4.23 shows the change in the average size of oxygen and carbon precipitates in the coalescence stage in the temperature range of 1423...300 K. At this stage of the calculations, the following temperature dependences of the diffusion coefficients of oxygen $D_O = 2.16 \cdot 10 \cdot \exp\left(-\frac{1.55}{kT}\right)$ cm^2/s [290] and carbon $D_C = 1.3 \cdot \exp\left(-\frac{3.3}{kT}\right)$ cm^2/s [286].

Calculations in Group II showed that the change in the thermal growth conditions leads to a decrease in the average radius of precipitates $R(t)$ in FZ-Si crystals in comparison with CZ-Si crystals of group I (Fig. 4.24) in the growth stage of precipitates, as well as a corresponding decrease in the sizes of precipitates in stage coalescence (Fig. 4.25) [267].

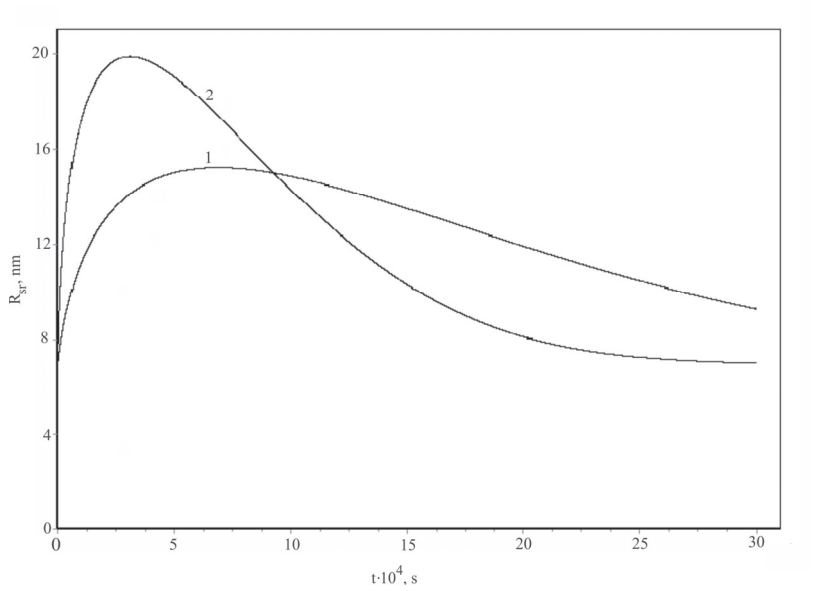

Fig. 4.23. The change in the average size of the precipitates of oxygen (1) and carbon (2) in the temperature range of cooling 1423...300K in CZ-Si crystals

On Fig. 4.26 shown the results of calculations of the change in the average size of oxygen precipitates in the coalescence stage for crystals of groups I, II and III, and Fig. 4.27 shows the results of calculations of the change in the average size of carbon precipitates in the coalescence stage for crystals of groups I, II and III. The joint nucleation and growth of new phase particles (oxygen and carbon precipitates) during the crystals cooling leads to a strong interaction between the evolution processes of these two subsystems of grown-in microdefects. The absorption of vacancies by the growing precipitates of oxygen leads to the emission of silicon atoms into the interstices. The silicon interstitial atoms, in turn, interact with growing carbon precipitates, which in the process of their growth supply vacancies for growing oxygen precipitates. Such interaction leads to accelerated transition of subsystems of oxygen and carbon precipitates to the coalescence stage, in comparison with the independent evolution of these two subsystems [268].

Despite on fact that the oxygen and carbon concentrations for crystals of groups I and II are the same, the change in thermal growth conditions

for small-scale single crystals of FZ-Si (high growth rates and axial temperature gradients) leads to the fact that here the coalescence stage occurs much earlier (at $T \approx T_m - 20K$).

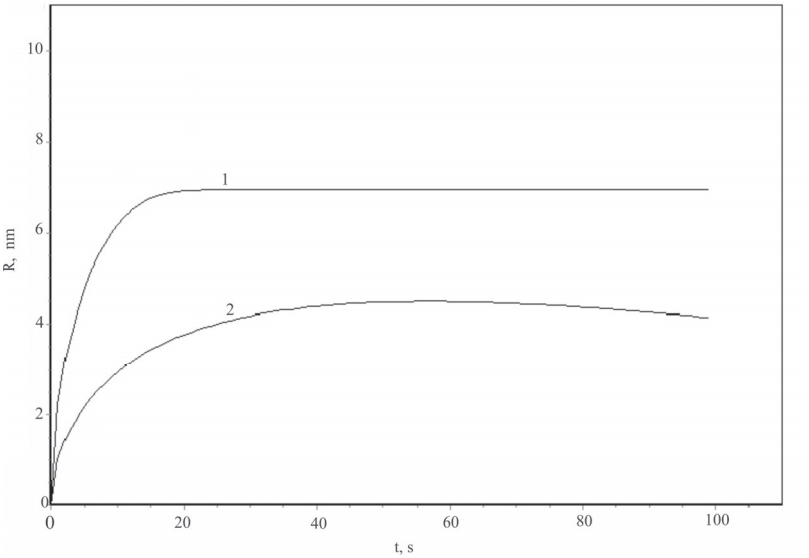

Fig. 4.24. The change in the average size of the precipitates of oxygen (1) and carbon (2) during the cooling of the FZ-Si crystal from the crystallization temperature

Very important are the results of calculations for crystals of groups III and IV. If the calculations for crystals of groups I and II are of theoretical interest for the case of limiting concentrations of oxygen and carbon under different thermal growth conditions, then for real crystals of groups III and IV we have experimental results carried out with the help of TEM [52].

The results of theoretical calculations show that with a decrease in the concentration of oxygen and carbon in crystals of groups III and IV occurs the further decrease of transit time of the growth stage of precipitates (for example, for crystals of group IV the coalescence stage occurs when $T \approx T_m - 5K$). Hence, a change in the thermal growth conditions of the crystals (increase in the growth rate and axial temperature gradient) significantly affects the growth stage of the precipitates. In turn, to a lesser extent, the decrease in the time of the growth stage of precipitates is due to a decrease in the concentration of impurities in the crystals. Ultimately,

these causes lead to a decrease in the average size of the precipitates (Figs. 4.25…4.27).

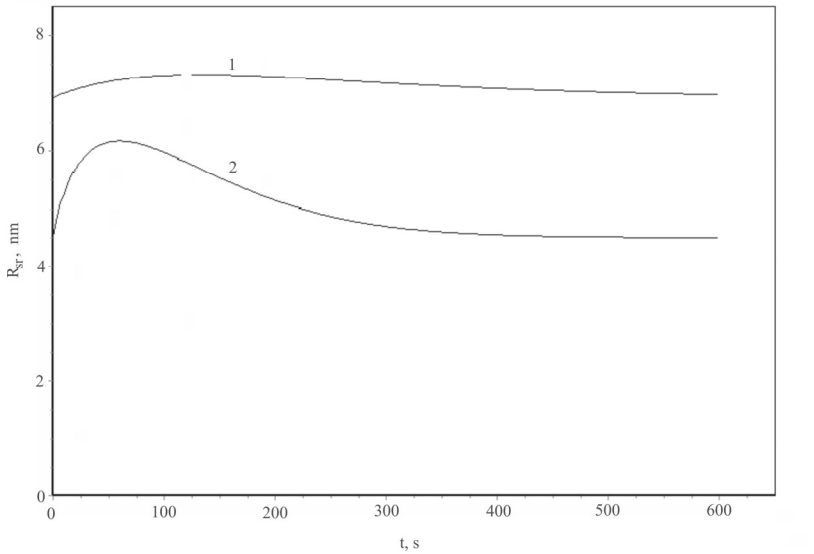

Fig. 4.25. The change in the average size of the precipitates of oxygen (1) and carbon (2) in the temperature range of cooling of 1423...300K of FZ-Si crystals

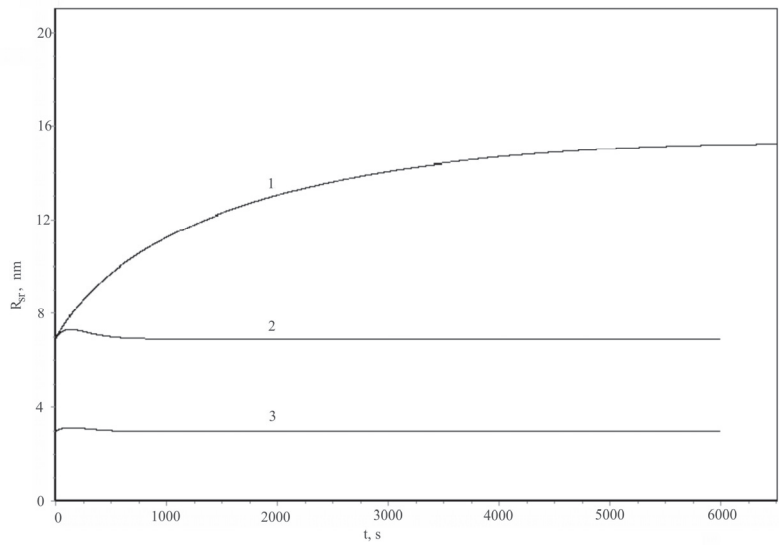

Fig. 4.26. Change in the average size of oxygen precipitates in the coalescence stage for crystals of I (1), II (2) and III (3) groups

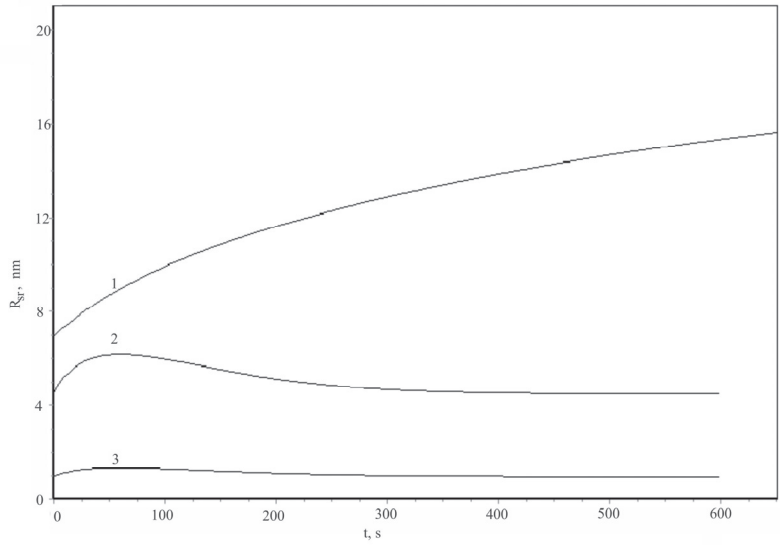

Fig. 4.27. The change in the average size of carbon precipitates in the coalescence stage for crystals of I (1), II (2) and III (3) groups

As a result of detailed TEM-studies it has been established that the precipitates of oxygen and carbon (grown-in D-microdefects under this thermal growth conditions) have sizes in the range 3...10 nm, and their concentration ~ 10^{13} cm^{-3} [52]. With a decrease in the crystal growth rate, the size of the defects increases [15]. Analysis of the results of computer simulation of crystals of group III shows that the calculated size of the precipitates is in the range 2.7...6.5 nm, and for crystals of group IV it is within 2.0...5.5 nm, which agrees very well with the experimental data [51].

The kinetic model of the decomposition of solid solutions of oxygen and carbon impurities not only makes it possible to simulate the processes of high-temperature precipitation during the crystal cooling in the temperature range 1683 ... 300 K, but also describes the available experimental data about precipitation of oxygen and carbon. The kinetic model of growth and coalescence of oxygen and carbon precipitates together with the kinetic models of their formation [8, 241] is a unified model of the high-temperature precipitation process in dislocation-free silicon single crystals. The mathematical apparatus of this model makes it possible, in the future, to take into account and analyze the interaction of IPDs not only with background impurities of oxygen and carbon, but also with other impurities (for example, transition metals, nitrogen, hydrogen, etc.), and considering the interaction "impurity + impurity".

Conclusions to chapter 4. Analysis of the kinetic processes of impurity interactions shows that as a transparent and informative mathematical model for the formation of mobile complexes, one should choose the strong complexation approximation of the model of successive diffusion, which allows a simple physical interpretation and is most adequate to the physical model under consideration.

A mathematical model of the process of formation of primary grown-in microdefects based on the dissociative process of impurity diffusion is formulated. The cases of interaction "oxygen + vacancy" and "carbon + silicon interstitial atom" near the crystallization front for undoped dislocation-free single crystals of FZ-Si and CZ-Si are considered. Approximate analytical expressions are consistent with the two-stage mechanism for the formation of grown-in microdefects and show that the processes of nucleation of defects begin near the crystallization front. The front boundary of the formation of complexes ("oxygen + vacancy" and "carbon + silicon interstitial atom") is at a distance ~ $3 \cdot 10^{-4}$mm from crystallization front. This calculated distance is a diffusion layer, after passing through which, during the crystal cooling, an excess (nonequilibrium) concentration of IPDs occurs.

The calculation of the formation of the "oxygen + vacancy" and "carbon + silicon interstitial atoms" complexes during the crystals cooling on the basis of an approximate solution of partial differential equations of the Fokker-Planck type is carried out. A good correlation is shown between these calculations and calculations based on the solution of differential equations of dissociative diffusion. The process of impurities precipitation begins near the crystallization front and is due to the disappearance of excess IPDs in sinks, whose role is played by the impurities of oxygen and carbon.

With the help of two theories of nucleation of particles of the second phase, which are based on various epistemological approaches (the classical theory of nucleation and Vlasov's model for solids), the results of experimental studies on high-temperature impurity precipitation are confirmed. Vlasov's model for solids can be used not only to study hypothetical ideal crystals, but also to describe the formation of a defective structure of real crystals.

CHAPTER FIVE

THE FORMATION OF MICROVOIDS AND INTERSTITIAL DISLOCATION LOOPS DURING CRYSTAL COOLING AFTER GROWING

Contradiction is not a sign of falsity, nor the want of contradiction a sign of truth
—Blaise Pascal (19.VI.1623 – 19.VIII.1662)
Pensées sur la religion et sur quelques autres sujets, 1670

If the decomposition of supersaturated solid solutions of impurities begins at temperatures near the crystallization front, then the decomposition of supersaturated solid solutions of IPDs (vacancies and silicon interstitial atoms) occurs during the crystal cooling in the temperature range 1423...1173 K [52].

Usually the formation of microvoids in large-scale single crystal silicon was modeled in the framework of the recombination-diffusion model of the formation of grown-in microdefects and the model of the point defects dynamics [6, 7, 112, 120, 156-170, 287-289]. Here, an analytical method is used to determine the temperature field on the basis of a generalization of data on two-dimensional temperature distributions in a growing silicon ingot. However, the main process in the framework of this model continues to be the recombination of IPDs. The mathematical model of the point defects dynamics in silicon quantitatively explains the homogeneous character of the formation of microvoids and interstitial dislocation loops [119]. In [256], an attempt was made to calculate the effect of the absence of recombination of IPDs on the formation of grown-in microdefects within the model of point defect dynamics.

5.1. Modeling of the processes of formation of microvoids and interstitial dislocation loops within the framework of point defects dynamic model

In modeling the nucleation of microvoids and interstitial dislocation loops, we proceeded from the fact that their formation begins at certain temperatures, when conditions arise for the occurrence of supersaturation on IPDs, while precipitates are already formed and between them pass competing processes of growth of some and dissolution of others. This assertion was based on the experimental facts that there is no recombination of IPDs in the high-temperature region when the crystal is cooled from the melting temperature [52]. The confirmation of these experimental results by theoretical calculations [213] allows the processes of analysis and calculation of the defect structure to consider as for three regions: (1) High-temperature region (~ 1682...1373 K), when the precipitates of impurities originate and grow. (2) Middle-temperature region (~ 1373...1070K), when nucleation and growth of microvoids or interstitial dislocation loops occur. (3) Low-temperature region (below 1070K), when the processes of integration of existing precipitates occurs.

The experimentally determined temperature range for the formation of microvoids in large-scale crystals is 1403...1343 K [119, 122], therefore, approximate calculations within the framework of a model of point defect dynamics were carried out for the range 1403...1073 K. The following data were used in the calculations [256]:

$\lambda_v = 650 erg/cm^2; k = 8.6153 \cdot 10^{-5} eV/K; D_v = 188.449 \exp(-1.917/kT);$

$C_{ve} = 1.11639 \cdot 10^{27} \exp(-3.9/kT); \rho = 5 \cdot 10^{22} cm^{-3}.$

Most mathematical models used to describe the process of nucleation of new particles can be classified [119] as:

- Systems of differential equations of diffusion growth of bimolecular clusters.
- Modifications of Fokker-Planck approximation for partial differential equations.

In complex systems, when one has to consider a large number of bimolecular reactions, the separate processing of such reactions is often not possible. Fokker-Planck formulas, which introduce a size in the model's consideration, make numerical solutions real but time-consuming and costly. The computational model uses the classical theory of nucleation and formation of stable clusters, being, strictly speaking, the distribution of the size of clusters (secondary grown-in microdefects) based on the time process of their formation and previous history [256].

The system of equations (2.2)-(2.3) is solved using exact spatial and time discretization. The algorithm includes the solution of the equation $V_g = \frac{dh}{dt}$ for the crystal growth rate with the simultaneous solution of equations (2.4)-(2.7) and the boundary and initial conditions (2.8)-(2.16). The size distribution is determined from the solution of equations (2.6)-(2.7) for the corresponding type of secondary grown-in microdefects (microvoids or A-microdefects). In accordance with the two-stage mechanism for the formation of grown-in microdefects, it was assumed in the calculations that the recombination factor $k_{IV} = 0$.

In the high-temperature region (1683 K < T < 1403 K, growth parameter $V_g/G_a > C_{crit}$) nucleation and growth of primary grown-in microdefects (impurity precipitates) occur. In this region the supersaturation of IPDs (vacancies) is low and, therefore, the rate of nucleation of microvoids is negligibly small. At T ≤ 1403 K supersaturation increases, which leads to increase in the rate of microvoids nucleation. After the formation of microvoids during their growth, there is a rapid expenditure of vacancies. As a result, supersaturation decreases and the rate of nucleation of microvoids decrease sharply. Hence, nucleation prevails in a narrow temperature range, and, therefore, outside zone of microvoids formation their nucleation is ignored. Furthermore, since the growth rate of microvoids decreases sharply due to an increase in their size and a corresponding decrease in the vacancy concentration, the growth of microvoids outside the nucleation zone is also not taken into account.

On Fig. 5.1 is shown the results of calculating the temperature dependence of the critical radius of microvoids, and on Fig. 5.2 shows temperature dependence of the concentration of microvoids.

In numerical and analytical calculations, the temperature field was used either as an approximation of Neimark [5] or as an approximation of Voronkov [6, 170]. Based on the analysis of the values of modern temperature fields with the growth of crystals using the Czochralski method, a fixed value G_a = 2.5 K/mm is accepted [256]. Modeling was carried out for crystals with a diameter of 150 mm, which were grown at growth rates V_g = 0.6 mm/min and V_g = 0.7 mm/min. These growth conditions correspond to the growth parameter $V_g/G_a > C_{crit}$, i.e., crystal was grown at the vacancy supersaturation.

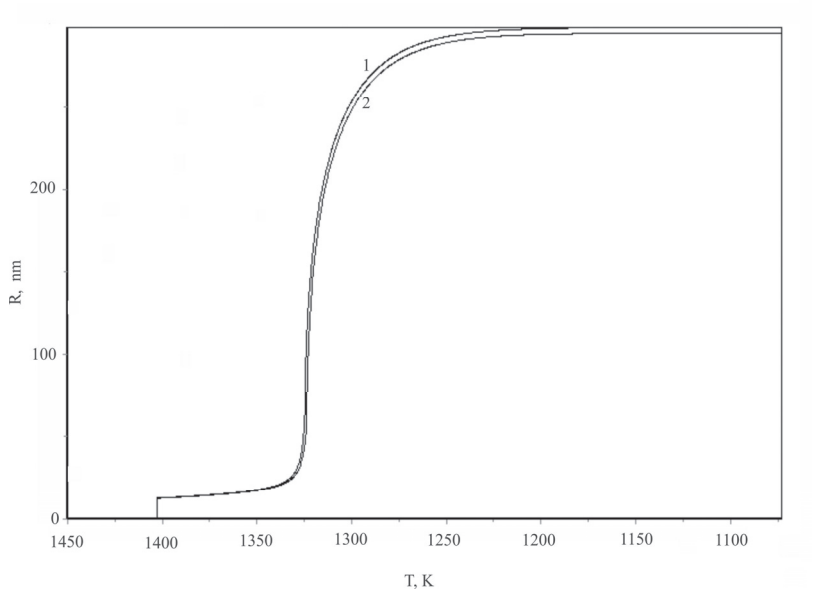

Fig. 5.1. Dependence of the critical radius of microvoids on the crystal cooling temperature during growth:
(1) growth rate V_g = 0.6 mm/min; (2) growth rate V_g = 0.7 mm/min.

The temperature of formation of microvoids is defined as the temperature at the highest nucleation rate, and it corresponds to ~ 1333 K (~ 1060^0C) (Fig. 5.1). The increase in the growth rate of the crystal slightly reduces the critical radius of the voids and slightly affects the nucleation temperature. To prevent the formation of microvoids (i.e., to achieve the condition when the microvoid radius $R_v \to 0$) we can by increasing of the cooling rate above the value 40 K/min [173]. Such conditions are satisfied when growing small-scale silicon crystals. At real growth rates of large-scale single crystals (with a diameter of more than 80 mm), the suppression of the formation of microvoids is impossible [290].

However, increase in the growth rate of a crystal almost doubles reduce the concentration of introduced defects (Fig. 5.2). An interesting fact is the appearance of a "shelf" (a weak increase in the critical radius in the temperature range ~ 1403...1360 K), which indicates that the formation of precipitates and microvoids near T ~ 1403 K passes in a certain temperature range, albeit with different but comparable rates of origins

(Fig. 5.1). In this temperature range the consumption by growing precipitates of vacancies decreases and, due to the growth of supersaturation of vacancies, microvoids with a relatively small critical radius will be formed. The places of their origin can serve as precipitates, which were formed earlier. These data are confirmed by experimental studies with the help of TEM of heat-treated silicon single crystals. Short-term (from 15 to 30 min) heat treatment at a temperature of T = 1373 K lead to a sharp reduction in the size of vacancy microvoids and the detection on their place of large precipitates [121, 122].

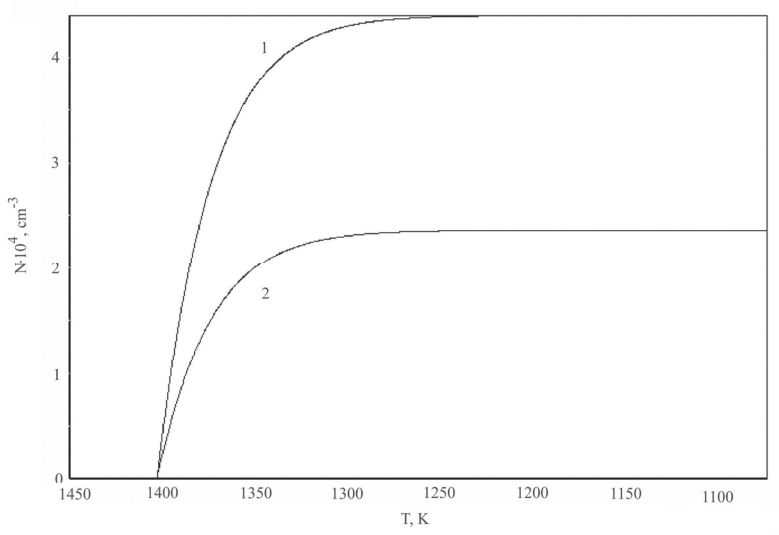

Fig. 5.2. Dependence of the concentration of microvoids on the crystal cooling temperature during growth:
(1) growth rate V_g = 0.6 mm/min; (2) growth rate V_g = 0.7 mm/min

This is possible only if precipitates of certain sizes already exist in this place and materials for their growth (vacancies and impurity atoms) are near. At the same time, in this temperature range the concentration of microvoids sharply increases (Fig. 5.2). The presence of a "shelf" is extremely important from the viewpoint of the coordination and continuity of defect formation processes when the crystal is cooled during growth. It can be assumed that in the entire region of formation and growth of microvoids the process of growth of precipitates passes at a low rate because of a violation of the balance of point defects and a decrease in the concentration of free impurity atoms. This leads to the fact that the

impurities settle on the walls of microvoids. This fact is confirmed by numerous experimental studies using Auger-spectroscopy, which revealed the presence of oxygen and carbon films on the walls of microvoids [114, 121, 122].

A further decrease in temperature favors the growth of supersaturation of vacancies, which leads to a sharp increase in the nucleation rate near ~ 1333 K. The nucleation region is small; microvoids grow and form in it. Behind the region of nucleation there is a region of growth of microvoids. In this area microvoids absorb vacancies and their growth rate slows down. It should be noted that in these areas a slight growth is observed with the subsequent formation of a certain concentration of microvoids (Fig. 5.2).

In the general case, the critical size of the microvoids weakly grows in the early stages of nucleation, then rapidly increases at a high nucleation rate and reaches asymptotic values (Fig. 5.1). On Fig. 5.3 is shown the distribution of sizes after complete growth of the voids ($\frac{\partial N_v}{\partial R_v} = f(R_v)$).

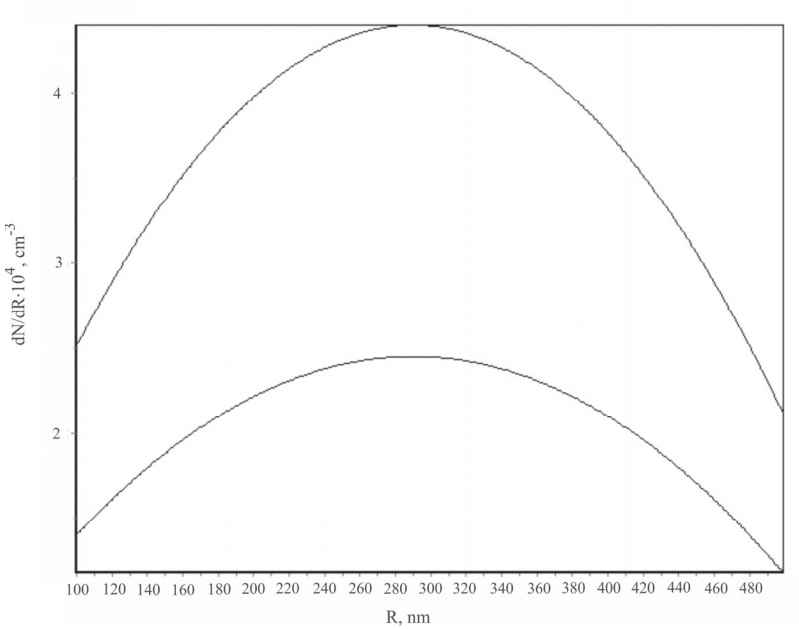

Fig. 5.3. The size distribution function of vacancy microvoids: (1) growth rate V_g = 0.6 mm/min; (2) growth rate V_g = 0.7 mm/min.

We note a negligibly small shift in the direction of large dimensions of the distribution function with increasing growth rate, which is due to the weak displacement $R_v(T)$ on Fig. 5.1.

These calculations were carried out within the framework of the model of point defect dynamics, i.e., for the same crystals and with the same parameters as in the paper about simulation of microvoids and interstitial dislocation loops (A-microdefects) [119]. But in [290] results were obtained that differ somewhat from the data of Ref. [119]. These differences are that:

- The rate of nucleation of microvoids at the initial stage of their formation zone is small and grows slightly with decreasing temperature.
- The sharp increase in the nucleation rate, which determines the nucleation temperature, occurs when T ~ 1333 K.
- A weak shift in the direction of large dimensions of the distribution function of microvoids with increasing crystal growth rate can be neglected.

These differences appear as a result of the fact that in calculations the recombination factor $k_{IV} = 0$ [290]. If $k_{IV} \neq 0$, then in the high-temperature region it is impossible to consider the interaction of impurity with IPDs, which is recognized by the authors of the model of the point defects dynamics [6, 7, 112, 120, 156-170, 289]. In this case a contradiction arises between the calculations of the mathematical model and the real physical system, which is manifested in ignoring the precipitation process during the growth of a silicon monocrystal.

The results of calculations of the formation of microvoids based on another model are presented in [290]. The analysis of the experimental and calculated data within this model shows that the formation of microvoids in dislocation-free silicon single crystals is due to the following: (1) A sharp decrease in the concentration of oxygen that is not bound into impurity agglomerates. (2) The large diameter of the crystal (more than 80 mm), which leads to the absence of a vacancy outflow from the central part of the crystal to its lateral surface. (3) The presence in the large-scale crystals of the ring of D-microdefects, which is formed as a result of the exit of the (111) facet onto the crystallization front and leads to impoverishment by the impurity atoms of the region inside this ring [290].

Modeling of the formation of interstitial dislocation loops (A-microdefects) in the framework of the model of point defect dynamics was carried out in a manner analogous to the calculation of the formation of microvoids [256] using the following computational data:

$\lambda_i = 1326\ \ erg/cm^2; k = 8.6153 \cdot 10^{-5} eV/K; D_i = 776.8 \exp(-2.0/kT);$

$C_{ie} = 2.52095 \cdot 10^{26} \exp(-3.7/kT); \rho = 5 \cdot 10^{22} cm^{-3}$

Based on the experimental data on the A-microdefect formation region, the sought temperature range of the calculation was from 1223 K to 1023 K [119]. In the high-temperatures region (1223 K < T < 1682 K, growth parameter $V_g/G_a < C_{crit}$) nucleation and growth of primary grown-in microdefects (impurities precipitates) occurs. In this region the supersaturation of IPDs (silicon interstitial atoms) is low, and, therefore, the rate of nucleation of A-microdefects is negligible. At T ≤ 1223 K supersaturation increases that leads to increase in the rate of nucleation of A-microdefects. After the formation of A-microdefects, during their growth there is a rapid expenditure of silicon interstitial atoms. As a result, supersaturation decreases and the rate of nucleation of A-microdefects decrease sharply. Hence, nucleation predominates in a narrow temperature range, and, therefore, outside the zone of A-microdefects formation their nucleation is ignored. Furthermore, since the rate of growth of A-microdefects decreases sharply due to increase in their size and corresponding decrease in the concentration of silicon interstitials atoms, the growth of A-microdefects outside the nucleation zone is also not taken into account.

On Fig. 5.4 is shown the results of calculating the temperature dependence of the critical radius of A-microdefects, and on Fig. 5.5 shows temperature dependence of concentration of A-microdefects. Similarly, a fixed value G_a = 2.5 K/mm is assumed in the calculations [119]. Modeling was carried out for crystals with a diameter of 150 mm, which were grown at growth rates V_g = 0.1 mm/min and V_g = 0.25 mm/min. These growth conditions correspond to the growth parameter $V_g/G_a < C_{crit}$, i.e., the crystal grown during interstitial supersaturation.

The temperature of formation of A-microdefects corresponds to ~ 1153 K (~ 880 ^{0}C) (Fig. 5.4). The increase in the growth rate of the crystal weakly decreases the critical radius of A-microdefects and weakly effects on the nucleation temperature. From Fig. 5.5 it can be seen that increase in the growth rate of a crystal almost doubles reduce the concentration of introduced defects [256].

Of considerable interest are the results of a computational experiment at the initial stage of the nucleation of A-microdefects in the region so-called "shelf" (Fig. 5.4). In contrast to Fig. 5.1 in this region for A-microdefects the increase in the critical radius in the temperature range ~ 1223...1160 K is negligible. In this temperature range the growing

precipitates are decrease the consumption of silicon interstitial atoms, and due to the increase of their supersaturation, A-microdefects with a very small critical radius will be formed. Unlike voids, it is impossible to remove A-microdefects, since thermal treatments lead only to the growth of A-microdefects due to the accelerated delivery of point defects to them [256].

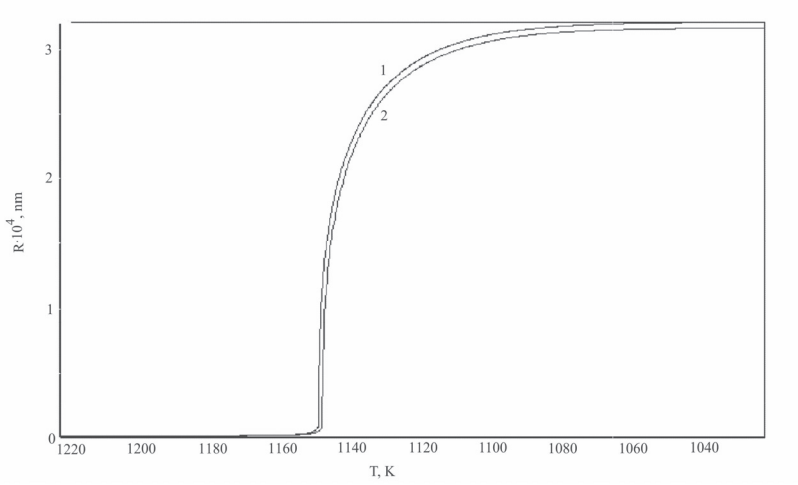

Fig. 5.4. Dependence of the critical radius of A-microdefects on the crystal cooling temperature during growth:
(1) growth rate V_g = 0.1 mm/min; (2) growth rate V_g = 0.25 mm/min

A further decrease in temperature promotes an increase in the supersaturation of silicon interstitials atoms, which leads to a sharp increase of the nucleation rate near ~ 1153 K. The nucleation region is small; A-microdefects grow and form in it. Behind the nucleation region there is a region of growth of A-microdefects. In this region A-microdefects absorb of interstitial silicon atoms and their growth rate slows down. In these regions a slight growth is observed followed by the formation of a certain concentration of A-microdefects (Fig. 5.5).

On Fig. 5.6 is shown the size distribution after growth of A-microdefects $\frac{\partial N_i}{\partial R_i} = f(R_i)$. We note a small shift in the direction of large dimensions of the distribution function with increase in the growth rate, which is due to the weak displacement $R_i(T)$ on Fig. 5.4.

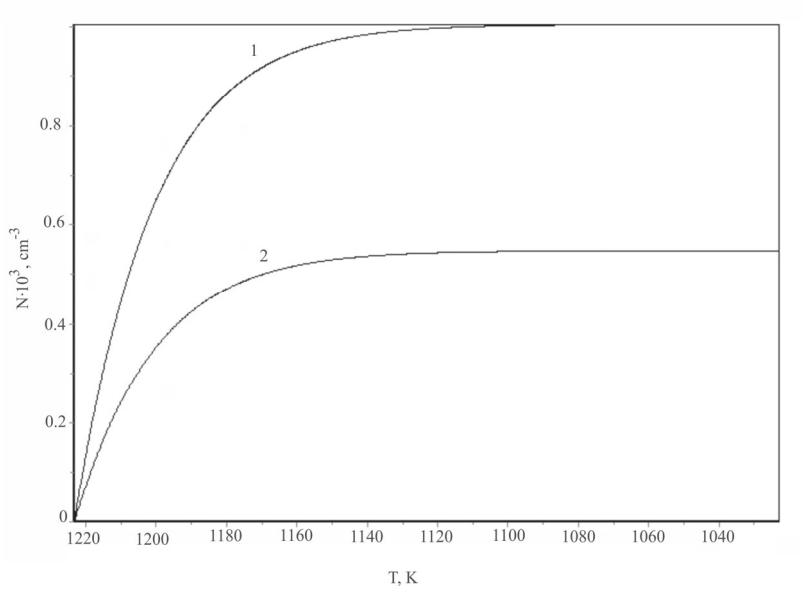

Fig. 5.5. Dependence of the concentration of A-microdefects on the crystal cooling temperature during growth:
(1) growth rate V_g = 0.1 mm/min; (2) growth rate V_g = 0.25 mm/min

The data of computational experiment for determining the concentration of microvoids correlate well with the experimentally observed results (10^4…10^5 cm^{-3}) [123]. For A-microdefects, when the experiments give a value of ~ 10^6 cm^{-3} [27, 42], the discrepancy reaches three orders of magnitude. This may be due to the fact that, in contrast to microvoids, which are formed only through the interaction of "IPD + IPD", the formation of A-microdefects occurs due to the action of two mechanisms: the interaction of "IPD + IPD" (coagulation mechanism) and the mechanism of prismatic extrusion [256].

The results of calculations in the framework of the modified model of the point defects dynamics indicate that the main contribution to the formation of A-microdefects is made by the mechanism of prismatic extrusion, when the formation of interstitial dislocation loops is associated with the removal of stresses around the growing precipitate [256]. Hence, impurity precipitation processes that occur when the crystal is cooled from the crystallization temperature are of a fundamental nature and determine

the whole process of defect formation during the growth of dislocation-free silicon single crystals.

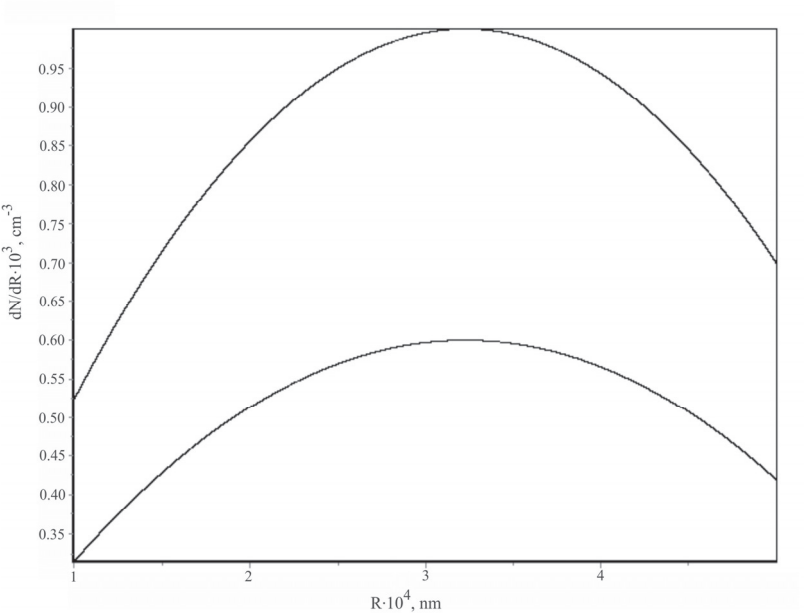

Fig. 5.6. The size distribution function of A-microdefects: (1) growth rate V_g = 0.1 mm/min; (2) growth rate V_g = 0.25 mm/min

The nucleation and growth of precipitates and also secondary grown-in microdefects (microvoids and interstitial dislocation loops) are spaced in time. The emergence of secondary grown-in microdefects begins under certain temperature conditions, when conditions arise for the occurrence of supersaturation on IPDs, while precipitates are already formed and between them there are competing processes of growth of some and dissolution of others. It should be taken into account that, in addition, the nucleation and growth of secondary grown-in microdefects (microvoids and interstitial dislocation loops) is spaced in space [256]. The important result of the calculations is confirmation of the coagulation process of formation of microvoids and the deformation process of the formation of interstitial dislocation loops [256].

The situation changes when considering the processes of nucleation and growth of post-growth microdefects that are formed in crystals during various technological influences. In this case the formation of precipitates

of various types, interstitial dislocation loops and stacking faults occurs simultaneously and for their calculations it is necessary to use approximate methods for calculating transport equations. However, such calculations should not come from zero, since the initial grown-in microdefects will play the main role, and they determine the magnitude and direction of the fluxes of point defects in the formation of post-growth defects. Therefore, only mathematical models that take into account the leading role of grown-in microdefects can adequately describe the defective structure of silicon crystals after various technological influences.

5.2. The vacancy condensation model

Within the framework of the two-stage mechanism for the formation of grown-in microdefects [291], a different approach was applied in modeling the formation of microvoids. This is due to the fact that the diffusion kinetics of impurities quite often passes very quickly. This is especially facilitated by the presence of interstitial component either as a separate diffusant or as a component of dissociative diffusion. This aspect leads to important features of the formation of impurity profiles in semiconductor samples subjected to heating. The basic mechanism that determines the features of the impurity profile in the near-surface layers is associated with the interaction of impurity atoms with vacancies, which always exist in excess in these layers. Previously, this mechanism was associated exclusively with injection of vacancies from the surface into the interior of the crystal, but it has now been established [292] that an important role is played by the process of combining vacancies with the formation of microvoids and then decorating them by impurity. The method of formation of an excess of nonequilibrium vacancies is not important.

Microvoids are formed in large-scale crystals (100 mm and higher), the growth of which is characterized by relatively high growth rates, small curvature of the crystallization front, and small axial temperature gradient. The temperature interval for the formation and growth of microvoids determined from the results of experimental studies is very narrows ~ 1403 ... 1343 K, and the interval of growth of the oxide film on their walls is ~ 1343 ... 1173 K [114, 121, 122]. From these data we assume that in the layer of a crystal with a thickness δ, that corresponds to the cooling conditions of the crystal during growth from 1403 K to 1343 K (Fig. 5.7), the excess of nonequilibrium vacancies arises n_0 (Fig. 5.8).

The reason for their appearance may be the binding of oxygen atoms into grown-in microdefects ((I+V)-microdefects) at a decrease in

temperature up to T < 1423 K. Under such conditions, the decay of the supersaturated vacancy solution proceeds at the first stage and simultaneously their diffusion occur. After most vacancies are spent on the formation of microvoids and the concentration of nonequilibrium vacancies becomes small, the process of diffusion of the remaining nonequilibrium vacancies to the surface and into the bulk of the crystal is accompanied by a process of coalescence of microvoids. At the end of this second stage, all excess vacancies go on the surface of the crystal [290].

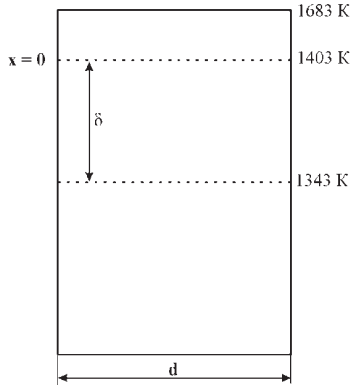

Fig. 5.7. The formation of a layer with a thickness δ , when the crystal is cooled, in which an excess of nonequilibrium vacancies occurs (*d* is a crystals diameter)

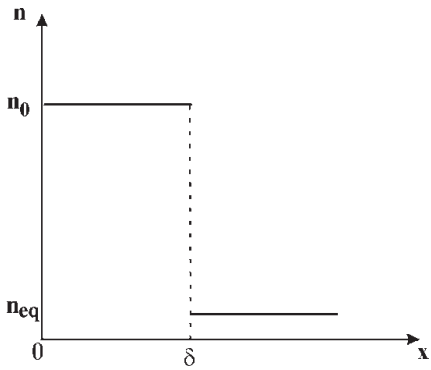

Fig. 5.8. Vacancy profile at the initial time (n_0 is the concentration of excess nonequilibrium vacancies; n_{eq} is the equilibrium concentration of vacancies)

In the first stage, following [292], the system can be described by equations

$$\frac{\partial n}{\partial t} = D\frac{\partial^2 n}{\partial x^2} - 4\pi NDrn \tag{5.1}$$

$$\frac{\partial r^2}{\partial t} = \frac{2n}{N_L}D \tag{5.2}$$

where n is the concentration of nonequilibrium vacancies; D is the diffusion coefficient of vacancies; r is the microvoid radius; N_L is the concentration of vacancies in the microvoid or the inverse volume per vacancy; N is the microvoids concentration.

In (5.1) on the right, the first term describes the diffusion of nonequilibrium vacancies from the surface (where the surface is the boundary between the volume of the crystal formed at 1423 K < T < 1682 K and a layer of thickness δ) into the sample, and the second term is the removal of part of vacancies from the diffusion flux (this part is goes to the formation of microvoids).

In accordance with Fig. 5.7 and Fig. 5.8 the boundary and initial conditions have the form:

$$n\big|_{x=0} = 0, \quad n\big|_{t=0} = \begin{cases} n_0, & at\ \ x \le \delta \\ 0, & at\ \ x > \delta \end{cases}, \quad r\big|_{t=0} = 0, \quad d\big|_{t=0} = \infty.$$

The condition $n\big|_{x=0} = 0$ assumes that a very rapid absorption of excess vacancies occurs at the surface (its role is played by the volume of the crystal formed at 1423 K < T < 1682 K). It follows that the characteristic absorption time of the excess concentration of vacancies at $x = 0$ is much less than all other characteristic times. The condition $d\big|_{t=0} = \infty$ assumes that in the process of solving the task, the output of vacancies on the side surface of the crystal is not taken into account.

Let us consider the solution of the task for the first stage. We substitute (5.2) into (5.1), integrate on time, and introduce new variables according to:

$$x = \mu\xi, \quad t = \nu\tau, \quad r^2 = \lambda q \tag{5.3}$$

where $\mu^6 = \frac{N_L}{2n_0}\frac{1}{(8/3\pi N)^2}$, $\nu = \frac{\mu^2}{D}$, $\lambda = \mu^{-4}(8/3\pi N)^{-2}$. In this case the equations (5.1), (5.2) acquire a dimensionless form:

$$\frac{\partial q}{\partial \tau} = \frac{\partial^2 q}{\partial \xi^2} - q^{3/2} + f(\xi) \tag{5.4}$$

$$n = n_0 \frac{\partial q}{\partial \tau} \tag{5.5}$$

where $f(\xi) = \begin{cases} 1, & at\ \xi \le \Delta \\ 0, & at\ \xi > \Delta \end{cases}, \quad \Delta = \frac{\delta}{\mu}$ (5.6)

with boundary and initial conditions $q\big|_{\tau=0} = 0, \quad q\big|_{\xi=0} = 0, \quad q\big|_{\xi=\infty} = 0$.

The function $f(\xi)$ can be found by substituting the initial conditions into equation (5.4).

The duration of the first stage τ_I depends on the time for which most of the excess vacancies leave the voids, which is determined from equation (5.4), with the elimination of the diffusion term $\partial^2 q / \partial \xi^2$ approximately equal to unity. A necessary condition for the formation of voids in a layer of thickness δ is the restriction $\tau_I \le \tau_S = \Delta^2$. In accordance with this condition, the time for the formation of the void must not be greater than the time for the vacancies to exit to the surface [292].

The characteristic times of the first stage of the process in the dimensional form have the form:

$$t_I = \nu \tau_I = \frac{\mu^2}{D} \tag{5.7}$$

$$t_S = \nu \tau_S = \frac{\delta^2}{D} \tag{5.8}$$

The established profile of the voids after the termination of the first stage $(\partial q / \partial \tau \approx 0)$ can be determined from equation

$$\frac{\partial^2 q}{\partial \xi^2} - q^{3/2} + f(\xi) = 0 \tag{5.9}$$

with boundary conditions $q\big|_{\xi=0} = 0, \ q\big|_{\xi\to\infty} = 0$. The parameter that determines the form of the voids profile is the value of Δ, which has the meaning of the ratio of the characteristic time of vacancy release onto the surface to the characteristic time of void formation. The solutions of equation (5.7) for three regions of variation of the coordinate ξ have the form [292]:

$$0 \le \xi \le \xi_{\max}, \quad \int_0^q \frac{dq}{\sqrt{2\left(\frac{2}{5}q^{5/2} - q + q_\Delta\right)}} = \xi \tag{5.10}$$

$$\xi_{\max} \le \xi \le \Delta, \quad \xi_{\max} + \int_q^{q_{\max}} \frac{dq}{\sqrt{2\left(\frac{2}{5}q^{5/2} - q + q_\Delta\right)}} = \xi \tag{5.11}$$

$$\Delta \le \xi < \infty, \qquad q = \frac{400}{(\xi + \xi_0)^4}, \tag{5.12}$$

where $\xi_{\max} = \int_0^{q_{\max}} \frac{dq}{\sqrt{2\left(\frac{2}{5}q^{5/2} - q + q_\Delta\right)}}, \quad \xi_0 = \left(\frac{400}{q_\Delta}\right)^{1/4} - \Delta,$

$q_\Delta, q_{\max}$ determined by equations

$$\frac{2}{5}q_{\max}^{5/2} - q_{\max} + q_\Delta = 0,$$

$$\int_{q_\Delta}^{q_{\max}} \frac{dq}{\sqrt{2\left(\frac{2}{5}q^{5/2} - q + q_\Delta\right)}} = \Delta - \xi_{\max}.$$

In the limiting cases we have

$$\Delta << 1 \quad q_{\max} \approx q_\Delta \approx \frac{\Delta^2}{2}, \quad \xi_{1/2} \approx 2{,}2\Delta + \frac{6{,}2}{\sqrt{\Delta}},$$

$$\Delta >> 1 \quad q_{\max} \approx 1, \quad \xi_{1/2} \approx \Delta + 2.5.$$

The duration of the second stage of the process (coalescence of the voids) can be estimated using the formula of the characteristic coalescence time [293]:

$$t_{II} = \frac{r^3 kT}{D\sigma\Omega^2 n_{eq}}, \tag{5.13}$$

where σ is the surface tension at the crystal-vacuum interface.

If the process of impurity diffusion passes in the crystal, then if the impurity has time to move a distance δ during the time t_{imp} which is less than t_{II}, this impurity will decorate the vacancy profile. Hence, the condition for the formation of impurity profile is the relation:

$$t_{imp} = \frac{\delta^2}{D_{imp}} \le t_{II}, \tag{5.14}$$

where D_{imp} is the impurity diffusion coefficient.

The values of the parameters required for the calculation are [290]: $N_L = \frac{1}{\Omega} = \frac{1}{2 \cdot 10^{-23}\ cm^3} = 5 \cdot 10^{22}\ cm^{-3}$; $N = 10^5\ cm^{-3}$; $G = 650\ erg/cm^2$; $D = 188.449 \exp(-1.917/kT)$; $k = 86153 \cdot 10^{-5}\ eV/K$; $D_o = 0.17 exp(-2.54/kT)$; $n = 1.11639 \cdot 10^{27} \exp(-3.9/kT)$; $r = 100\ nm = 10^{-5}\ cm$; $D_c = 1.9 \exp(-3.1/kT)$.

The temperature profile along the length of growing CZ-Si and FZ-Si crystals is described by equation [7]: $\frac{1}{T} = \frac{1}{T_m} + \frac{1}{T_m^2} G_a x$. Using the standard value G_a = 2.5 K/mm for the majority of CZ-Si crystals and the temperature interval for the formation of vacancy microvoids of 1403...1343 K [114, 121, 122], we obtain δ ≈ 3,75 cm. Then μ = 0,384 cm and Λ = 9,767 >> 1. With this value of Λ we determine from equations (5.10)-(5.12) q_{max} = 0.99659, ε_{max} = 5.284. The results of the calculations are shown on Fig. 5.9.

The estimate of the characteristic times of the first and second stages of the process, which made in the temperature range of formation of microvoids, shows that perform the relation $t_I << t_S << t_{II}$ take place [290].

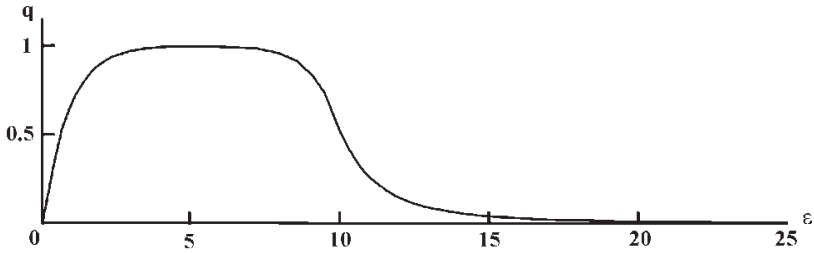

Fig. 5.9. Dependence of the square of the radius of the microvoid on the distance to the initial boundary of the temperature interval of their formation (in dimensionless units, Δ = 9.767)

From this follows an unambiguous conclusion that in the process of growth of a silicon crystal in the case of creating an excess concentration of vacancies in the temperature range of crystal cooling 1403...1343 K, a quasi-stationary voids profile are formed. The conditions for decorating

microvoids by background impurities of carbon and oxygen (5.14) in the temperature range 1343...1173 K [121, 122] are well satisfied in the entire indicated interval. These results confirm the fact that the higher the temperature, the less likely the decoration of the pore profile by impurities [233] and refute the position of the model of the point defects dynamics about formation of microvoids near the crystallization front [119].

The statement of the task did not take into account the output of vacancies onto the lateral surface of the crystal. The presence of a lateral surface limits the conditions for the formation of microvoids in the cross section of the crystal by a minimum requirement of $d_{min} > 2\delta$. Hence, under certain temperature growth conditions in real industrial single crystals, vacancy microvoids will be formed starting with a crystal diameter greater than 70 mm [290].

Thus, the vacancy-condensation model, in contrast to the recombination-diffusion model for the formation of grown-in microdefects makes the following:

- Explains the reason for the formation of an excess of nonequilibrium vacancies in the observed temperature range.
- Explains the reason for the absence of microvoids in small-scale crystals.
- Introduces a mathematical apparatus, which is in good agreement with each other theoretical calculations and experimental data.
- Gives an understanding of the physics of defect formation in dislocation-free silicon single crystals.
- Is in good agreement with available experimental data.

Theoretical calculations and experimental studies show that the formation of microvoids is due to the appearance of a nonequilibrium concentration of vacancies upon cooling of the crystal as a result of the binding of impurity atoms to primary grown-in microdefects (impurity precipitates).

In contrast to the model of the point defects dynamics, the formation of microvoids during the cooling of the crystal in the temperature range 1423...1343 K is associated with the experimental results and theoretical calculations on the formation of a microdefective structure upon cooling of the crystal in the temperature range 1683...1423 K. The consideration of the problem of the formation of microvoids confirms that the diffusion of point defects in the temperature gradient field controls the process of defect formation in dislocation-free silicon single crystals.

5.3. Kinetic model of formation and growth of interstitial dislocation loops

In the previous section, a calculation was made of the formation of microvoids and interstitial dislocation loops in accordance with the strict approximation of the model of point defect dynamics under the condition that there is no recombination of IPDs at high temperatures. It was confirmed that the process of formation of microvoids is homogeneous. However, the formation of interstitial dislocation loops is mainly determined by the deformation mechanism. This conclusion was made on the basis of a discrepancy in three orders of magnitude between the experimentally observed concentration of interstitial dislocation loops and their calculated value [256]. From these results, a kinetic model of the formation and growth of interstitial dislocation loops was developed during the cooling of the crystal after growing on the basis of a deformation mechanism [107].

As was shown above, the kinetics of the high-temperature impurity precipitation process involves three stages: the formation of new-phase nuclei, the growth of precipitates, and the coalescence stage [268, 282]. Typically, precipitates arise as a result of self-organization processes in the crystal bulk (elastic interaction of point defects) and are initially present in a coherent elastically deformed state when the lattice distortions near the precipitate-matrix interface are small and one atom from the precipitate side corresponds to one atom on the side of the matrix [13]. Elastic deformations and associated mechanical stresses cause the transfer of excess (missing) matter from the precipitate or to it. The accumulation of elastic energy during the growth of precipitate causes a loss of coherence with the matrix, when it is already impossible to establish a one-to-one correspondence between atoms on different sides of the interface. This leads to a structural relaxation of precipitates, which occurs with the help of formation and movement of dislocation loops.

To model the stress state of the precipitate and the surrounding matrix, it is sufficient to investigate the precipitate of the simplest spherical shape, since solutions for it can be found analytically [294, 295]. As the initial model, let us take theoretical and experimental studies of the stress relaxation of bulk quantum dots [296-301]. In accordance with these concepts, as the precipitate grows, its elastic field causes the formation of circular interstitial dislocation loops of mismatch, which contributes to a reduction in the total elastic energy of the system. It is shown that in the bulk of the crystal the matrix material displaced by the growing precipitate forms an interstitial dislocation loop near the precipitate simultaneously

with the formation of a loop of a mismatch dislocation at the precipitate itself [300]. In this case, the critical sizes of the precipitates, at which the process of dislocation formation is energetically favorable, are of the same order with the critical size of dislocation loops [300].

In the silicon bulk the precipitate creates a stress field due to the discrepancy between the parameters of the precipitate lattice (a_1) and the surrounding matrix (a_2) [301]. Then the intrinsic deformation of the precipitate is defined as

$$\varepsilon = \frac{a_1 - a_2}{a_1} \tag{5.15}$$

In general, the intrinsic deformation of the precipitate in the bulk of the matrix can be written in the following form:

$$\varepsilon^* = \begin{pmatrix} \varepsilon_{xx} & \varepsilon_{xy} & \varepsilon_{xz} \\ \varepsilon_{xy} & \varepsilon_{yy} & \varepsilon_{yz} \\ \varepsilon_{zx} & \varepsilon_{zy} & \varepsilon_{zz} \end{pmatrix} \delta(\Omega_{pr}), \tag{5.16}$$

where the diagonal terms are the dilatational discrepancy between the crystal lattices of the precipitate and the matrix; the other terms are the shear components; $\delta(\Omega_{pr})$ is a Kronecker symbol. The elastic fields of precipitates (stresses σ_{ij} and deformations ε_{ij}) and the field of total displacements are calculated taking into account the intrinsic deformation (5.16) and the region of localization of the precipitate $\delta(\Omega_{pr})$. Calculation of the elastic fields of precipitate is carried out according to a known scheme using elastic modules, Green's function or its Fourier image [107].

Let us consider the simplest model of a spherical precipitate with an equiaxed intrinsic deformation $\varepsilon_{ii}^* = \varepsilon, \varepsilon_{ij}^* = 0 (i \neq j; i, j, = x, y, z)$. The elastic energy of a strained spheroidal defect with equiaxial uniform intrinsic deformation with increasing precipitate radius (R_{pr}) increases in cubic order [300]:

$$E_{pr} = \frac{32 \cdot \pi}{45 \cdot (1 - \upsilon)} \cdot J \cdot \varepsilon^2 \cdot R_{pr}^3, \tag{5.17}$$

where J is a shear modulus; υ is a Poisson coefficient. From some critical value of the radius R_{crit} the mechanism of discharge of the elastic energy of the precipitate begins to operate. This mechanism leads to the formation of a prismatic interstitial dislocation loop. The energy criterion

for such a mechanism is the condition $E^{initial} \geq E^{final}$, here $E_{initial}, E_{final}$ is the elastic energy of the system with precipitate before and after relaxation.

In the case of a precipitate of spherical shape with equiaxed intrinsic deformation, the calculation of the elastic fields of precipitate is much simpler. Suppose that the intrinsic elastic energy of the precipitate before and after the formation of the misfit dislocation loop remains constant $E_{pr}^{initial} = E_{pr}^{final}$. Then the criterion for the origin of the discrepancy loop can be represented by the condition $0 \geq E_D + E_{prD}$, where E_D is an energy of discrepancy dislocation loop; E_{prD} is a interaction energy of precipitate with a dislocation loop.

To estimate, we assume that the misfit dislocation loop has an equatorial location on the spheroidal precipitate $R_D = R_{pr}$, and the intrinsic energy of the prismatic loop is [296]

$$E_{loop} = \frac{J \cdot b^2 \cdot R_D}{2 \cdot (1 - \upsilon)} \cdot \left(\ln \frac{4 \cdot d}{f} - 2 \right), \qquad (5.18)$$

where d is a loop diameter; f is a radius of the loop core; b is a Burgers vector.

The threshold value of the precipitate radius at which a loop forms on the precipitate [301]

$$R_{crit} = \frac{3b}{8\pi(1+\nu)\varepsilon} \left(\ln \frac{1.08\alpha R_{crit}}{b} \right), \qquad (5.19)$$

where α is a contribution constant of the dislocation core. Formula (5.19) is approximate and can only be used to determine the value of the critical radius R_{crit}.

In [302] the kinetics of the integration of dislocation loops at the stages of growth and coalescence of loops is theoretically considered. It is assumed that in the general case growth is controlled either by energy barrier when the atom is captured by a loop or by the activation energy of the diffusion of interstitial atom. In the conditions of crystal cooling after growth, we assume that the decisive role is played by the diffusion processes. Further, in the calculations of the evolution of the distribution of loops in size and evolution of loop density, the model [303] is used.

At the stage of coalescence, dislocation loops with a radius $R > R_{crit}$ will increase in size, while small dislocation loops with a radius $R < R_{crit}$ will dissolve [284, 302-304]. The growth of a dislocation loop during the

crystal cooling takes place both by dissolving small loops with sizes smaller than the critical ones and by supersaturation on interstitial silicon atoms, under growth conditions, when the growth parameter of the crystal $V_g / G_a < C_{crit}$. At the same time, at $V_g / G_a > C_{crit}$, when there is a supersaturation in vacancies, dissolution of interstitial dislocation loops will occur. The growth of the radius of the interstitial dislocation loop as a function of the time of the cooling of the crystal can be determined from [303]:

$$R(t) = \sqrt{R_{crit}^2 + j \cdot D(t) \cdot t}, \quad (5.20)$$

where $D(t)$ is a diffusion coefficient of interstitial silicon atoms, t is a crystal cooling time, j is a coefficient of proportionality. The value of the crystal cooling time is determined from the dependence $T(t) = \frac{T_m^2}{T_m + U \cdot t}$, where T_m is the crystallization (melting) temperature; $U = V_g \cdot G_a$ is the crystal cooling rate.

Suppose that the formation of dislocation loops is determined only by the deformation mechanism. Then the concentration of dislocation loops during the crystal cooling can be considered as a function of the concentration of precipitates. In turn, at the stage of growth and coalescence of precipitates, their concentration is a function of the cooling time of the crystal [268]. Hence, the dependence of the loop concentration on the crystal cooling time is [303]:

$$N(t) = \frac{M(t)}{1 + D(t) \cdot t / 2 \cdot R_{crit}^2}, \quad (5.21)$$

where $M(t)$ is a precipitates concentration.

Two separate groups of calculations were carried out, which simulated the formation of interstitial dislocation loops during the growth of large-scale and small-scale FZ-Si and CZ-Si crystals. The first group of calculations (I) was carried out with the following parameters: crystal growth rate V_g = 0.3 mm/min, the axial temperature gradient G_a = 25.0 K/cm. These conditions correspond to the growth of large-scale CZ-Si crystals with the growth parameter $V_g / G_a < C_{crit}$. The second group of calculations (II) was carried out with the following parameters: crystal growth rate V_g = 3.0 mm/min, the axial temperature gradient G_a = 190.0 K/cm. These conditions correspond to the growth of small-scale FZ-Si

crystals. For all groups of calculations $T = \frac{T_m^2}{T_m + V_g G_a t}$, where T_m is the melting temperature; a_1 = 0.768 nm (SiO_2), a_1 = 0.4359 nm (SiC), υ = 0.333, $k = 8.6153 \cdot 10^{-5} eV / K$, $b = 0.384\ nm$, a_2 = 0.5431 nm, f = 0.96 nm, $D = 0.19497 \cdot \exp\left[-\frac{0.9(eV)}{kT}\right]$ cm^2/s.

The formation of precipitates leads to the appearance of local fields and the concentration of stresses that effect on the generation and kinetics of dislocation loops. The intrinsic deformations of precipitates determined through the parameters of the discrepancy between the crystal lattices of silicon and precipitates, constitute ε_{SiO_2} = 0.293, ε_{SiC} = -0.246. The result of relaxation of elastic energy by a precipitate is the appearance of one or more dislocation loops [300]. The critical radii of precipitates, at which the generation of a dislocation loop is energetically favorable, will be R_{crit} = 3.028 nm (SiO_2) and R_{crit} = 3.402 nm (SiC). It is assumed that the nucleated loop has a radius equal to the radius of the precipitate, and the decrease in the elastic energy is due to the diffusion of silicon atoms adjacent to the precipitate [300]. The dislocation loop at the precipitate boundary is a misfit dislocation loop. In the general case, such loops can be several and surround the precipitate they can in different directions. In addition, simultaneously with the misfit dislocation loop, a concomitant dislocation satellite loop can be formed [298]. The radius of the satellite loops (R_1) is directly proportional to the radius of the mismatch loop (R_2): $R_1 = \beta \cdot R_2, \beta = \sqrt{\frac{b_2}{b_1}}$, where b_1 and b_2 is a Burgers vectors of a satellite loop and mismatch loop, accordingly [300].

The results of calculations for the evolution of the loop radius in time for the crystals of group I are shown on Fig. 5.10. On Fig. 5.11 is shown the calculation of the change in the radius of the dislocation loop as a function of the cooling rate of the crystal. The results of the computational experiment show that the maximum value of the radius of a dislocation loop, the growth of which is determined by the diffusion mechanism, is achieved for crystals of both groups at a cooling temperature of ~ 1423 K. The final size of the dislocation loops for group I of crystals is 35.4 μm, and for group II of crystals is 4.1 μm. The increase in the crystal cooling rate causes a sharp decrease in the size of the loop and increase of their concentration (Fig. 5.12 and 5.13).

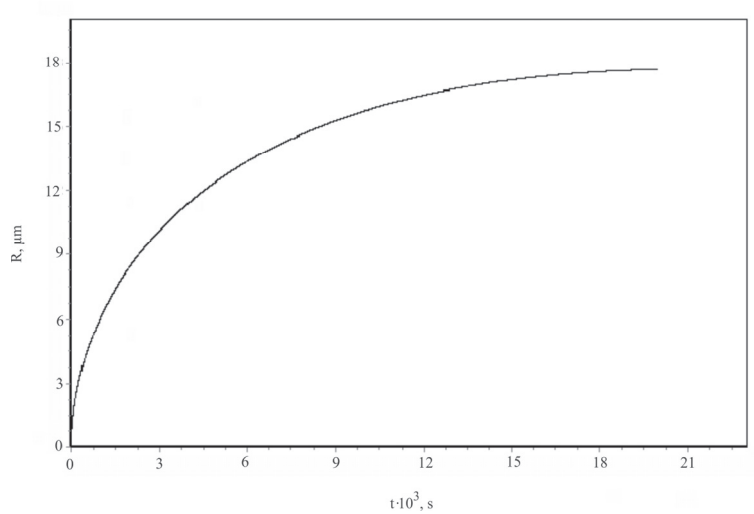

Fig. 5.10. Evolution of the radius of a dislocation loop for crystals of group I

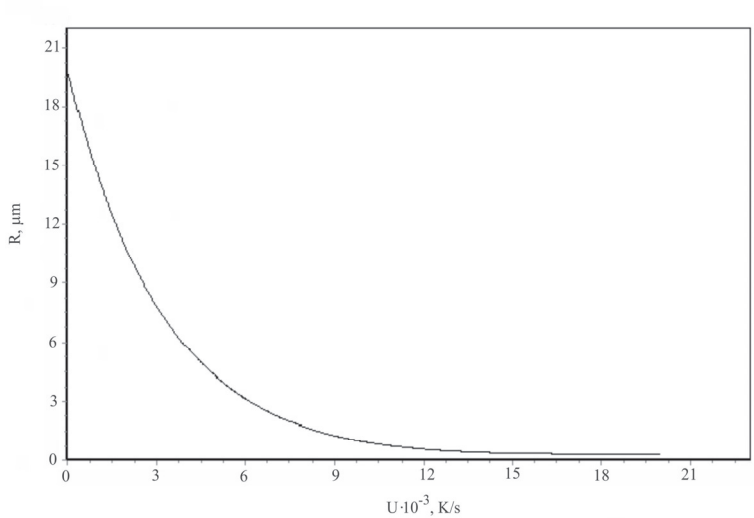

Fig. 5.11. The change in the radius of the dislocation loop as a function of the cooling rate of the crystal of group I

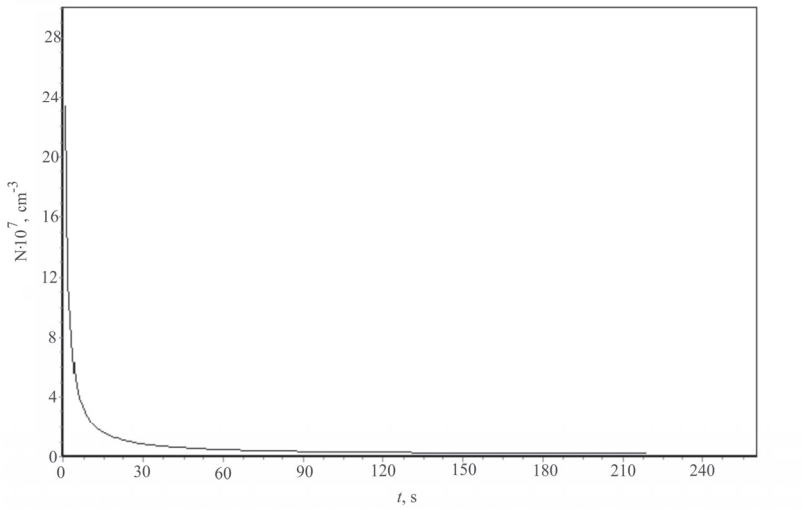

Fig. 5.12. Dependence of the concentration of dislocation loops on time for crystals of group II

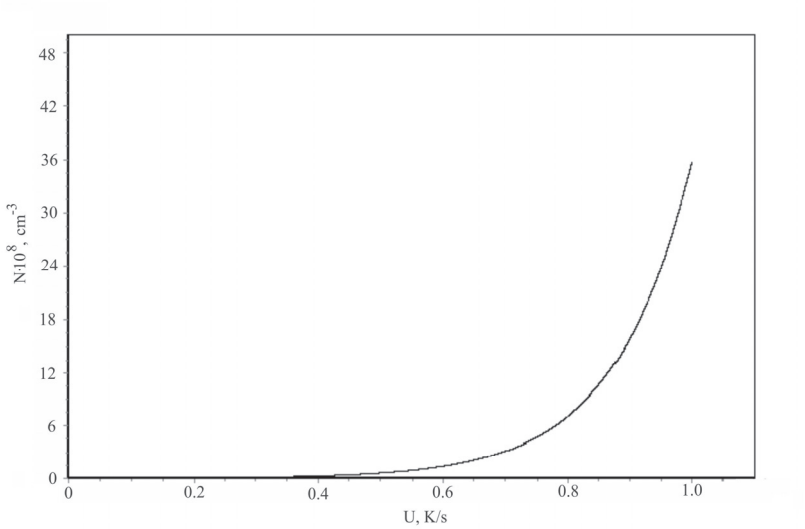

Fig. 5.13. Dependence of the concentration of dislocation loops on the cooling rate of a crystal

Depending on the initial concentration of precipitates, the final concentration of dislocation loops varies within the range from $2.45 \cdot 10^5$ to $2.45 \cdot 10^7$ cm^{-3}. For example, at $M = 5 \cdot 10^{13}$ cm^{-3} the final concentration of dislocation loops for the group II of crystals reaches $2.45 \cdot 10^7$ cm^{-3}.

Analyzing TEM-data on the study of precipitates in silicon single crystals obtained under different growth conditions, we can speak about the presence of followings: (1) Coherent precipitates not containing any dislocation defects nearby. (2) Precipitates with single dislocation loops. (3) Precipitates with multiple dislocation loops (Fig. 5.14) [52]. Precipitates can play the role of stoppers for dislocation loops, first hampering their propagation and reproduction processes, and then promote the formation of dislocation loops by the action of Bardeen-Herring or Frank-Read sources [25, 304]. These processes lead to the proliferation and formation of dislocation loops of a complex type (Fig. 5.14).

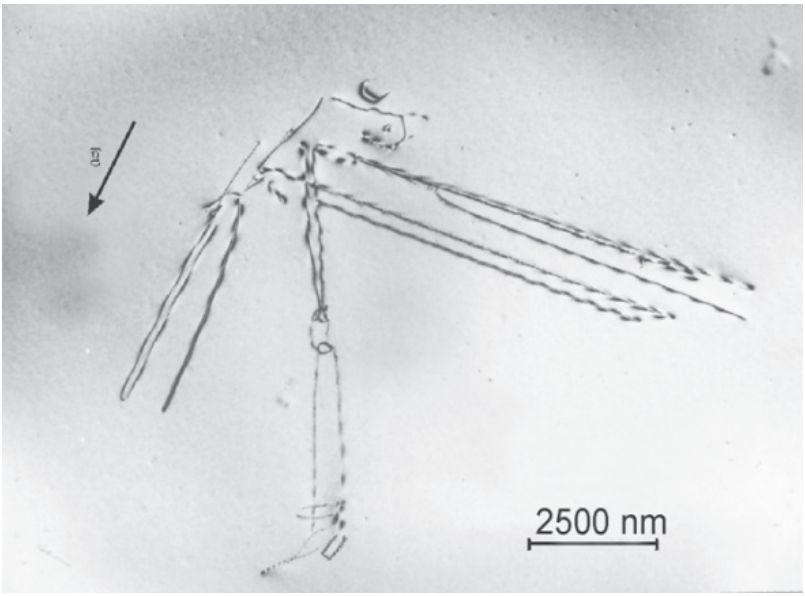

Fig. 5.14. TEM-image of A-microdefect in the form of proliferated dislocation loops, $\bar{g} = (0\bar{2}2)$

The kinetic model of the formation and growth of interstitial dislocation loops shows that the formation and development of dislocation loops is due to high-temperature precipitation of background impurities,

when a discrepancy arises between the parameters of the crystal matrix and precipitate. The growth and coalescence of dislocation loops is provided, mainly, due to the generation of interstitial silicon atoms by growing precipitates, as well as the dissolution of small dislocation loops. To relax the stresses caused by the precipitate growing during cooling, it is necessary that the precipitate either generate of interstitial silicon atoms into the interstices or adsorb vacancies. The first case corresponds to the crystal growth parameter $V_g / G_a < C_{crit}$ and was considered in Ref. [107]. The second case corresponds to the crystal growth parameter $V_g / G_a > C_{crit}$, which leads to suppression of the formation of interstitial dislocation loops and to the formation under certain thermal conditions of microvoids [6, 52].

Conclusions to chapter 5. Experimental and theoretical studies of ultrapure dislocation-free silicon single crystals showed that the formation of a defect structure during crystal growth proceeds in such direction: from high-temperature impurity precipitation to the formation of secondary grown-in defects (microvoids or dislocation loops).

Mathematical models of the formation of precipitates and secondary grown-in microdefects (microvoids and dislocation loops) confirm the experimental results on which the heterogeneous (two-stage) mechanism of grown-in microdefect formation is based. The process of interaction of IPDs with impurities, which begins near the crystallization front, is a fundamental (primary) process; it is decisive in the formation of the defect structure of highly perfect dislocation-free silicon single crystals during their growth. In the process of crystal cooling, depending on the thermal growth conditions due to the loss of impurity atoms onto precipitates formed, conditions are created for exceeding the equilibrium values of the concentrations of IPDs, which leads to the formation of microvoids and interstitial dislocation loops in different regions of the crystal. In this case impurity precipitates serve as condensation sites for IPDs.

The model of high-temperature precipitation together with the kinetic models of the formation and growth of interstitial dislocation loops and microvoids is a mathematical apparatus that allows one to theoretically describe the processes of formation and transformation of grown-in microdefects in dislocation-free single crystals of FZ-Si and CZ-Si any diameter. The use of these mathematical approaches is based on a physical model based on a theoretically and experimentally established fact that there is no recombination of IPDs during the crystal cooling at high temperatures. The heterogeneous (two-stage) mechanism of formation and

transformation of grown-in microdefects adequately describes the real defect structure of dislocation-free silicon single crystals formed under different thermal conditions of crystal growth. This solidarity of physical and mathematical models allows us to say that a new theoretical model for the formation of grown-in microdefects has been developed, which is based on a heterogeneous (two-stage) mechanism and mathematical models for the formation of precipitates and secondary grown-in microdefects. Proceeding from the basic processes underlying the process of defect formation in dislocation-free silicon single crystals, we define this model as a diffusion model.

CHAPTER SIX

GENERAL APPROACH TO THE ENGINEERING OF DEFECTS IN SEMICONDUCTOR SILICON

Nothing gives certainty but truth; nothing gives rest but the sincere search for truth.
—Blaise Pascal (19.VI.1623 – 19.VIII.1662)
Pensées sur la religion et sur quelques autres sujets, 1670

Solid-state physics is the physics of real crystals that contain structural defects [11]. The problem of obtaining materials and structures with given properties is a common problem of materials science and, in particular, materials science of semiconductors. In semiconductor silicon the types, concentration and behavior of structural defects (grown-in and structural microdefects) are very diverse and depend on the nature, conditions of production and the nature of the external influences (temperature processing, pressure, irradiation, impurities, mechanical effects, etc.). Therefore, the creation of defects with the necessary properties, both in the process of crystal growth and the process of manufacturing the device, is the main way to control the properties of solid-state devices with predictable and controlled characteristics.

A set of defects determines the properties of real crystals and structures, and the additional introduction of nonequilibrium point defects during technological impacts can significantly change the thermodynamic state of crystals and structures, as well as their most important physical properties. Control of atomic processes at interfaces, reactions between impurities and defects in materials and structures becomes one of the main trends in modern materials science and the basis of a new direction in materials science of semiconductors the defect engineering. Technologies of defect engineering are a necessary and inseparable part of semiconductor silicon manufacturing technologies and devices based on it.

6.1. Necessary conditions for the engineering of defects during the crystal growth

Historically, the study of defect formation in silicon was fragmentary. This fragmentation was associated with attempts to explain the causes of the appearance of structural defects depending on a particular technological process (crystal growth, technological processing in the creation of devices). The researchers received large databases of empirical data on defect formation in various technological areas of production of silicon devices, which, however, only with very great difficulty and very little confidence could be linked together.

The review of K.V. Ravi (1981) can be called the first attempt to bring together disparate data on defects in semiconductor silicon [39]. A great organizational and informational value is given by the GADEST (Gettering and Defect Engineering in Semiconductor Technology) conferences held for more than thirty years. These conferences discuss a wide range of issues, from theoretical consideration of the fundamental aspects of defect physics in semiconductors and strategies for the development of modern semiconductor electronics to the practical solutions of modern technologies. As the basic subjects it is possible to note: growth of mono- and multicrystalline silicon; IPDs, impurities and dislocations in silicon; properties and gettering of transition metals; thermal, optical properties of semiconductors; defect engineering in silicon micro- and nanoelectronics and others (for example, a series of conferences [305-309]).

There are good reviews on defect engineering in various areas of silicon technology. In [310] the questions of the development of the physical foundations of defect engineering in the technology of silicon power high-voltage devices and light-emitting diodes. Techniques were developed here that make it possible to control nonequilibrium IPDs and their behavior at different stages of the technological process. In addition, complex studies were considered that take into account the interrelationship of manufacturing conditions, structural, optical and electro-physical properties in power high-voltage and light-emitting structures, and allow monitoring the processes of formation and suppression of nonequilibrium IPDs and the entire system of defects formed at different stages of the process [310]. The paper [311] presents the results of studies that allowed laying the foundations of defect engineering in the technology of light-emitting structures based on single-crystal silicon implanted with erbium ions. The reviews [312, 313] present the results of investigations of defect-impurity interaction in implanted silicon. The factors influencing the course of quasi-chemical reactions are analyzed: temperature, ionization level,

elastic stress fields and internal electric fields. Also here are examples of practical implementation of defect-impurity engineering in microelectronics [313].

In general, any original scientific work on the study of defect formation, as well as in other silicon technologies, can be considered as an attempt to engineer the defective structure of the crystal (or device) for certain conditions (see, for example, reviews [314-316]). There are a lot of such works and often they do not follow a single approach to defect formation processes in crystals. The logic of creating silicon devices suggests that firstly the initial defect structure (grown-in microdefects) is formed in the process of growing the crystal. Then, under different technological influences on the crystal, two interrelated processes occur. First, the grown-in microdefects are transformed and, secondly, new structural imperfections are formed. As a result, a new defective structure (post-growth microdefects) is formed, which is determined by the type and nature of the various technological impacts or their combinations.

Hence, the role of the original defective structure is basic and determines the properties and quality of silicon devices created during technological impacts. From this viewpoint, as an example, you can pay attention to the reviews [191, 317-319]. In these reviews are considered: the structural imperfections that are formed during the growth of silicon single crystals and structures based on it; the mechanisms of their formation; the elements of defect engineering in crystals, wafers and structures; the methods for studying defects. All these questions are considered from the viewpoint of the recombination-diffusion model of the formation of grown-in microdefects and the corresponding mathematical variations of the model of the point defects dynamics. Therefore, for these reviews are inherent all the previously mentioned shortcomings of physical and mathematical models (in particular, the negation of impurity precipitation during crystal growth). At the same time, all physical models proceed from the established fact that the types, sizes and concentrations of grown-in microdefects are determined by the thermal growth conditions of the crystals (growth method, crystal diameter, growth rate and temperature gradients in the crystal).

Recently, in connection with the intensive development of mathematical methods and the growth of computers powers, the methods of mathematical modeling have found the greatest application for determining optimal ways of improving the technology of growing single crystals. Modern software allows to calculate with high accuracy the temperature fields in growth chambers taking into account all their features and properties of materials used in the construction, as well as to

improve previously created thermal units in order to create the required temperature distribution and reduce heat losses. In addition, the application of methods of mathematical modeling makes it possible to improve the technological process and accelerate the development of new technologies for growing dislocation-free silicon single crystals with a specified minimized content of grown-in microdefects.

Solving practical problems of improving the quality of single crystals and optimizing technological regimes in many cases requires studies of melt hydrodynamics and complex conjugate heat-mass transfer in growth chambers. Actual in this connection is the solution of the problem of the relationship between crystal growth conditions and their bulk crystallographic characteristics. A number of authors working in this direction are engaged in forecasting not only the hydrodynamics of the melt (in particular, in the boundary layer at the crystallization front) and gas dynamics in the region above the melt surface and in the volume of the growth chamber, but also the temperature field in the crystal throughout the growth stage. Physical modeling is used here [320, 321], and also numerical modeling [322, 323], consistent complex approach [324], global numerical simulation of complex conjugate heat-mass transfer in the whole growth chamber or thermal node [325, 326], three-dimensional hydrodynamic modeling for the crucible-melt-crystal system [327-329].

So, in a number of papers by the authors working in this direction, it has been shown that the growth of so-called "defect-free" regions, i.e., regions with primary oxygen-vacancy and carbon-interstitial precipitates, is possible by significantly increasing the rate of cooling of the ingot [7, 170, 193, 330-333]. In these studies, various versions of the design of thermal zones were calculated and proposed, where the variation in the cooling rates was achieved by different positions of the thermal shields in the crucible region. It was shown in [332-334] that the introduction of the so-called "crucible screen" significantly affects the magnitude of the axial temperature gradient in the temperature range 1573...1273 K of the growing crystal. The values of the microvoids density of $2.2 \cdot 10^5$ cm^{-3} with a size of 117 nm were obtained at a cooling gradient of 6.0 K/cm and $7.5 \cdot 10^5$ cm^{-3} with a size of 78 nm with a cooling gradient of 15.0 K/cm [170]. The authors of [170] noted that the results obtained are acceptable for the use of such crystals in the manufacture of integrated microcircuits. It should be noted that similar results (increase in the concentration of defects with a decrease in their sizes) were observed for primary grown-in microdefects in small-scale crystals [52].

It was shown in [173] that the limiting value of the cooling rate is 40 K/cm. At gradients above 40 K/cm, microvoids are not detected, and

impurity precipitates begin to dominate over the volume of the crystal (in [173] is assumed only the oxygen precipitates). This result agrees well with the results of experimental observations of small-scale crystals FZ-Si (30 mm) and CZ-Si (50 mm): microvoids are not formed in such crystals, since their cooling rate is always greater than 40 K/cm. Thus, it is necessary to say that the direction associated with obtaining crystals at high cooling rates is very important and promising from the viewpoint of controlling the quality of the single crystals.

However, the conditions for growing real industrial single crystals (diameters in excess of 200 mm) are now such that one has to talk not about obtaining them without secondary microdefects, but about a low content of these defects (at high cooling rates). An ideal method for obtaining small-scale crystals of FZ-Si and CZ-Si with uniform distribution of primary microdefects (impurity precipitates) was their growing at high growth rates and subsequent quenching [52]. This led to a "freezing" of the early stages of the defect formation process, and subsequent heat treatments of such samples did not lead to their significant deterioration. Since for large-scale crystals this method is inapplicable, it is necessary to find ways to grow crystals whose defective ensemble will be in the state of the early stages of the defect formation process.

In one of the modifications of the Czochralski and float zone methods [335], in order to improve the quality of the crystal around the growing single crystal, a cylindrical or cone-shaped body is introduced that divides the space of the container above the melt into the inner and outer parts. In this case, the body has one opening through which an inert gas directed to the interior of the container space can reach its outer part.

In the device for obtaining silicon single crystals in order to improve the quality of the crystal, the directions of rotation of the crucible and crystal coincide, and the ratio of the rotational speeds of the crucible and the crystal is calculated by the special formula [336]. In the patented device [337], the rotation speed of the crucible and the crystal is gradually increased, keeping the ratio of the rotational speeds of the crucible and the crystal approximately constant. This makes it possible to obtain silicon single crystals with a uniform radial distribution of dopant and oxygen and with a uniform oxygen distribution along the length of the crystal. In the device [338], a gas-guiding cylindrical screen is additionally introduced, into which an additional annular screen is included.

In another device [339], the following steps were taken: (1) pulling the ingot from the melt to the seed, (2) detaching it from the melt, (3) separating the ingot from the seed, (4) replenishing the melt, and pulling out the next ingot, in which the morphology of its surface is controlled and

when the growth of the facets of the single crystal disappears are made the detachment of the ingot from the melt. In [340] polycrystalline silicon is charged in a quartz crucible, a cylindrical screen 235-240 mm in diameter is placed coaxially with the grow single crystal, the lower end of which is placed above the melt plane at an altitude h determined by the formula $h = (A - D)/B$, where D is the given diameter of the grown ingot equal to 76-150 mm; A is the size coefficient, B is the dimensionless coefficient. The chamber is sealed, an inert gas is supplied at a flow rate of 15 L/min. The melt is seeded and a monocrystal is grown. The ingot with a uniform distribution of impurities is obtained, which was called "defect-free" by the inventors.

In [341], the invention is described as follows: an apparatus for growing a silicon single crystal from a melt contains a (1) chamber with holes for evacuation of a gas stream in which a (2) crucible for melt located in a stand on a rod is placed, (3) an upper gas-guide screen forming a gas flow above the melt, (4) and a heater. The device is equipped with a lower gas-guide annular screen (located above the heater) with a central hole for moving the stand. The holes for the evacuation of the gas flow are made in the chamber between the upper and lower gas-guiding screens. The space between the casing, the lower gas-guide ring screen, the heater and the rod is filled with a backfill, for example, silicon carbide. The heater can be sectional. In this case, the filling is fixed between the heater sections by means of sealing inserts, for example, of graphite felt. Around the rod, the backfill can be fixed by means of a sealing ring. The device allows significantly increasing the productivity of the growing process, improving the quality characteristics of grown silicon single crystals and reducing their cost, as well as extending the life of the thermal unit, reducing the cost of maintenance and repair.

In [342], it was proposed to grow single CZ-Si crystals and then use them in the manufacture of semiconductor devices, in particular power transistors, power diodes, thyristors, etc. The invention makes it possible to increase the yield of suitable products, both in the growth of single-crystal silicon and in the manufacture of semiconductor devices based on such silicon. This is achieved by the partial doping with phosphorus during the growing of the single crystal, and the additional doping to a given level of specific resistance is carried out by thermal donors by annealing silicon at a 623...773 K, combining it with temperature treatments containing these temperatures in the manufacturing cycle of the device. The distribution of donors due to doping with phosphorus, as well as the content and distribution of thermal donors, are chosen so that the

total concentration of donors in each point of a single crystal in the finished devices corresponded to a given level of specific resistance.

In [343], a variant of obtaining single crystals by the Czochralski method was proposed. The essence of the method is as follows: the melting device for growing monocrystals from the melt consists of a quartz crucible placed in a graphite stand rigidly fixed to the rod. The stand is made composite in the form of upper and lower disks mounted coaxially to each other, the upper disc having a larger diameter than the lower one and can being fixed to the lower disc and crucible. The lower disc is fixed to the rod, and around the crucible a "wrapper" is fixed in the form of a foil of finely divided graphite. This invention reduces the downtime of the melting device between reboots, improves the technological purity of silicon single crystal production, reduces the irretrievable loss of silicon and ensures the integrity of the device during cooling after the growing process. Another variant of the melting device [344] consists of a quartz crucible placed in a graphite stand rigidly fixed to the rod.

A number of papers [345-349] proposed a method for growing crystals under conditions of an axial heat flux near the crystallization front. This method pursued the goal of creating a tool for quantitative study of heat and mass transfer and interfacial kinetics, which makes it possible to accurately compare the crystallization conditions near the crystallization front with the quality of the crystal, and the possibility of growing large-scale crystals. The axial heat flux was the one-dimensional thermal field near the crystallization front, suppressing natural convection near the crystallization front and thus creating weak laminar melt flows. Such flows can ensure, under crystallization, regimes close to the diffusion regime of mass transfer and, hence, high macrohomogeneity. According to the data of [345, 348] for weak laminar melt flows, the thickness of the diffusion layer is comparable with the height of the melt zone near the crystallization front and its contribution to the heat transfer is small, which creates the theoretical possibility of separate control of heat transfer and mass transfer.

The authors of [349] proposed the construction of apparatus for growing crystals using the effect of noncontact excitation of forced convection in a melt by rotating the thermal field. Here is proposed: (1) the rejection of mechanical rotary devices (both crucible and seed) while keeping the possibility of controlling convective heat and mass transfer, (2) the possibility of partial or complete sealing of the growth space, (3) construction of a thermal control system in the dynamic connection mode of heating elements of the growth furnace.

Finally, in [350] a technique is proposed that combines the elements of heat and mass transfer control and the application of magnetic fields. The essence of the technique is as follows: to create supercooling in the boundary layer between the melt and the facet of the growing crystal with use electromagnetic fields that drive the melt. As a result, the heat removal is carried out mainly through the melt. The process productivity with its optimization increases up to 10 times for crystal diameters of 300...500 mm.

The disadvantages of all these solutions is that only private tasks are solved for optimizing the growth parameters of dislocation-free silicon single crystals.

In solving problems of obtaining uniformly doped single crystals, great importance is given to the processes of magnetohydrodynamic action on the melt during growth. In addition, doping with unconventional impurities (isovalent impurities, rare-earth element impurities) as well as various radiation effects on the material can be described as examples of attempts to influence the defect structure of single-crystal silicon in order to practically create the energy spectrum of levels in the band gap by creating sufficiently thermostable electrically active complexes with the necessary ionization energy [351].

In [324], the solution of the problem of controlling microvoids is achieved by the fact that a monocrystal growing from a melt has a temperature of 1623...1523 K before the end of growth due to additional heat treatment, and after this his rapidly cooled. This is achieved by introducing into the growth units additional heaters and gas-guiding screens supplying an inert gas for cooling.

It can be concluded that in the engineering of grown-in microdefects, the problem of controlling the composition and state of the ensemble of point defects in crystals is put forward, requiring deep penetration into the problem of their interaction. With the solution of this problem, new approaches to the management of the properties of single crystals must be associated. The key to solving such a problem can be the diffusion model for the formation of grown-in microdefects, which gives a complete quantitative and qualitative picture of the interaction of point defects in the process of growth and cooling of dislocation-free silicon single crystals.

6.2. Structure of the diffusion model

Theoretical studies of defect formation in semiconductor silicon play a crucial role in the production of breakthrough ideas for next generation technologies. It is extremely important not only to grow crystals with a

previously known defective structure, but also to manage this structure during the technological processes of creating devices. From this viewpoint, the diffusion model, which fully describes the kinetics of the diffusion decay processes of supersaturated solid solutions of point defects during crystal cooling after growing, depending on the thermal growth conditions, can be a convenient tool for such control [255].

In the diffusion model for the formation of grown-in microdefects, all parameters of precipitates, microvoids, and dislocation loops are determined through the thermal parameters of crystal growth. Determination of the type of defect structure and calculation of the formation of grown-in microdefects is performed depending on the value of crystal growth rate, temperature gradients and cooling rate of the crystal [352]. Depending on the thermal growth conditions of the crystals, grown-in microdefects of three types are formed: precipitates, dislocation loops and microvoids. Experimental and theoretical studies of ultrapure dislocation-free silicon single crystals showed that the formation of a defect structure during crystal growth proceeds in the direction: from high-temperature impurity precipitation to the formation of secondary grown-in defects (microvoids or dislocation loops). The diffusion model for the formation of grown-in microdefects is based on the experimentally confirmed positions of the physical model of their formation and includes a high-temperature model of precipitation and kinetic models for the formation of microvoids and dislocation loops (Fig. 6.1).

The diffusion model is based on an experimentally and theoretically established fact that there is no recombination of IPDs at high temperatures. The model of high-temperature impurity precipitation describes the elastic interaction between IPDs and background impurities of oxygen and carbon during cooling of dislocation-free silicon single crystals after growing in the temperature range 1683K...300K. The high-temperature precipitation model includes all three stages of the classical theory of the formation of a second-phase particle: the formation of a critical nucleus, the growth and coalescence of precipitate. The process of precipitation begins near the crystallization front and is due to the disappearance of excess IPDs in the sinks, whose role is played by the impurities of oxygen and carbon. The size of the critical nucleus of the precipitate is minimal near the crystallization front and increases with decreasing temperature upon cooling of the crystal.

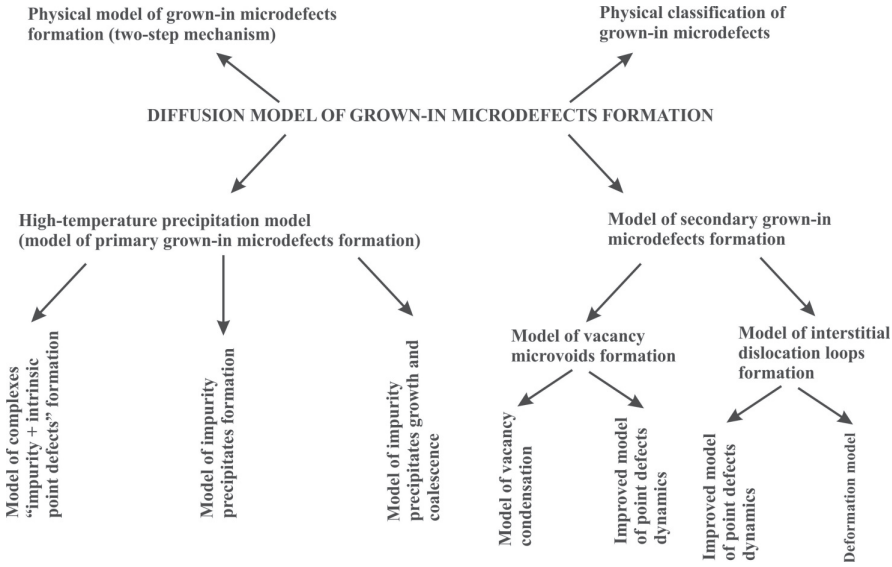

Fig. 6.1. Structural diagram of the diffusion model for the formation of grown-in microdefects

Under certain thermal conditions for crystal growth, depending on the growth parameter V_g/G_a in the temperature range of cooling 1403K...1223K, either microvoids or dislocation loops are formed. Kinetic models of their formation show that the formation of microvoids has a homogeneous character, while the formation of dislocation loops occurs due to the action of the deformation mechanism. Improved models of the point defects dynamics are calculated in the absence of recombination of IPDs at high temperatures.

A number of questions remain in the theory of defect formation in solids, which until recently did not receive a satisfactory solution, for example, (1) the problem of the correct description of the formation of structural defects during crystal growth, (2) the construction of a consistent microscopic theory of the formation of defects in solids, etc. The absence of a general algorithm for solving problems of defect formation in solids leads researchers to the necessity of their phenomenological analysis for each type of crystals separately. At the same time, many phenomena occurring in different crystals have a general character, for example, (1) the interaction of point defects with one

another, (2) their interaction with dislocations, (3) the formation and transformation of dislocations, etc.

Correction of traditional ideas about the dominant role of IPDs showed that semiconductor silicon, being extremely pure and perfect in structure, can itself be considered as the initial model for constructing theoretical models of defect formation in other semiconductor materials and metals. The obtained mathematical models and the proposed methods for their solution in silicon make it possible to formulate and solve many tasks in the kinetics of diffusion processes in solids. The diffusion model of defect formation has a sufficient generality and is applicable to the mathematical description of such processes as impurity precipitation, voids formation, the formation of dislocation loops in crystals, etc. Two stages of the decomposition of a supersaturated solution of point defects (according to the vacancy and interstitial mechanisms) make it possible to describe reactions of interaction between IPDs and impurities, as well as modifications of the defect-impurity system during crystal cooling after growing. The primary nature of the processes of high-temperature precipitation is a fundamental feature that determines the general kinetics of defect formation in highly perfect crystals, both semiconductors and metals [255].

The generality of the approach does not exclude the presence of specific features of the application of the diffusion model for various materials that are associated with different thermal conditions for the growth of crystals and various types of their crystal structure. Specificity of defect formation at high temperatures in metals, especially close-packed ones, is due to the fact that the concentration of equilibrium interstitial atoms is many orders of magnitude lower than the equilibrium vacancies [353]. When the crystal is cooled, condensation of nonequilibrium vacancies occurs in the form of vacancy disks [354]. As a result of the collapse of the vacancy disks, prismatic dislocation loops are formed [355]. This mechanism is analogous to the mechanism of formation of microvoids in a loose lattice of semiconductors, which, however, does not lead to the formation of dislocation loops in semiconductors. At the same time, the process of high-temperature impurity precipitation in metals promotes the deformation mechanism of the formation of dislocation loops. It is possible that the joint action of the vacancy and deformation mechanisms of the formation of dislocation loops is the main reason why the growth of dislocation-free single crystals of metals is more difficult compared with semiconductors. At the same time, in the case of growing crystals of semiconductor compounds containing a volatile component, an

important additional source of dislocation loops can be the deviation of the composition from stoichiometry.

The specificity of growing and distinguishing the crystal structure of various dislocation-free single crystals must necessarily be taken into account in the physical model and mathematical constructions of the diffusion model. However, in any case, the algorithm of its application is based on the high-temperature precipitation process, which determines the entire subsequent course of formation of the defective crystal structure. The diffusion model of defect formation can be an ideal platform for a multifunctional solution of many key problems of modern solid state physics, such as defect formation in solids, defect engineering in solids, control of the physical properties of solid structures, etc. For detailed confirmation of these judgments (assumptions), theoretical work of specialists is needed that investigate other solid materials.

The practical importance of developing the theory of defect formation in crystals is due to the fact that the formation of structural defects and their transformations accompany industrial technological processes for the production of crystals and devices. From the emerging microstructure, the electrical, optical, mechanical, and other properties of crystals and devices are strongly depending. Knowledge of the patterns of the formation of defects in solids can be used to improve the technologies for obtaining materials and instruments with specified properties, to solve problems of controlling the type, density, and spatial distribution of structural imperfections.

In this regard, with the practical application of the diffusion model of defect formation, two topical issues arise that are related to the purview of the model and the methodology for constructing information complexes for the engineering of defects. First of all, it is necessary to include the problem of an adequate description of the formation and development of a defective (real) crystal structure both at the stage of their growth and at the stage of creating devices based on them. This line of research is extremely relevant for the development of the theory of solids and, moreover, has great practical importance for industrial production. Therefore, the answer to the first question implies that any theoretical model should link together the consideration of the processes of formation and development of a defective structure during the growth of a crystal and its technological treatments. The answer to the second question requires that the information system is based on the technique of analysis and calculation of grown-in microdefects adequate to the real defective structure of semiconductor silicon.

6.3. Diffusion model of the formation of grown-in microdefects as applied to the description of defect formation in heat-treated silicon single crystals. Thermal donors and thermal acceptors

An important factor determining the rate and nature of the reactions in crystals is the temperature. The temperature dependence is determined by the energy parameters of formation and decay of defective associations, and in the case of low temperatures and migration of defects. During the creation of devices, the main technological effects on the crystal are thermal treatments that critically affect the defective structure of the crystals and lead to the formation of post-growth microdefects. The post-growth defects determine the quality of silicon semiconductor devices. The possibility of using the mathematical apparatus of the diffusion model for the formation of grown-in microdefects in the formation of a defect structure in an undoped dislocation-free silicon single crystal as a result of thermal treatments was considered in [356].

As estimate of the application of the diffusion model to describe the formation of the defect structure of heat-treated crystals, a hypothetical model of ideal crystal was used [356]. Suppose that there is a "defect-free" undoped silicon single crystal at a temperature of T = 300 K, which was grown by the Czochralski method. As shown by numerous experimental studies when the crystal is heated in the temperature range 623...823 K, structural imperfections are formed which are the nuclei of precipitates SiO_2 [190]. Let us assume that T = 723 K is the minimum temperature for the formation of structural imperfections in dislocation-free silicon single crystals. We apply for the chosen crystal model the diffusion model for the formation of grown-in microdefects.

In accordance with the diffusion model for the formation of grown-in microdefects, the formation of "impurity + IPDs" complexes is the determining factor in the onset of the defect formation process. The formation of complexes between IPDs and impurities is determined, on the one hand, by the fact that both are sources of internal stresses in the lattice (elastic interaction) and, on the other, Coulomb interaction between them (if defects and impurities are present in a charged condition). In the diffusion model, only the elastic interaction is taking into account. Elastic deformations and associated mechanical stresses cause the transfer of excess (missing) matter from the precipitate or to it. The accumulation of elastic energy during the growth of precipitate causes a loss of coherence with the matrix, when it is already impossible to establish a one-to-one correspondence between atoms on different sides of the interface. This

leads to a structural relaxation of precipitates, which occurs by the formation and movement of dislocation loops.

The critical size of the precipitates of oxygen (SiO_2) and carbon (SiC) is determined in accordance with formulas (4.59)-(4.60). In this case, the temperature dependence has the form $T(t) = const$. The number of impurity atoms in compressed precipitates with radii r_O and r_C is determined in accordance with formula (4.61). The average number of particles at the nucleation centers and the average radius of the precipitate at the growth stage were found from formulas (4.69) and (4.74), respectively. The average size of the precipitates in the coalescence stage is proportional to the cubic root of time (4.86).

As the precipitate grows, its elastic field causes the formation of a circular interstitial dislocation loop of mismatch, which contributes to a decrease in the total elastic energy of the system. In the bulk of the crystal, the material of the matrix displaced by the growing precipitate forms an interstitial dislocation loop near the precipitate, simultaneously with the formation of a mismatch dislocation loop at the precipitate itself [298].

In this case, the critical sizes of the precipitates, at which the process of dislocation formation is energetically favorable, are of the same order with the critical size of dislocation loops [300]. The value of the critical radius of the loop [107]:

$$R_{crit} = \sqrt[3]{\frac{45 \cdot (1-\upsilon) \cdot b^2 \cdot d \cdot \ln(\frac{4 \cdot d}{f} - 2)}{128 \cdot \pi (1-\upsilon) \cdot \varepsilon^2}} \qquad (6.1)$$

where d is a diameter of loop; f is a radius of the loop core; b is a Burgers vector; υ is a Poisson coefficient.

The growth of the radius of the interstitial dislocation loop as a function of the time of the thermal treatment of the crystal can be determined from (5.20). Dependence of the concentration of loops on the time of thermal treatment of the crystal [301]:

$$n(t) = \frac{M}{10^3 \cdot t^{0.8}}, \qquad (6.2)$$

where M is the precipitates concentration.

The following data were used in the calculations: $V_p = 4.302 \cdot 10^{-2}$ nm^3 (SiO_2); $V_p = 2.04 \cdot 10^{-2}$ nm^3 (SiC); σ = 310 erg/cm^2 (SiO_2); σ = 1000 erg/cm^2 (SiC); $\mu = 6.41 \cdot 10^{10}$ Pa; δ = 0.3; ε = 0.15; $\gamma_i = 0.4; \gamma_v = 0.1$; $k = 8.6153 \cdot 10^{-5} eV / K$; a = 0.25 nm;

$b = 0.384\ nm;\ D_O = 0.17\exp(-2.54/kT);\ D_c = 1.9\exp(-3.1/kT);$
$D_i = 0.19497 \cdot \exp\left[-\frac{0.9(eV)}{kT}\right]$ cm^2/s; $\upsilon = 0.333$, f = 0.96 nm; x = 1.5.

The analysis was carried out in the approximation that the growth of precipitates occurs at a fixed number of nucleation centers under the diffusion mechanism of growth. The model considers the precipitation homogeneous in bulk.

Four separate groups of calculations were carried out, which simulated the precipitation processes during the thermal treatment of "defect-free" undoped silicon single crystals grown by the Czochralski method. The first group of calculations (I) was carried out at the annealing temperature T = 730 K. The second group of calculations (II) was carried out at the annealing temperature T = 1000 K. The third group of calculations (III) was carried out at the annealing temperature T = 1100 K. The fourth group of calculations (IV) was carried out at the annealing temperature T = 1510 K. For all four calculation groups $N(0) = 10^{18}$ cm^{-3} for oxygen and carbon concentrations, $N(0) = 0.1N_E$ [282], $N_c = 10^{13}$ cm^{-3}, $\alpha = 1/3$.

On Fig. 6.2 is shown the dependence of the critical radius of precipitates of oxygen (1) and carbon (2), respectively.

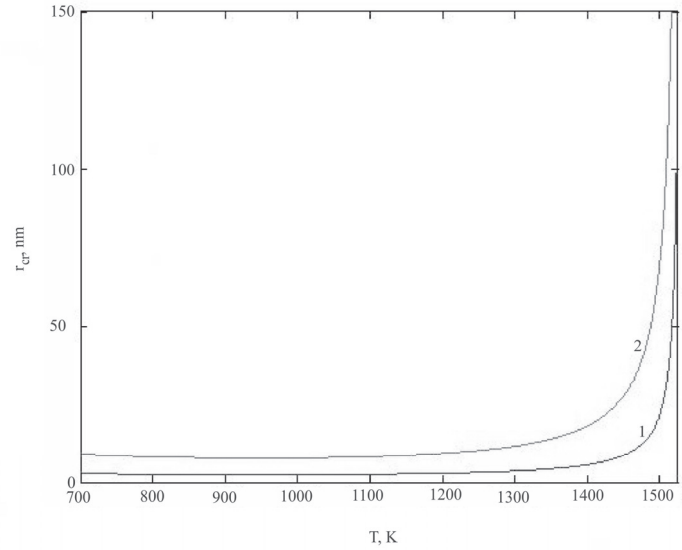

Fig. 6.2. Dependence of the critical radius of precipitates of oxygen (1) and carbon (2) on the heat treatment temperature

During the thermal treatment at T = 730 K, the size of the critical nucleus of the oxygen precipitate (SiO_2) is 2.7 nm, and the size of the critical nucleus of the carbon precipitate (SiC) is about 8.7 nm. The minimum values of the critical radii of precipitates are reached in the initial state at T = 730 K and increase with increasing temperature. With increase in the annealing temperature of the crystals, the sizes of the critical nuclei of precipitates also increase. In addition, with increase in the oxygen concentration at a constant annealing temperature, the size of the critical nucleus decreases.

The increase in the critical radius of precipitates during the heating of the crystal leads to a sharp decrease in their growth rate and, accordingly, to a sharp decrease in the kinetics of their precipitation. The kinetics of precipitation when the crystal is heated is analogous to the precipitation kinetics during the cooling of the crystal. However, increase in the critical radius of precipitates during the crystal cooling occurs with a decrease in temperature from 1682 K to 300 K [241]. This difference is due to the influence of the growth parameters V_g and G_a, which determine the processes of defect formation during crystal growth and are taken into account in the dependence $T(t) = \dfrac{T_m^2}{T_m + V_g G_a t}$, where T_m is a melting temperature.

The condition of transition to the coalescence stage $R(t) \approx R_{cr}(t)$, which is satisfied for the first three groups of crystals (Fig. 6.3).

In this case, the higher the annealing temperature of the crystal, the faster the transition to the coalescence stage. Calculations of the fourth group of crystals show that during annealing at T > 1500 K, the coalescence stage does not occur at real annealing times.

The condition of transition to the coalescence stage $R(t) \approx R_{cr}(t)$ upon precipitation of carbon does not hold for all four groups of crystals. These results of calculations together with the large value of the size of the critical nucleus of carbon precipitate in comparison with the size of the critical nucleus of oxygen precipitation may indicate that at the thermal treatments are mainly oxygen precipitations. In this case, with the formation and growth of oxygen precipitates, vacancies are consumed, and carbon can go to the formation of "oxygen + carbon" complexes. In addition, with the growth of oxygen precipitates, interstitial silicon atoms are emitted into the solid solution of point defects. As a result, a supersaturation occurs in the crystal on interstitial silicon atoms and the formation of microvoids during heat treatment cannot occur. These calculated data are in good agreement with the experimental results

obtained with the help of TEM-studies of crystals with microvoids [122]. Short-term heat treatments of such crystals at T = 1373 K resulted in a sharp decrease in the size of microvoids or their disappearance [114, 121, 122]. At the same time, the growth of precipitates and supersaturation on interstitial silicon atoms contribute to the formation and growth of interstitial dislocation loops in a crystal.

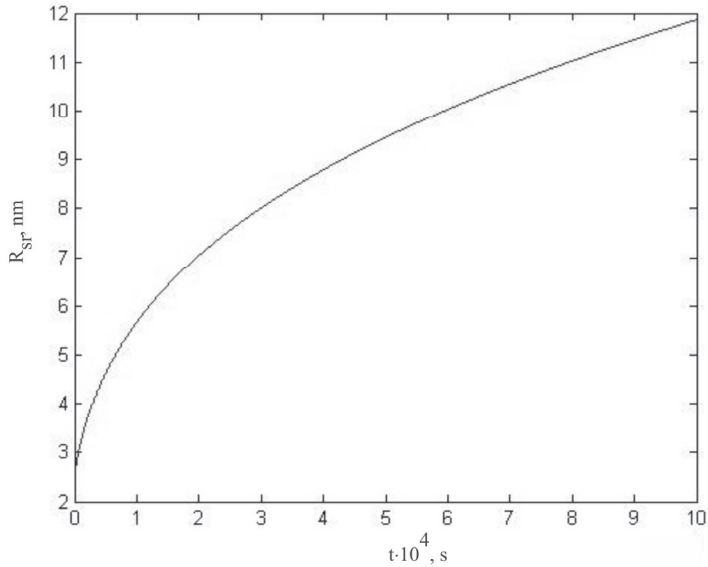

Fig. 6.3. Dependence of the change in the average radius of oxygen precipitate in the coalescence stage at a constant annealing temperature *T* = 1100 K

On Fig. 6.4 is shown the variation of the radius of an interstitial dislocation loop as a function of the time of the heat treatment process at *T* = 1100 K.

The growth of a dislocation loop during the thermal treatment of a silicon single crystal occurs both as a result of supersaturation on interstitial silicon atoms, and due to the dissolution of small loops with sizes less than the critical. The results of the computational experiment show that the maximum value of the radius of a dislocation loop, whose growth is determined by the diffusion mechanism, for crystals of four groups is reached at the heat treatment temperature T = 1510 K. Increasing the time of heat treatment causes an increase in the size of the loop and a

decrease in its concentration (Fig. 6.5). For example, at M = 10^{12} cm^{-3} concentration of dislocation loops is reached $6.31 \cdot 10^5$ cm^{-3}.

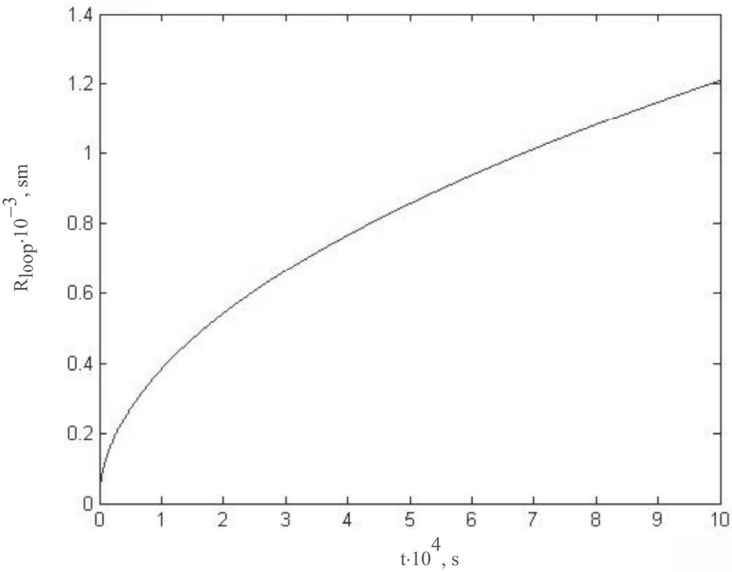

Fig. 6.4. Change in the radius of an interstitial dislocation loop as a function of the time of the heat treatment process at T = 1100 K

Calculations of the formation of a defect structure in a hypothetically ideal undoped dislocation-free silicon single crystal as a result of thermal treatments using the mathematical apparatus of the diffusion model for the formation of grown-in microdefects have shown that the precipitation process during the thermal treatment of the crystal is mainly due to the precipitation of oxygen. The growth of precipitates causes supersaturation of the crystal on interstitial silicon atoms. This process leads to the formation and growth of interstitial dislocation loops. This mechanism of defect formation during thermal treatments of crystals does not contradict numerous experimental and theoretical works. Hence, the diffusion model for the formation of grown-in microdefects makes it possible to describe the formation and development of a defect structure during thermal treatments of silicon single crystals.

Real silicon single crystals contain grown-in microdefects that take an active part in the processes of defect formation during thermal treatments. Grown-in microdefects mainly serve as sinks for IPDs and impurity atoms.

As a result, defect growth occurs and the transformation of the original defect structure. Since the distribution of grown-in microdefects in the bulk of a crystal is nonuniform, it is simultaneously possible the formation and growth of defects as a result of the mechanism discussed above. Both the transformation of the initial defect structure and the formation of new defects lead to supersaturation of the crystal by silicon interstitial atoms. Therefore, the formation of new microvoids does not occur, and the microvoids that formed during the growth of the crystal shrink in size or dissolve [122]. It can also be assumed that the formation of thermal donors and thermal acceptors after thermal treatments of dislocation-free silicon single crystals is due to the initial stages of oxygen precipitation.

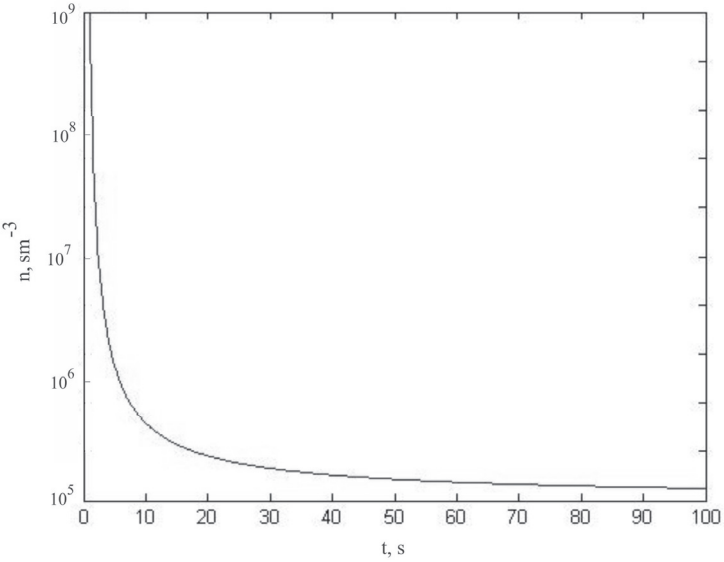

Fig. 6.5. The change in the concentration of dislocation loops from the annealing time

The application of the diffusion model for the formation of grown-in microdefects to the formation of a grown-in and post-growth defect structure allows one to describe from a single point the formation of a defect structure in single-crystal silicon, from crystal growth to the creation of a device. The construction of a general (complete) model of defect formation provides prediction of the features of formation of microdefects at various stages of the technological process.

At the same time, the application of the probabilistic approach (Vlasov's model for solids) to complexation processes during thermal treatments of silicon crystals leads to a slightly different result (Fig. 6.6).

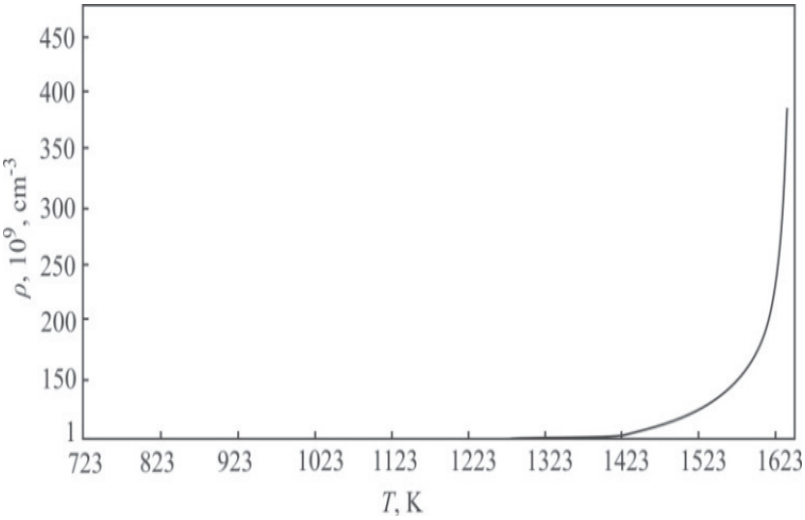

Fig. 6.6. Temperature dependence of the distribution density of "silicon-oxygen" complexes upon annealing of a crystal

It is widely known that after thermal treatments of different durations in the temperature range 573...1473 K in silicon crystals, significant changes in the electrophysical and structural properties take place. As shown by numerous studies, the main reason for changing the properties of silicon during thermal treatments is the transformation of the initial defect structure [37, 52]. The change in the electrophysical properties is due to the formation of donor (thermal donor-I and thermal donor-II) and acceptor (thermal acceptor) centers. Thermal donors-I are formed during heat treatments in the temperature range 623...823K and disappear after a short annealing at temperatures above 823K. Heat treatment at a higher temperature (873...1073K) also leads to the appearance of donor activity (thermal donor-II or "new thermal donors"), which break down at temperatures of ≈ 1173 K and higher [37, 357]. In a some of cases, thermal treatments lead to the formation of thermal acceptors, which accompany thermal donors-II [37].

Over the past 60 years, a number of models for the formation of these centers have been proposed on the basis of experimental data obtained in

the study of the kinetics of their formation, as well as electrical, optical, and paramagnetic properties. The theoretical basis for these models was based on the classical approach using the classical theory of nucleation and growth of particles of the second phase in solids. The analysis of these models and experimental data on the study of electric centers in silicon was carried out, for example, in Refs. [37, 357]. Summarizing the obtained results, it can be said that thermal donors-I are oxygen and silicon complexes and are the initial stage of formation of precipitates. At the same time, thermal donors-II are precipitates of oxygen at the stages of their growth and coalescence [37]. Some authors have come to the conclusion that thermal donor-I and thermal donor-II are of the same nature [358].

However, according to Vlasov's model for solids, the complexation process at a temperature $T = 730K$, which corresponds to the average temperature of formation of the thermal donors, is unlikely (Fig. 6.6). Complexation in silicon at thermal treatments is possible only at high temperatures [359].

At first glance, there is an insurmountable contradiction between the results of the two approaches. However, as indicated above, the development of precipitate passes through three stages: the complexation stage (nucleation), the growth stage, and the coalescence stage. During crystal growth, nucleation occurs near the crystallization front. The basis of nucleation is the processes of complexation between intrinsic and impurity point defects. When a certain critical size is reached, the defects begin to grow. At some specific cooling temperatures of the crystal ($\sim T_m - 20K$ for small-scale crystals and $\sim T_m - 300K$ for large-scale crystals) the stage of coalescence of precipitates begins [268]. During the coalescence stage, part of the precipitates continues to grow. At the same time, some of the smaller precipitates go through the reverse process: they dissolve [268]. Depending on the growth thermal conditions, a defective crystal structure is formed which includes precipitates, dislocation loops or microvoids [52]. At least in undoped small-scale (diameter 30 mm) FZ-Si single crystals grown at a V_g=5…6.0 mm/min, precipitates of oxygen and carbon are formed [52]. After the crystal growth is complete, the development of precipitates in the defective silicon structure continues and, at a temperature of $T = 300K$ is fixed in the coalescence stage [268].

Vlasov's model for solids indicates the absence of complexation during thermal treatments of crystals. Hence, the stage of nucleation at heat treatments of the crystal is absent. However, thermal treatments activate

the very weak processes of coalescence of precipitates at $T = 300K$. As the annealing temperature increases, the rates of growth and dissolution of precipitates increase. Vlasov's model says that it is necessary to consider not processes of formation and growth of complexes, but processes of dissolution of precipitates already created during growth. Analysis of experimental and theoretical studies shows that in this case, the complexes "Si-O", "Si-C" and "C-O" can act as electrical centers in undoped silicon single crystals. In the case of doped crystals, the formation of electrical centers can occur on the basis of precipitates of other nature (for example, nitrogen). Thermal treatments of silicon crystals take place at the stage of coalescence of precipitates. At this stage, some of the precipitates continue to grow, while the other part of the precipitates of smaller size dissolves. Dissolved precipitates are responsible for the formation and annealing of electrical centers in silicon. A characteristic feature of such analysis is not the negation, but the consideration of various model concepts about the nature of electric centers, starting with the Kaiser model [360].

Hence, Vlasov's model for solids makes it possible to tie together the processes of creating a defective structure during crystal growth and its subsequent transformation due to thermal treatments. In this case, it is possible to select the optimal model for the nature of electrical centers in silicon, which are formed as a result of thermal treatments.

Vlasov's model for solids allows us to take a fresh look at already known facts and discover new phenomena and patterns in the study of real solids. This thesis is confirmed when considering the origin of donor and acceptor centers in silicon during thermal treatments. The proposed qualitative model for the formation of electrical centers directly relates their origin to the initial defect structure of silicon. The formation of electrical centers is due to the processes of dissolution of impurity precipitates during the thermal treatment that were created during crystal growth. Hence, high-temperature impurity precipitation is directly related to the subsequent transformation of grown-in microdefects in the production process of silicon devices and is the foundation for the creation and development of a defective structure of semiconductor silicon.

6.4. The technique of virtual research of defect structure

The mathematical apparatus of the diffusion model with the help of modern information technologies can be used as a basis for a software complex for analyzing and calculating the formation of grown-in and post-growth microdefects in dislocation-free silicon single crystals [361]. With

the help of the software complex, it is possible to determine the necessary conditions for crystal growth and the modes of its processing to obtain a precisely defined defect structure [362, 363]. By improving and developing such software products, it is possible to calculate the defective crystal structure, both in general and at each of its points. To create such software products, a research (calculation) technique is needed that would link each point of the crystal to its real structure. The technique of virtual research of a defective structure should be verified by experimental studies.

In [364] a technique was proposed for determining and calculating the defect structure as a function of the growth conditions of the crystal (growing method, crystal growth rate, axial and radial temperature gradients, crystal cooling rate).

As shown above, the formation and transformation of grown-in microdefects is controlled by the thermal conditions for growing dislocation-free silicon single crystals. Therefore, the basis of the technique for determining and calculating the grown-in defect structure is the parameter that connects the main thermal conditions of crystal growth $V_g / G_a = C_{crit}$.

To condition $V_g / G_a = C_{crit}$ in real crystals corresponds to the V-shaped distribution of D-microdefects in a plane parallel to the growth axis, or the annular distribution of D-microdefects in a plane perpendicular to the growth direction [13, 52]. As already mentioned above, in the scientific literature the condition $V_g / G_a = C_{crit}$ is correlated with the so-called OSF-ring ("oxidation-induced stacking faults"), which is observed in crystals after thermal treatments [81, 83, 84, 86]. The use of such a name is not entirely true, since the stacking faults are not grown-in's but post-growth defects. The formation of stacking faults is the result of the transformation of grown-in microdefects (precipitates) in the course of thermal effects. It has been experimentally established that D-microdefects are precipitates of oxygen and carbon and their concentration in the ring region is almost an order of magnitude higher than outside the ring [52].

On Fig. 6.7 a standard picture of the distribution of grown-in microdefects in dislocation-free silicon single crystals grown by the Czochralski method with a variable growth rate is shown. It is similar to the scheme of distribution of grown-in microdefects as a function of the growth rate shown on Fig. 1.13b. Crystal diameter 50 mm, the growth rate varied from V_{gmin} = 0.5 mm/min to V_{gmax} = 3.0 mm/min [364].

There are three areas of defect formation: region (1) (above the V-shaped precipitate distribution), region (2) (V-shaped precipitate distribution region) and region (3) (below the V-shaped precipitate distribution). In small-scale silicon crystals in the region (1) the grown-in microdefects (precipitates) of interstitial and vacancy types are formed at comparable concentrations; in the region (2), the same defects are formed as in region (1), and outside the V-shaped distribution's the interstitial dislocation loops and predominantly interstitial precipitates are formed [13, 52]. In crystals with a diameter of more than 70 mm in the regions (1), (2) (inside the V-shaped distribution), microvoids are formed [13]. In the region (3) dislocation loops and precipitates of predominantly interstitial type are formed [52].

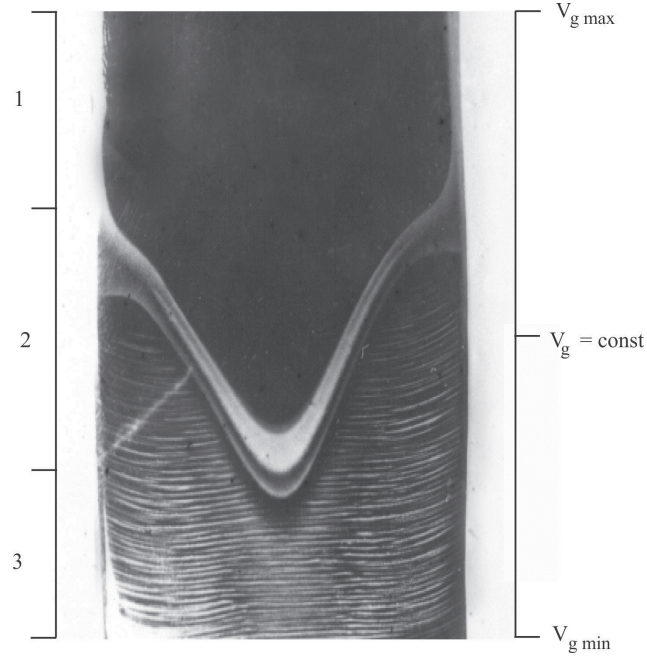

Fig. 6.7. The standard picture of the distribution of grown-in microdefects in dislocation-free silicon single crystals grown by the Czochralski method with a variable growth rate

As the diameter of the crystal increases, the thermal growth conditions of the crystal change and the picture of the defect formation in the

longitudinal section of the crystal undergoes changes that are the rather rapid disappearance of the regions (1) and (3) [53]. For example, in modern large-scale silicon single crystals (diameter 150...300 mm) grown by the Czochralski method, the general picture of defect formation corresponds only to the region (2) on Fig. 6.7 [53].

At $V_g/G_a > C_{crit}$ in small-scale crystals in the region (1) the concentration of vacancies is comparable with the concentration of interstitial silicon atoms (high crystal growth rates). At $V_g/G_a < C_{crit}$ in small-scale crystals in region (3) the concentration of vacancies is small compared with the concentration of interstitial silicon atoms (low crystal's growth rates). For large-scale crystals at $V_g/G_a > C_{crit}$ supersaturation on vacancies is created due to the presence of V-shaped distribution of precipitates, which leads to a exhaustion of impurity atoms inside the V-shaped distribution of precipitates and the creation of conditions for the homogeneous formation of microvoids. Hence, growth parameter V_g/G_a controls a system of interacting point defects during crystal cooling after growing.

The first step of the technique is to specify a certain crystal diameter. Since $V_g/G_a = C_{crit}$ it is determined theoretically and experimentally in a certain range (0.06 mm^2/K·min ≤ C_{crit} ≤ 0.3 mm^2/K·min) [6, 42, 168], then for calculation we select a certain value C_{crit}.

In the second step of the procedure, the values of the axial temperature gradient at the center of the crystal (G_a), as well as the values of the minimum (V_{gmin}) and the maximum (V_{gmax}) crystal growth rate are selected. For each crystal diameter, these values can be determined from analysis of the experimental and theoretical data [362].

The third step is the choice of the axial temperature gradient at the edge of the crystal (G_e) in the range of values G_e/G_a = 1.0…2.5. Parabolic radial distribution of the axial temperature gradient $G(r) = G_a + (G_e - G_a) \cdot \left(r/R_s\right)^2$, where R_s is a crystal radius; r is a current coordinate in the range from 0 to R_s [364].

The last step is that, from the dependence $V_g(r)/G_a(r) = C_{crit}$, a graphical dependence of the critical growth rate on the crystal radius is constructed. Then, on the calculated dependence of the critical growth rate is superimposed the real growth rate of the crystal, which makes it possible to determine the form of the defective structure of the real crystal. It is clear that for a crystal of a given diameter, depending on the position of the straight line $V_g = const$ relatively to the curve $V_g(r)$ three regions of the defect structure can be (Fig. 6.7) [364].

On Fig. 6.7 some value $V_g = const$ is given as example. In this case, we are in the region (2). Based on the analysis of the defect structure of this region inside the V-shaped precipitate distribution, the formation of precipitates is calculated, and outside the V-shaped precipitate distribution, the formation of precipitates and dislocation loops is calculated. Calculation of the formation of precipitates is carried out within the framework of the classical theory of nucleation, growth and coalescence of precipitates using analytical and approximate calculations [241, 267, 268]. Calculation of the loops formation is carried out within the framework of the deformation model for the formation of dislocation loops and makes it possible to determine such parameters as the critical radius, the dependence of the loop diameter on the growth rate of the crystal, and the loops concentration [107].

We note two main advantages of the method of analysis and calculation of the grown-in defect structure of dislocation-free silicon single crystals. The first advantage lies in the fact that the technique is fairly simple and can easily be implemented as a software product that can become a convenient virtual experimental device in the study of various properties of dislocation-free silicon single crystals. The second advantage lies in the fact that the analysis and calculation of the defect formation process is determined only by the thermal growth conditions. In this case, of the three controlling growth parameters, the two parameters are strictly defined (the diameter of the crystal and its growth rate), and the axial temperature gradient is specified in a certain range of values. This uncertainty in the value of the axial temperature gradient introduces deviations in the analysis and calculation of the formation of grown-in microdefects, which can be reduced if we experimentally determine the values of G_a and G_e during crystal growth.

The reliability of the procedure can be verified experimentally by selective etching of the longitudinal or transverse planes of the crystal. In the case of deviations from the experimental pattern, it is possible to select

the parameters G_a, G_e, C_{crit} to achieve the complete correspondence of the calculated and experimental data. Such experimental check will avoid the difficulties of the experimental determination of G_a and G_e, especially for large-scale crystals.

The technique allows analyzing and calculating the formation of grown-in microdefects based on the temperature conditions for growing dislocation-free silicon single crystals (crystal growth rates, axial and radial temperature gradients). This fact provides opportunities for programming crystal growth processes with a predefined and regulated structure, as well as for developing the necessary equipment of furnaces in order to obtain growth parameters that will provide the given defective structure.

In addition, this technique should find wide application in the scientific and research practice not only of technologists, but also of physicists, materials scientists, designers. For example, for physicists such a technique will allow to associate fluctuations in the determination of a particular parameter (properties) on different crystals with the dependence of this parameter (property) on a certain initial defect structure.

The method of analysis and calculation of the formation of grown-in microdefects in dislocation-free silicon single crystals is easy to implement on a personal computer in technological and research practice. Theoretical study of the real structure of crystals depending on their thermal growth conditions with the help of the original virtual technique of analysis and calculation of the formation of grown-in microdefects is a new technique of experiment. Furthermore, this technique allows you to replace the experimental studies of the structure with adequate theoretical studies, so the software product developed on the basis of the proposed method will be a new virtual experimental device.

6.5. Use of information technologies for analysis and management of defect structure of initial single crystals and devices based on them

Mathematical models of the formation of grown-in microdefects gave the equivalent of the object (the process of defect formation during crystal growth), which in mathematical form reflects its most important properties: the positions to which it obeys, and the connections inherent in its constituent parts [364]. Mathematical models are presented in a form that is convenient for the application of numerical methods, and the computational algorithm not only determines the sequence of computational

and logical operations for finding the required quantities with a given accuracy, but, as the results of calculations have shown, does not distort the basic properties of the model and, therefore, the initial object. The electronic equivalent of object for direct testing on a computer was programs that translated mathematical models and algorithms into computer-accessible language (C++). The software complex for the analysis and calculation of grown-in microdefects consists of two consecutive parts: a block for determining the type of the defective structure and the calculation and graphic block (Fig. 6.8) [362, 364].

At the stage of determining the type of defective structure, the software works as follows. First, a method is chosen for growing dislocation-free silicon single crystals (the Czochralski method or float zone melting), and then a defines of crystal diameter. Since $V_g(r)/G_a(r) = C_{crit}$ it is determined theoretically and experimentally in a certain range (0.06 mm^2/K·min $\leq C_{crit} \leq$ 0.3 mm^2/K·min), then for calculation we select a certain value C_{crit}.

Fig. 6.8. The initial form of the software

For a given diameter, in some ranges of values, the value of the axial temperature gradient at the center of the crystal (G_a), is chosen, as well as the values of the minimum and maximum growth rates of the crystal. For each crystal diameter, these values are determined from analysis of the experimental and theoretical data.

Further, an axial temperature gradient is selected at the crystal edge (G_e) in the range of values G_e/G_a = 1.0…2.5. From the dependence $\frac{V_{gcrit}(r)}{G(r)} = C_{crit}$, a graphical dependence of the critical growth rate on the crystal radius is constructed.

As was mentioned above, depending on the position of the straight line $V_g = const$ relatively to the curve $V_{gcrit}(r)$ there are three possible areas of defective structure, the calculation of which is carried out by the calculation and graphic block of the software complex (Fig. 6.9).

The first calculation region is characterized by high crystal growth rates, when only microvoids and precipitates are formed above the V-shaped distribution. The second calculation area is characterized by average crystal growth rates, when a ring of precipitates is formed in a plane perpendicular to the direction of growth. In this case, precipitates and microvoids are formed inside the ring, and outside the ring precipitates and interstitial dislocation loops are formed. The third area of calculation is characterized by low crystal growth rates, when precipitates and interstitial dislocation loops form below the V-shaped distribution (Fig. 6.9).

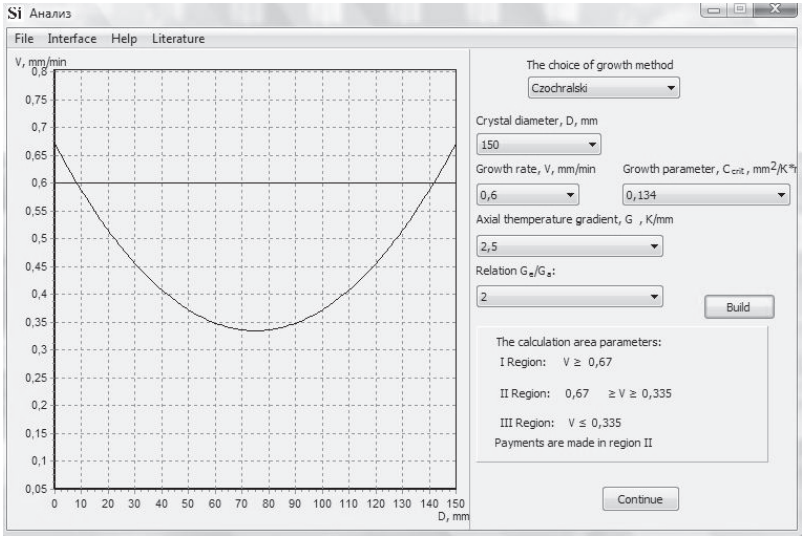

Fig. 6.9. Form of defect structure analysis

Calculation of precipitates is carried out within the framework of the classical theory of nucleation, growth and coalescence of precipitates using analytical and approximate calculations. Parameters characterizing the processes of precipitation of oxygen and carbon are determined, among them, for example, the critical radii of precipitates, the size distribution of precipitates, the change in the average size of the precipitates during crystal cooling, etc.

The algorithm for calculating the defect structure is based on the high-temperature precipitation process, which determines the entire course of formation of the defective crystal structure (Fig. 6.10).

A comparison of virtual calculations with experiment is carried out using a database of experimental studies. The database of experimental studies should contain all known experimental data on the crystal. For example, it can be data: (1) the crystal structure, the growth method, and the thermal parameters of crystal growth, (2) the types of defects, their sizes and concentrations, and the formation temperatures of defects, (3) the physical model of defect formation, etc. The data (the list) are fed to the input of the algorithm for the calculation of the defect structure using the high-temperature precipitation model.

Calculation of precipitates is carried out within the framework of probabilistic and classical theories of nucleation, growth and coalescence of precipitates using analytical and approximate calculations. Parameters characterizing the processes of precipitation of oxygen and carbon are determined, among them, for example, the critical radii of precipitates, the size distribution of precipitates, the change in the average size of the precipitates during crystal cooling, etc. (Fig. 6.11). Mathematical models and calculation of parameters are given in the papers [255, 351, 364].

Further, the secondary defect structure of the crystals is calculated and analyzed (dislocation loops, microvoids). The results of calculations are compared with the database of experimental studies. With good agreement with the database of experimental studies, the results of calculations can serve as characteristics of the initial defect structure of the crystal. If the reconciliations cannot be obtained, the calculations are repeated again until the results are obtained with the specified deviation. At the same time, it is possible to refine mathematical models and (or) experimental results.

In the calculation of microvoids, the presence of conditions for their formation is first checked, since microvoids are not formed at a cooling rate of the crystal $V_{cool} \geq 40$ K/min [173] and in crystals with a diameter of less than 70 mm [290]. Calculation of microvoids and interstitial dislocation loops makes it possible to determine for each of these types of defects such parameters as critical radius, and concentrations.

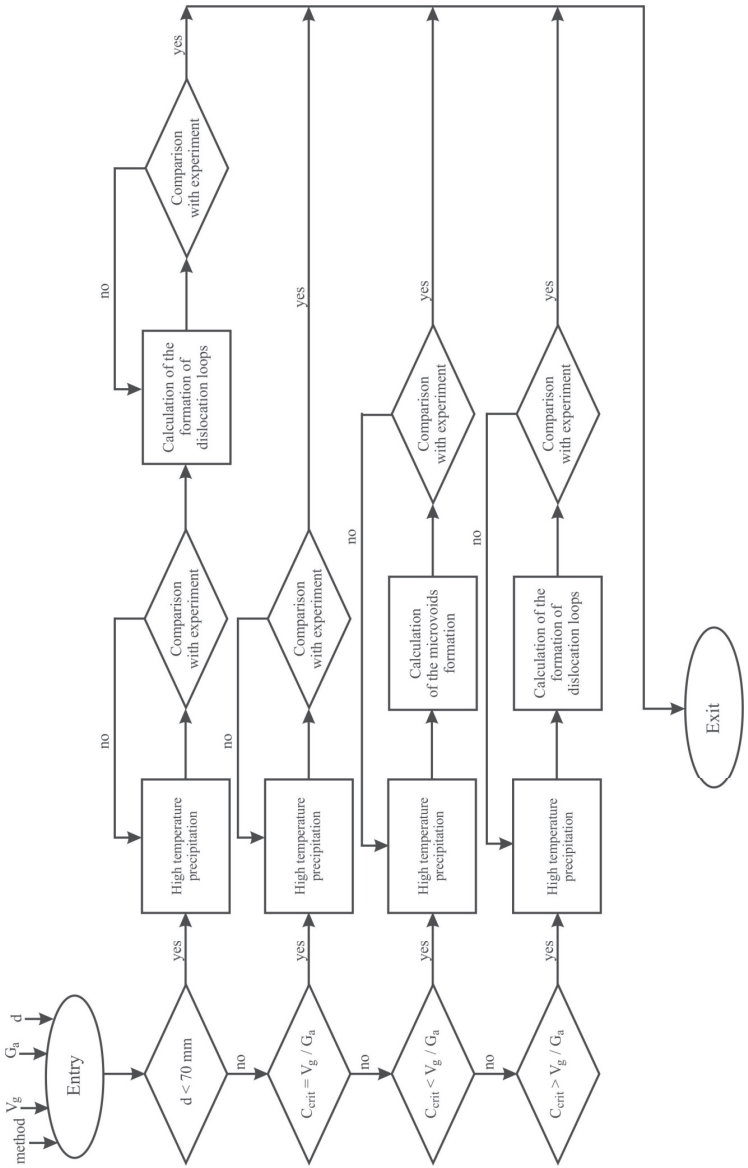

Fig. 6.10. Algorithm for calculating the defect structure of semiconductor silicon

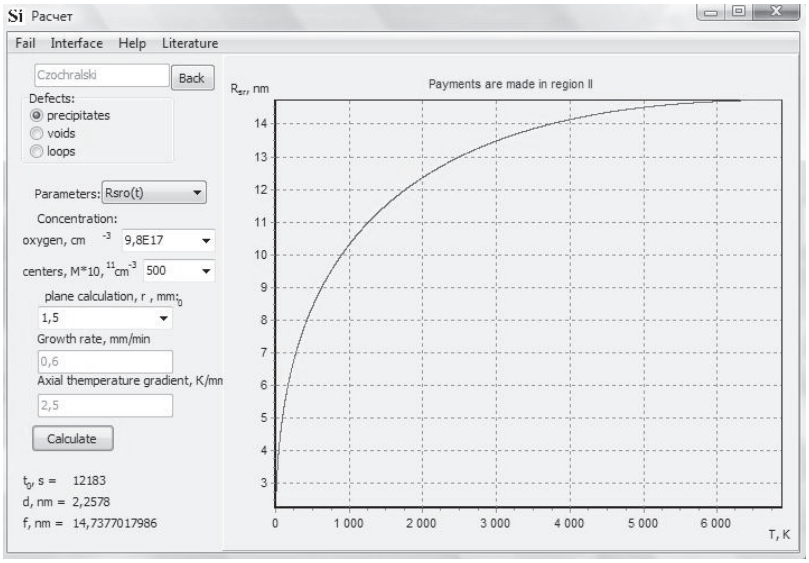

Fig. 6.11. Form of defect structure calculation

The advantage of calculating the formation and growth of precipitates, microvoids and interstitial dislocation loops is that the input and control parameters of the computational and graphic part are the growth parameters: the rate of crystal growth and the axial temperature gradient, which is chosen in a certain range of values depending on the diameter of the crystal being grown. Of the three growth parameters, the two parameters are strictly defined (the diameter of the crystal and its growth rate), and the axial temperature gradient is specified in a certain range of values. This uncertainty in the value of the axial temperature gradient introduces a deviations in the analysis and calculation of the formation of grown-in microdefects, which can be reduced by experimentally determining the values of G_a and G_e during crystal growth. In addition, the errors of the approximate computational methods used contribute to the overall deviation of the virtual experimental device.

The development of a software for the analysis and calculation of the formation of grown-in microdefects in dislocation-free silicon single crystals became possible after the creation of a precipitation model during the cooling of the crystal after growth, which, together with the kinetic models of the formation and growth of interstitial dislocation loops and

vacancy microvoids, allows us to theoretically describe the processes of formation and transformation of grown-in microdefects in dislocation-free silicon single crystals of any diameter [255].

The created software allows to save significant funds and time that was previously spent on conducting experimental studies of the defective structure with the help of optical microscopy, TEM, and X-ray methods for observing defects. The experimental difficulties in the detection and determination of the individual characteristics of ultra-small grown-in microdefects have led to the fact that the microdefects that have been studied to date have been the post-growth microdefects that are formed after various technological influences (thermal treatments, irradiation). Since the post-growth microdefects are mainly the result of transformation of the initial grown-in defect structure, it becomes possible to create software for analysis and calculation of post-growth microdefects, the basis of which will necessarily be the already developed software.

Since the adequacy of the developed triad "mathematical model + algorithm + program" of the initial physical model is certified by carrying out computational experiments and their comparison with the results of experiments [13, 52], replacing the experimental studies with adequate theoretical studies using the software, allows to say that the software is a new virtual experimental device. Since the method of application of the software is original, it is a new technique of experiment.

The solution of practical problems of controlling the defect structure of dislocation-free silicon single crystals requires optimization of technological growth regimes as a result of hydrodynamics studies of melt and complex conjugate heat and mass transfer in growth plants. The problem of the correlation of the crystal growth conditions and its bulk crystallographic characteristics is extremely relevant and requires prediction of (1) melt hydrodynamics in the boundary layer at the crystallization front, (2) gas dynamics in the region above the melt surface and in the volume of the growth chamber, (3) the temperature field in the crystal at all growth stages. Solutions to this complex problem, based on the theory of similarity, develop on models of different levels and purposes: physical modeling, numerical modeling, and integrated approach. In recent years, global numerical models [365, 366] have been developed that claim to calculate the complex conjugate heat and mass transfer in the entire growth chamber or in a thermal node. Their particular case is the three-dimensional hydrodynamic models for the crucible-melt-crystal system [367, 368]. At the present time, it is possible to combine simulation with the control of the structural perfection of the grown single crystal [369-371]. In this case, the problem involves a conjugate solution of three

interrelated modeling tasks: (1) processes of heat transfer in modern thermal units and heat treatment of single-crystal silicon; (2) stress state of single crystals and silicon wafers; (3) defect formation processes in single crystals and silicon wafers. An example of one such problem is the growth of crystals from a melt by the Czochralski method, in which an accurate calculation of the thermal field is necessary for the adequate calculation of the thermally stressed state and the formation of microdefects in the crystal, taking into account hydrodynamics in the melt, the process of crystallization and heat exchange by radiation in a growing plant [372].

In [371] the program complex CrystmoNet is presented, allowing to solve such and similar conjugate problems of thermomechanics in the mode of remote access. It uses the Crystmo and Defects modules to calculate heat transfer and defect formation, as well as commercial modules: Fluent for fluid mechanics (Ansys® Fluent® [373]), Marc and Mentat (MSC.Marc® Mentat® [374]) for solid-state mechanics and Tecplot (Tecplot®-360 [375]) for graphical presentation of results. With all the merits of the software CrystmoNet, it has a very significant drawback. The module for calculating the defect structure is based on the recombination-diffusion model for the formation of grown-in microdefects. And this means that the researcher will receive information only about the homogeneous formation of microvoids and interstitial dislocation loops, and no other information.

At the same time, the software proposed in [351, 362] also has a number of significant drawbacks. Such drawbacks are following: (1) one-dimensional modeling (application only for the calculation of grown-in microdefects), (2) absence of modular building of applications, (3) no class for calculation. To eliminate the shortcomings and take into account the influence of technological treatments on the defective structure of silicon, when creating a new model of the information system, C# was used on the .NET platform [362]. A class of calculations for automated information system for the study of as-grown single crystals of silicon was created. C# is fully object-oriented, provides cross-platform, provides tools and capabilities for scaling and developing projects based on this class, as well as the availability of user-friendly development environments for different operating systems.

The possibilities of applying a diffusion model for the description of defect formation during crystal growth and during technological processing were taken into account in the development of a specialized information system for analyzing and managing the defect structure of dislocation-free silicon single crystals (Fig. 6.12).

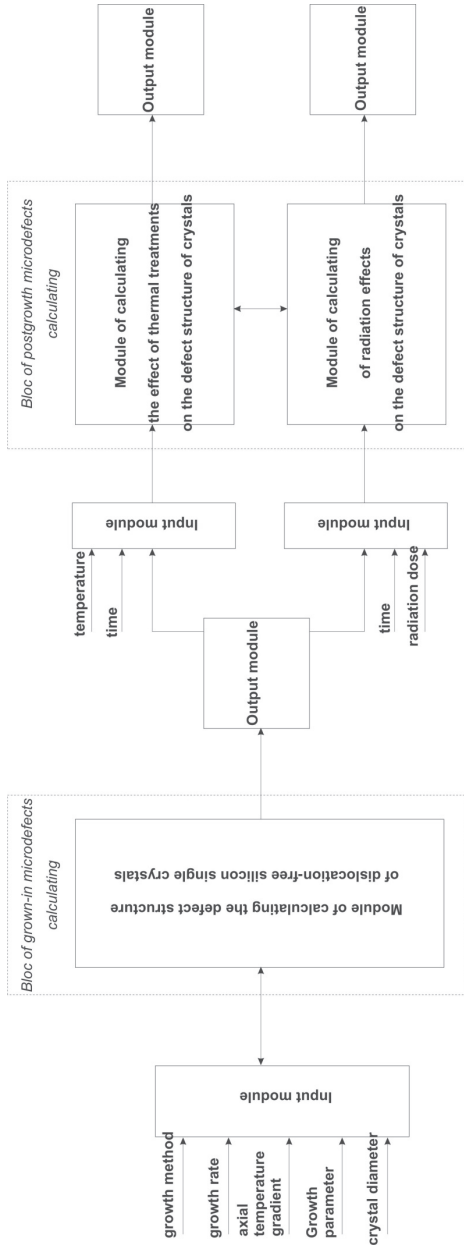

Fig. 6.12. Information-logic diagram of the information system

The input of the system receives the growth parameters of dislocation-free silicon single crystals (growth method, growth rate V_g, axial temperature gradient G_a, Voronkov's growth parameter $V_g / G_a = C_{crit}$, crystal diameter). The output module of the growth microdefect calculation bloc provides information on the type of defect, its size and concentration.

During the manufacture of semiconductor devices, the transformation of a defective structure occurs due to thermal treatments and the action of radiation. The bloc for calculating the post-growth microdefects contains modules for calculating the effect of thermal treatments and irradiations on the defective structure of devices. The modules are interrelated, since the thermal treatment is used for annealing radiation damage. The inputs of these modules receive information about the initial defective structure of the crystals together with the parameters of technological influences (temperature, time, radiation dose). From the output modules of the bloc for calculating the post-growth microdefects, information on the type of defects, their dimensions and concentration are obtains [362].

The bloc for the calculation of grown-in microdefects occupies a central place in the information system. This is due to the fact that the initial defect structure of the crystal determines the defective structure of the devices. It is possible to investigate with the help of this bloc the defective structure of a grown crystal with given temperature growth conditions. Conversely, it is possible to specify the defective structure of the crystal and determine the temperature conditions for growing it. Hence, the information system is not only a virtual experimental device, but also a method for the engineering of crystal defects. A similar approach can be applied to the bloc for calculating the post-growth microdefects.

The diffusion model shows that impurity precipitation plays the main role in the defect formation process. Therefore, the algorithm for its application is based on the high-temperature precipitation process, which determines the entire subsequent course of formation of the defective crystal structure.

Conclusions to chapter 6. Theoretical study of the real structure of crystals depending on their thermal growth conditions with the help of the original virtual technique of analysis and calculation of the formation of grown-in microdefects is a new technique of experiment. This technique allows you to replace the experimental studies of the structure with adequate theoretical studies, so the software developed on the basis of the proposed method will be a new virtual experimental device.

The software complex is the first experience of using a virtual experimental device to study the real structure of dislocation-free silicon single crystals. At present, it can be used to analyze and calculate the defect structure of undoped silicon monocrystals. In this case, the software complex acts as a basis, whose improvement and refinement (for example, taking into account the interaction of point defects, dopant atoms, transition metals, nitrogen, etc.), one can expand and optimize the modeling process. Hence, the software complex for the analysis and calculation of the formation of grown-in microdefects is a universal, flexible and inexpensive tool that allows one to describe and construct real defect formation processes in dislocation-free silicon single crystals. It provides practical levers for controlling the defect structure of perfect dislocation-free silicon single crystals directly during crystal growth.

The possibility of applying a diffusion model to both crystals during their growth and to crystals after thermal effects indicates the universality of this model. The diffusion model represents a unified approach to studying the physics of defect formation processes in technologies for growing silicon crystals and technological processing of structures based on it. Hence, it is possible to analyze from a general viewpoint the formation and transformation of the defective structure of silicon crystals from growth to the creation of various devices. Such analysis is impossible without the creation, both separate software complexes, and a single information system for analyzing the development of a defective structure. These software products can be used:

- To simulating the engineering of defects in silicon crystals during their growth.
- To simulating the engineering of defects in silicon crystals during the manufacture of devices.
- For use as a tool for studying defect formation processes in silicon.

SUMMARY

We know truth, not only by the reason, but also by the heart, and it is from this last that we know first principles
—Blaise Pascal (19.VI.1623 – 19.VIII.1662)
Pensées sur la religion et sur quelques autres sujets, 1670

The structural defects have a significant effect on the characteristics, as well as the operational reliability of semiconductor devices. This is due to the fact that the basic electro-physical properties of semiconductor silicon depend not only on the content of foreign impurities, but also on the perfection of the crystalline structure. In this connection, most of the parameters of dislocation-free silicon single crystals, which are structurally sensitive, depend on the initial defect structure. The success in creating high-quality single crystals and devices with controlled and predicted parameters is largely determined by the achievements in the management of the state of the ensemble of point defects

This book is a concentrated expression of ideas about the formation of a defective structure of silicon single crystals during their growth and subsequent technological treatments. At the same time, the book can be consider as a report on the research and scientific works of the Zaporozhye (Russian) scientific group of material scientists over the past 45 years. The results of the first twenty years of work can be formulated on the basis of fundamental ideas in the field of semiconductor physics, which are of paramount importance for semiconductor materials science and semiconductor technology as a whole:

1. The conceptual and physic-technical development of numerous problems associated with the physics of the formation of a defect structure of dislocation-free silicon single crystals, as well as original solutions of technically topical problems associated with obtaining perfect single crystals of semiconductor silicon.
2. Qualitative elaboration of the basic principles of the model for the formation of grown-in microdefects ((1) diffusion of IPDs to the nucleation centers in the form of atoms of background impurities of carbon and oxygen, (2) a continuous sequence of nucleation,

development, and transition of one type of grown-in microdefects to another).

3. Development of classical (experimental or letter's) classification of grown-in microdefects in small-scale dislocation-free silicon single crystals.
4. Logically consistent and physical development of a complex of experimental studies aimed at solving the problem of the formation of the initial defect structure (grown-in microdefects) in dislocation-free silicon single crystals.
5. Obtaining experimental data on the individual characteristics of grown-in microdefects (the sign of the crystal lattice deformation, shape, dimensions, and concentration) in small-scale silicon crystals grown by the float zone method ((I+V), D-, C-, B-microdefects).

Over the past 25 years, the following scientific results have been achieved:

1. Obtaining experimental data on the individual characteristics of grown-in microdefects (the sign of the crystal lattice deformation, shape, dimensions, and concentration) in small-scale silicon crystals grown by Czochralski method ((I+V), D-, C-, B-microdefects).
2. Statistically significant patterns of the distribution of grown-in microdefects are obtained depending on the growth rate of the crystal, which can be used as a basis for a database on defects in the structure of dislocation-free silicon single crystals.
3. A physical classification of grown-in microdefects in dislocation-free silicon monocrystals of any diameter is developed.
4. A high-temperature impurity precipitation model has been developed that extends the effect of the classical theory of the formation and growth of second-phase particles on the cooling of a crystal after its growth.
5. A deformation model of the formation and growth of interstitial dislocation loops and a vacancy-condensation model for the formation of microvoids during crystal growth have been developed.
6. The problem of describing the formation of a defective silicon structure by applying Vlasov's model for solid is solved. Based on the solution obtained, three main conclusions can be drawn: (1) Vlasov's theory is a far-reaching and natural extension of classical

mechanics. (2) Vlasov's equation can be used to describe any aggregate state of matter. (3) Vlasov's equation is a universal tool for describing the processes taking place in the physical world (both in the macrocosm and in the microcosm). These results and conclusions we believe are the most important among all our results.

7. The heterogeneous (two-stage) mechanism of formation and transformation of grown-in microdefects is substantiated and experimentally confirmed, which is based on such positions: (1) recombination of IPDs at high temperatures can be neglected; (2) background impurities of carbon and oxygen are involved in the process of defect formation as nucleation centers; (3) decomposition of a supersaturated solid solution of point defects upon cooling of silicon crystals from the crystallization temperature is carried out by two independent mechanisms: vacancy and interstitial; (4) the basis of the defect formation process is the primary agglomerates that are formed during the cooling of silicon crystals from the crystallization temperature due to the interaction of point defects "impurity + IPDs"; (5) in the process of crystal cooling at a temperature below 1423K, depending on the thermal growth conditions, secondary grown-in microdefects are formed due to the interaction "IPD + IPD"; (6) formation of secondary grown-in microdefects is due to the action of coagulation (microvoids) and deformation (interstitial dislocation loops) mechanisms; (7) vacancy and interstitial branches of the heterogeneous mechanism have a symmetry that is due to the parallelism of the course of defect formation processes in the decay of a supersaturated solid solution of point defects, the consequence of which is the formation of vacancy and interstitial grown-in microdefects of the same type and the growth of dislocation-free silicon single crystals in the vacancy-interstitial mode of crystal growth.
8. A diffusion model for the formation and transformation of grown-in microdefects has been developed, which is based on the physical classification of grown-in microdefects, the main positions of the heterogeneous (two-stage) mechanism of formation and transformation of grown-in microdefects and mathematical models for the formation of primary and secondary grown-in microdefects.
9. On the basis of modern information technologies, software complexes have been developed that solve problems of research

and management of the defective structure of a crystal, both during its growth and during the manufacture of various devices.

Experimental and theoretical studies of defect formation in semiconductor silicon play a crucial role in the production of breakthrough ideas for next generation technologies. We believe that the diffusion model of defect formation can be an ideal platform for a multifunctional solution of many key problems of modern solid-state physics, such as defect formation in solids, defect engineering in solids, control of the physical properties of solid structures, etc. Therefore, we hope that this book will serve as a necessary tool for young researchers with the help of which it will be possible to move on.

REFERENCES

1. Zulehner, W. "Czochralski grown of silicon." *J. Cryst. Growth* 65 (1983): 189-213.
2. Capper, P. "Bulk crystal growth - methods and materials." In *Springer Handbook of Electronic and Photonic Materials*, edited by P. Capper, and S. Kasap, 231-254. Leipzig: Springer US, 2006.
3. Abe, T., H. Harada, and J. Chikawa. "Swirl defects in float zone silicon." *Physica BC* 116 (1983): 139-147.
4. Dash, W.C. "The growth of silicon crystals free from dislocations." In *Growth and Perfection of Crystals*, edited by R.H. Doremus, B.W. Roberts, and D. Turnbull, 361-385. New York: John Wiley & Sons, 1958.
5. Neymark, K.N., B.A. Sakharov, V.F. Chulitsky, and M.I. Osovskiy. "Study of the thermal field in the growth of silicon single crystals by the method of crucibleless zone melting." In *Silicon and germanium*,
6. Voronkov, V.V. "Mechanism of swirl defects formation in silicon." *J. Cryst. Growth* 59 (1982): 625-642.
7. Verezub, N.A., M.G. Milvidsky, and A.I. Prostomolotov. "Parametric analysis of the formation of vacancy microdefects in silicon single crystals." *Proceedings of universities. Materials of electronic engineering* no. 2 (2004): 29-34.
8. Talanin, V.I., I.E. Talanin, and A.A. Voronin. "About formation of grown-in microdefects in dislocation-free silicon single crystals." *Can. J. Phys*. 85 (2007): 1459-1471.
9. Sally, I.V., and E.S. Falkevich. *Control the shape of crystal growth*. Kiev: Naukova Dumka, 1989.
10. Tilli, M., and A. Haapalinna. "Properties of silicon." In: *Handbook of silicon based MEMS materials and technologies*, edited by V. Lindroos, M. Tilli, A. Lehto, and T. Motooka, 3-17. Oxford: Elsevier Publ., Inc., 2010.
11. Bueren, van H.G. *Imperfections in crystals*. Amsterdam: North-Holland Publ. Company, 1960.
12. Talanin, V.I., I.E. Talanin, and D.I. Levinson. "Physical model of paths of microdefects nucleation in dislocation-free single crystals float-zone silicon." *Cryst. Res. & Technol*. 37 (2002): 983-1011.

13. Talanin, V.I., and I.E. Talanin. “Mechanism of formation and physical classification of the grown-in microdefects in semiconductor silicon.” *Defect & Diffusion Forum* 230-232 (2004): 177-198.
14. Abe, T., T. Samizo, and S. Marujama. “Etch pits observed in dislocation-free silicon crystals.” *Jpn. J. Appl. Phys*. 5 (1966): 458-463.
15. Kock, A.J.R. de. “The elimination of vacancy-clusters in dislocation-free silicon crystals.” *J. Electrochem. Soc*. 118 (1971): 1851-1856.
16. Kock, A.J.R. de, P.I. Roksnoer, and P.G.T. Boonen. “Effect of growth parameters on formation and elimination of vacancy-clusters in dislocation-free silicon crystals.” *J. Cryst. Growth*, 22 (1974): 311-320.
17. Hu, S.M. “Defects in silicon substrates.” *J. Vac. Sci. and Technol*. 14 (1977): 17-31.
18. Foll, H., V. Gosele, and B.O. Kolbesen. “The formation of swirl defects in silicon by agglomeration of self-interstitials.” *J. Cryst. Growth* 40 (1977): 90-108.
19. Kock, A.J.R. de, P.I. Roksnoer, and P.G.T. Boonen. “The introduction of dislocations during the growth of floating-zone silicon crystals as a result of point defects condensation.” *J. Cryst. Growth* 30 (1975): 279-294.
20. Neymark, K.N., E.G. Sheikhet, I.Yu. Litvinova, and E.S. Falkevich. “Influence of growing conditions on the distribution of microdefects in dislocation-free single crystals of silicon.” *Proceedings of the USSR Academy of Sciences. Inorganic materials* 15 (1979): 184-187.
21. Sitnikova, A.A., L.M. Sorokin, I.E. Talanin, K.L. Malyshev., E.G. Sheikhet, and E.S. Falkevich. “Investigation of the nature of microdefects in dislocation-free single crystals of silicon.” *Physics of the Solid State (Fizika Tverdogo Tela)* 28 (1986): 1829-1833.
22. Vitman, R.F., N.B. Guseva, A.A. Lebedev, A.A. Sitnikova, E.S. Falkevich, and N.F. Chervony. “Interrelation of the structure-sensitive properties with the genetic characteristics of silicon single crystals.” *Physics of the Solid State (Fizika Tverdogo Tela)* 36 (1994): 697-704.
23. Talanin, V.I., and I.E. Talanin. “Physical nature of grown-in microdefects in Czochralski-grown silicon and their transformation during various technological effects.” *Phys. Stat. Sol. (a)* 200 (2003): 297-306.
24. Jeske, W., and B. Jakowlew. “The swirl defects A-type as a source of dislocation generation on the macroscopic scale during growth of float zone silicon single crystals.” *Electron Technology* 12 (1979): 97-106.

25. Guseva, N.B., E.G. Sheikhet, V.V. Shpeizman, and I.L. Shulpina. "Dislocation activity of microdefects in silicon single crystals." *Physics of the Solid State (Fizika Tverdogo Tela)* 28 (1986): 3192-3194.
26. Bernewitz, L.J., B.O. Kolbesen, K.R. Mayer, and G.E. Shuh. "TEM observations of dislocation loops correlated with individual swirl defects in as-grown silicon." *Appl. Phys. Lett*. 25 (1974): 277-279.
27. Petroff, P.M., and A.J.R. de Kock. "Characterization of swirl defects in floating-zone silicon crystals," *J. Cryst. Growth* 30 (1975): 117-124.
28. Kock, A.J.R. de, P.I. Roksnoer, and P.G.T. Boonen. "Formation and elimination of growth striations in dislocation-free silicon crystals." *J. Cryst. Growth* 28 (1975): 125-137.
29. Kamm, J.B., and R. Muller. "Two dimensional plotting of semiconductor resistivity by scanning electron microscope." *Sol. State Electr*. 20 (1977): 105-108.
30. Abe, T., Y. Abe, and J. Chikawa. "The structure and origin of growth striations in dislocation-free silicon crystals." In: *Semiconductor Silicon*, edited by H.R. Huff and R.R. Burgess, 95-99, New Jersey: Electrochem. Soc., 1973.
31. Watkins, G.D., and K.L. Brower. "EPR observation of the isolated interstitial carbon atom in silicon." *Phys. Rev. Letts.* 36 (1976): 1329-1332.
32. Sheikhet, E.G., E.S. Falkevich, K.N. Neimark, I.F. Chervoniy, and V.A. Shershel. "Formation of microdefects in the growth of silicon monocrystals." *Physics of the Solid State (Fizika Tverdogo Tela)* 26 (1984): 207-213.
33. Run, van A.M.J.G. "A critical pulling rate for remelt crystal growth." *J. Cryst. Growth* 53 (1981): 441-443.
34. Tempelhoff, K., and N. van Sung. "Formation of self-disorder agglomerates in dislocation-free silicon." *Phys. Stat. Sol (a)* 70 (1982): 441-449.
35. Kolbesen, B.O., and A. Muhlbauer. "Carbon in silicon: properties and influence on devices." *Sol. State Electronics* 25 (1977): 1561-1582.
36. Drevinsky, P.J., C.E. Caefer, L.C. Kimerling, and J.L. Benton. "Carbon-related defects in silicon." In: *Defect Control in Semiconductors*, edited by K. Sumino, 341-345, Amsterdam: North Holland, 1990.
37. Babich, V.M., N.I. Bletskan, and E.F. Wenger. *Oxygen in single crystals of silicon*. Kiev: Interpress LTD, 1997.

38. Bourret, A., J. Thibault-Desseaux, and D.N. Seidman. “Early stages of oxygen segregation and precipitation in silicon.” *J. Appl. Phys*. 55 (1984): 825-835.
39. Ravi, K.V. *Imperfections and impurities in semiconductor silicon*. New York: Wiley, 1981.
40. Voronkov, V.V., and M.G. Milvidsky. “The role of oxygen in the formation of microdefects in the growth of dislocation-free single crystals of silicon.” *Kristallografiya (Crystallography Reports)* 33 (1988): 471-477.
41. Roksnoer, P.J., W.J. Bartels, and C.W.T. Bulle. “Effect of low cooling rates on swirls and striations in dislocation-free silicon crystals.” *J. Cryst. Growth* 35 (1976): 245-248.
42. Foll, H., and B.O. Kolbesen. “Formation and nature of swirl defects in silicon.” *Appl. Phys*. 8 (1975): 319-331.
43. Kock A.J.R. de. “Microdefects in dislocation-free silicon.” *Philips Res. Rept. Suppl.*, no. 1 (1973): 1-104.
44. Kock, A.J.R. de, P.I. Roksnoer, and P.G.T. Boonen. “Microdefects in swirl-free silicon crystals.” In: *Semiconductor Silicon* edited by H.R. Huff and R.R. Burgess, 83-88, New Jersey: Electrochem. Soc., 1973.
45. Talanin, V.I., I.E. Talanin, and D.I. Levinson. “Physics of the formation of microdefects in dislocation-free monocrystals of float-zone silicon.” *Semicond. Sci. & Technol*. 17 (2002): 104-113.
46. Veselovskaya, N.V., E.G. Sheikhet, K.N. Neimark, and E.S. Falkevich. “Defects of the type of clusters in silicon single crystals.” In: *Growth and alloying of semiconductor crystals and films* edited by F.A. Kysnetsov, 284-288, Novosibirsk: Nauka, Vol. 2, 1977.
47. Kock, A.J.R. de, W.T. Stacy, and W.M. van de Wijgert. “The effect of doping on microdefect formation in as-grown dislocation-free Czochralski silicon crystals.” *Appl. Phys. Lett.* 34 (1979): 611-616.
48. Kock, A.J.R. de, and W.M. van de Wijgert. “The effect of doping on microdefect formation in as-grown dislocation-free Czochralski silicon crystals.” *J. Cryst. Growth* 49 (1980): 718-734.
49. Sitnikova, A.A., L.M. Sorokin, and E.G. Sheikhet. “Investigation of D-type microdefects in silicon single crystals.” *Physics of the Solid State (Fizika Tverdogo Tela)* 29 (1987): 2623-2628.
50. Roksnoer, P.J., and M.M.B. van den Boom. “Microdefects in a non-striated distribution in floating-zone silicon crystals.” *J. Cryst. Growth* 53 (1981): 563-573.
51. Sitnikova, A.A., L.M. Sorokin, I.E. Talanin, E.G. Sheikhet, and E.S. Falkevich. “Vacancy type microdefects in dislocation-free silicon single crystals.” *Phys. Stat. Sol. (a)* 90 (1985): K31-K35.

52. Talanin, V.I., and I.E. Talanin. “Formation of grown-in microdefects in dislocation-free silicon monocrystals.” In: *New research on semiconductors* edited by Thomas B. Elliot, 31-67, New York: Nova Science Publishers, Inc., 2006.
53. Ammon, W. von, E. Dornberger, and P.O. Hansson. “Bulk properties of very large diameter silicon single crystal.” *J. Cryst. Growth* 198-199 (1999): 390-398.
54. Muraoka, S. “Current status of 300 mm silicon crystal growth and its future status.” *Oyo Buturi* 66 (1997): 673-677.
55. Zhang, T., G.-X. Wang, F. Ladeinde, and V. Prasad. “Turbulent transport of oxygen in the Czochralski growth of large silicon crystal.” *J. Cryst. Growth* 198-199 (1999): 141-146.
56. Gulyaeva, A.S., L.V. Liner, O.A. Pervova, O.A. Remizov, and S.U. Slobodova. “Influence of the growth rate on the formation of microdefects in silicon.” *Tsvetnye Metally (Non-ferrous metals)* no. 10 (1986): 57-59.
57. Murgai, A., H.C. Gatos, and W.A. Westdorp. “Effect of microscopic growth rate on oxygen microsegregation and swirl defect distribution in Czochralsri-grown silicon.” *J. Electrochem. Soc*. 126 (1979): 2240-2245.
58. Pimentel, C.A., and F.B.C. Brito. “Point defect aggregates in boron doped dislocation-free Czochralski silicon crystals.” *J. Cryst. Growth* 62 (1983): 129-140.
59. Gulyaeva, A.S., Liner L.V., S.U. Slobodova, and N.Ya. Shushlebina. “Effect of impurities of boron and phosphorus on the formation of microdefects in the heat treatment of silicon.” *Proceedings of the USSR Academy of Sciences. Inorganic materials* 23 (1987): 880-882.
60. Litvinov, V.V., A.N. Petukh, and Yu.M. Pokotilo. “Microinhomogeneity of oxygen distribution in large-diameter silicon ingots.” *Proceedings of universities. Nonferrous metallurgy* no. 5 (1997): 29-32.
61. Muhe, A., R. Backofen, J. Fainberg, G. Muller, E. Dornberger, E. Tomzig, W. von Ammon. “Oxygen distribution in silicon melt during a standart Czochralski process studied by sensor measurements and comparison to numerical simulation.” *J. Cryst. Growth* 198-199 (1999): 409-413.
62. Bulyarsky, S.V., V.V. Svetukhin, and O.V. Prikhodko. “Modeling of oxygen precipitation in silicon.” *Proceedings of universities. Materials of electronic engineering* no. 3 (1999): 11-17.
63. Gall, P., J.-P. Fillard, J. Bonnafe, T. Rakotomavo, H. Rufer, and H. Schwenk. “Role of oxygen in nucleation of microprecipitates in silicon

materials." In: *Defect control in semiconductor* edited by K. Sumino, 255-259, Amsterdam: North Holland, 1990.
64. Enischerlova, I.L., G.G. Shmeleva, and E.M. Temper. "The influence of a number of factors on the processes of precipitation of oxygen in silicon." *Inorganic materials* 28 (1992): 936-941.
65. Voronkov, V.V., M.G. Milvidsky, V.Ya. Reznik, N.I. Puzanov, and A.M. Eidenzon. "Precipitation of oxygen in silicon with various growth microdefects." *Kristallografiya (Crystallography Reports)* 35 (1990): 1197-1204.
66. Voronkov, V.V., M.G. Milvidsky, and V.Ya. Reznik. "Influence of growth microdefects on the precipitation of oxygen in dislocation-free silicon." *Kristallografiya (Crystallography Reports)* 35 (1990): 1205-1211.
67. Puzanov, N.I., and A.M. Eidenzon. "Influence of growth conditions of silicon single crystals on the precipitation of oxygen in high-temperature treatments." *Kristallografiya (Crystallography Reports)* 37 (1992): 1244-1253.
68. Ogino, M. "Supression effect upon oxygen precipitation in silicon by carbon for a two-step thermal anneal." *Appl. Phys. Lett*. 41 (1983): 847-849.
69. Swaroop, R.B. "Advances in silicon technology for the semiconductor industry." *Sol. State Technol*. 26 (1983):, 111-114.
70. Gupta, S., S. Messoloras, J.R. Schneider, R.J. Stewart, and W. Zulehner. "Oxygen precipitation in carbon-dopes silicon." *Semicond. Sci. and Technol*. 7 (1992): 5-11.
71. Yamanaka, H. "Formation kinetics and infrared absorption of carbon-oxygen complexes in Czochralski silicon." *Jpn. J. Appl. Phys*. 33 (1994): 3319-3329.
72. Ueki, T., M. Itsumi, and T. Takeda. "Carbon in grown-in defects in Czochralski silicon and its influence on gate-oxide defects." *Jpn. J. Appl. Phys*.38 (1999): 5695-5699.
73. Iida, S., Y. Aoki, Y. Sugita, T. Abe, and H. Kawata. "Grown-in microdefects in a slowly grown Czochralski silicon crystal observed by synchrotron radiation topography." *Jpn. J. Appl. Phys*. 39 (2000): 6130-6135.
74. Kim Young, K., S. Ha Tae, J.K. Yoon. "Growth parameters on the defects formation in a grown silicon crystal." *J. Mater. Sci*. 33 (1998): 4627-4632.
75. Puzanov, N.I., and A.M. Eidenzon. "Classification of microdefects in dislocation-free silicon grown by the Czochralski method." *Tsvetnye Metally (Non-ferrous metals)* no. 4 (1988): 69-72.

76. Puzanov, N.I., and A.M. Eidenzon. “Relaxation in the system of point defects of a growing dislocation-free silicon crystal.” *Kristallografiya (Crystallography Reports)* 31 (1986): 373-379.
77. Puzanov, N.I., and A.M. Eidenzon. “Effect of transient crystallization regimes on microdefects in silicon.” *Izv. Academy of Sciences of the USSR. Inorganic Materials* 22 (1986): 1237-1242.
78. Puzanov, N.I., A.M. Eidenzon, and V.I. Rogovoi. “Influence of growing conditions on the formation of microdefects in dislocation-free silicon.” *Kristallografiya (Crystallography Reports)* 34 (1989): 461-469.
79. Puzanov, N.I., and A.M. Eidenzon. “The effect of thermal history during crystal growth on oxygen precipitation in Czochralski-grown silicon.” *Semicond. Sci. and Technol*. 7 (1992): 406-413.
80. Puzanov, N.I., and A.M. Eidenzon. “The role of intrinsic point defects in the formation of oxygen precipitation centers in dislocation-free silicon.” *Crystallography Reports* 41 (1996): 134-141.
81. Voronkov, V.V., and R. Falster. “Vacancy-type microdefect formation in Czochralski silicon.” *J. Cryst. Growth* 194 (1998): 76-88.
82. Shimizu, H., C. Munakata, N. Honma, S. Aoki, and Y. Kosaka. “Observation of ring-distributed microdefects in Czochralski-grown silicon wafers with a scanning photon microscope and its diagnostic application to device processing.” *Jpn. J. Appl. Phys*. 31 (1992): 1817-1822.
83. Harada, K., H. Tanaka, T. Watanabe, and H. Furuya. “Defects in the oxidation-induced stacking fault ring region in Czochralski silicon crystal.” *Jpn. J. Appl. Phys*. 37 (1998): 3194-3199.
84. Sadamitsu, S., S. Umeno, Y. Koike, M. Hourai, S. Sumita, and T. Shigematsu. “Dislocations, precipitates and other defects in silicon crystals.” *Jpn. J. Appl. Phys*. 32 (1993): 3675-3679.
85. Puzanov, N.I., and A.M. Eidenzon. “Observation of stacking faults rings in silicon crystal.” *J. Cryst. Growth* 137 (1994): 642-645.
86. Dornberger, E., and W. von Ammon. “The dependence of ring-like distributed stacking faults on the axial temperature gradient of growing Czochralski silicon crystals.” *J. Electrochem. Soc*. 143 (1996): 1648-1654.
87. Yamagishi, H., I. Fusegawa, N. Fuyimaki, and M. Katayama. “Recognition of D-defects in silicon single crystal by preferential etching and effect on gate oxide integrity.” *Semicond. Sci. and Technol*. 7 (1992): A135-A140.

88. Kato, M., T. Yoshida, Y. Ikeda, and Y. Kitagawara. “Transmission electron microscope observation of “IR scattering defects” in as-grown Czochralski Si crystals.” *Jpn. J. Appl. Phys*. 35 (1996): 5597-5601.
89. Miyazaki, M., S. Miyazaki, Y. Yanase, T. Ochiai, and T. Shigematsu. “Microstructure observation of “crystal-originated particles” on silicon wafers.” *Jpn. J. Appl. Phys*. 34 (1995): 6303-6307.
90. Umeno, S., M. Okui, M. Hourai, M. Sano, and H. Tsuya. “Relationship between grown-in defects in Czochralski silicon crystals.” *Jpn. J. Appl. Phys*. 36 (1997): L591-L594.
91. Nishimura, M., S. Yoshino, H. Motoura, S. Shimura, T. Mchedlidze, and T. Hikone. “The direct observation of grown-in laser scattering tomography defects in Czochralski silicon.” *J. Electrochem. Soc*. 143 (1996): L243-L246.
92. Voronkov, V.V., and R. Falster. “Nucleation and growth of faceted voids in silicon crystals.” *J. Cryst. Growth* 198-199 (1999): 399-403.
93. Nango, N., S. Iida, and T. Ogawa. “An optical study on dislocation clusters in a slowly pulled silicon crystals.” *J. Appl. Phys*.86 (1999): 6000-6004.
94. Iida, S., Y. Aoki, K. Okitsu, Y. Sugita, H. Kawata, and T. Abe. “Microdefects in as-grown Czochralski silicon crystal studied by synchrotron radiation section topography with aid of computer simulation.” *Jpn. J. Appl. Phys*. 37 (1998): 241-246.
95. Bublik, V.T., and N.M. Zotov. “Microdefects detected by diffuse X-ray scattering in dislocation-free single crystals of silicon grown by the Czochralski method.” *Crystallography Reports*. 42 (1997): 1103-1113.
96. Nishikawa, H., T. Tanaka, Y. Yanase, M. Hourai, M. Sano, and H. Tsuya. “Formation of grown-in defects during Czochralski silicon crystal growth.” *Jpn. J. Appl. Phys*. 36 (1997): 6595-6601.
97. Tempelhoff, K., and van Sung. “Formation of vacancy agglomerates in quenched dislocation-free silicon.” *Phys. Stat. Sol. (a)* 72 (1982): 617-622.
98. Rauh, H. D. Sieger, and A. Wright. “Morphology of oxygen precipitates in CZ silicon studied by small angle neutron scattering (SANS).” In: *Defect Control in Semiconductor*, edited by K. Sumino, 1541-1545, Amsterdam: North Holland, 1990.
99. Sheikhet, E.G., V.I. Shakhovtsov, and V.F. Latyshenko. “Interaction of radiation defects with growth microdefects in single crystals of silicon.” *Ukrainian Physical Journal* 33 (1988): 1851-1855.
100. Prostomolotov, A.I., and N.A. Verezub. “Two-dimensional model of the intrinsic point defects behaviour during CZ silicon crystals growth.” *Proc of SPIE*. 44 (2000): 97-103.

101. Talanin, V.I., I.E. Talanin, and D.I. Levinson. "On the identity of defect formation processes in small-sized single crystals of FZ-Si and CZ-Si." *Proceedings of universities. Materials of electronic engineering* no. 3 (2003): 30-34.
102. Kock, de A.J.R. "Vacancy clusters in dislocation-free silicon." *Appl. Phys. Lett*. 16 (1970): 100-102.
103. Falkevich, E.S., A.A. Veselkova, and K.N. Neimark. "Pits of etching in dislocation-free single crystals of silicon." In: *Silicon and germanium*, edited by E.S. Falkevich, and D.I. Levinzon, 42-46. Moscow: Metallurgy, 1970.
104. Talanin, V.I., and I.E. Talanin. "Microdefect structure of semiconductor silicon." *Proceedings of universities. Materials of electronic engineering* no. 4 (2002): 4-15.
105. Tan, T.Y., and W.K. Tice. "Oxygen precipitation and the generation of dislocations in silicon." *Phil. Mag*. 34 (1976): 615-631.
106. Yang, K.H., R. Anderson, and H.F. Kappert. "Identification of oxide precipitates in annealed silicon crystals." *Appl. Phys. Lett*. 33 (1978): 225-229.
107. Talanin, V.I., and I.E. Talanin. "A kinetic model of the formation and growth of interstitial dislocation loops in dislocation-free silicon single crystals." *J. Crystal Growth* 346 (2012): 45-49.
108. Talanin, I.E., V.I. Talanin, and D.I. Levinson. "Model of formation and transformation of microdefects in dislocation-free single crystals of silicon." *J. Surf. Invest.: X-Ray, Synchrotron Neutron Tech*. no. 3 (2002): 72-76.
109. Talanin, V.I., and I.E. Talanin. "Vacancy microdefects in dislocation-free single crystals of silicon." *Proceedings of universities. Materials of electronic engineering* no. 1 (2006): 14-19.
110. Danilchuk, L.N., A.O. Okunev, V.A. Tkal, and Yu.A. Drozdov. "Experimental determination of the physical nature of growth microdefects in dislocation-free silicon grown by the Czochralski method." *J. Surf. Invest.: X-Ray, Synchrotron Neutron Tech*. no. 7 (2005): 13-22.
111. Kock, de A.J.R. "Swirl defects in as-grown silicon crystals." In: *Defects in semiconductors*, edited by J. Narayan and T.Y. Tan, 309-316, New York, North-Holland Publ. Co., 1981.
112. Voronkov, V.V. "Formation of vacancy pores upon cooling of Ge and Si." *Kristallografiya (Crystallography Reports)* 19 (1974): 228-236.
113. Lee, W.P., W.S. Seow, H.K. Yow, and T.Y. Tou. "Analysis of atomic force microscopy images of crystal originated "particles" on silicon

wafers treated with $NH_4OH:H_2O_2:H_2O$ solution." *Jpn. J. Appl. Phys*. 40 (2001): 18-23.

114. Yanase, Y., H. Nishihata, T. Ochiai, and H. Tsuya. "Atomic force microscope observation of the change in shape and subsequent disappearance of "crystal-originated particles" after hydrogen-atmospfere thermal annealing." *Jpn. J. Appl. Phys*. 37 (1998): 1-4.
115. Ravi, K.V., and C.J. Varker. "Oxidation induced stacking faults in silicon. Electrical effects in p-n diodes." *J.Appl. Phys*. 45 (1974): 272-287.
116. Okui, M., and M. Nishimoto. "Effect of axial temperature gradient on the formation of grown-in defect regions in Czochralski silicon crystals; reversion of the defect regions between the inside and outside of the Ring-OSF." *J. Cryst. Growth* 237-239 (2002): 1651-1656.
117. Milvidsky, M.G., and V.B. Osvensky. *Structural defects in single crystals of semiconductors*. Moscow: Metallurgy, 1984.
118. Furukawa, J., H. Tanaka, Y. Nakada, N. Ono, and S. Shiraki. "Investigation on grown-in defects in CZ-Si crystal under slow pulling rate." *J. Cryst. Growth* 210 (2000): 26-30.
119. Kulkarni, M.S., V, Voronkov, R. Falster. "Quantification of defect dynamics in unsteady-state and steady-state Czochralski growth of monocrystalline silicon." *J. Electrochem. Soc*. 151 (2004): G663-G669.
120. Prasad, M., and T. Sinno. "Internally consistent approach for modeling solid-state aggregation. I. Atomistic calculations of vacancy clustering in silicon." *Phys. Rev. B* 68 (2003): 45207-45220.
121. Ueki, T., M. Itsumi, T. Takeda, K. Yoshida, A. Takaoka, and S. Nakajima. "Shrinkage of grown-in defects in Czochralski silicon during thermal annealing in vacuum." *Jpn. J. Appl. Phys*. 37 (1998): L771-L773.
122. Itsumi, M. "Octahedral void defects in Czochralski silicon." *J. Cryst. Growth* 237-239 (2002): 1773-1778.
123. Sitnikova, A.A., L.M. Sorokin, I.E. Talanin, E.G. Sheikhet, and E.S. Falkevich. "Electron-microscopic study of microdefects in silicon single crystals grown at high speed." *Phys. Stat. Sol. (a)* 81 (1984): 433-438.
124. Talanin, I.E., D.I. Levinson, and V.I. Talanin. "Formation and transformation of microdefects in dislocation-free single crystals of silicon." *Proceedings of universities. Materials of electronic engineering* no. 4 (2000): 21-27.

125. Bender, H. "Investigation of the oxygen-related lattice defects in Czochralski silicon by means of electron microscopy techniques." *Phys. Stat. Sol. (a)* 86 (1984): 245-261.
126. Yonemura, M., K. Sueoka, and K. Kamei. "Analysis of local lattice strain around oxygen precipitates in Czochralski-grown silicon wafers using convergent beam electron diffraction." *Jpn. J. Appl. Phys*.38 (1999): 3440-3447.
127. Kamura, Y., F. Hashimoto, and M. Yoneta. "Oxygen precipitation at 400-700^{0}C in Czochralski silicon: thermal donors, new donors and rod-like defects." In: *Defect control in semiconductors* edited by K. Sumino, 233-238, Amsterdam: North Holland, 1990.
128. Itsumi, M., M. Maeda, S. Ohfuji, and T. Ueki. "Two kinds of impurity-related mark on thermal oxides originating in octachedral void defects." *Jpn. J. Appl. Phys*. 38 (1999): 5720-5724.
129. Ojima, K., K. Sakai, and T. Yamagami. "Morphology change of octachedral oxide precipitates in Czochralski silicon wafers stretched by tension." *Jpn. J. Appl. Phys*. 39 (2000): 5723-5726.
130. Sakai, K., T. Yamagami, and K. Ojima. "Change in shape of oxygen precipitate grown by thermal annealing." *J. Cryst. Growth* 210 (2000): 65-68.
131. Sheikhet, E.G., I.F. Chervoniy, and E.S. Falkevich. "Investigation of microdefects in neutron-doped single crystals of high-purity silicon." *High-purity substances* no. 2 (1989): 50-55.
132. Jones, K.S., S. Prussin S., and E.R. Weber. "A systematic analysis of defects in ion-implanted silicon." *Appl. Phys. A* 45 (1988): 1-34.
133. Possel, M., B. Schmidt, C.S. Murthy, T. Feudel, and K. Suzuki. "Modeling of damage accumulation during ion implantation into single-crystalline silicon." *J. Electrochem. Soc*. 144 (1997): 1495-1504.
134. Tamura, M., Y. Hiroyama, A. Nishida, and M. Horiuchi. "Secondary defects in low-energy As-implanted Si." *Appl. Phys. A* 66 (1998): 373-384.
135. Libertino, S., J.L. Benton, D.C. Jakobson, D.J. Eaglesham, J.M. Poate, S. Coffa, P. Kringhoj, P.G. Fuochi, and M. Lavalle. "Evolution of intfrstitial- and vacancy-type defects upon thermal annealing in ion-implanted Si." *Appl. Phys. Lett.* 71 (1997): 389-391.
136. Prussin, S. "Defects in silicon substrates." *J. Appl. Phys*. 45 (1974): 1635-1638.
137. Furuno, S., K. Izui, and H. Otsu. "Nature of secondary defects in silicon produced by high temperature electron irradiation." *Jpn. J. Appl. Phys*. 18 (1979): 203-207.

138. Pasemann, M., D. Hoehl, A.L. Aseev, and O.P. Pchelyakov. "Analysis of rod-like defects in silicon and germanium by means of high-resolution electron microscopy." *Phys. Stat. Sol. (a)* 80 (1983): 135-139.
139. Terrasi, A., E. Rimini, V. Raineri, F. Iacona, F. La Via, S. Loeorra, and S. Molilo. "Precipitation of As in thermally oxidized ion-implanted Si crystals." *Appl. Phys. Lett*. 73 (1998): 2633-2635.
140. Vavilov, I.S., V.F. Kiselev, and B.N. Mukashev. *Defects in silicon and on its surface*. Moscow: Nauka, 1990.
141. Emtsev, V.V., and T.V. Mashovets. "Impurities and point defects in semiconductors." Moscow: Radio and Communication.
142. Popov, V.P., A.V. Dvurechenskii, B.P. Kashnikov, and A.I. Popov. "Defects in supersaturated solid solution of arsenic in silicon at rapid thermal annealing." *Phys. Stat. Sol. (a)* 94 (1986): 569-572.
143. Talanin, V.I. *Modeling and properties of the defect structure of dislocation-free silicon monocrystals*. Zaporizhzhya" Publishing house of the ZIGMU, 2007.
144. Kazakevich, L.A., and P.F. Lugakov. "Recombination of charge carriers in dislocation-free silicon containing growth microdefects of various types." *Semiconductors* 32 (1998): 129-131.
145. Kolkovsky, I.I., V.F. Latyshenko, E.G. Sheikhet, and V.V. Shusha. "Effect of electron irradiation on the recombination activity of microdefects in dislocation-free single crystals of silicon." *Soviet Physics Semiconductors* 21 (1986): 1821-1824.
146. Sheikhet, E.G., V.F. Latyshenko, V.P. Shapovalov, and V.A. Nazarenko. "Electrical activity of microdefects in dislocation-free single crystals of silicon." *Ukrainian Physical Journal* 27 (1982): 1679-1684.
147. Seeger, A.K., and K.P. Chick. "Diffusion mechanism and point defects in silicon and germanium." *Phys. Stat. Sol*. 29 (1968): 455-542.
148. Van Vechten, J.A., and C.D. Thurmond. "Comparison of theory with quenching experiments for the entropy and enthalpy of vacancy formation in Si and Ge." *Phys. Rev. B* 14 (1976): 3551-3555.
149. Schnittler, C., G. Teichmann, W. Kaufmann, and H. Schneider. "A thermodynamic model for the formation and growth of B-defects in silicon." *Phys. Stat. Sol. (a)* 69 (1982): 227-233.
150. Schnittler, C., G. Teichmann, W. Kaufmann, and H. Schneider. "Energetic calculations concerning the A-defect structure and formation in silicon." *Phys. Stat. Sol. (a)* 68 (1981): K135-K137.
151. Chikawa, J., and S. Shirai. "Melting of silicon crystals and a possible origin of swirl defects." *J. Cryst. Growth* 39 (1977): 328-340.

152. Chikawa, J., and S. Shirai. “Swirl defects in silicon crystals.” *J. Appl. Phys*. 18 (1979): 153-164.
153. Pullner, E.O. “Kinetics of the formation of microdefects in the process of growth of dislocation-free single crystals of silicon.” *High-purity substances*no. 5 (1995): 19-24.
154. Van Vechten, J.A. “Formation of interstitial type dislocation loops in tetrahedral semiconductors by precipitations of vacancies.” *Phys. Rev. B* 17 (1978): 3197-3206.
155. Sirtl, E. “Mechanism of formation complexes defects in silicon”. In: *Semiconductor silicon*, edited by H.R. Huff and E. Sirtl, 4-19, Princeton: Electrochem. Soc., 1977.
156. Roksnoer, P.J. “Mechanism of formation of microdefect in silicon.” *J. Cryst. Growth* 58 (1984): 596-612.
157. Wijaranakula, W. “Numerical modeling of the point defect aggregation during the Czochralski silicon crystal growth.” *J. Electrochem. Soc*. 139 (1992): 604-616.
158. Falster, R., and V.V. Voronkov. “A perspective from crystal growth and wafer processing on the properties of intrinsic point defects in silicon.” *Defect & Diffusion Forum* 200 (2002): 202-214.
159. Okada, Y. “Concentration of native point defect in Si single crystals at high temperatures.” *Phys. Rev. B* 41 (1990): 10741-10743.
160. Okino, T., and M. Onishi. “Point and swirl defects in silicon.” *Jpn. J. Appl. Phys*. 33 (1994): 6642-6647.
161. Falster, R., and V.V. Voronkov. “The engineering of intrinsic point defects in silicon wafers and crystals.” *Mater. Sci. Eng. B* 73 (2000): 69-76.
162. Sinno, T., and R.A. Brown. “Modeling microdefect formation in Czochralski silicon.” *J. Electrochem. So*c. 146 (1999): 2300-2312.
163. Voronkov, V.V., and R. Falster. “Dopant effect on point defect incorporation into growing silicon crystal.” *J. Appl. Phys*. 87 (2000): 4126-4129.
164. Voronkov, V.V., and R. Falster. “Intrinsic point defects and impurities in silicon crystal growth.” *J. Electrochem. Soc*. 149 (2002): G167-G174.
165. Porrini, M., V.V. Voronkov, and R. Falster. “Dopant effect on point defect incorporation into growing silicon crystal.” *Mat. Sci. Eng. B* 134 (2006): 185-189.
166. Milvidsky, M.G. “Features of defect formation in dislocation-free single crystals of semiconductors.” *Proceedings of universities. Materials of electronic engineering* no. 3 (1998): 4-12.

167. Dornberger, E., W. von Ammon, J. Virbulis, B. Hanna., and T. Sinno. "Modeling of transient point defect dynamics in Czochralski silicon crystal." *J. Cryst. Growth* 230 (2001): 291-299.
168. Sinno, T., R.A. Brown, W. von Ammon, E. and Dornberger. "Point defects dynamics and the oxidation-induced stacking-faults in Czochralski-grown silicon crystals." *J. Electrochem. Soc*. 145 (1998): 302-318.
169. Larsen, T.L., L Jensen, A. Ludge, H. Riemann, and H.Lemke. "Numerical simulations of point defects transport in floating-zone silicon single crystal growth." *J. Cryst. Growth* 230 (2001): 300-304.
170. Prostomolotov, A.I., N.A. Verezub, and V.V. Voronkov. "Modeling the formation of growth microdefects in dislocation-free single crystals of large-diameter silicon." *Proceedings of universities. Materials of electronic engineering* no. 2 (2005): 48-53.
171. Habu, R., and A. Tomiura. "Distribution of grown-in crystal defects in silicon crystals formed by point defect diffusion during melt-growth: disappearance of the oxidation induced stacking faults-ring." *Jpn. J. Appl. Phys*. 35 (1996): 1-9.
172. Lemke, H., and W. Sudkamp. "Analytical approximations for the distributions of intrinsic point defects in grown silicon crystal." *Phys. Stat. Sol. (a)* 176 (1999): 843-865.
173. Nakamura, K., T. Saishoji, and J. Tomioka. "Grown-in defects in silicon crystals." *J. Cryst. Growth* 237-239 (2002): 1678-1684.
174. Akatsuka, M., M. Okui, S. Umeno, and K. Sueoka. "Calculation of size distribution of void defects in CZ silicon." *J. Electrochem. Soc*. 150 (2003): G587-G590.
175. Voigt, A., C. Weichmann, J. Nitschkowski, E. Dornberger, and R. Holz. "Transient and quasi-stationary simulation of heat and mass transfer in Czochralski silicon crystal growth." *Cryst. Res. & Technol*. 38 (2003): 499-508.
176. Borghesi, A., B. Pivac, A. Sassella, and A. Stella. "Oxygen precipitation in silicon." *J. Appl. Phys*. 77 (1995): 4169-4235.
177. Ikari, A., O. Yoda, Y. Ujihira, H. Haga, and A. Uedono. "Nucleation of oxygen precipitates in Czochralski single-crystal quenched from high temperature." *Nippon Steel Technical Report* 57 (1993): 62-66.
178. Kulkarni, M.S. "Defect dynamics in the presence of oxygen in growing Czochralski silicon crystals." *J. Cryst. Growth* 303 (2007): 438-448.
179. Kulkarni, M.S. "Defect dynamics in the presence of nitrogen in growing Czochralski silicon crystals." *J. Cryst. Growth* 310 (2008): 324-335.

180. Pitaevsky, L.P., and E.M. Lifshits. *Physical kinetics*. Oxford: Butterworth-Heinemann, 1981.
181. Cristian, J.W. *The theory of transformations in metals and alloys*. London: Pergamon Press, 1965.
182. Haimi, E.. "Oxygen in silicon." In: *Handbook of silicon based MEMS materials and technologies*, edited by V. Lindroos, M. Tilli, A. Lehto, and T. Motooka, 59-72. Oxford: Elsevier Publ., Inc., 2010.
183. Abe T., and T. Takahashi. "Intrinsic point defect behavior in silicon crystals during growth from the melt: A model derived from experimental results." *J. Cryst. Growth* 334 (2011): 16–36.
184. Vanhellemont. J. "Intrinsic point defect incorporation in silicon single crystals grown from a melt, revisited." *J. Appl. Phys*. 110 (2011): 063519-063522.
185. Vanhellemont, J. "Response to «Comment on 'Intrinsic point defect incorporation in silicon single crystals grown from a melt, revisited'»." *J. Appl. Phys*. 111 (2012): 1161021-16105.
186. Voronkov, V.V., and R. Falster. "Intrinsic point defects and grown-in microdefects in silicon crystals — comment on: «Intrinsic point defect behaviour in silicon crystals during growth from the melt: A model derived from experimental results», T. Abe, T. Takahashi, J. Crystal Growth 334 (2011)." *J. Cryst. Growth* 351 (2012):: 115–117.
187. Voronkov, V. V., and R. Falster. "Comment on «Intrinsic point defect incorporation in silicon single crystals grown from a melt, revisited» [J. Appl. Phys.110, 063519 (2011)]." *J. Appl. Phys*. 111 (2012): 116102-116105.
188. Kulkarni, M.S. "A selective review of the quantification of defect dynamics in growing Czochralski silicon crystals." *Ind. Eng. Chem. Res*. 44 (2005): 6246-6263.
189. Nakamura. K., T. Saishoji, T. Kubota, T. Iida, Y. Shimanuki, T. Kotooka, and J. Tomioka. "Formation process of grown-in defects in Czochralski grown silicon crystals." *J. Cryst. Growth* 180 (1997): 61-72.
190. Wang, Z., and R.A. Brown. "Simulation of almost defect-free silicon crystal growth." *J. Cryst. Growth* 231 (2001): 442-452.
191. Brown, R.A., Z. Wang, and T. Mori. "Engineering analysis of microdefects formation during silicon crystal growth." *J. Cryst. Growth* 225 (2001): 97-112.
192. Voronkov, V.V., B. Dai, and M.S. Kulkarni. "Fundamentals and engineering of the Czochralski growth of semiconductor silicon crystals." *Compr. Sem. Science and Technol*. 3 (2011): 81-169.

193. Verezub, N.A., and A.I. Prostomolotov. “The study of heat transfer in the growth node of the Czochralski process on the basis of the conjugate mathematical model.” *Proceedings of universities. Materials of electronic engineering* no. 3 (2000): 28-34.
194. Sinno, T., E. Dornberger, W. von Ammon, R.A. Brown, and F. Dupret. “Defects engineering of Czochralski single-crystals silicon.” *Mater. Sci. Eng*. 28 (2000): 149-198.
195. Pat. 6197111 B1 USA, MKI WITH 30 V 27/02. Heat shield assembly for crystal puller / W.I. Ferry, S. Ishii: MEMC Inc. 06/03/2001.
196. Berghols, W., M.J. Binns, G.R. Booker, J.C. Hutchinson, S.H. Kinder, S. Messoljras, R.C. Newman, R.J. Stewart, and J.G. Wilkes. “A study of oxygen in silicon using high-resolution transmission electron microscopy, small-angle neutron scattering and infrared absorption.” *Phil. Mag. (b)* 59 (1989): 499-522.
197. Senkader, S., J. Esfandyari, and G. Hobler. “A model for oxygen precipitation in silicon including bulk stacking fault growth.” *J. Appl. Phys*. 78 (1995): 6469-6476.
198. Ko, B.G., and K.D. Kwack. “Growth/dissclution model for oxygen precipitation based on the kinetics of phase transformations.” *J. Appl. Phys*. 85 (1999): 2100-2107.
199. Kapur, S.S., M. Prasad, J.C. Crocker, and T. Sinno. “Role of configurational entropy in the thermodynamicalof clusters of point defects in crystalline solids.” *Phys. Rev. (b)* 72 (2005): 14119-14131.
200. Talanin, V.I. “Interaction of point defects in the process of growth of dislocation-free single crystals of silicon.” *Proceedings of universities. Materials of electronic engineering* no. 4 (2007): 27-40.
201. Talanin, V.I., I.E. Talanin, and D.I. Levinson. “Microdefects in semiconducting silicon.” *Functional Materials* 10 (2003): 1-7.
202. Talanin, V.I., I.E. Talanin, A.A. Voronin, and A.V. Sirota. “The aggregation of point defects in dislocation-free silicon single crystals.” *Functional Materials* 14 (2007): 1-5.
203. Talanin, V.I., I.E. Talanin, and D.I. Levinson. “Formation of microdefects in semiconductor silicon.” *Crystallography Reports* 49 (2004): 188-192.
204. Fedina, L., A. Gutakovskii, A. Aseev, J. van Landujt, and J. Vanhellemont. “Extended defects formation in Si crystals by clustering of intrinsic point defects studied by in – situ electron irradiation in an HREM.” *Phys. Stat. Sol.(a)* 171 (1999): 147-157.
205. Fedina, L., and A. Gutakovskii, A. Aseev. “In situ HREM irradiation study of an intrinsic point defects clustering in FZ-Si.” *Cryst. Res. Technol*. 35 (2000): 775-786.

206. Fedina, L.I., A.K. Gutakovskiy, and A.L. Aseev. “New types of extended defects in silicon crystals, arising from the joint clustering of vacancies and interstitial atoms.” *Proceedings of universities. Materials of electronic engineering* no. 3 (2000): 19-25.
207. Fedina, L.I. “Recombination and interaction of point defects with the surface during the clustering of point defects in silicon.” *Semiconductors* 35 (2001): 1120-1127.
208. Seeger, A., W. Frank, and U. Gosele. “Diffusion in elemental semiconductors: new developments.” In: *Defects and radiation effects in semiconductors* edited by J.H. Albany, 148-167, Bristol & London: IOP, 1979.
209. Gosele, U., W. Frank, and A. Seeger. “About the secret of self-interstitial atoms in silicon.” *J. Appl. Phys*. 23 (1980): 361-367.
210. Gosele, U., W. Frank, and A. Seeger. “An entropy barrier against vacancy-interstitial recombination in silicon.” *Solid State Commun*. 45 (1983): 31-33.
211. Benneman, K.H. “New method treating lattice point defects in covalent crystals.” *Phys. Rev*. 137 (1965):: A1497-A1514.
212. Seeger, A., H. Foll, and W. Frank. “Intrinsic interstitial atoms, vacancies and their clusters in silicon and germanium.” In: *Radiation. Effects in Semiconductors* edited by N. B. Urli and J. W. Corbett, 12-37, Bristol & London: IOP, 1976.
213. Talanin, V.I., and I.E. Talanin. “On the recombination of intrinsic point defects in dislocation-free silicon single crystals.” *Physics of the Solid State* 49 (2007): 467-471.
214. Tognato, R. “On the formation of swirl defects in silicon and germanium.” *Phys. Stat. Sol. (a)* 98 (1986): K133-K136.
215. Pizzini, S. “Chemistry and physics of segregation of impurities at extended defects in silicon.” *Phys. Stat. Sol. (a)* 171 (1999): 123-132.
216. Dzelme, J., I. Ertsinsh, B. Zapol, and A. Misiuk. “Structure of oxygen and silicon interstitials in silicon.” *Phys. Stat. Sol. (a)* 171 (1999): 197-201.
217. Ian Hodge, M. “Adam-Gibbs formulation of enhalpy relaxation near the glass transition.” *J. Res. Natl. Inst. Stand. Technol*. 102 (1997): 195-202.
218. Tang, M., L. Colombo, J. Zhu, and T. Diaz de la Rubia. “Intrinsic point defects in crystalline silicon: tight-binding molecular dynamics studies of self-diffusion, interstitial-vacancy recombination and formation volumes.” *Phys. Rev. B* 55 (1997): 14279-14289.

219. Mayer, J.H., H. Mehrer H., and K. Maier. “About a self-diffusion in silicon.” In: *Radiation Effects in Semiconductors 1976*, edited by N. B. Urli and J. W. Corbett, 186-197, Bristol & London: IOP,, 1977.
220. Bracht, H., E.E. Haller, and R. Clark-Phelps. “Silicon self-diffusion in isotope heterostructures.” *Phys. Rew. Lett*. 81 (1998): 393-396.
221. Adam, G., and J.H. Gibbs. “On the temperature dependence of cooperative relaxation properties in glass-forming liquids.” *J. Chem. Phys*. 43 (1965): 139-148.
222. Antoniadis, D.A., and I. Moskowitz. “Diffusion of substitutional impurities in silicon at short oxidation times: an insight into point defect kinetics.” *J. Appl. Phys*. 53 (1982): 6788-6796.
223. Vanhellemont, J., and C. Claeus. “A theoretical study on the critical radius of precipitates and its application to silicon oxide in silicon.” *J. Appl. Phys*. 62 (1987): 3960-3967.
224. Talanin, V.I., and I.E. Talanin. “On the problem of the consistency of the high-temperature precipitation model with the classical nucleation theory.” *Physics of the Solid State* 56 (2014): 2043-2049.
225. Wright, M.R. *Fundamental chemical kinetics*. Woodhead Publishing, 1999.
226. Kukushkin, S.A., and A.V. Osipov. “A new method for the synthesis of epitaxial layers of silicon carbide on silicon owing to formation of dilatation dipoles.” *J. Appl. Phys*. 113 (2013): 024909-024916.
227. Kukushkin, S.A., and A.V. Osipov. “First-order phase transition through an intermediate state.” *Physics of the Solid State* 56 (2014): 792-800.
228. Fistul, V.I. *Decay of supersaturated solid-state solid solutions*. Moscow: Metallurgy, 1977.
229. Vas'kin, V.V. “Influence of the internal electric field on the simultaneous and sequential diffusion of impurities in semiconductors.” *Soviet Physics Semiconductors* 2 (1968): 102-109.
230. Vas'kin, V.V., and V.A. Uskov. “Effect of complexation on the diffusion of impurities in semiconductors.” *Physics of the Solid State (Fizika Tverdogo Tela)* 10 (1968): 1239-1241.
231. Vas'kin, V.V., and V.A. Uskov. “Complexation and diffusion of impurities in semiconductors.” *Physics of the solid (Fizika Tverdogo Tela)* 11 (1969): 1763-1769.
232. Uskov, V.A. “Multicomponent diffusion in monoatomic and binary semiconductors.’ In:: *Properties of doped semiconductors* edited by V.S.Zemskov, 129-134, Moscow: Nauka, 1977.
233. Bulyarsky, S.V., and V.I. Fistul. *Thermodynamics and kinetics of interacting defects in semiconductors*. Moscow: Fizmatlit, 1997.

234. Prokopev, E.P. “Mathematical model of gettering of metal impurities in silicon.” *High-purity substances* no. 4 (1992): 47-53.
235. Damask, A.C., and J. Dienes. *Point defects in metals*. New York: Gordon & Breach, 1963.
236. Ershov, S.N., V.A. Panteleev, S.N. Nagornykh, and V.V. Chernyakhovsky. ’The energy of migration of intrinsic point defects in a different charge state in silicon and germanium.” *Physics of the solid state (Fizika Tverdogo Tela)* 19 (1977): 322-323.
237. Panteleev, V.A. "Vacancy paradox" in germany and silicon and its solution.” *Physics of the solid state (Fizika Tverdogo Tela)* 19 (1977): 1801-1803.
238. Groot de, S.R., and P. Mazur. *Non-equlibrium thermodynamics*. Amsterdam: North-Holland, 1962.
239. Talanin, I.E., and V.I. Talanin. “Features of the heterogeneous mechanism of formation and transformation of growth microdefects in dislocation-free single crystals of silicon.” *Proceedings of universities. Materials of electronic engineering* no. 2 (2004): 14-24.
240. Talanin, V.I., and I.E. Talanin. “Modeling of the defect structure in dislocation-free silicon single crystals.” *Crystallography Reports* 53 (2008): 1124-1132.
241. Talanin, V.I., and I.E. Talanin. “Kinetics of high-temperature precipitation in dislocation-free silicon single crystals.” *Physics of the Solid State* 52 (2010): 2063-2069.
242. Vanhellemont, J. “Diffusion limited oxygen precipitation in silicon: precipitate growth kinetics and phase formation.” *J. Appl. Phys*. 78 (1995): 4297-4299.
243. Voronkov, V.V., and R. Falster. “Nucleation of oxide precipitates in vacancy containing silicon.” *J. Appl. Phys*. 91 (2002): 5802-5810.
244. Albrecht, M., S.B. Aldabergenova, S.B. Baiganatova, G. Frank, T.I. Taurbaev, S. Christiansen, and H.P. Strunk. “Carbon containing platelets in silicon and oriented diamond growth.” *Cryst. Res. Technol*. 35 (2000): 899-906.
245. Vlasov. A.A. “Generalization of the concept of electron plasma.” *Izvestia Academy of Sciences of the USSR, Physical Series* 8 (1944): 248-266.
246. Landau, L.D. “On the vibration of the electronic plasma.” *J. Phys. USSR* 10 (1946): 25-34.
247. Pegoraro, F., F. Califano, G. Manfredi, and P.J. Morrison. “Theory and applications of the Vlasov equation.” *Eur. Phys. J. D*. 69:68 (2015): 1-3.

248. Vlasov, A.A. “On the theory of the solid state.” *Journal of Physics* 9 (1945): 130-139.
249. Vlasov, A.A. “Thread-like and plate-like structures in crystals and liquids.” *Theoretical and Mathematical Physics* 5 (1970): 1228-1241.
250. Ginzburg, V.L., L.D. Landau, M.A. Leontovich, and V.A. Fok. “About inconsistency of works by A.A.Vlasov on general theory of plasma and physics of solid body.” *J. Exp. Theor. Phys.* 16 (1946): 246-252.
251. Ginzburg, V.L. “About some grief-historians of physics.” *Questions of History of Science and Technology* no. 4 (2000): 5-14.
252. Kozlov, V.V. “The generalized Vlasov kinetic equation.” *Russian Math. Surveys* 63 (2008): 691-726.
253. Vedenyapin, V.V. *Boltzmann and Vlasov kinetic equations*. Moscow: Fizmatlit, 2001.
254. Agrafonov, Yu.V., and G.A. Martynov. “Statistical theory of the crystalline state.” *Theoretical and Mathematical Physics* 90 (1992): 113-127.
255. Talanin, V.I., and I.E. Talanin. “Diffusion model of the formation of growth microdefects: a new approach to defect formation in crystals (review).” *Physics of the Solid State* 58 (2016): 427-437.
256. Talanin, V.I., and I.E. Talanin. “Kinetics of formation of vacancy microvoids and interstitial dislocation loops in dislocation-free silicon single crystals.” *Physics of the Solid State* 52 (2010): 1880-1886.
257. Mazhukin, V.I., A.V. Shapranov, and A.V. Rudenko. “Comparative analysis of interatomic interaction potentials for crystalline silicon.” *Mathematica Montisnigri* XXX (2014): 56-75.
258. Mattoni, A., M. Ippolito, L. Colombo. “Atomistic modeling of brittleness in covalent materials.” *Phys. Rev. B*, 76 (2007): 224103-224111.
259. Eremin, RA, Kh.T. Kholmurodov, V.I. Petrenko, L. Rosta, and M.V. Avdeev. “Analysis of small-angle neutron scattering by a solution of stearic acid in benzene using molecular dynamic modeling.” *Physics of the Solid State* 56 (2014): 86-89.
260. Gritsenko, V.A. “Atomic structure of amorphous nonstoichiometric oxides and silicon nitrides.” *Uspekhi Fizicheskikh Nauk* 178 (2008): 727-737.
261. Davydov, S.Yu., A,A. Lebedev, and N.Yu. Smirnova. “To the construction of the model of thermal destruction of silicon carbide for the purpose of obtaining graphite layers.” *Physics of the Solid State* 51 (2009): 452-454.

262. Magomedov, M.N. “On self-diffusion and surface energy in the compression of diamond, silicon and germanium.” *Journal of Theoretical Physics* 83 (2013): 87-96.
263. Magomedov, M.N. “On the parameters of formation of vacancies in crystals of a subgroup of carbon.” *Semiconductors* 42 (2008): 1153-1164.
264. Magomedov, M.N. “On the calculation of the parameters of the Mi-Lennard-Jones potential.” *Thermophysics of High Temperatures* 44 (2006): 518-533.
265. Magomedov, M.N. *Study of interatomic interaction, formation of vacancies and self-diffusion in crystals*. Moscow: Fizmatlit, 2010.
266. Boda, D., and D. Henderson. “The effects of deviations from Lorentz-Berthelot rules on the properties of a simple mixture.” *Molecular Physics* 106 (2008): 2367-2370.
267. Talanin, V.I., and I.E. Talanin. “Complex formation in semiconductor silicon within the framework of the Vlasov model of a solid state.” *Physics of the Solid State* 58 (2016): 2050-2054.
268. Talanin, V.I., and I.E. Talanin. “Kinetic model of growth and coalescence of oxygen and carbon precipitates during cooling of as-grown silicon crystals.” *Physics of the Solid State* 53 (2011): 119-126.
269. Ham, F.S. “Diffusion-limited growth of precipitate particles.” *J. Appl. Phys*. 30 (1969): 1518-1525.
270. Kelton, K.F., R. Falster, D. Gambaro, M. Olmo, M. Comara, and P.F. Wei. “Oxygen precipitation in silicon: experimental studies and theoretical investigations with the classical theory of nucleation.” *J. Appl. Phys*. 85 (1999): 8097-8111.
271. Sueoka, K., N. Ikeda, T. Yamamoto, and S. Kobayachi. “Morphology and growth process of thermally induced oxygen precipitation in Czochralski silicon.” *J. Appl. Phys*. 74 (1993): 5437-5444.
272. Esfandyari, J., S. Schmeiser, S. Senkader, G. Hobler, and B. Murphy. “Computer simulation of oxygen precipitation in Czochralski-grown silicon during anneals.” *J. Electrochem. Soc*. 143 (1996): 995-1001.
273. Wei, P.F., K.F. Kelton, and R. Falster. “Coupled-flux nucleation modeling of oxygen precipitation in silicon.” *J. Appl. Phys*. 88 (2000): 5062-5070.
274. Zirkelbach, F., B. Stritzker, K. Nordlund, J. K. N. Lindner, W. G. Schmidt, and E. Rauls. “Defects in carbon implanted silicon calculated by classical potentials and first-principles methods.” *Phys. Rev. B* 82 (2010): 094110-094114.
275. Zirkelbach, F., B. Stritzker, K. Nordlund, J. K. N. Lindner, W. G. Schmidt, and E. Rauls. “Combined ab initio and classical potential

simulation study on silicon carbide precipitation in silicon." *Phys. Rev. B* 84 (2011): 064126-064129.
276. Kyslovskyy, Ye.M., T.P. Vladimirova, S.I. Olikhovskii, V.B. Molodkin, E.V. Kochelab, and R.F. Seredenko. "Evolution of the microdefect structure in silicon at isothermal annealing as determined by X-ray diffractometry." *Phys. Stat. Sol. (a)* 204 (2007): 2591-2597.
277. Prostomolotov, A.I., and N.A. Verezub. "Simplistic approach for 2D grown-in microdefects modeling." *Phys. Stat. Sol. (c)* 6 (2009): 1878-1881.
278. Kulkarni, M.S., and V.V. Voronkov. "Simplified two-dimensional quantification of the microdefect distributions in silicon crystals grown by the Czochralski process." In: *High Purity Silicon VIII* edited by C.L. Claeys, M. Watanabe, R. Falster and P. Stallhofer, 71-95, New Jersey: Electr. Soc. Inc., 2004.
279. Bulyarsky, S.V., V.V. Svetukhin, and O.V. Prikhodko. "Modeling of oxygen inhomogeneity in the volume of precipitation in silicon." *Semiconductors* 33 (1999): 1281-1286.
280. Senkader, S., G. Hobler, and C. Schmeiser. "Determination of the oxide-precipitate – silicon-matrix interface energy by considering the change of precipitate morphology." *Appl. Phys. Lett*. 69 (1996): 2202-2204.
281. Van Kampen, N.G. *Stochastic processes in physics and chemistry*. Amsterdam: North Holland, 2007.
282. Slezov, V.V., and V.V. Sagalovich. "Diffusive decomposition of solid solutions." *Uspekhi Fizicheskikh Nauk*, 151 (1987): 67-104.
283. Lifshitz, I.M., and V.V. Slezov. "Coalescence kinetics in spatially inhomogeneous media." *Journal of Experimental and Theoretical Physics* 35 (1958): 479-490.
284. Slezov, V.V., and S.A. Kukushkin. "To the theory of nonisothermal coalescence in the decay of supersaturated solid solutions." *Physics of the Solid State (Fizika Tverdogo Tela)* 29 (1987): 1812 – 1818.
285. Landau, L.D., and E.M. Lifshitz. *Statistical physics*. Oxford: Pergamon Press, 1980.
286. Talanin, V.I., I.E. Talanin, A.I. Mazursky, and M.L. Maksimchuk. "Modeling of the kinetics of the process of coalescence of primary growth microdefects in dislocation-free single crystals of silicon." *Proceedings of universities. Materials of electronic engineering* no. 1 (2010): 4-9.
287. Wang, Z. "Modeling microdefects formation in crystalline silicon: the roles of point defects and oxygen." PhD diss., Massachusets institute of technology, 2002.

288. Henke, S., B. Stritzker, and B. Rauschenbach. “Synthesis of epitaxial beta-SiC by C60 carbonization of silicon.” *J. Appl. Phys*. 78 (1995): 2070-2074.
289. Plekhanov, P.S., U.M. Gosele, and T.Y. Tan. “Modeling of nucleation and growth of voids in silicon.” *J. Appl. Phys*. 84 (1998): 718-726.
290. Talanin, V.I., and I.E. Talanin. “Modeling of defect formation processes in dislocation-free silicon single crystals.” *Cryst. Reports* 55 (2010): 632-637.
291. Talanin, V.I., I.E. Talanin, S.A. Koryagin, and M.Yu. Semikina. “Modeling vacancy microvoids formation in dislocation-free silicon single crystals.” *Semiconductor Physics, Quantum Electronics & Optoelecrtronics* 9 (2006): 77-81.
292. Fistul, V.I., V.I. Petrovsky, N.S. Rytova, and P.M. Grinshtein. “Formation of a near-surface impurity profile.” *Soviet Physics Semiconductors* 13 (1979): 1402-1410.
293. Fistul, V.I., and M.I. Sinder. “Vacancy porosity in the near-surface region of a semiconductor.” *Soviet Physics Semiconductors* 15 (1981): 1182-1186.
294. Golgstein, R.V., M.V. Mezhennyi, M.G. Mil’vidskii, V.Ya. Reznik, K.B. Ustinov, and P.S. Shushpannikov. “Experimental and theoretical investigation of formation of the oxygen-containing precipitate-dislocation loop system in silicon.” *Physics of the Solid State* 53 (2011): 527-538.
295. Collected Works of J.D. Eshelby. Eds. X. Markenscoff and A. Gupta. Amsterdam: Springer Netherlands, 2006.
296. Bert, N.A., A.L. Kolesnikova, A.E. Romanov, and V.V. Chaldyshev. “Elastic behavior of a spherical inclusion with a given uniaxial dilatation.” *Physics of the Solid State* 44 (2002): 2240-2250.
297. Chaldyshev, V.V., N.A. Bert, A.E. Romanov, A.A. Suvorova, A.L. Kolesnikova, V.V. Preobrazhenskii, M.A. Putyato, B.R. Semyagin, P. Werner, N.D. Zakharov, and A. Claverie. “Local stresses induced by nanoscale As–Sb clusters in GaAs matrix.” *Appl. Phys. Lett*. 80 (2002): 377-379.
298. Chaldyshev, V.V., A.L. Kolesnikova, N.A. Bert, and A.E. Romanov. “Investigation of dislocation loops associated with As-Sb nanoclusters in GaAs.” *J. Appl. Phys*. 97 (2005): 024309-024312.
299. Bert, N.A., V.V. Chaldyshev, A.L. Kolesnikova, and A.E. Romanov. “Stress relaxation phenomena in buried quantum dots. In: *Self-Assembled Quantum Dots*, edited by Z.M. Wang, 297-336. New York: Springer Science, , 2008.

300. Kolesnikova, A.L., A.E. Romanov, and V.V. Chaldyshev. “Elastic-energy relaxation in heterostructures with strained nanoinclusions.” *Physics of the Solid State* 49 (2007): 667-674.
301. Bert, N.A., A.L. Kolesnikova, V.N. Nevedomsky, V.V. Preobrazhenskii, M.A. Putyato, A.E. Romanov, V.M. Seleznev, B.R. Semyagin, and V.V. Chaldyshev. “Formation of dislocation defects in the process of burying of InAs quantum dots into GaAs.” *Semiconductors* 43 (2009): 1387-1393.
302. Bonafos, C., D. Mathiot, and A. Claverie. “Ostwald ripening of end-of-range defects in silicon.” *J. Appl. Phys*. 83 (1998): 3008-3018.
303. Burton, B., and M.V. Speight. “The coarsening and annihilation kinetics of dislocation loops.” *Philosophical Magazine A* 53 (1985): 385-402.
304. Kosevich, A.M. “How the crystal flows.” *Uspekhi Fizicheskikh Nauk* 114 (1974): 509-532.
305. “GADEST XVI 2015, Bad Staffelstein, Germany”. In: *Solid State Phenomena 242*, edited by P. Pichler.
306. “GADEST XV 2013, Oxford, UK”. In: *Solid State Phenomena 205-206*, edited by J.D. Murphy.
307. “GADEST XIV 2011, Loipersdorf, Austria”. In: *Solid State Phenomena 178-179*, edited by W. Jantsch and F. Schäffler.
308. “GADEST XIII 2009, Döllnsee, Germany”. In: *Solid State Phenomena 156-158*, edited by M. Kittler and H. Richter.
309. Sobolev, N.A. *Defect Engineering in Semiconductor Technology*. Berlin: LAP Lambert Academic Publishing, 2011.
310. Sobolev, N.A. “Silicon, doped with erbium, is a new semiconductor material for optoelectronics.” *Russian Chemical Journal* XLV (2001): 95-101.
311. Chelyadinsky, A.R., and F.F. Komarov. “Defect-impurity engineering in implanted silicon.” *Uspekhi Fizicheskikh Nauk* 173 (2003): 813-846.
312. Sobolev, N.A. “Engineering defects in implanted technology of silicon light-emitting structures with dislocation luminescence.” *Semiconductors* 44 (2010): 3-25.
313. *Defects and impurities in silicon materials. An introduction to atomic-level silicon engineering*. Eds. Y.Yoshida, and G. Langouche. Tokyo: Springer, 2015.
314. *Advanced microelectronics*. Eds. V.A. Perevostchikov, and V.D. Skoupov. Berlin: Springer, 2005.
315. *Silicon, germanium, and their alloys. Growth, defects, impurities, and nanocrystals*. Eds. G. Kissinger, and S. Pizzini. Boca Raton: CRC Press, Taylor & Francis group, 2015.

316. *Handbook of silicon based MEMS materials and tech*nologies. Eds. V. Lindroos, M. Tilli, A. Lehto, and T. Motooka. Oxford: Elsevier Publ., Inc., 2010.
317. Valek, L., and J. Sik. "Defect engineering during Czochralski crystal growth and silicon wafer manufacturing." In: *Modern aspects of bulk crystal and thin film preparation* edited by N. Kolesnikov, 43-70. Rijeka: INTECH Publ., 2012.
318. Eranna, G. *Crystal growth and evaluation of silicon for VLSI and ULSI*. Boca Raton: CRC Press, Taylor & Francis group, 2015.
319. Nguyen, T.H.T., J,C. Chen, C. Hu, C.H. Chen, Y.H. Huang, H.W. Lin, A. Yu, B. Hsu, M. Yang, and R. Yang. "Numerical study of the thermal and flow fields during the growth process of 800 kg and 1600 kg silicon feedstock." *Crystals* 7 (2017): 74-84.
320. Berdnikov, V.S., V.V. Vinokurov, V.I. Panchenko, and S.V. Soloviev. "Heat transfer in the classical Czochralski method." *Engineering and Physics Journal* 74 (2001): 122-127.
321. Berdnikov, V.S., V.I. Polezhaev, and A.I. Prostomolotov. "The flow of a viscous liquid in a cylindrical vessel as the disk rotates." *Proceedings of the USSR Academy of Sciences. Mechanics of Liquids and Gas* no. 5 (1985): 33-40.
322. Muller, G. "Experimental analysis and modeling of melt growth processes." *J. Cryst. Growth* 237-239 (2002): 1628-1637.
323. Pat. 21853 UA, MKI C30B13/00, C30B15/00. The method of growing melt-free dislocation silicon single crystals. Talanin V.I., Talanin I.E., and Sirota A.V. Publ. 10.04.07.
324. Xiao, Q., and I.I. Derby. "Three dimensional melt flow in Czochralski oxide growth: high-resolution, massively parallel, finite element computations." *J. Cryst. Growth* 152 (1995): 169-181.
325. Chen, Q.S., V. Prasad, A. Chatterjee, and J. Larkin. "A porous media-based transport model for hydrothermal growth." *J. Cryst. Growth* 198-199 (1999): 710-717.
326. Polezhaev, V.I., O.A. Bessonov, N.V. Nikitin, and S.A. Nikitin. "Convective interaction and instabilities in GaAs Czochralski model." *J. Cryst. Growth* 230 (2001): 40-47.
327. Nikitin, N.V., and V.I. Polezhaev. "Three-dimensional convective instability and temperature oscillations during the growth of crystals by the Czochralski method." *Mechanics of Liquids and Gas* no. 3 (1999): 26-38.
328. Prostomolotov, A.I., N.A. Verezub, and Kh.X. Ilyasov "Remote and conjugate modeling of heat and mass transfer and defect formation in

technological processes." *Proceedings of universities. Materials of electronic engineering* no. 1 (2015): 31-36.
329. Bornside, D.E., T.A. Kinney, and R.A. Brown, "Minimization of thermoelastic stresses in Czochralski grown silicon: application of the integrated system model." *J. Cryst. Growth* 108 (1991): 779-805.
330. Pat. 6197111 B1 USA, MKI C30B27/02. Heat shield assembly for crystal puller. Ferry W.I., and Ishii S. Publ. 03.06.01.
331. Pat. 6340392 B1 USA, MKI C30B15/02. Pulling methods for manufacturing monocrystalline silicone ingots by controlling temperature at the center and edge of an ingot-melt interface. Park J.G. Publ. 01.12.02.
332. Verezub, N.A., M.G. Milvidsky, and A.I. Prostomolotov. "Heat transfer in plants for growing single crystals of silicon by the Czochralski method." *Material Science* no. 3 (2004): 2-6.
333. Berdnikov, V.S., A.I. Prostomolotov, and N.A. Verezub. "The phenomenon of "cold plume" instability in Czochralski hydrodynamic model: Physical and numerical simulation." *J. Cryst. Growth* 401 (2014): 106-110.
334. Pat. 2102539 C1 RF, MKI C30B15/14. A device for growing a single crystal and a method for growing a single crystal. Wilzmann P., and Pinzkhoffer H. Publ. 01.20.98.
335. Pat. 2001131737A RF, MKI C30B15/20. Method for the production of single-crystal silicon. Remizov O.A., and Jay J.K. Publ. 10.08.04.
336. Pat. 2278912 C1 RF, MKI C30B15/20. Method for producing single-crystal silicon (variants). Remizov O.A. Publ. 27.06.06.
337. Pat. 2241078 C1 RF, MKI C30B15/00. Method of growing a single crystal of silicon from a melt. Alekseev S.V., Makeev Kh.I., and Makeev M.Kh. Publ. 27.11.04.
338. Pat. 2189407 C2 RF, MKI C30B15/02. Method for the preparation of silicon single crystals in the case of a breakdown of single-crystal growth. Beringov S.B., Ushankin Yu.V., and Shulga Yu.G. Publ. 20.09.02.
339. Pat. 2200775 C2 RF, MKI C30B15/00. Method of growing a single crystal of silicon from a melt. Beringov S.B., Rudenko S.V., and Shulga Yu.G. Publ. 20.03.03.
340. Pat. 2241079 C1 RF, MKI C30B15/00. Device for growing a single crystal of silicon from a melt. Alekseev S.V., Batashov M.V., Makeev Kh.I., and Makeev M.Kh. Publ. 27.11.04.
341. Pat. 93035824 A RF, MKI C30B15/04. Method of doping of silicon single crystals. Salnik Z.A., Miklyaev Yu.A., Naumov A.V., Salnik O.S., Fomichev A.V., and Volkov V.I. Publ. 10.05.96.

342. Pat. 2241080 C1 RF, MKI C30B15/10. Melting device for growing single crystals of silicon from the melt. Alekseev S.V., Batashov M.V., Makeev Kh.I., and Makeev M.Kh. Publ. 27.11.04.
343. Pat. 2003117510 A RF, MKI C30B15/10. Melting device for growing single crystals of silicon from the melt. Alekseev S.V. Batashov M.V., Makeev Kh.I., and Makeev M.Kh. Publ. 27.12.04.
344. Pat. 1800854 C1 RF, MKI C30B15/10. Device for growing crystals. Golyshev V.D., and Gonik M.A. Publ. 15.02.90.
345. Kakimoto, K. "Heat and mass transfer in semiconductors melt during single-crystal growth processes." *J. Appl. Phys*. 77 (1995): 1827-1833.
346. Kalaev, V., Y. Makarov, V. Yuferev, and A. Zhmakin. "Modeling of semitransparent bulk cryatal growth." In: *Crystal growth technology: from fundamentals and simulation to large-scale production*, edited by H.J. Scheel, and P. Capper, 205-227. London: John Wiley & Sons, 2011.
347. Bykova, S.V., V. D. Golyshev, M.A. Gonik, V.B. Tsvetovsky, I.V. Frjasinov, and M.P. Marchenko. "Features of mass transfer for the laminar melt flow along the interface." *J. Cryst. Growth* 237-239 (2002): 1886-1891.
348. Gonik, M.A., and A. Croll. "Silicon crystal growth by the modified FZ technique." *CrystEngComm*. 15 (2013): 2287-2293.
349. Kokh, A.E., V.E. Kokh, and N.G. Kononova. "Installation for growing crystals under conditions of rotation of the thermal field." *Devices and Technics of the Experiment* no. 1 (2000): 157-168.
350. Pat. 2203987 C2 RF, IPC C30B30/04. A method for accelerated growth of semiconductor crystals of large diameter by cooling through a melt and the action of electromagnetic fields to create a supercooling of the melt. Prokhorov A.M., Petrov G.N., Borisov V.T., and Lyashchenko B.G. Publ. 10.05.03.
351. Talanin, V.I., and I.E. Talanin. "The diffusion model of grown-in microdefects formation during crystallization of dislocation-free silicon single crystals." In: *Advances in crystallization processes* edited by Y. Mastai, 611-632. Rijeka: INTECH Publ., 2012.
352. Damask, A. C., and G. J. Dienes. *Point defects in metals*. New York: Gordon & Breach, 1963.
353. Bolling, C.F., and D. Finestein. "On vacancy condensation and the origin of dislocations in growth from the melt." *Philosophical Magazine* 25 (1972): 45-66.
354. Zasimchuk, I.K., and E.P. Pavlova. "Crystallographic and morphological characteristics of dislocations in malodislocational zinc

single crystals grown from a melt." *Kristallografiya (Crystallography Reports)* 33 (1988): 673-678.
355. Talanin, V.I., and I.E. Talanin. "Diffusion model of the formation of growth microdefects as applied to the description of defect formation in heat-treated silicon single crystals." *Physics of the Solid State* 55 (2013): 282-287.
356. Newman, R.C. "Oxygen diffusion and precipitation in Czochralski silicon." *J. Phys.: Condens. Matter* 12 (2000): R335-R365.
357. Babitsky, Yu.M., and P.M. Grinshtein. "Kinetics of formation of second oxygen donors in silicon." *Soviet Physics Semiconductors* 18 (1984): 604-609.
358. Talanin, V.I., I.E. Talanin, and V.I. Lashko. "Description of the real monocrystalline structure on the basis of the Vlasov model for solids." In: *New research on silicon – structure, properties, technology* edited by V.I.Talanin, 5-9. Rijeka: INTECH Publ., 2017.
359. Bytkin, S.V., and T.V. Kritskaya. "Comparative analysis of electrophysical parameters of silicon single crystals subjected to long-term storage at 300K." *Proceedings of universities. Materials of electronic engineering* no. 3 (2010): 14-17.
360. Kaiser, W. "Electrical and optical properties of heat-treated silicon." *Phys. Rev*. 105 (1957): 1751-1756.
361. Talanin, V.I., I.E. Talanin, and N.Ph. Ustimenko. "Structural scheme of information system for defect engineering of dislocation-free silicon single crystals." *Science and Technology* 2 (2012): 130-134.
362. Talanin, V.I., I.E. Talanin, and N.Ph. Ustimenko. "Analysis and calculation of the formation of grown-in microdefects in dislocation-free silicon single crystals." *Crystallography Reports* 57 (2012): 898-902.
363. Talanin, V.I., and I.E. Talanin. "A selective review of the simulation of the defect structure of dislocation-free silicon single crystals." *The Open Condensed Matter Physics journal* no. 4 (2011): 8-31.
364. Talanin, V.I., I.E. Talanin, and N.Ph. Ustimenko. "A new method for research of grown-in microdefects in dislocation-free silicon single crystals." *Science and Technology* 1 (2011): 13-17.
365. Li, M., N. Imaishi, and T. Tsukada. "Global simulation of a silicon Czochralski furnace." *J. Cryst. Growth* 234 (2002): 32–46.
366. Virbulis, J., T. Wetzel, A. Muiznieks, B. Hanna, E. Dornberger, E. Tomzig, A. Muhlbauer, and W. von Ammon. "Numerical investigation of silicon melt flow in large diameter CZ-crystal growth under the influence of steady and dynamic magnetic fields." *J. Crystal Growth* 230 (2001): 92-99.

367. Miller, W. “Numerical simulation of bulk crystal growth on different scales: silicon and GeSi.” *Phys. Status Solidi B* 247 (2010): 885-869.
368. Kalaev, V.V., D.P. Lukanin, V.A. Zabelin, Yu.N. Makarov, J. Virbulis, E. Dornberger, and W. von Ammon. “Calculation of bulk defects in CZ Si growth: Impact of melt turbulent fluctuations.” *J. Cryst. Growth* 250 (2003): 203–208.
369. Prostomolotov, A.I., N.A. Verezub, and M.G. Milvidskii. “Thermal Optimization of Cz silicon single crystal growth.” In: *Gettering and Defect Engineering in Semiconductor Technology XIII* edited by M Kittler, and H Richter, *Solid State Phenomena* 156-158 (2010): 217-223370.
370. Prostomolotov, A., H. Ilyasov, and N. Verezub. “CrystmoNet remote access code for Czochralski crystal growth modelling.” *Science and Technology, 2013, Special Iss.*: 18-25.
371. Goncharov, A.L., M.T. Devdariani, A.I. Prostomolotov, and I.V. Fryazinov. “Approximation and numerical method for solving three-dimensional Navier-Stokes equations on orthogonal meshes.” *Mathematical Modeling* 3 (1991): 89-109.
372. ANSYS FLUENT Tutorial Guide: Release 14.0. 2011. ANSYS Inc.
373. Introduction to MSC.Marc and Mentat: MAR101 course notes. 2007. Msc.Software Inc.
374. Tecplot 360: User’s Manual. 2009. Tecplot Inc.

SUPPLEMENT

(A) Personal composition of the Zaporozhye Scientific Group in the 1970s-1980s

Dr. E.S. Falkevich, Dr. V.F. Latyshenko, I.Yu. Litvinova, Dr. K.N. Nerimark, Dr. E.G. Sheikhet (Head of Zaporozhye Scientific Group up to 1988), Dr. V.A. Shershel, Dr. I.E. Talanin, M.Sc. A.S. Trainin, M.Sc. N.V. Veselovskaya.

(B) Personal composition of the Zaporozhye (Russian) Scientific Group since 1990s to a present time

M.Sc. S.A. Koryagin, M.Sc. V.I. Lashko, M.Sc. M.L. Maximchuk, M.Sc. A.I. Mazurskii, Prof. Dr. I.E. Talanin (Head of Zaporozhye (Russian) Scientific Group since 1989 to a present time), Prof. Dr. V.I. Talanin, M.Sc. N.Ph. Ustimenko, M.Sc. A.A. Voronin.

(C) Short biography of Prof. Dr. I.E. Talanin

Dr. Igor Evgenievich Talanin was born into a Russian noble family. He is a Full Professor and Chief of the Computer Science and Software Engineering Department of the Institute of Economics and Information Technologies, Zaporozhye, Ukraine. He has published extensively in material science and semiconductor physics, and in software engineering. His publications include five books and around 300 scientific papers.

(D) Short biography of Prof. Dr. V.I. Talanin

Dr. Vitalyi Igorevich Talanin was born into a Russian noble family. He is a Full Professor and Vice-Chief of the Computer Science and Software Engineering Department of the Institute of Economics and Information Technologies, Zaporozhye, Ukraine. He has published extensively in material science and semiconductor physics, and in software engineering, as well as in Russian history and genealogy. His publications include 11 books and around 200 scientific papers. He is a Member of the Editorial Boards of *Journal of Crystallization Process and Technology*, *Science and Technology*, and *Journal of Information Systems & Engineering and Management*.